

The Oxidation Of Dissolved Organic Compounds By Redbed Sandstones

By

Omar Nabhan Al AZZO

A thesis submitted to

The University of Birmingham

for the degree of

Doctor of Philosophy

School of Geography, Earth & Environmental Sciences.

The University of Birmingham

August 2016

UNIVERSITY OF
BIRMINGHAM

University of Birmingham Research Archive

e-theses repository

This unpublished thesis/dissertation is copyright of the author and/or third parties. The intellectual property rights of the author or third parties in respect of this work are as defined by The Copyright Designs and Patents Act 1988 or as modified by any successor legislation.

Any use made of information contained in this thesis/dissertation must be in accordance with that legislation and must be properly acknowledged. Further distribution or reproduction in any format is prohibited without the permission of the copyright holder.

Acknowledgements

I am sincerely thankful to my lead supervisor Professor John Tellam, for the unlimited advice and audience during this study. Also many thanks must be extend to my second supervisor Mike Rivett.

I am grateful to the all staff of Earth Sciences for their assistanceas well as to all of my colleagues, especially Mahmood Jaweesh, for his friendship and help.

I am sincerely grateful to my sponsor (Higher Education Development Committee in Iraq (HCED)) for providing funding this study.

Specially thank you goes to my wife Noor for being patient and understanding during the study period. Without her vital support, it is impossible to finish this work.

Final I am deeply indebted to my mother, aunt, sisters and brother for their steadfast support. Without our family support and prayer, I cannot reach the UK.

DEDICATION

This thesis is dedicated

To my mother

To soul of my father

الإهداء

إلى الوالدة الغالية اطل الله عمرها

إلى روح أبي الطاهرة رحمت الله عليه

Abstract

The aim of this research was to investigate the ability of red sandstone to oxidise dissolved organic carbon (DOC). Ascorbic acid (H_2A) has been used as a relatively simple representative of DOC, because it has functional groups in common with more complex natural organics, is relatively easy to analyse, safe and environmentally friendly. Preliminary experiments revealed that ascorbic acid is able to reductively dissolve oxide in sandstone and showed that Mn as well as Fe oxides are involved. Before running final batch experiments studies were undertaken on sorption of ascorbic acid, Fe and Mn to sandstone. Sorption was similar to that seen for synthetic hematite (possibly a two- slope linear isotherm). Two sets of batch experiments were undertaken under anoxic conditions one under biotic and one under abiotic condition. The results showed that the release of Fe and Mn depends on the concentration of H_2A and pH. The decrease in H_2A concentration was greater than the increase in Fe and Mn concentrations (corrected for sorption of metals on the sandstone surfaces) and this was ascribed to sorption. A revised possible sorption model was proposed that included sorption of both ascorbate and dehydroascorbic acid (main product of H_2A oxidation). The rate of H_2A oxidation was higher in biotic experiments than in abiotic experiments. It was concluded that this was due to the difference of pH between two sets of experiments rather than due to bacteria presence. The rate of ascorbic acid oxidation by natural oxides was higher than found by previous researchers for synthetic hematite. This result was not expected because less crystalline and newly prepared synthetic hematite is usually considered more reactive than geological hematite, though the rates recorded here also include the effect of Mn oxides. However, the processes determined by the synthetic mineral studies do seem appropriate also to geological systems. Many questions are left to investigate but the present study has shown that the sandstone will provide a possibly significant natural oxidative attenuation of some organics.

Table of contents

1. Introduction.....	1
1.1 Background.....	1
1.2 Previous Research.....	3
1.2.1 Introduction.....	3
1.2.2 Oxide Reduction in Sedimentary Aquifers.....	3
1.2.3 Lab Studies on Synthetic Minerals.....	4
1.2.4 Lab Studies on Natural Sediment.....	6
1.2.5 Studies of the Roles of Bacteria in the Reductive Dissolution of Oxides.....	7
1.2.6 Oxidation of dissolved organic carbon	9
1.2.7 The effect of mineral properties	9
1.3 Aim	11
1.4 Approach	12
1.5 Thesis format	13
2 Preliminary experiments.....	14
2.1 Introduction.....	14
2.2 Materials and Analysis.....	15
2.2.1 Ascorbic Acid.....	15
2.2.2 Sandstone.....	16
2.2.3 Analysis for Fe and Mn ⁺⁺	17
2. 3. High [H ₂ A], generally high temperature experiments.....	19

2.3.1	<i>Introduction.....</i>	19
2.3.2	<i>Will high [H₂A] reduce hematite at high temperatures?.....</i>	20
2.3.3	<i>Reductive dissolution dependence on temperature.....</i>	21
2.3.4	<i>Reductive dissolution dependence on H₂A concentrations at high temperature.....</i>	25
2.3.5	<i>Reductive dissolution at lower H₂A concentrations at lower and high temperatures.....</i>	27
2.3.6	<i>How does reductive dissolution by high concentration H₂A change with sandstone mass at high temperatures over long time interactions.....</i>	28
2.3.7	<i>Monitoring the colour change of the solution and sandstone at high temperature.....</i>	31
2.3.8	<i>The effects of filtration and acidification at high temperature.....</i>	32
2.3.9	<i>Combining previous experiment results to look at how concentrations vary over longer times at high temperature.....</i>	33
2.3.10	<i>The effect of contact with oxygen at high H₂A concentration at lab temperature</i>	35
2.3.11	<i>Measurement of dissolved oxygen in ascorbic acid solutions.....</i>	36
2.3.12	<i>Variation in TOC with time at high temperatures.....</i>	39
2.4	<i>Low concentration H₂A, lab temperature experiments</i>	41
2.4.1	<i>Will low concentration H₂A reduce sandstone oxides measurably at low temperatures?.....</i>	41
2.4.2	<i>Does filtering and shaking affect dissolution at low H₂A concentrations and low temperatures.....</i>	43
2.4.3	<i>Effect of shaking at lab temperatures and without shaking at higher temperatures.....</i>	44
2.5	<i>What is the effect of initial conditions on dissolution at low H₂A concentrations and low temperatures?.....</i>	46
2.5.1	<i>The release of Fe and Mn⁺⁺ from sandstone by HCl.....</i>	46
2.5.2	<i>The effect of washing sandstone with dilute HCl on the reductive dissolution of oxides by H₂A.....</i>	49
2.5.3	<i>Effect on reductive dissolution of saturation of the surface of the oxides with Ca⁺⁺.....</i>	54

2.6 Summary and Conclusion.....	57
3 The Analysis of Ascorbic Acid Using the Reduction of KMnO_4.....	59
3.1 Introduction.....	59
3.2 KMnO_4 solutions at equilibrium	61
3.3 The absorbance (A) as a function of pH in pure KMnO_4 solutions.....	62
3.4 The absorbance of KMnO_4 solutions as a function of concentration.....	63
3.5 Reaction between KMnO_4 and H_2A	65
3.6 Effect of different $[\text{KMnO}_4]$ on the absorbance of ascorbic acid.....	68
3.7 Effect of Fe on the measurement of $[\text{H}_2\text{A}]$	69
3.7.1 <i>Effect of adding Fe(III) to KMnO_4</i>	69
3.7.2 $\text{KMnO}_4 + \text{Fe(III)} + \text{H}_2\text{A}$	70
3.7.3 $\text{KMnO}_4 + \text{Fe (II)}$	71
3.7.4 $\text{KMnO}_4 + \text{H}_2\text{A} + \text{Fe(II)}$	74
3.8 Effect of Mn^{+2} on measurement of $[\text{H}_2\text{A}]$	76
3.8.1 <i>Effect of Mn on the absorbance of KMnO_4</i>	76
3.8.2 <i>Effect of $\text{KMnO}_4 + \text{H}_2\text{A} + \text{Mn}^{++}$</i>	78
2.8.3 <i>Correcting H_2A Measurements for the Presence of Mn^{++}</i>	81
3.9 The stability of ascorbic acid.....	82
3.10 Recommendations for H_2A Analysis Using KMnO_4	85
4 Sorption of ascorbic acid on sandstone.....	87
4.1 Introduction.....	87
4.2 Sorption	87
4.2.1 <i>Introduction</i>	87

4.2.2	The distribution coefficient (K_d) and Isotherms.....	87
4.2.3	Speed of Sorption Reactions and K_d Values and What Dependence On.....	89
4.2.4	Mechanisms of Sorption Reactions.....	90
4.2.5	Implications from Literature for Experiments on Sandstone.....	93
4.3	Sorption Batch Experiments	93
4.3.1	Initial sorption experiment with higher mass of sandstone: (Experiments E_1 & E_2).....	93
4.3.2	Sorption of ascorbic acid using a higher concentration range of H_2A (E_3).....	99
4.3.3	Sorption of ascorbic acid using a lower mass of sandstone and lower concentration range of $[H_2A]$ (E_4).....	102
4.3.4	Confirming the drift of the UV-vis spectrophotometer.....	104
4.3.5	Sorption of ascorbic acid using 10g sandstone and a moderate range of concentrations of H_2A (E_5).....	105
4.4	Discussion and Conclusion.....	110
5	Cation exchange	113
5.1	Introduction.....	113
5.2	Cation Exchange.....	113
5.3	Measurement of Cation Exchange Capacity of Sandstone Samples Using Strontium Chloride	116
5.4	Selectivity Coefficients	120
5.5	Experiments on Fe (II) Exchange.....	125
5.6	Sorption of Mn^{++}	127

5. 7	Conclusions.....	128
6	Reaction of Ascorbic Acid and English Triassic sandstone	130
6.1	Introduction	130
6.2	Methods.....	130
6.3	Results and Initial Observations.....	135
6.4	Rate of Apparent reductive dissolution	143
6.5	mass balance and surface interaction	148
6.6	Rates of reductive dissolution of sandstone oxides coatings.....	156
6.7	conclusions	162
7.1	Summary of Results	164
7.2	Implications.....	168
7.3	Recommendation and future research	169
7.1	Conclusions.....	165
7.1.1	introduction	165
7.1.2	Preliminary batch experiments.....	165
7.1.3	Development of methods to analyse ascorbic acid.....	166
7.1.4	Sorption of ascorbic acid on the red sandstone	166
7.1.5	Cation exchange /total sorption of Fe and Mn ⁺⁺ on the red sandstone	167
7.1.6	Reductive dissolution mechanisms	167
7.2	Review of objectives	169
7.3	Implications.....	171
7.4	Recommendation and future research	172
References	174

List of figures

Figure 1-1: Suter et al.'s (1991) model for the reductive dissolution of synthetic hematite by ascorbic acid.....	5
Figure 2-1: Comparison of the absorption of various concentrations of ferrous iron prepared in DIW and in 10 Mm ascorbic acid solution.....	18
Figure 2-2: Comparison of the absorption of various concentrations of Mn^{+2} prepared in DIW and in 10 Mm ascorbic acid solution.....	19
Figure 2-3: The relationship between the concentration of Fe and time of contact of 10 g sandstone and 500 ml of 10 mM ascorbic acid solution at 42 °C.....	20
Figure 2-4: The concentration of Fe released after 24 hours of contact of 1g of sandstone with 500 ml of 10 mM ascorbic acid solution at pH=3	21
Figure 2-5: Plot of Fe and Mn concentration for samples stored at lab temperature against the Fe and Mn for samples stored in fridge at 4°C.....	22
2-6: A linearised Arrhenius relationship plot for the apparent rate constant of the experiments shown in Figure 2.4.....	24
2-7: The concentration of Mn released after 24 h reaction under four different temperatures, using 10 mM ascorbic acid at pH =3.....	24
Figure 2-8: The relationship between filtered (0.45µm) sample concentrations and unfiltered sample concentrations at 60 °C.....	25
Figure 2-9: The amount of Fe and Mn released from 1 g of sandstone by 500 ml of 75, 50 and 25 mM H_2A at 60 C.....	26
Figure 2-10: The relationship between the Fe concentration extrapolated to time = 0 and initial hydrogen ion concentration in sandstone	27
Figure 2-11: The concentration of Fe released from 1 g mass sandstone using 500 ml of 1 and 0.75 mM H_2A at 20 and 80 °C.....	28
Figure 2-12: The effect of filtration through 0.2 µm filters.....	29
Figure 2-13: Fe released (average of filtered and unfiltered samples) on contact of 500 ml of 10 mM H_2A solution (pH~3.2) with sandstone at 80 °C.....	30
Figure 2-14: Mn^{++} released (average of filtered and unfiltered samples) on contact of 500 ml of 10 mM H_2A solution (pH~3.2) with sandstone at 80 °C.....	31
Figure 2-15: The change of colour of 10 mM ascorbic acid as it reacts with 10 g red sandstone.....	32

Figure 2-16: Fe release from 1 g mass sandstone using 500 ml of 10 mM H ₂ A (pH~2.93) at 90°C using different sample treatments.....	33
Figure 2-17 The relationship between time vs Fe concentration at higher temperatures from a combination of several experiments.....	35
2-18: Fe and Mn release from 1g sandstone using 500 ml of 10 mM H ₂ A under aerobic and anaerobic conditions	36
2-19: Dissolved oxygen variation with time for 500 ml of DIW with 1 g sandstone.....	38
Figure 2-20: Dissolved oxygen variation with temperature for deionised water with sandstone, ascorbic acid alone and ascorbic acid with sandstone.....	39
Figure 2-21: The relation between TOC and iron using 10 mM H ₂ A with 1 g sandstone at 50 and at 90 °C.....	40
Figure 2-22: Comparison of TOC variation with time between 10 mM H ₂ A solutions in contact with and not in contact with sandstone at 50 and at 90 °C.....	41
Figure 2-23: Plot of Fe concentration versus time at 50 and 90 °C	41
Figure 2-24: Fe and Mn ⁺⁺ concentrations as a function of H ₂ A concentration at lab temperature. 10 g sandstone with 0.04 l of H ₂ A solutions.....	42
Figure 2-25: The effect of shaking on the rate of reductive dissolution of Fe and Mn oxides in 10g sandstone samples.....	43
Figure 2-26: Fe and Mn release after 2 hours of shaking 10 g sandstone in 40 ml H ₂ A solution under lab temperature.....	45
Figure 2-27: Fe and Mn release from 10 g sandstone at lab temperature	48
Figure 2-28 The relationship of [Fe] and [Mn] with pH.....	49
Figure 2-29: The amount of Fe and Mn released from 10 g of sandstone washed with dilute HCl and unwashed using ascorbic acid.....	51
Figure 2-30: The amount of Fe and Mn released from unwashed and dilute HCl -washed sandstone by ascorbic acid.....	53
Figure 2-31: The variation of Fe and Mn concentration and pH in the washing supernatants.....	54
Figure 2-32: The relationship between pH and the concentration of Fe and Mn after H ₂ A contact with the sandstone for unwashed and HCl-washed sandstone samples.....	54

Figure 2-33: Concentrations of Fe and Mn released by contact of ascorbic acid with unwashed sandstone samples and CaCl ₂ -washed sandstone samples.....	56
Figure 2-34: The variation of Fe and Mn concentration and pH in the washing supernatants. All Fe concentrations are below detection limit.....	56
Figure 2-36: Concentrations of Fe and Mn as a function of pH for unwashed and CaCl ₂ -washed sandstone.....	57
Figure 3-1: Modelling of KMnO ₄ solutions at equilibrium using phreeqc.....	62
Figure 3-2: The absorbance of a 100 ppm solution of KMnO ₄ at different pH values.....	63
Figure 3-3: Dependence of absorbance on [KMnO ₄].....	64
Figure (3-4) Absorbance against [H ₂ A].....	65
Figure 3-5: H ⁺ change (positive is rise) after adding KMnO ₄ as a function of [H ₂ A] initially present in solution.....	67
Figure 3-6: Measurements of the absorbance of H ₂ A using KMnO ₄	69
Figure 3-7: The effect on absorbance of KMnO ₄ solutions by various concentrations of Fe(III). (a) 40 ppm of KMnO ₄ ; (b) 100 ppm of KMnO ₄	70
Figure 3-8: The effect of addition of 4 ppm of Fe(III) on absorbance of KMnO ₄ / H ₂ A solutions.....	70
Figure 3-9: Effect of ferrous iron on KMnO ₄ solution absorbance.....	72
Figure 3-10: Addition of Fe ⁺² to KMnO ₄ solutions in the presence of H ₂ A: a) Absorbance against [H ₂ A] ppm; b) absorbance against [FeII] for each [H ₂ A].....	75
Figure 3-11: Addition of Fe ⁺² to KMnO ₄ solutions in the presence of H ₂ A.....	76
Figure 3-12: Addition of Mn ⁺² to KMnO ₄ solutions.....	78
Figure 3-13: The effect of the addition of Mn ⁺² on Absorbance	79
Figure 3-14: The dependence of {A _{[Mn]>0} - A _{[Mn]=0} } for H ₂ A solutions in the presence of Mn (II) under oxic conditions. (a) all data; (b) data averaged for each [Mn].....	80
Figure 3-15: The dependence of A for all H ₂ A solutions investigated in the presence of Mn (II) under oxic conditions.....	80
Figure 3-16: Change of absorbance under oxic conditions over time.....	83
Figure3-17: Change of H ₂ A under oxic conditions over time.....	83

Figure 3-18: Change of absorbance under anaerobic conditions over time.....	84
Figure 3-19: Change of H_2A under anaerobic conditions over time.....	84
Figure (4-1): Sorption isotherm for E_1 various $[H_2A]$ with 20 g mass of sandstone.....	94
Figure (4-2): Sorption isotherm for E_2 various $[H_2A]$ with 15 g mass sandstone.....	95
Figure (4-3): Sorption isotherm for various concentrations of ascorbic acid with 20 and 15 g sandstone :(E_1 and E_2).....	95
Figure (4-4): Experiment E_1	97
Figure (4-5):Experiment E_2	98
Figure (4-6): Sorption isotherm plot for experiment E_3	100
Figure (4-7): Experiment E_3	101
Figure (4-8): Sorption isotherms for E_4	102
Figure (4-9): Experiment E_4 . (a) Langmuir fit (b) corrected for $[Mn]$	103
Figure (4-10) Monitoring the absorbance of different $[KMnO_4]$ over time.....	104
Figure (4-11) Relation between $[H_2A]$ and pH.....	106
Figure (4-12). A plot of the (absorption –intercept) for $[H_2A]$ analysis against time.....	107
Figure (4-13) The relationship between the absorbance and $[H_2A]$	107
Figure (4-14) The sorption isotherm plot for E_5 for a range of ascorbic acid with 10 g sandstone, after correction.....	108
Figure (4-15). Experiment E_5	109
Figure (4-16) All experimental isotherms plotted together	111

Figure (4-17) Langmuir sorption isotherm for ascorbic acid on the surface of synthetic hematite (α Fe ₂ O ₃) at 25°C from (Afonso et al., 1990).....	112
Figure (5-1) Typical ranges of values for cation exchange capacities of different soil texture and clay minerals (data from Dragn, 1988).....	115
Figure (5-2) Concentrations of cations released from 10 g sandstone in contact with various initial concentrations of ferrous iron solutions.....	126
Figure (5-3) Results of Phreeqc modelling of the FeCl ₂ experiments.....	127
Figure (5-4): The isotherm for the Mn experiments.....	128
Figure (6-1) Agar plates after 3 weeks of incubation of untreated sandstone (left) and heat-treated sandstone (right).....	133
Figure 6-2 Amount of Fe and Mn released into the solution and concentration of H ₂ A for biotic experiments using an initial H ₂ A of 100 ppm.....	136
Figure 6-3 Amount of Fe and Mn released in the solution and concentration of H ₂ A for abiotic experiment using initial H ₂ A of 100 ppm.....	137
Figure 6-4 Amount of Fe and Mn released in the solution and concentration of H ₂ A for biotic experiment using initial H ₂ A of 80 ppm.....	137
Figure 6-5 Amount of Fe and Mn released in the solution and concentration of H ₂ A for abiotic experiment using initial H ₂ A of 80 ppm.....	138
Figure 6-6 Amount of Fe and Mn released in the solution and concentration of H ₂ A for biotic experiment using initial H ₂ A of 60 ppm.....	138
Figure 6-7 Amount of Fe and Mn released in the solution and concentration of H ₂ A for abiotic experiment using initial H ₂ A of 60 ppm.....	139
Figure 6-8 Amount of Fe and Mn released in the solution and concentration of H ₂ A for biotic experiment using initial H ₂ A of 40 ppm.....	139
Figure 6-9 Amount of Fe and Mn released in the solution and concentration of H ₂ A for abiotic experiment using initial H ₂ A of 40 ppm.....	140
Figure 6-10 Amount of Fe and Mn released in the solution and concentration of H ₂ A for biotic experiment using initial H ₂ A of 20 ppm.....	140
Figure 6-11 Amount of Fe and Mn released in the solution and concentration of H ₂ A for abiotic experiment using initial H ₂ A of 20 ppm.....	141

Figure (6-12) Plot of pH and E_h against time for all experiments.....	142
Figure 6-13. Variation of the sum of $Fe/2$ and Mn concentrations as a function of time in the biotic experiments.....	145
Figure 6-14. Plot of average pH for each initial $[H_2A]$ against the intercept on a time = 0 on a $[Fe]/2 + [Mn]$ against time plot	146
Figure (6-15) Decrease in $[H_2A]$ plotted against increase in metal concentration for (a) biotic and (b) abiotic conditions.....	147
Figure 6-16. Comparison of rates of dissolution of Fe and $2M$ ($2 \times \{[Fe]/2 + [Mn]\}$). $2M$ is used as Suter et al. (1991) data is in terms of moles of Fe	148
Figure (6-17) Mass balance variation with time for the 100ppm H_2A case.....	150
Figure (6-18) Plots of the sorbed HA^- estimated from the mass balance against $[H_2A]_{aq}$ and pH for the 100ppm experiments.....	152
Figure (6-19) Comparison of the DHA sorption model predictions and the lab data for the biotic experiment results.....	154
Figure 6-20 Comparison of the DHA sorption model predictions and the lab data for the abiotic experiment results.....	155
Figure (6-21) the rate of decrease in $[H_2A]$ with time as a relation of $[H_2A]$	157
Figure (6-22): The rate of change of $[Fe]/2 + [Mn]$ with time plotted against average $[H_2A]$ for each of 100,80,60,40 and 20ppm experiments.....	158
Figure (6-23): Comparing the rates of reductive dissolution for biotic and abiotic experiments.....	159
Figure(6-24): the rate of metal reduction versus sorbed of $[HA]^-$	160
Figure(6-25): The relationship between pH and oxidation rate of H_2A for all experiments.....	161
Figure (6-26): (a) Total HA^- sorbed as estimated using the model for this study (biotic and abiotic) and all data from Suter et al. (1991).....	162

List of tables

Table 2-1: The relative concentration of Fe and Mn in all comparable experiments.....	45
Table 3-1: Some chemical and physical properties of ascorbic acid.....	60
Table 3-2: Values for absorptivity for KMnO_4 from the literature and this study.....	64
Table 3-3: pH of $[\text{H}_2\text{A}]$ solutions before and after adding KMnO_4	67
Table 3-4: Observations on particle formation in H_2A after addition of KMnO_4 and leaving for 24 h.....	68
Table 3-5: Variation in colour for different $[\text{H}_2\text{A}]$ in presence of 40 and 100 ppm of KMnO_4	69
Table 3-7: Observations on particle formation in H_2A solutions after adding 4 and 1 ppm of Mn^{+2} after the solutions have been left for 24 h.....	81
Table 4-1: Values of net zero point of charge for some natural mineral and materials.....	92
Table 4-2: Summary of sorption isotherm parameters for all sorption experiment.....	111
Table 5-1: The concentrations in solution obtained after contact of deionised water and strontium chloride solutions with the sandstone. Calcium ions dominate. Iron was not detectable using FAAS.....	118
Table 5-2: Concentration of cations corrected for concentrations from deionised water experiments and resulting total CEC for the sandstone samples.....	120
Table 5-3 :Equations used to determine selectivity coefficient for different pairs of cations using Gaines and Thomas convection used in this study.....	123
Table 5-4: Gaines-Thomas selectivity coefficient values.....	124
Table 5-5: Gaines-Thomas selectivity coefficients from the literature for sandstones and sandy sediments.....	125

Table (6-1) Replication of samples.....	131
---	-----

List of appendices

Appendices chapter -2

Appendices chapter -3

Appendices chapter-4

Appendices chapter -5

Appendices chapter -6

1. Introduction

1.1 Background

On the Earth, groundwater is the largest resource of fresh water available (Freeze and Cherry, 1979). Many countries rely heavily on groundwater for their water supplies; therefore to understand the groundwater geochemistry and to protect groundwater quality are considered top priorities. Sandstone aquifers are a common type of aquifer worldwide, and a common type of sandstone aquifer are redbed continental sandstones of moderate intergranular permeability and fracture permeability (Barker and Tellam, 2006). About 25% of the total groundwater abstraction from licensed wells in the UK comes from the Permo-Triassic Sandstones (Allen et al. 1997).

Redbed sandstones provide a potentially significant amount of oxidative capacity from hematite (Fe_2O_3) grain coatings that could naturally attenuate either natural dissolved organic matter or dissolved organic contaminants coming from human activity. If we could quantify the oxidation process, we would be much more better able to estimate the natural attenuation of organic pollutants which took place in different areas like, rural areas where natural organic matter or farm wastes / sewage leakage to groundwater, urban and industrial leakage, beside landfill leachate leakages. Lovely and Anderson (2000) point out that generally sandstone aquifers often have a reddish colour due to the presence of iron oxide, while after contamination by organic carbon the colour of the sediment converts to grey or even white (bleaching), especially under higher temperatures. Heron et al. (1994) mention that oxides present in aquifer sediments can make significant potential contributions to natural attenuation and control of many kinds of contaminations. Canfield et al. (1993) point out that iron oxides in sediment free from sulphide minerals contribute about three-quarters of the oxidation of organic carbon in sediments world-wide. However the oxidation capacity of

sediment varies considerably from high to low oxidation capacity depending on the amount, types and characteristics of oxide grain coatings on sediment (Heron et al., 1994).

Furthermore oxic and anoxic conditions have also considerable effect on the oxidation rate of organic carbon in sediment. For instance, Heron et al. (1994) give anaerobic sediment examples where organic matter oxidation capacity ranges from 4 to 10 $\mu\text{mol/g}$, and examples of aerobic sediment with higher oxidation capacity ranging from 25 to 30 $\mu\text{mol/g}$, the difference being due to the absence of oxide species like Fe(III) and Mn(IV) oxides in the aquifer sediments under anoxic conditions (Heron et al., 1994).

Oxidization of dissolved organic carbon in aquifers converts possibly toxic or unwanted dissolved organic carbon in water to relatively non-toxic inorganic carbon forms like carbon dioxide CO_2 and bicarbonate. Oxidation, e.g. by oxides, can act to limit the expansion of organic contamination plumes in groundwater (Heron and Christensen, 1995; Tuccillo et al., 1999). However, oxidation of organic matter coupled with reductive dissolution of Mn and Fe (III) oxides creates concern because of significant rise of Fe^{++} and Mn^{++} concentrations (Thomas et al., 1994; Hiscock and Grischek, 2002). Moreover the oxidizing of organic compounds could play a significant role in diagenesis.

Redox reactions are important in a number of ways in natural aquatic environments. Firstly release of dissolved inorganics occurs, e.g. Mn^{++} which is more available to uptake by plants roots. Secondly oxidation of organic compounds increases humification. Thirdly many types of hazardous and toxic compounds which leach to aquatic environment as a result of man-made actions can be removed before affecting ecosystems (Bertino and Zepp, 1991).

Reeburgh (1983) pointed out that there is no full understanding of the mechanisms of oxidation of dissolved organic matter by sediment oxides, and though there has been much

progress since his paper there is still a basic lack of understanding. Therefore more studies are required.

1.2 Previous Research

1.2.1 Introduction

In this section a lot of previous studies will be mentioned that deal with the reactions that take place between oxides (synthetic and natural) and organic acids, especially ascorbic acid, and also mention the role of bacteria in this kind of reaction. Purpose is to provide some background for the later chapters.

1.4.2 Oxide Reduction in Sedimentary Aquifers

All kinds of soils and sediments have their own capacity to withstand changes in redox conditions, but this redox buffering capacity varies for each sediment according to the type, quantity and availability of electron donors and acceptors present in the system (Davranche and Bollinger, 2000). In subsurface anaerobic environments, solubility and quantity of iron oxides in sediments play a key role in determining the rate of organic carbon oxidation (Sulzberger et al. 1989).

Froelich et al. (1979) and Champ et al. (1979) report that oxygen is likely to be the first electron acceptor for organic carbon oxidation. Then under anoxic condition when oxygen has been used up, nitrate and Mn oxides are the next electron acceptors. After depletion of both of these, ferric oxides are the next electron acceptor followed by sulphate and finally CO₂ (methanogenesis).

Iron reduction often predominates in contaminated anoxic aquifers containing higher concentrations of dissolved organic carbon especially in the absence of NO₃ and Mn(IV) as terminal electron acceptors. However in the presence of these terminal electron acceptors less

iron reduction may take place (Lovely and Chapelle 1995, mentioned in Lovely and Anderson, 2000).

Lindsay (1991) cites a lot of studies to explain that when plants suffer from a deficiency of available iron, addition of organic matter (e.g. manure) compensates for this shortage of available iron to the plants. The addition corrects this lack by promoting reductive dissolution and making Fe more available to plants roots.

Under anaerobic conditions, iron oxides present in sediment are often considered the principle electron acceptors for many kinds of aliphatic and aromatic organic compounds, with the oxidation mediated by microorganisms (Lovely, 1991; Lohmayer et al., 2014). Heron and Christensen (1995) found that iron oxides in contaminated sediments collected from a landfill site in Denmark were completely removed by the effect of organic contamination over a period of 15 yr. Larsen et al. (2006) observed a sharp rise of $[\text{Fe}^{++}]$ in groundwater in pristine sandy aquifers in Denmark from below detection limit to around 0.5 mM that were coupled with an increase in alkalinity and depth. They interpret this as indicating oxidation of organic matter with the rate increasing with depth due to iron oxide reductive dissolution.

1.2.3 Lab Studies on Synthetic Minerals

There is three general mechanisms that explain the dissolution of iron oxides as listed below (Zinder et al., 1986 ; Suter et.al., 1991):

- 1-. Protonation mechanism (e.g. dissolution by inorganic acids like HCl)
- 2-reductive dissolution mechanisms (e.g. by ascorbic acid)
- 3-complexation mechanisms (e.g. by oxalic acid).

Suter et al.(1991) use ascorbic acid to reductively dissolve synthetic hematite, determining the rates of reduction. They proposed (Figure 1-1) that attachment of ascorbic acid to the surface of iron oxides led to the formation of FeIII/ascorbic acid surface complexes that allowed an electron to be transferred to the FeIII in the hematite. The resulting ascorbate radical was released and the now ferrous surface ion was released into solution. Suter et al. (1991) state that the reductive dissolution mechanism takes place quicker than other kinds of dissolution mechanism.

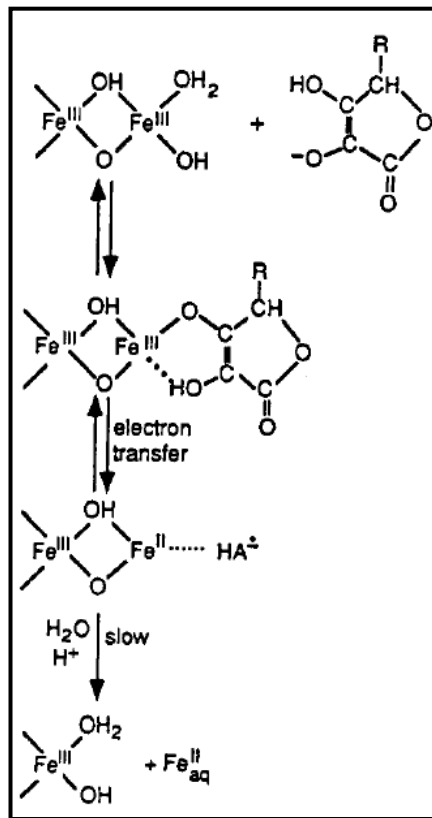


Figure (1-1) Suter et al.'s (1991) model for the reductive dissolution of synthetic hematite by ascorbic acid. $>\text{Fe}^{\text{III}}\text{OH}_2^+$ is the ferric surface site and $>\text{Fe}^{\text{III}}\text{HA}$ is the surface ascorbate complex.

Banwart et al. (1989) found that the rate of reduction dissolution of synthetic hematite by ascorbic acid at pH =3 increased around four times in presence of oxalate (from $1.48 \times 10^{-7} \text{ mol m}^{-2} \text{ h}^{-1}$ to $6 \times 10^{-7} \text{ mol m}^{-2} \text{ h}^{-1}$). On the other hand the rate of reductive dissolution dropped by about one order of magnitude (to $0.21 \times 10^{-7} \text{ mol m}^{-2} \text{ h}^{-1}$) if they used just oxalate alone.

The rate of reductive dissolution depends on the kinds of oxide minerals present. For instance, Larsen and Postma (2001) attempted to reductively dissolve three types of synthetic iron oxides namely poorly crystalline goethite, lepidocrocite and ferrihydrite using 10 mM of ascorbic acid. They found considerable variation in rate of dissolution, the least being with goethite (with an initial first order in Fe rate of $5.4 \times 10^{-6} \text{ s}^{-1}$), while the highest dissolution rate being for ferrihydrite (with an initial rate two orders of magnitude higher at $(7 \times 10^{-4} \text{ s}^{-1})$).

pH is often considered a master parameter in reductive dissolution of oxides. The rate of reductive dissolution varies considerably with change in pH. In general with decline in pH there is a rise of reductive dissolution rate in synthetic hematite dissolution facilitated by ascorbic acid. However at pH above six the reductive dissolution of hematite was not recognized by Suter et al. (1991). With a drop in pH, the solubility of ferric iron rises significantly and vice versa (Stumm and Morgan, 1996). Generally ferrous iron Fe^{++} oxidizes to ferric iron Fe^{+++} in the presence of oxygen, while not being affected by oxygen at pH values less than 4. In this case Fe^{++} still exists in solution even if exposed to oxic conditions. This means that ferrous ion is more stable in acidic conditions (Weber et al., 2006).

1.2.4 Lab Studies on Natural Sediment

Larsen et al. (2006) used ascorbic acid to reductively dissolve natural iron oxides present in sandy aquifer samples collected from Denmark and found that there was more than three orders of magnitude variation in rate of dissolution of iron oxide (first order rate constants of 1×10^{-3} to $7 \times 10^{-6} \text{ s}^{-1}$). They interpreted this as indicating the wide range of reactivity of natural iron oxides compared synthetic iron oxides prepared in the lab. Larsen et al. (2006) also studied reductive dissolution of natural hematite coated sandy sediment collected from a pristine aquifer using HCl and ascorbic acid in separate experiments. They found that the

amount of ferrous iron released using HCl acid was about 2 times less than the amount released using ascorbic acid.

1.2.5 Studies of the Roles of Bacteria in the Reductive Dissolution of Oxides

Taylor et al. (1997) studied the effect of iron bacteria on the redox reactions of groundwater samples collected from a contaminated aquifer in New York. They found that the presence of iron reducing bacteria (*Shewanella sp.*) catalyses reductive dissolution of iron hydroxide in these sediments, and this leads to the rise of Fe^{++} concentration in groundwater (8 to 18 mg/l).

Lovely et al. (1987) note at the same time as the reduction of oxides mediated by bacteria, the bacteria also significantly contributed to the oxidation of dissolved aromatic organic carbon in contamination aquifers.

Wahid and Kamalam (1993) also studied the ability of soil bacteria to convert crystalline iron oxide to amorphous iron oxides and release Fe^{++} into soil solution. After carrying out the experiments under sterilized and unsterilized conditions, they found soil irradiated for 2, 6 and 20 days released about 25, 40 and 80 $\mu\text{g/g}$ of Fe respectively, while the Fe released by unsterilized soils was significantly higher at about 500, 5000 and 9000 $\mu\text{g/g}$. Ferrous iron release reached around 3 orders of magnitude greater from unsterilized soils.

Petruncice et al. (2005) carried out column experiments on sandstone collected from Fredericton, Canada, to investigate the effect of bank infiltration on the oxidation of high dissolve organic carbon (DOC). In terms of reaction between DOC and MnO_2 oxides, they found unsterilized columns released significantly more Mn^{++} than sterilized columns.

Munch and Ottow (1980) and Ottow (1981) suggest that both anaerobic bacteria and aerobic bacteria are able to mediate reductive dissolution of iron oxide but anaerobic bacteria are more active in reductive dissolution in soil.

The degree of crystallinity of Fe (III) oxide in the soil and sediment may also have a significant effect on the rate of reductive dissolution of oxides when mediated by bacteria. For instance, Wahid and Kamalam (1993) carried out a lab experiment to examine two kinds of wetland soils, the first dominated by crystalline iron oxides and the second dominated by amorphous iron oxides. They found that the soil rich in crystalline iron oxide did not participate significantly in reductive dissolution by soil bacteria while the soil containing predominantly amorphous iron oxide did.

Mn (IV) and Fe oxide reduction can take place with bacterial mediation (Lovley et al., 2004) and without (abiotic reduction) (Ehrlich, 1981) but the first is more prevalent in the natural environment. Iron oxides are able to oxidize aromatic organic carbons without microorganism mediation (McBride, 1987; Stone and Morgan, 1987) and with microorganism mediation (Lovely, 1991). The rate of oxidation of organic matter is higher when the interaction between oxides and organic matter is mediated by bacteria (Lovely, 1991). Iron oxide reduction mediation by microorganisms plays an important role not just in natural environments but also in applied industrial systems. For example Lee et al. (1999) were able to remove about 45% of iron oxide from kaolin clay by injecting bacteria with 5%(w/w) of glucose (a reducing agent), that led to a decline in the redness intensity and increase of whiteness colour of kaolin in comparison with the same experiment but without bacteria. Some researchers mention that microorganisms are able to reductively dissolve both low and high crystallinity iron oxide (Roden and Zachara, 1996; Neal et al., 2003; Hansel et al., 2004; Gonzalez-Gil et al., 2005). While other researchers point out that the biotic reduction only took place at a considerable rate in the cases of amorphous and poor crystalline iron oxides rather than highly crystalline iron oxides (Lovley and Phillips, 1986; Glasauer et al., 2003). This means that up to date there is no consensus about the effect of the degree of iron oxide crystallinity on reductive mediation by microorganisms.

Larsen and Postma (2001) studied the biotic reduction rate of groups of synthetic iron oxide minerals by ascorbic acid. They found an increase in the following sequence from low to high reduction rate: hematite, then goethite, then lepidocrocite and finally ferrihydrite.

Microorganism attachment on the surface of iron oxides facilitates biotic reduction of these oxides in the sediment. This process is considered a key mechanism in the biotic reduction (Lovley et al., 2004). Moreover Lovley (1987) and Nealson and Saffarini (1994) point out that without this direct attachment of bacteria the microbial reduction of oxides might not occur.

1.2.6 Oxidation of dissolved organic carbon

Oxidizing of organic matter occur in many environments for example in submersible soil the reduction of ferric iron and Mn oxides occurs under anoxic conditions and that leads to the oxidizing of organic matter in for example paddy fields (Ponnamperuma,1972).

Lee and Bennett (1998) found high concentrations of ferrous iron Fe^{++} and Mn^{++} in shallow glacial aquifers in one site at Cape Cod, Massachusetts, USA, reaching up to 13 and 7 mg/l respectively. These high concentrations of metal result from the involvement of microorganisms in reductive dissolution of manganese and iron oxides in glacial outwash sediments as a result of infiltration of sewage effluent into this aquifer. Biotic oxidation of the organic carbon in this sewage water led to a drop of DOC concentration as organic carbon was converted to inorganic carbon. This chemical process was considered one of the defences against the spread of contamination in the aquifer.

1.2.7 The Effect of Mineral Properties

There are many properties of iron oxides that have a significant effect on its stability and dissolution, including specific surface area. For instance hematite has less specific surface

area by about 10 fold than ferrihydrite which means the hematite is more stable and will be less easy to dissolve than ferrihydrite in nature (Cornell and Schwertmann, 2003). In general there is a decline in rate of reductive dissolution of iron oxides with decrease in the specific surface area of oxides (Larsen et al., 2006). However, Larsen et al. (2006) suggest that both natural and artificial iron oxide reductive dissolution takes place at the same order of magnitude in spite of the fact that natural iron oxide is more variable in terms of its surface area and degrees of crystallinity. Natural iron oxides contain mixtures of oxides with significant variations in their degree of crystallization from excellent crystallinity and low reactivity to very poorly crystalline or amorphous iron oxides (Larsen et.al, 2006). As mentioned above, crystallinity is thought to be important. Munch and Ottow (1983) also report the degree of iron oxide crystallinity affects dissolution rates. For example crystalline iron oxides like hematite have a lower dissolution rate in comparison with more poorly crystalline (amorphous) iron oxides like ferrihydrite.

In aquatic environments with increase of dissolved organic matter (DOM) there is often an increase of metal solubility and mobility (Blaser, 1994; Piccolo, 1994; Zsolnay, 1996). Also the presence of ferrous iron in solution can be more effective in chemical reduction of Mn oxides than even biotic reduction (Nealson, and Myers ,1992 cited in Benelli, 2015).

Levy et.al (1992) point out one of the most vital sink in sediment for many dissolved metals are Mn and iron oxides and that depend on redox potential and pH conditions. In addition to oxidization of various organic pollutants, these oxides also have some ability to absorb dissolved metals and metalloids. For instance Mulvaney et al. (1988) point out that hematite has a strong ability to sorb dissolved ferrous iron at pHs higher than 5. Another situation where oxidation of organic carbon by oxides is important therefore is in the release of arsenic under reducing conditions occurring in young sedimentary aquifers for example in Bangladesh and West Bengal. In this case low pH favours sorption as As will usually be

present as an anion. Here microorganisms play a significant role according to Bose and Sharma (2002). The release of As poses a major health issue for those people who use groundwater for drinking.

1.3 Aim

The primary aim of this research is to determine the capacity and mechanism of oxides present in redbed sandstone to oxidize dissolved organic carbon. The secondary aim is to determine the possibility of using the results from previous experiments carried out on synthetic iron oxides in predicting the oxidation of dissolved organic matter in the much more mineralogically complex system of the sandstones.

The sandstone chosen for the research was from the Triassic Sandstone of the English Midlands. This has a coating of hematite and also contains manganese oxides and clays. The sandstone used has no carbonate cement.

Ascorbic acid was chosen to represent dissolved organic matter (DOM). It is well known that natural dissolved organic matter can be extremely complex in its chemical composition and difficult to analyze, therefore an alternative simple organic carbon compound (ascorbic acid) was chosen to study some of the mechanisms involved. Ascorbic acid can

be relatively easy to analyze and therefore monitor during experiments. It is also cheap, non-hazardous and environmental friendly. Perhaps most important, there have been previous studies (Suter et al., 1991; Banwart et al., 1989; Afonsa et al., 1990) that have shown that synthetic hematite can oxidize ascorbic acid suggesting that it is possible that natural hematite may be able to do so as well. If there is agreement between the behaviour of synthetic and natural hematite then lab studies could be used with more confidence in predicting behaviour in field systems.

This study focuses on determining the rate of reductive dissolution of Mn and Fe oxides in sandstone, and concurrently determining the rate of the oxidation of ascorbic acid in aqueous solution. Moreover the project involves a study of the effect of microorganisms on the rates of reduction of oxides and oxidation of organic carbon by comparing the results of experiments completed under heat –treated (Abiotic) and unsterilized conditions. The experimental procedure has been used to produce data from which the kinetics of the reactions involved are being determined, and these will be used to deduce a conceptual model of the mechanisms involved in the reactions.

This approach looks only at the reductive dissolution mechanism associated with the functional groups of ascorbic acid. Future experiments would then look at the roles of other functional groups and also consider the role of complexation (e.g. by oxalic acid; Suter et al., 1991).

1.4 Approach

The basic approach has been to use batch experimentation with disaggregated sandstone and ascorbic acid solutions.

First work was to undertake a wide range of preliminary experiments to determine under what conditions ascorbic acid reacts with the sandstone. Trials were made under various temperatures, concentrations, times, shaking rates and filtering until reliable results under low temperature were achieved.

Next a method was developed for ascorbic acid analysis in the presence of Mn and Fe.

Next the sorption of ascorbic acid to the sandstone was investigated with the aim of quantifying it.

Next a series of ion exchange experiments were completed. When Fe and Mn are released by reductive dissolution of sandstone oxides the Fe^{+2} and Mn^{+2} released will be taken up by clays and oxides in the sandstone. So this had to be quantified to enable corrections to be made to the final batch experiment results.

Finally the final batch experiments were undertaken under anaerobic conditions, analysed using the ascorbic acid method developed earlier and processed using the ion exchange results. In addition, an MSc project (Benelli, 2015) was helped to be supervised who repeated some of the batch experiments under heat –treated conditions for comparison with the unsterilized batch experiments.

1.5 Thesis Format

Chapter 2 outlines a set of preliminary experiments designed to determine whether ascorbic acid reacts with the English sandstone chosen, what the approximate rates of dissolution are, the effects of temperature and concentration on the dissolution, and the most appropriate experimental procedures.

Chapter 3 develops a method for the analysis of ascorbic acid and investigates the stability of ascorbic acid.

Chapter 4 attempts to quantify the sorption of ascorbic acid onto the sandstone.

Chapter 5 quantifies the ion exchange properties of the sandstone, specially the exchanges of Fe and Mn.

Chapter 6 report on the detailed anaerobic batch experiments under unsterilized and heat – treated conditions using results from previous chapters.

Chapter 7 is the conclusion and provides recommendations for future work.

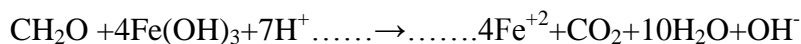
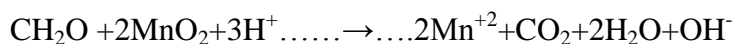
2. Preliminary experiments

2.1 Introduction

This chapter reports on preliminary experiments on the reductive dissolution of oxides in sandstone by ascorbic acid (H_2A), under different conditions, including: rock water ratio; H_2A concentration; pH; redox conditions; and different procedural techniques. The aim of the experiments was to provide the data needed to design the final experiments that would be necessary to achieve the aim laid out in Chapter 1.

There are many potential impacts of the reduction of iron and manganese hydroxides in natural environments. For example, Reddy and Delaune (2008) point out one of these effects of reduction of oxides in a wetland soil was a significant increase in dissolved Mn^{++} and ferrous iron (Fe^{++}) concentration in pore waters. Presence and absence of oxygen (aerobic and anaerobic condition) also effect on the reduction of these oxides in sediment; for instance Weng et al. (2007) studied the groundwater chemistry in the Hang jia-Hu-plain aquifer in China and found that there is a decrease of dissolved oxygen over depth that is associated with an increase of Mn^{++} and Fe^{++} concentrations. The $[\text{Mn}]$ increased from 0.03 to 3.87 ppm, and $[\text{Fe}^{++}]$ increased from 0 and 8 ppm over depth in this aquifer.

Lovely and Phillips (1998) suggest that reductive dissolution reactions for oxides in aquifers occurs as follows



where CH_2O (formaldehyde) represents the organic matter (organic carbon), and MnO_2 and $\text{Fe}(\text{OH})_3$ represent the solid oxide phases coating sediment grains. The reduction reactions are

mediated by bacteria. The reductive dissolution of Mn oxide occurs before the iron oxide reduction in the absence of oxygen and nitrate as a terminal electron acceptor (TEAP).

The aims of the work described in this chapter were to:

- i. determine if and under what conditions H_2A will react with the sandstone oxides;
- ii. determine what effects experimental methods have on the results so as to help to plan the final more quantitative experimental work.

No H_2A analysis was undertaken, as the analytical method required developing and it was necessary first to find out roughly what reaction happened between sandstone and ascorbic acid. So experiments looked mainly at determining Fe and Mn concentrations. An introduction to the properties of ascorbic acid will be given in Chapter 3.

The experiments concentrated on high H_2A concentration, elevated temperature experiments as these yielded higher concentrations of Fe and Mn more quickly.

As experience was gained, more realistic conditions were investigated, i.e. lower concentrations of H_2A and lower temperatures.

2.2 Materials and Analysis

2.2.1 Ascorbic Acid (H_2A)

Ascorbic acid has been chosen to represent dissolved organic matter to simulate the reaction between oxides in sandstone and dissolved organic carbon in terms of reductive dissolution oxides, as explained in Chapter 1. The ascorbic acid was obtained from Sigma-Aldrich Company Ltd., $\geq 99.0\%$.

2.2.2 Sandstone

All experiments were carried out using red sandstone samples collected from an outcrop located at Quatt in Worcestershire (national reference grid SO75528823)(Batty, 2016). The sandstone was chosen because it is typical of the English Midlands in most ways but because it is from shallow depth it has no carbonate cement. This avoids problems with much dissolution of carbonates when the ascorbic acid is added and means that the rock can be prepared for batch experiments easily as it is friable. It was used for other experimental work by Batty (2016) who describes the sandstone in detail.

Batty (2016) found the sandstone consists mainly of quartz (40-50% by volume) and feldspar (mainly alkali; 15-20%), but with lithic fragments, mica, and clay minerals. All grains are coated in hematite with some Mn oxides. Porosity is about 20% (Batty, 2016).

Most of the oxide in the red sandstone is hematite (Plant et al., 1999), but there will also be a range of other Fe oxide phases, including possibly goethite and magnetite. In addition there will be a range of Mn oxides, including forms of MnO_2 , mixed oxidation state Mn oxides and hydroxides. Fe and Mn will also occur in lithic fragments and biotite. So the sandstone is a complex mix of minerals. These minerals cannot easily be separated out for experimentation. Even identifying the exact mineral phases in many cases is challenging as they are present in amounts that are too small for XRD to resolve in the background of other minerals present. Another technique to find out where Fe and Mn are present in the sandstone would be microprobe analysis, but this was not available and would have in anycase still required probably optical identification of the phases concerned and this would be difficult. Often Mn oxides appear to be more reactive than Fe oxides, but Mn oxides are present in smaller concentrations than Fe oxides (Plant et al., 1999),so the latter may be more important in oxidation .The sandstone is friable and was lightly disaggregated for experimental work

following the procedure of Batty (2016). This was initial breaking of the rock into about centimetre cubes and then carefully breaking these pieces up using a mortar and pestle. The resulting separate grains were thoroughly mixed by hand before use.

2.2.3 Analysis for Fe and Mn⁺⁺

Concentration of Fe and Mn⁺⁺ were determined using flame atomic absorption spectroscopy (FAAS) in the Public Health laboratory of the University of Birmingham. Even at low concentrations (< 1ppm), if repeatability exceeded 7% the value was excluded from the results, and the analysis repeated again until a better level of precision was obtained.

The iron measured using the FAAS method represents the total iron, which equals the sum of ferrous iron Fe(II) and ferric iron Fe(III). However, most Fe is expected to be FeII. There will be some FeIII released due to dissolution at low pH, but this is small in comparison with the Fe released when ascorbic acid is present, strongly suggesting that reductive dissolution is occurring and the product will be FeII. Any FeIII present will be converted quickly to FeII by ascorbic acid. Though the Pt electrode E_H values cannot be used as thermodynamic valid values, their low values (<130 mV; see Chapter 6), also suggests also that the predominant form of Fe is FeII. For the experiments in aerobic conditions there may be some oxidation of FeII to FeIII by atmospheric oxygen and a significant amount of the FeIII produced in this way would be stable in the lowest pH experiments. However, in the main anaerobic experiments the only likely oxidant is MnO₂, and this would result in FeIII oxide precipitation at the pHs involved, or FeIII would be reduced by the ascorbic acid, and this possibility has been taken into account in the processing of the results of the final experiments. Though it would have been interesting to see whether there is FeII present, the ferrozine method (Viollier et al., 2000) is labour intensive and the results would not have helped in the interpretation, as any FeIII identified could have come from either MnO₂ reduction or non-reductive dissolution of hematite.

Before undertaking experiments on sandstone / H_2A interactions, it is necessary to determine if the method used for determination of Fe and Mn, flame atomic absorption spectrometry (FAAS), is affected by high concentrations of H_2A .

To do this, Fe and Mn^{++} standards were made up in deionised water (DIW) and 10 mM H_2A solutions, and then analysed using FAAS. The results are given in Figures 2.1, 2.2 and appendix 2.1, which indicate that there are at most only minor effects of the presence of 10mM of ascorbic acid on the absorption values for Fe and Mn. No account was therefore taken of H_2A concentration in the analysis. In the great % of experiments undertaken in the research the H_2A concentrations were less than 0.6 mM.

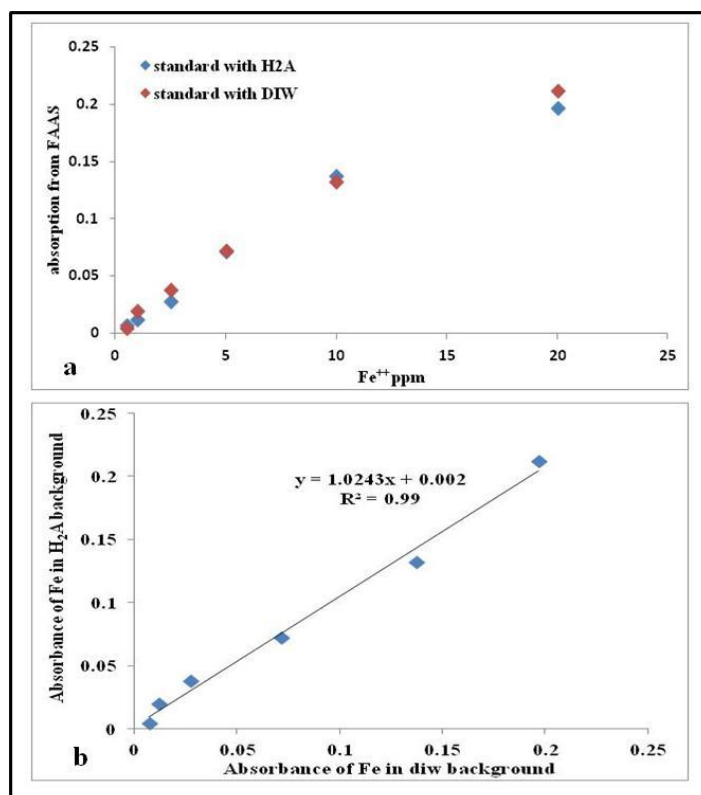


Figure 2-1: Comparison of the absorption of various concentrations of a) Fe prepared in DIW and b) in 10 Mm ascorbic acid solution.

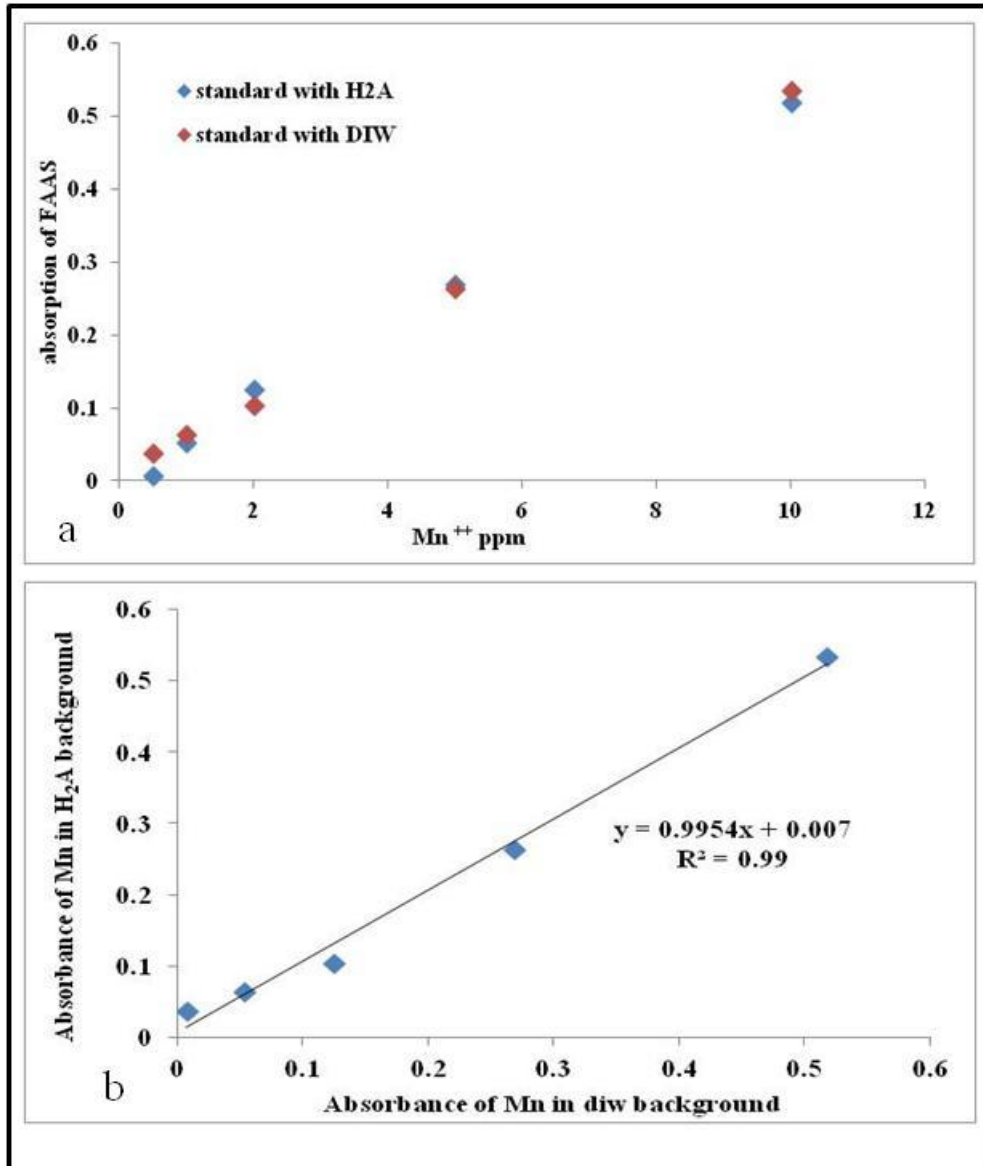


Figure 2-2: Comparison of the absorption of various concentrations of a) Mn⁺⁺ prepared in DIW and b) in 10 Mm ascorbic acid solution.

2. 3. High [H₂A], generally high temperature experiments

2.3.1 Introduction

Initial experiments, carried out using 1 g of sandstone and 500 ml of 10 mM H₂A (initial rock/water ratio = 0.002 g/ml) at lab temperature periodically hand-stirred, indicated no FAAS-detectable Fe or Mn was released over a period of time up to 72 hours.

As results, the experiments were repeated using a greater mass of sandstone (10 g), and at a higher temperature. These experiments are described in this section (Section 2.3). In later sections lower temperature experiments will be described.

2.3.2 Will high $[H_2A]$ reduce hematite at high temperatures?

The experiments were done using a mass of sandstone of 10 g and in a water bath at a temperature of 42 °C (Appendix 2.2). The volume of H_2A solution was 500 ml, making the rock/water ratio 0.02 g/ml initially (each sample extracted was of 5 ml). Again, the reaction vessel was periodically hand stirred.

The results are shown in Figure 2.3. It is clear from Figure 2.3 that there is a linear increase of iron concentration with time, reaching 3.92 mg/l after 195 hours of reaction at pH around 3. From Figure 2.3 a reaction rate constant (k) can be calculated of about 0.2×10^{-7} mol/g/h. The approximately 15% drop in volume during the experiment due to the taking of the samples looks like to have no significant effect on the rate. It is concluded that H_2A is capable of reductively dissolving hematite from English Triassic sandstone samples at 42 °C in this rock water ratio.

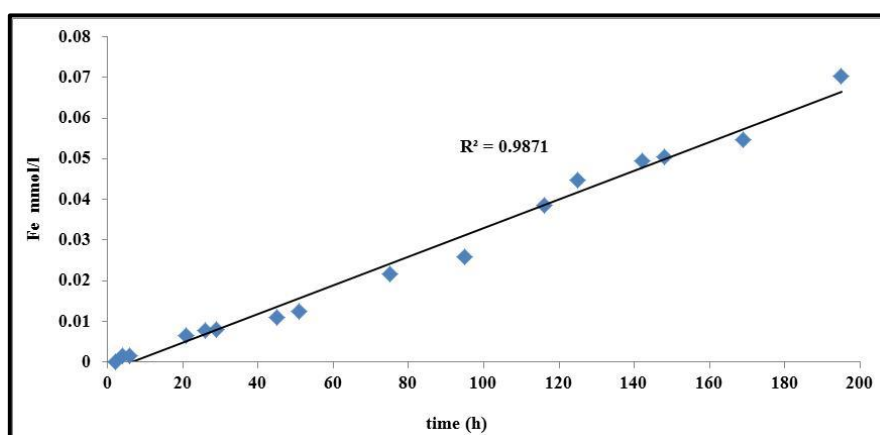


Figure 2-3: The relationship between the concentration of Fe and time of contact of 10 g sandstone and 500 ml of 10 mM ascorbic acid solution at 42 °C.

2.3.3 Reductive dissolution dependence on temperature

The main aim of this experiment was to find out the effect of temperature on the rate of iron and Mn oxide hydroxide reductive dissolution in red sandstone. In addition, the effect of storage temperature was also investigated.

500 ml of 10 mM ascorbic acid was added to each of four beakers containing 1 g of disaggregated sandstone. Each beaker was put in a water bath under four different temperatures (50, 60, 75 and 90 °C), and samples were collected at intervals of 1.5 hours after an initial 24 hours of reaction time. Each sample was split into two subsamples, one stored under lab temperature and the second at 4 °C.

The concentration / time results are presented in Figure 2.4 and Appendix 2.3. Figure 2.5 shows that the increase of temperature considerably enhanced the rate of reductive dissolution of ferric iron.

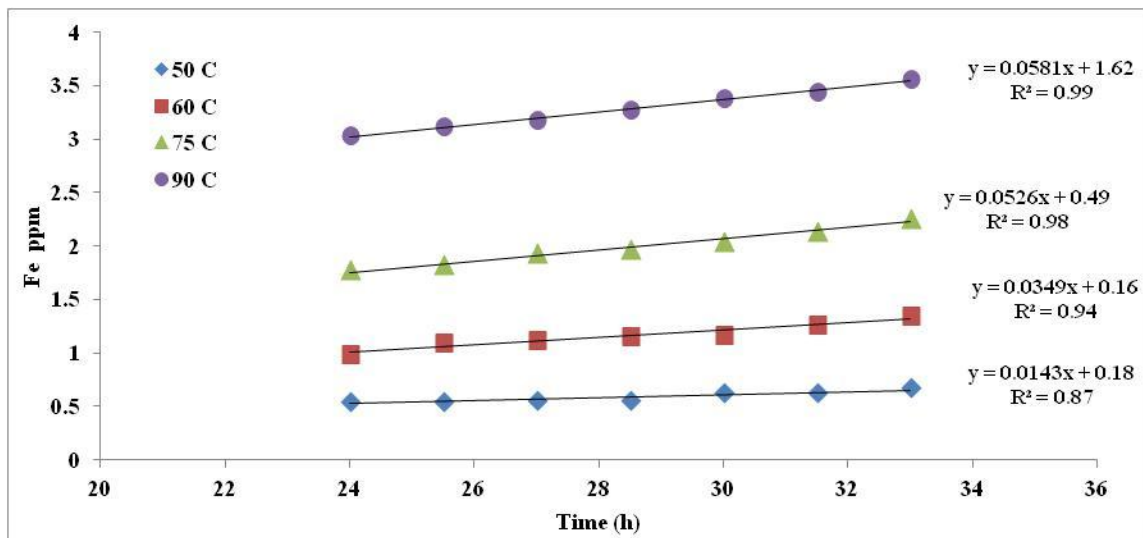


Figure 2-4: The concentration of Fe released after 24 hours of contact of 1g of sandstone with 500 ml of 10 mM ascorbic acid solution at pH = 3.

Figure 2.5 shows plots of Fe and Mn concentrations when the samples were stored at lab temperature against the Fe and Mn concentrations when the samples were stored at 4 °C (in fridge).

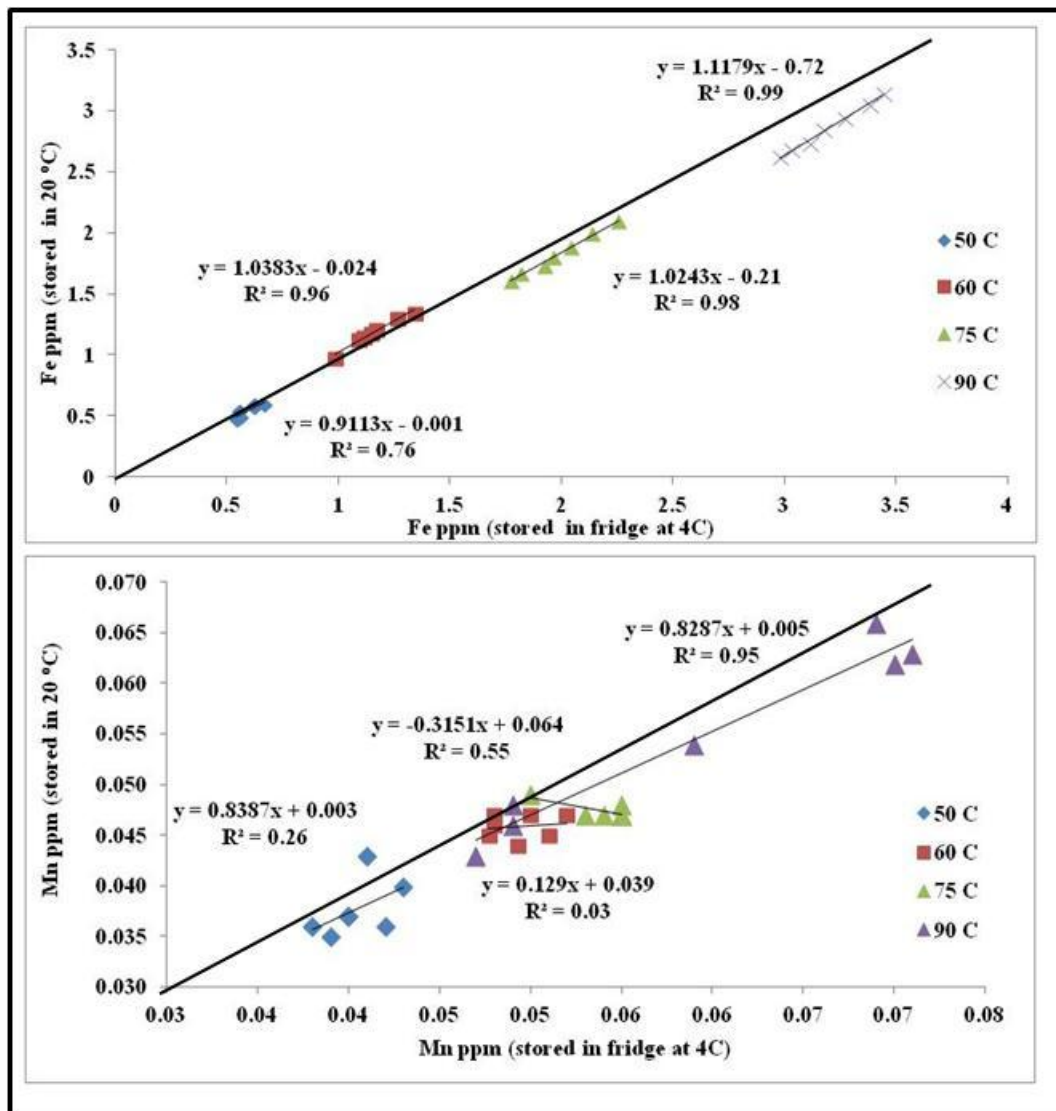


Figure 2-5. Plot of Fe and Mn concentration for samples stored at lab temperature against the Fe and Mn for samples stored in fridge at 4°C. Black lines in A and B is 1:1 line.

At 50 and 60°C there is no significant effect of sample storage conditions on concentration of Fe and Mn. However the Mn relationship was weak at 50 and 60 C. This may be due to the very low concentration of Mn that was close to detection limit for FAAS. Above 60°C the concentrations are underestimated (about 13%) if the samples are stored at 20°C.

The slope of each line in Figure 2.4 represents an apparent rate constant k for the experiment under the conditions run for Fe. The rate constant possibly appears to be a zero order rate constant in Fe and Mn because the concentrations of Fe are still very low even after over 24 hours of reaction time, i.e. the reaction is still far from equilibrium.

The Arrhenius equation has been used to allow determination of rate constant (k) as a function of time. The Arrhenius equation is:

$$k = A \exp[-E_a/(RT)]$$

where A is the pre-exponential factor and E_a is the activation energy. k was the rate constant and T represents absolute temperature. R represents gas constant.

On a plot of $\ln(K)$ against temperature $1/T$, see Figure 2.6, the slope represents $-E_a/R$, and the intercept represents $\ln A$. Though Figure 2.6 has an approximately linear relationship, but it is not quite linear may be indicating a change in conditions as temperature rises. From the plot, $A = 0.031 \text{ mol/g/h}$ and $E_a = 30.7 \text{ kJ/mol}$. At 10°C the about temperature of shallow UK groundwaters, the predicted k would be $6.7 \times 10^{-8} \text{ mol/g/h}$.

Torres et al. (1989) report that a drop in pH and a rise in temperature leads to an increase number of reactive sites on the hematite surface and a significant acceleration of the dissolution. However, they did not use ascorbic acid in their experiments.

Figure 2.7 shows the Mn released during the same experiments. Mn^{+2} release was significant lower than for Fe for this water rock ratio and close to detection limits. The release of Mn^{++} happened before 24 hours of contact time, with insignificant increase with time after 24 hours.

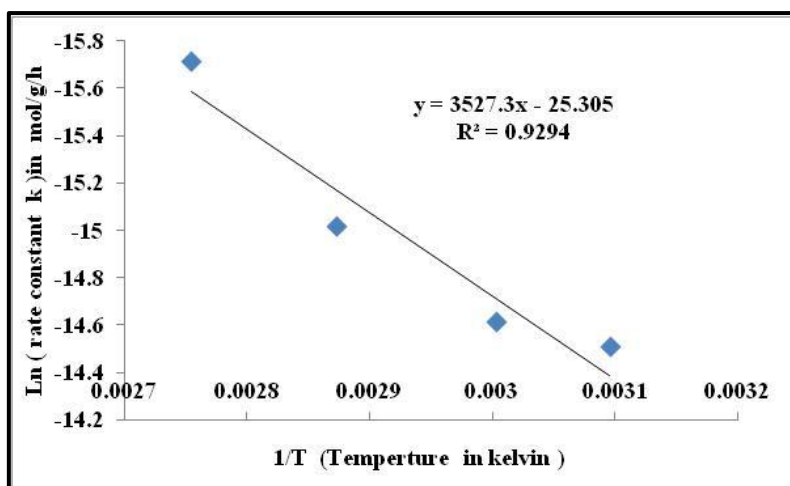


Figure 2-6: A linearised Arrhenius relationship plot for the apparent rate constant of the experiments shown in Figure 2.4.

It is probable that the MnO_2 content of the rock is small and effectively all of the Mn was dissolved out. In general there is a slight increase in concentration with temperature suggesting that perhaps a small amount of Mn is released from sources other than MnO_2 , e.g. possibly from silicates.

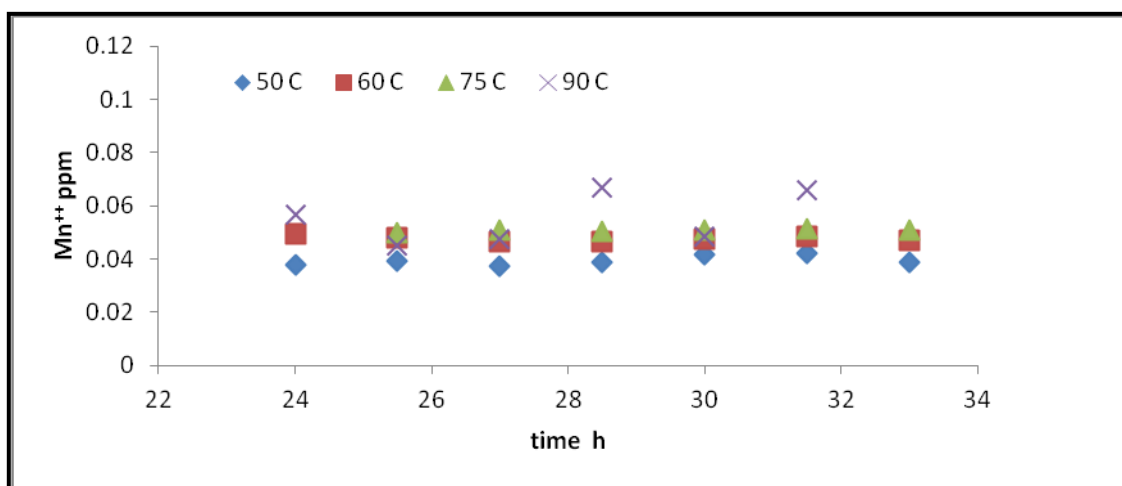


Figure 2-7: The concentration of Mn released after 24 h reaction under four different temperatures, using 10 mM ascorbic acid at pH =3.

2.3.4 Reductive dissolution dependence on H_2A concentrations at high temperature

The aim of this experiment was to find out the effect of ascorbic acid concentration on reductive dissolution at constant temperature (60 °C). To achieve this goal, 1 g of red sandstone was put in each of 3 beakers. 500 ml of 75, 50 and 25 mM H_2A was added to each beaker, and all beakers put in a water bath at 60 °C. There is slight increase of pH with decrease of concentration of ascorbic acid, the pH of these solutions being 1.8, 1.95 and 2.04 for 75, 50 and 25 mM H_2A respectively. Half the samples were filtered before analysis using a 0.45 micron filter, and half were analysed unfiltered. It was found that filtering made no significant difference (Figure 2.8). Details are given in Appendix 2.4.

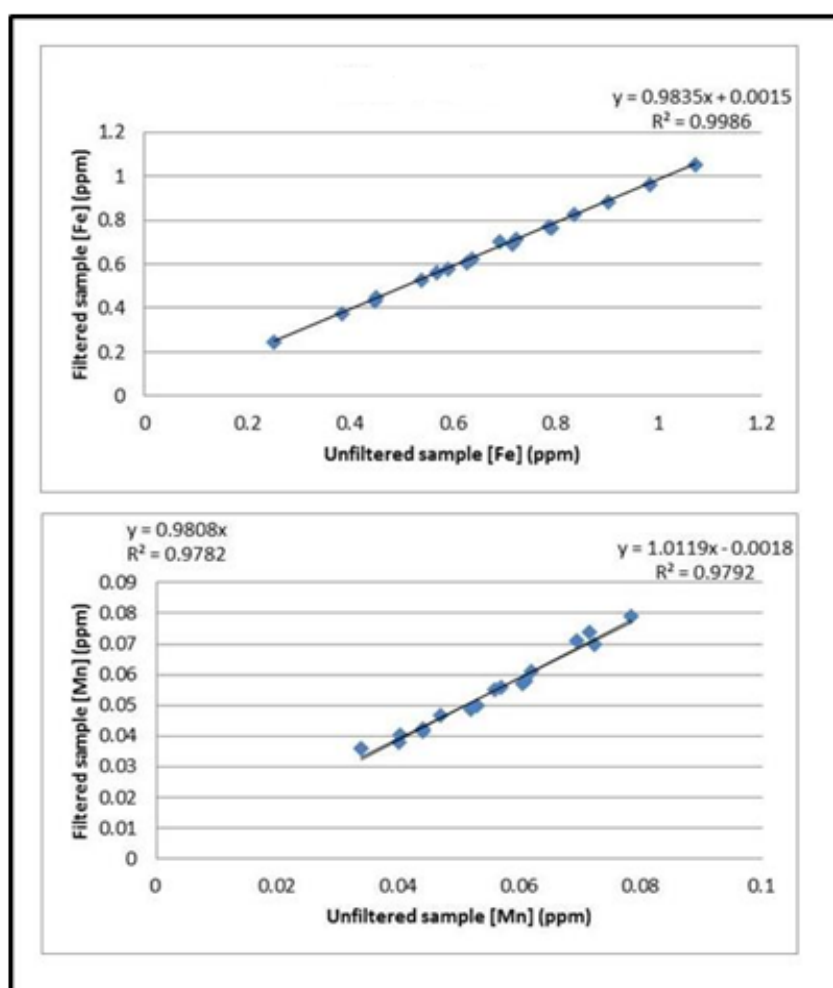


Figure 2-8: The relationship between filtered (0.45µm) sample concentrations and unfiltered sample concentrations at 60 °C.

Figure 2.9 shows the results of this experiment. It is clear from Figure 2.9 that an increase in concentration of ascorbic acid increases the total amount of reductive dissolution of Fe oxides. Joseph et al. (1996) also found that increasing the amount of ascorbic acid (from 10 to 80mM), but in presence of EDTA and citric acid too, also increased the iron release into solution from hematite during 8 h of batch experiment.

However, the rate of increase of Fe concentration with time is approximately constant. The difference between the experiments at different concentrations is the intercept at time = 0. The simplest explanation is that this is due to the different initial pH, lower pHs resulting in greater initial solution (Figure 2.10).

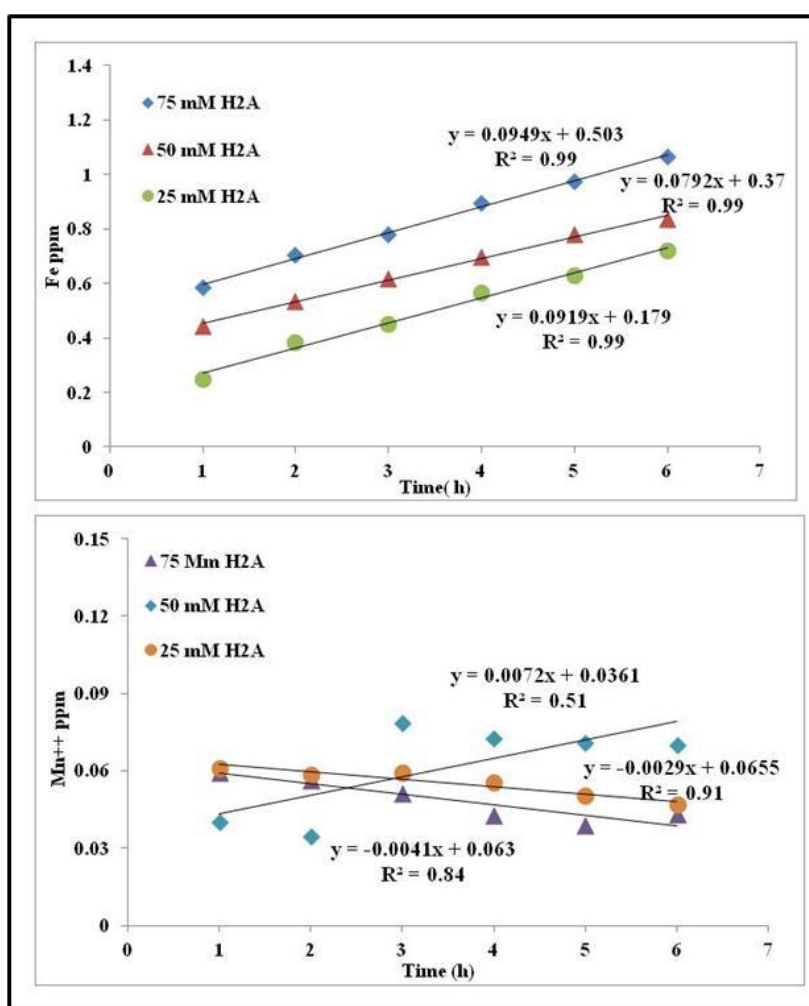


Figure 2-9: The amount of Fe and Mn released from 1 g of sandstone by 500 ml of 75, 50 and 25 mM H₂A at 60 °C.

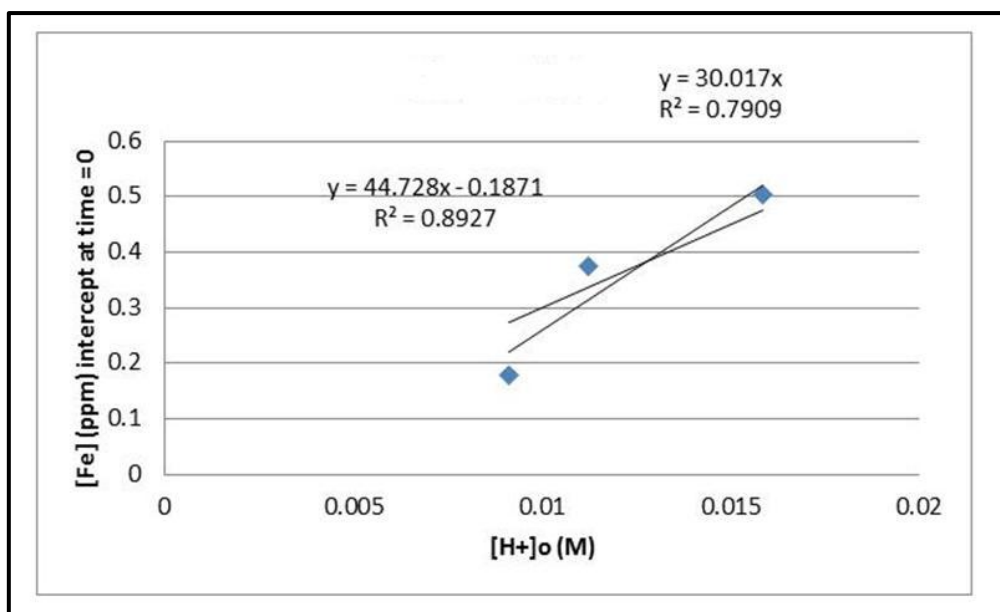


Figure 2-10: The relationship between the Fe concentration extrapolated to time = 0 and initial hydrogen ion concentration in sandstone / H₂A (75, 50, 25 mM) experiments at 60 °C.

Mn concentrations remain approximately constant (Figure 2.9) or even have a slight decrease. They have reached their maximum concentration within one hour of contact with the sandstone. This is consistent with the data of the previous experiment (Figure 2.7).

2.3.5 Reductive dissolution at lower H₂A concentrations at lower and high temperatures

Experiments were carried out using 10 times lower H₂A concentrations than the experiments described in Section 2.3.4 under two temperatures (20 and 80 °C), but for longer times of reaction. 1 g masses of sandstone were reacted with 500 ml of 1 and 0.75 mM H₂A (rock water ratio = 0.002 g/ml) at 20 and 80° C.

Figure 2.11 and appendix 2.5 shows the results. No Fe measurable by FAAS was released in the 20 °C experiments. (No Fe is released by experiments repeated using DIW also (though the pHs for these experiments would have been different)). At 80 °C, the rise in Fe

concentrations appears to slow down for both the 0.75 and 1 mM H_2A solutions. However, this cannot be explained by lack of H_2A as the amount of Fe released is much smaller than the initial H_2A mass. It may therefore be that the concentrations increase beyond 72 hours. The 1 mM solutions have significantly greater Fe concentrations. This could be because of a difference in the initial pH values. These pH were 3.79 and 4.07 for 1 and 0.75 of mM H_2A . However, could also be due to dependence of rate on H_2A concentration.

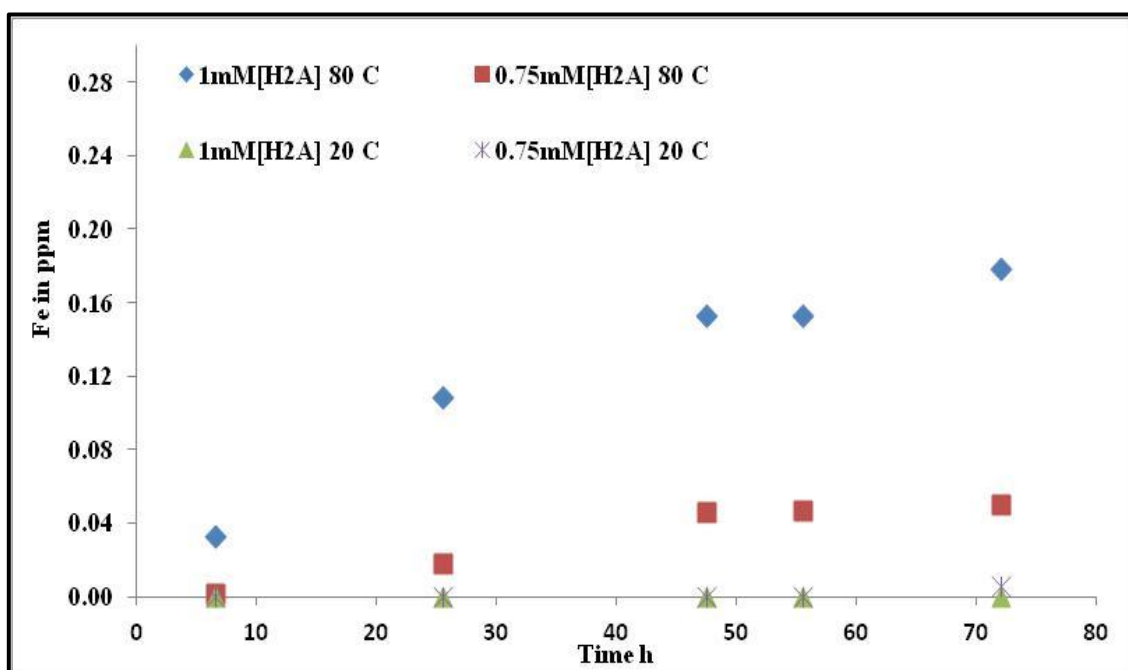


Figure 2-11: The concentration of Fe released from 1 g mass sandstone using 500 ml of 1 and 0.75 mM H_2A at 20 and 80 °C.

2.3.6 How does reductive dissolution by high concentration H_2A change with sandstone mass at high temperatures over long time interactions

The purpose of this experiment was to determine if the oxide dissolution rate changed significantly with time and as the total amount of dissolved oxide got close to the total amount of oxide on the sandstone.

1, 5 and 10 g of sandstone and 500 ml of 10 mM H_2A (pH = 3.21) solution were used at 80 °C and the reaction monitored by taking samples over the period 163 to 400 hours (Appendix 2.6 a & b). No shaking was undertaken and the reaction vessels were open to the atmosphere, i.e. potentially aerobic. The samples were analysed unfiltered and also after passed through a 0.2 micron filter. There was no effect of filtration on Fe or Mn concentrations as shown in Figure 2.12.

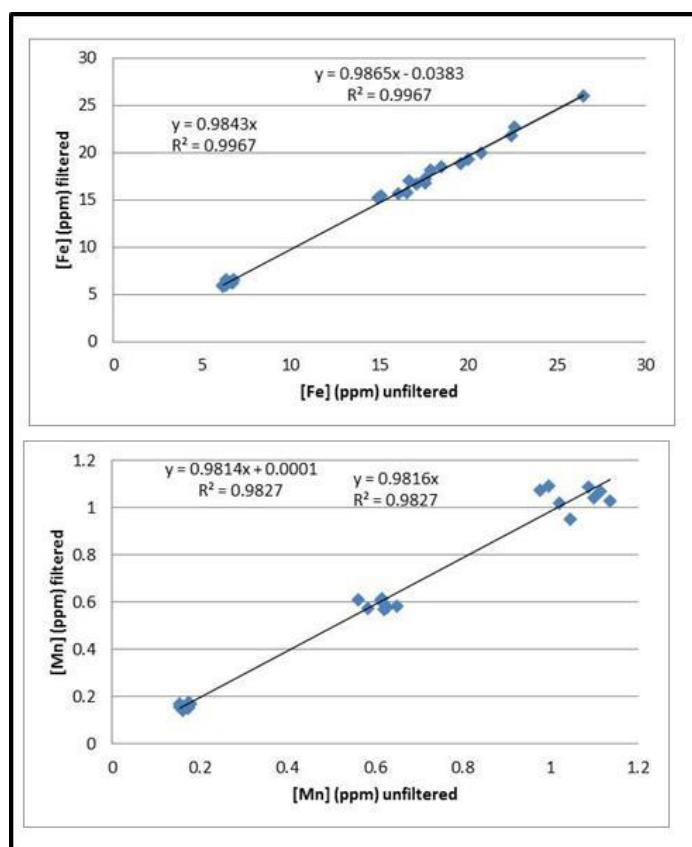


Figure 2-12: The effect of filtration through 0.2 µm filters

As shown in Figure 2.13 the concentrations increase with mass of sandstone used. The concentrations increase with time and the rock is still not changed to white colour and the moles of Fe removed are much less than the moles of H_2A available. So there is still oxide and reductant available. The mass released from 5 g of sandstone is only 2.6 times greater than the mass released from 1 g of sandstone. It is concluded that the reductive dissolution is

still occurring even if very slowly. This slowness may be because the reactors are not stirred. It is clear from Figure 2.13 that the release rate must have been greater at earlier times because there are big intercept values. The release rates increase with mass of sandstone used. Comparing the release rates in this experiment with that in Section 2.3.3 (Figure 2.4) indicates that at about 24 hours the rates were greater (about 0.05 ppm/h compared with 0.003-0.03 ppm/h). As the current experiment was not stirred, this may be the main reason for the slower rates, and all subsequent experiments were stirred.

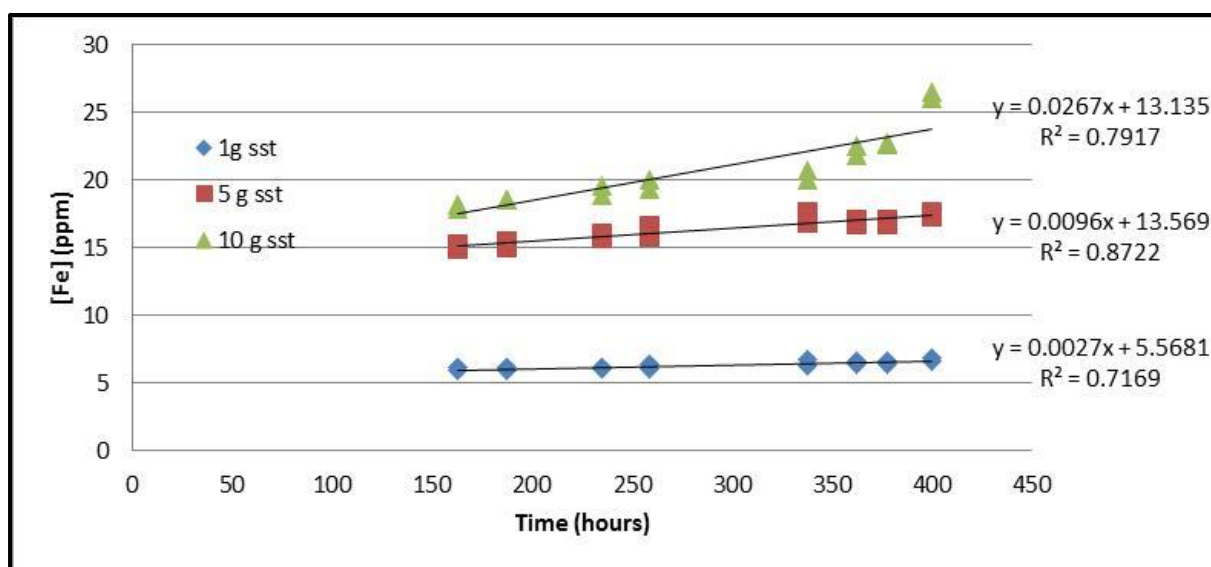


Figure 2-13: Fe released (average of filtered and unfiltered samples) on contact of 500 ml of 10 mM H_2A solution (pH~3.2) with sandstone at 80 °C.

Figure 2.14 shows the release of Mn^{++} in the same experiment. The Mn^{++} released is less than the Fe released. However, similar comments can be made about the very slow increase in Mn^{++} concentration occurring and how it must have been at a greater rate at earlier times (when the rate may be was less dependent on diffusion from the sediment?). The increase in Mn^{++} released is not proportional to the sandstone mass as was also found for Fe. Fe concentration increase for the 5 g sample is 2.7 times that for the 1 g sample, while for Mn the concentration increase for 5 g sample is 3.6 times that for the 1 g sample. The explanation

may be that there is proton-promoted dissolution (pH is about 3.2) as well as reductive dissolution. But also that the controlling factor is diffusion through the sediment.

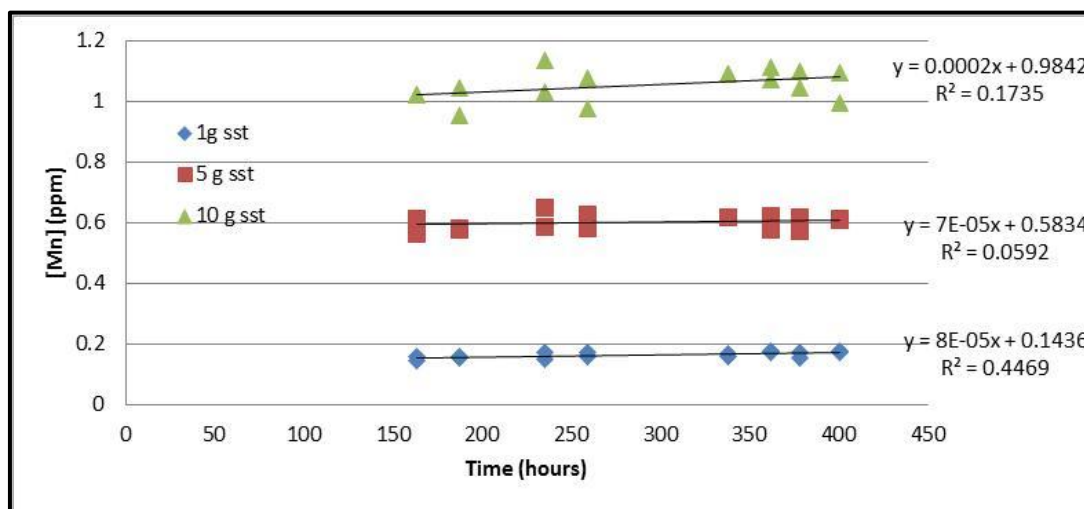


Figure 2-14: Mn^{++} released (average of filtered and unfiltered samples) on contact of 500 ml of 10 mM H_2A solution (pH~3.2) with sandstone at 80 °C.

2.3.7 Monitoring the colour change of the solution and sandstone at high temperature

A simple experiment has been carried just to monitor the colour of ascorbic acid solution after put in contact with sandstone at high temperature over time. Three beakers were prepared each one containing 10 mM of H_2A and 10 g sandstone. All beakers were put in a water bath at 80 °C.

It was observed that the solution changed from colourless during the first 4 h of reaction, to yellow, to dark yellow and eventually to dark brown after 150 hours of reaction (Figure 2.15). The sandstone sediment became partly bleached, but not completely white. This indicates the increase of released Fe and Mn over time. As the pH was about 3 and there is no difference in measured concentrations between filtered and unfiltered samples, it is likely that the colour is due to Fe being present as ferric complexes ($[Fe(H_2O)_6]^{+++}$). Observations of other

experiments at lower temperatures and higher pHs indicated that colour did not change though leaving a reactor for about 3 weeks resulted in a pale yellow colour. It is concluded that in these high temperature low pH experiments, Fe^{+++} is released partly by non-reductive dissolution as suggested in Section 2.3 and also some of the Fe^{++} released is oxidized according to:

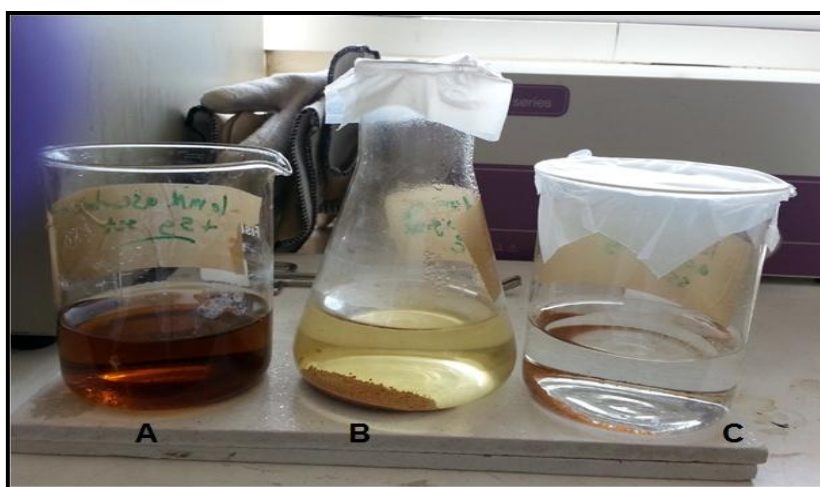
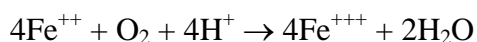


Figure 2-15: The change of colour of 10 mM ascorbic acid as it reacts with 10 g red sandstone. A) dark brown colour, 168 hours; B) yellow colour, 72 hours; C) colourless solution, 4 hours. The sandstone becomes lighter with time but never completely white.

2.3.8 The effects of filtration and acidification at high temperature

Further experiments were undertaken to study the effect of filtration and also to investigate the effect of acidification of samples by nitric acid were undertaken. 500 ml of 10 Mm (pH=2.93) of H_2A were put with 1 g mass of sandstone at 90 °C. The reactors were monitored from around 20 h to 90 h with 15 ml samples collected. The samples were divided into three sub-samples: the first 5 ml were left unfiltered; the second 5ml sample was filtered through a

0.2 μ m syringe filter; and to the third 5ml sample was added 20 μ l of 1 M HNO₃ without filtration in order to reduce the pH to 2.09.

Figure 2.16 (and Appendix 2.7) shows that the filtering, as previous experiments have indicated, does not affect the results. It also shows that acidification of the samples after separated from the sediment does not affect the results.

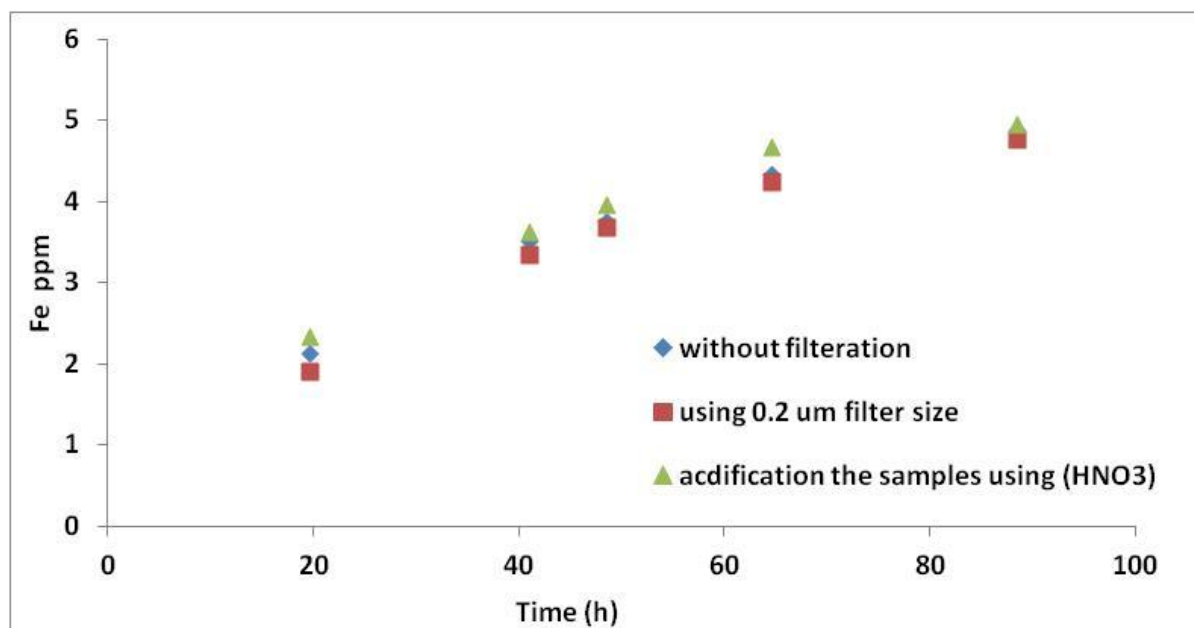


Figure 2-16: Fe release from 1 g mass sandstone using 500 ml of 10 mM H₂A (pH~2.93) at 90°C using different sample treatments.

2.3.9 Combining previous experiment results to look at how concentrations vary over longer times at high temperature

The rates of dissolution appear to be different in some of the previous experiments. Results from two experiments at 80°C and one at 90°C under same conditions were combined to see how these differences were related to time. Results are shown in Figure 2.17 (combination from Figures 2.4, 2.13 and 2.16). It is clear from this plot the curve comes from a first order reaction in Fe:

$$d[\text{Fe}]/dt = k([\text{Fe}]_{\text{max}} - [\text{Fe}])$$

where [] indicates concentration and subscript max indicates the maximum concentration.

Integrating from $t=0$ to $t=t$,

$$t = -1/k \{ \ln[1 - [\text{Fe}]/[\text{Fe}]_{\text{max}}] \}, \text{ i.e. } [\text{Fe}] = [\text{Fe}]_{\text{max}} \{ 1 - \exp(-kt) \}.$$

A fit to the data was made by trial and error using Excel (Figure 2.17B), giving

$$k = 0.019 \text{ h}^{-1} = 5.3 \times 10^{-6} \text{ s}^{-1} \text{ and } [\text{Fe}]_{\text{max}} = 6.5 \text{ ppm } (1.2 \times 10^{-4} \text{ mol/l}).$$

So the apparently linear increases with time shown in all previous plots are the result of short time intervals. The dependence on $([\text{Fe}]_{\text{max}} - [\text{Fe}])$ suggests that the actual dependence may be on $[\text{H}_2\text{A}]$, as it would be expected that $[\text{H}_2\text{A}]$ decreased as $([\text{Fe}]_{\text{max}} - [\text{Fe}])$ decreased. The proper rate would have to use $[\text{H}_2\text{A}]$ concentrations, which could be estimated with the data, but also take into account Mn concentrations.

Larsen et al. (2006) found the rate constant of reductive dissolution of natural iron oxides in a sandy aquifer sediment collected from Denmark by 10 mM ascorbic acid at pH =3 varied between 7×10^{-6} and $1 \times 10^{-3} \text{ s}^{-1}$, similar to the approximate figure obtained here. Joseph et al. (1996) found that the rate constant of dissolution of synthetic hematite using ascorbic acid alone was $1.98 \times 10^{-5} \text{ s}^{-1}$ using 80 mM of $[\text{H}_2\text{A}]$. While Roden (2004) determined the rate constant of iron oxides present in soil and sediment ranged between 3×10^{-6} to $1.6 \times 10^{-6} \text{ s}^{-1}$ using the same concentration and pH of H_2A as in the experiments of Figure 2.17.

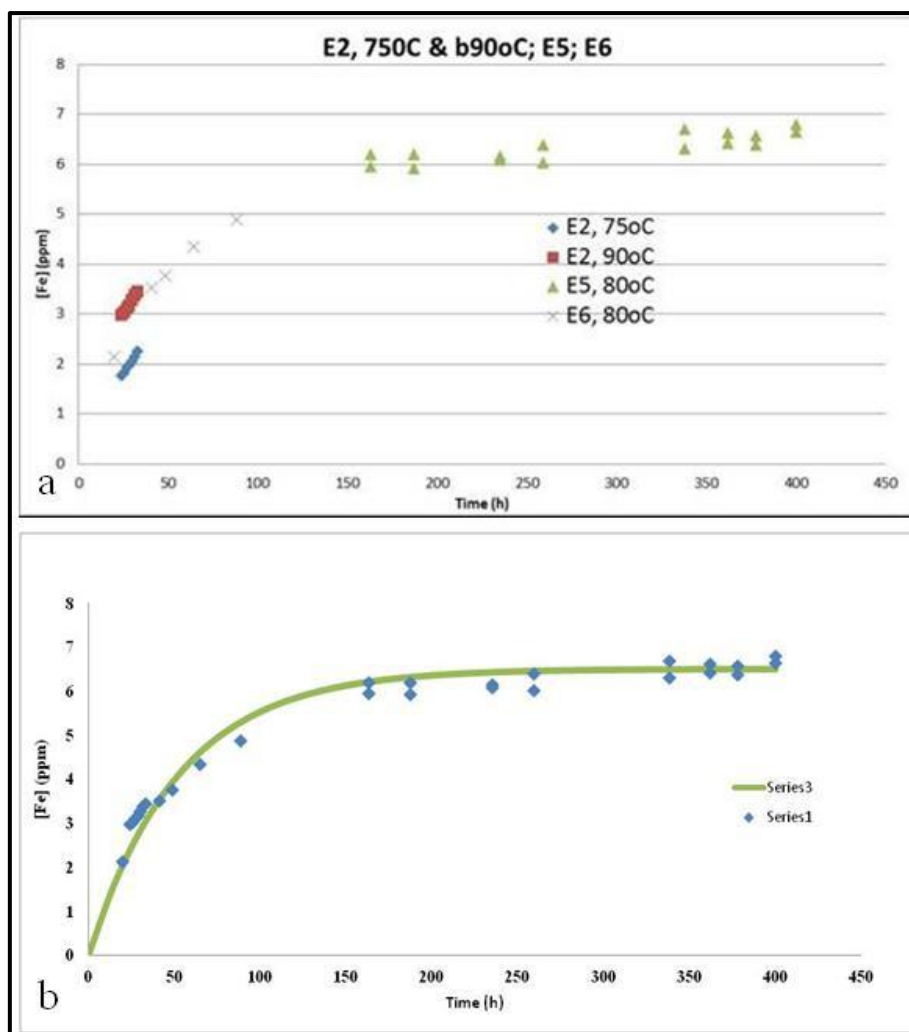


Figure 2-17. The relationship between time vs Fe concentration at higher temperatures from a combination of several experiments. A the experiments at 75, 80 and 90°C. B the experiments at 80 and 90°C with a fitted first order reaction relationship.

2.3.10 The effect of contact with oxygen at high H_2A concentration at lab temperature

In order to represent the aquifer under anaerobic conditions, the techniques to compare the effects of aerobic and anaerobic conditions on the rate of reductive dissolution must be developed. The purpose of this experiment is to monitor the amount of Fe and Mn^{++} released during long term reaction under aerobic and anaerobic conditions at lab temperature (21 °C).

To achieve this goal, two 500 ml aliquots of 10 mM ascorbic acid (pH=3) with 1 g of red sandstone were placed in beakers. One beaker was purged by N₂ gas for 10 min to remove dissolved oxygen before placing it in an anaerobic chamber. The second beaker was maintained under oxic conditions at lab temperature. Neither beaker was shaken as putting the shaker in the anaerobic chamber was not easy (but was resolved for experiments Chapter 6). Samples were collected from both beakers. The samples from the anaerobic chamber were put in glass vials with rubber stoppers and aluminium caps sealed to prevent sample exposure to oxygen until analysis. Figure 2.18 (and Appendix 2.8) presents the results. The anaerobic experiments resulted in higher concentrations of Fe and Mn. Fe concentrations are greater than Mn concentrations in both anaerobic and aerobic experiments. It is concluded that in future experiments anaerobic conditions should be attempted.

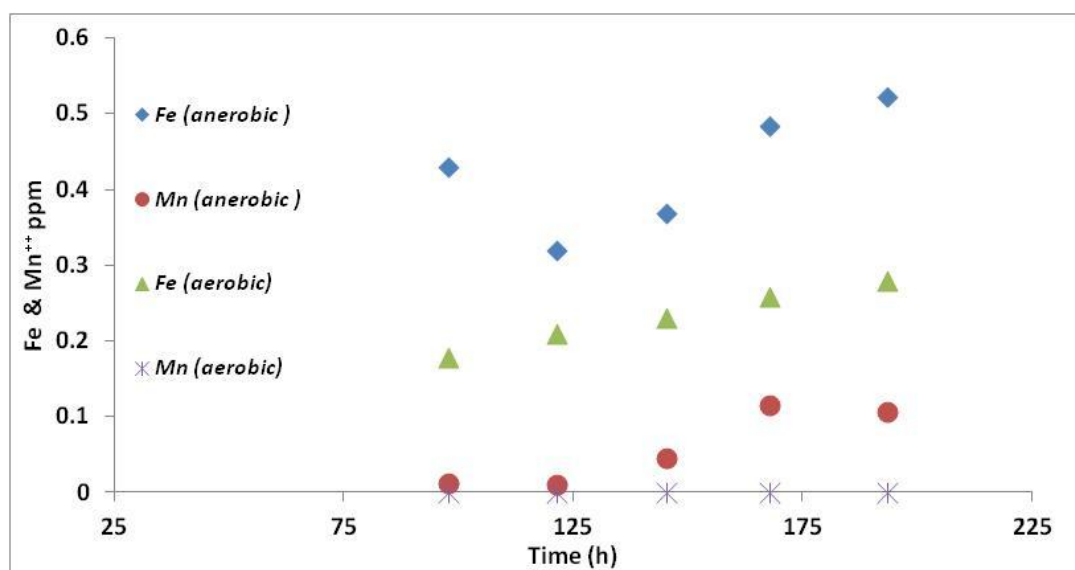


Figure 2-18: Fe and Mn release from 1g sandstone using 500 ml of 10 mM H₂A under aerobic and anaerobic conditions at 21 °C.

2.3.11 Measurement of dissolved oxygen in ascorbic acid solutions

As previous experiments indicated that the presence of oxygen significantly affected the rate of release of Mn and Fe, another experiment has been carried out to find out the effect of ascorbic acid alone and with the sandstone on the dissolved oxygen (D.O.) content of the

solutions. 500 ml of 10 mM H_2A solution was put in a beaker containing 1 g of red sandstone. Another 500 ml of ascorbic acid was put in a second beaker without sandstone. Also 500 ml of deionised water was put in a third beaker that contained 1 g of sandstone. Dissolved oxygen measurement was carried out using a dissolved oxygen probe (pro DO, YSI) whilst the beakers were gently shaken. This experiment was undertaken four times and once at 5 mM H_2A . It was not possible to operate the DO probe at high temperatures but it would be expected that there would be lower concentrations of dissolved gases.

The results are shown in Figure 2.19 (see Appendixes 2.9, 2.10 and 2.11). The experiments show similar patterns of change in dissolved oxygen concentrations. The deionised water with sandstone experiments showed the least change in DO. A slight increase or decrease was observed possibly because of change in temperature. Figure 2.20 shows D.O. plotted against temperature together with the saturation relationship and it confirms that the concentrations in the DIW/sandstone experiments is control by temperature-dependent saturation. The H_2A alone and with sandstone produced drops in D.O. that were similar suggesting that H_2A reacts with O_2 and that the sandstone does not make significant difference. The drop in D.O. was up to about sixth millimole per litre over up to 70 hours, so rather limited. The drop appeared to stabilised, possibly because the solutions were not stirred sufficiently perhaps. This experiment therefore revealed that ascorbic acid has some capacity to decrease the dissolved oxygen in the solution. The DO in the H_2A / sandstone experiment was lower than in the case of the H_2A experiment in some experiments. The latter is explained by H_2A reductive dissolution of hematite releasing Fe(II) that then reacts with the DO.

These results are interesting when compared with the data from measuring H_2A stability with time (chapter 3). In latter the concentrations of H_2A dropped quicker in anaerobic conditions though did drop under oxic conditions too.

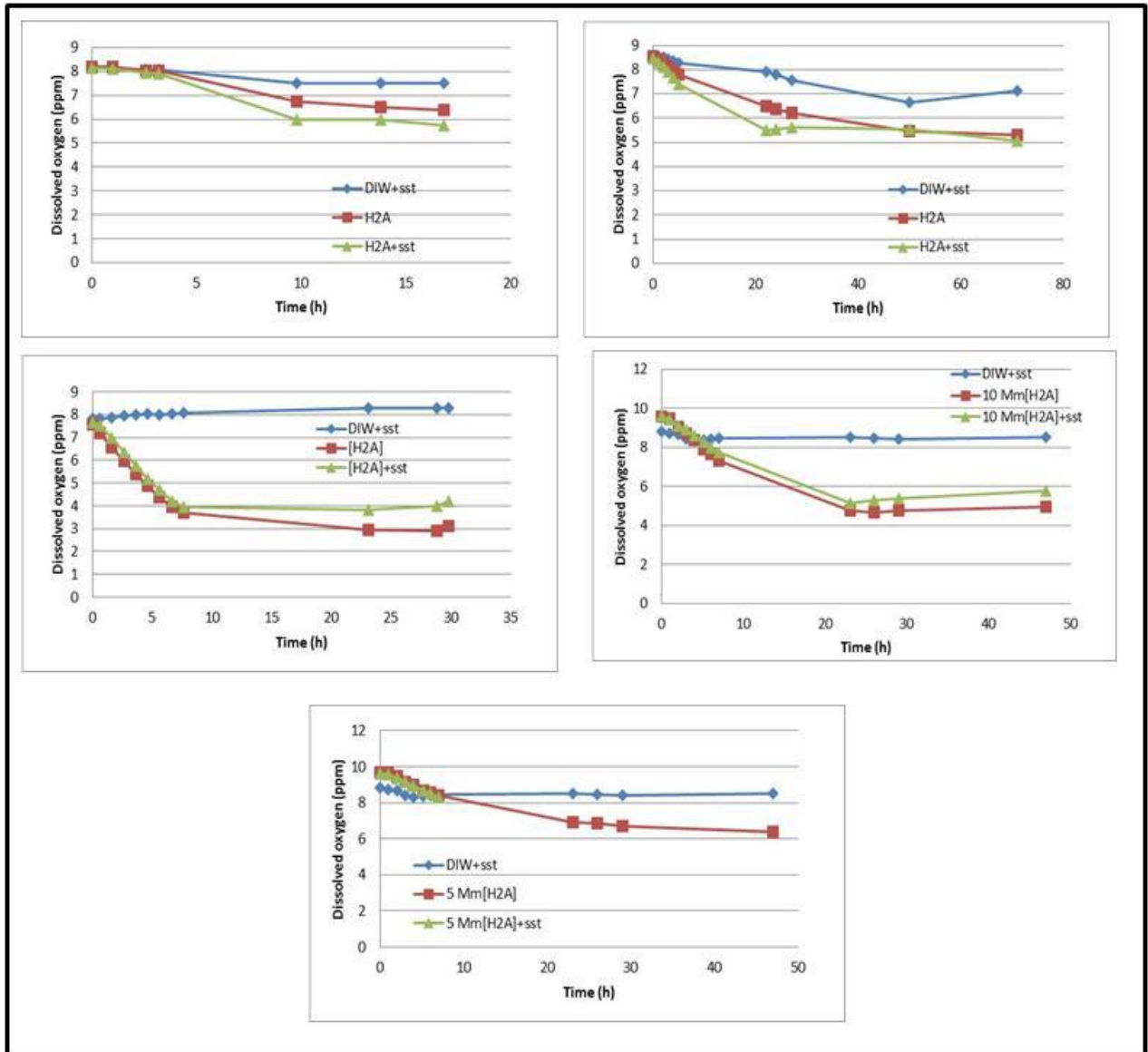


Figure 2-19: Dissolved oxygen variation with time for 500 ml of deionised water with 1 g sandstone, 500 ml of 10 mM ascorbic acid alone and 500 ml of 10 mM ascorbic acid with sandstone, all at lab temperature for different time . The last plot is for a repeat experiment at 5mM of ascorbic acid.

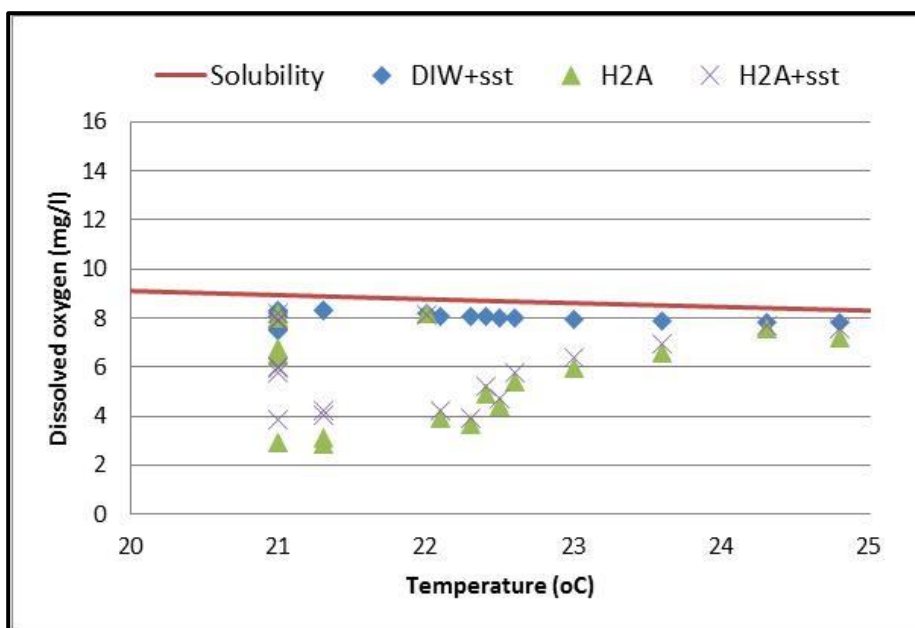


Figure 2-20: Dissolved oxygen variation with temperature for deionised water with sandstone, ascorbic acid alone and ascorbic acid with sandstone. Also the solubility of oxygen(http://www.engineeringtoolbox.com/oxygen-solubility-water-d_841.html). Generally time increases right to left. The H₂A solutions were approximately O₂ saturated at the start of the experiments.

2.3.12 Variation in TOC with time at high temperatures

Experiments have been undertaken to see if there is any loss of total organic carbon (TOC) detectable during the reaction of H₂A and sandstone.

10Mm of H₂A solution was reacted with 1 g mass of sandstone at two different temperatures (50 °C and 90 °C). Seven samples were collected 24 to 33 h of reaction (see Appendix 2.12).

Figure 2.21, 2.22 and 2.23 shows the results. Fe concentration slightly increases during the experiments at a greater rate at the higher temperature and with higher concentrations at the higher temperature. TOC falls at similar rates with time at the two temperatures (see Figure 2.22).

Figure 2.21 shows the relationship between Fe and TOC. TOC falls as Fe rises, but much more TOC is removed from solution than Fe released. A decrease of 0.5 moles of H_2A would be expected for one mole of Fe released. However, if H_2A reduces Fe oxides then the product is thought to be dehydroascorbic acid (Suter et al., 1991), i.e. all C remains organic C and TOC remain constant. But there may be some sorption of H_2A (Chapter 4) or some sorption of Fe (Chapter 5) or release of Mn (see above). Also may be there is some non-Fe related degradation of H_2A at the higher temperatures used here. Figure 2-22 includes data of TOC against time for experiments completed at the same time but without sandstone present (i.e. just H_2A). TOC concentrations do appear to decrease with time in both cases in similar way to when in the presence of sandstone. At 90 but not at 50 °C the TOC concentrations are less for the sandstone experiments suggest that the sandstone may possibly have some influence at the higher temperature but this could just be coincidence. As yet the implications of these results are not clear but possibly the decrease is related to the decrease in D.O. and is independent of the sandstone presence. D.O. dropped by about 0.2 mmol/l over 30 hours at most (but at lab temperatures)(Section 2.3.11) and $[\text{H}_2\text{A}]$ here drops by about at most the same amount. So may be degradation of H_2A by oxidation by O_2 but why then is DOC less as the product is likely to be organic. H_2A stability is looked at again in Chapter 3.

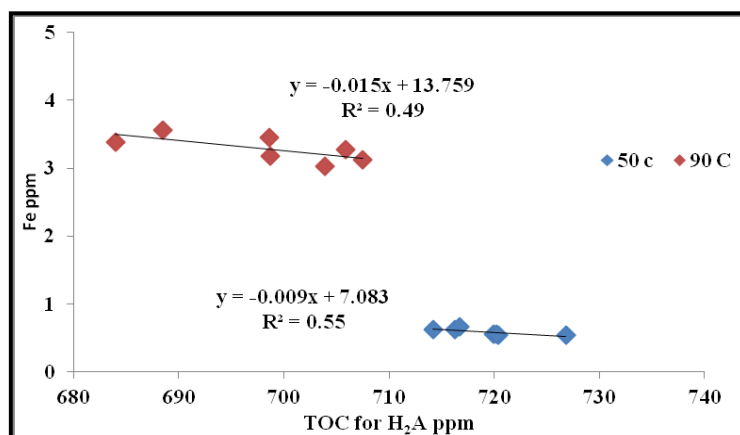


Figure 2-21: The relation between TOC and iron using 10 mM H_2A with 1 g sandstone at 50 and at 90 °C.

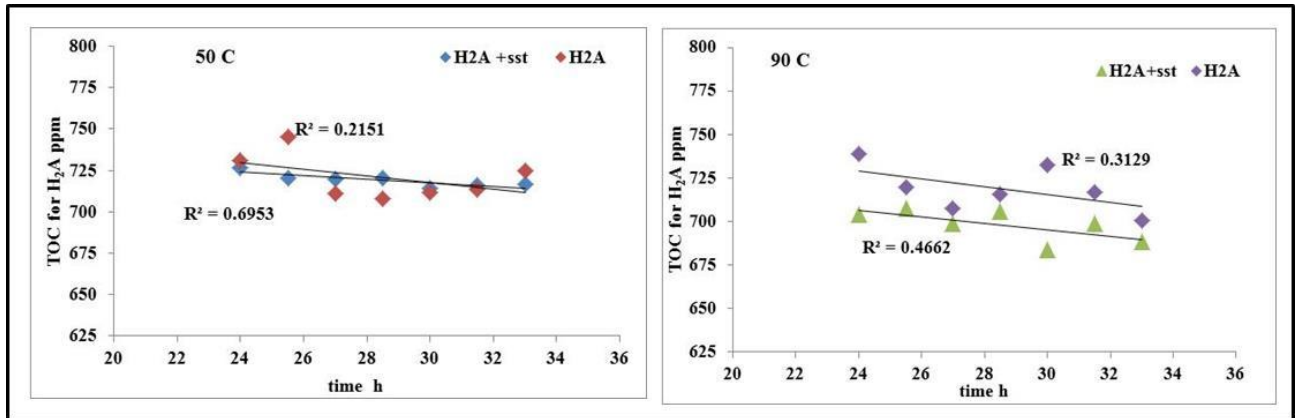


Figure 2-22: Comparison of TOC variation with time between 10 mM H₂A solutions in contact with and not in contact with sandstone at 50 and at 90 °C.

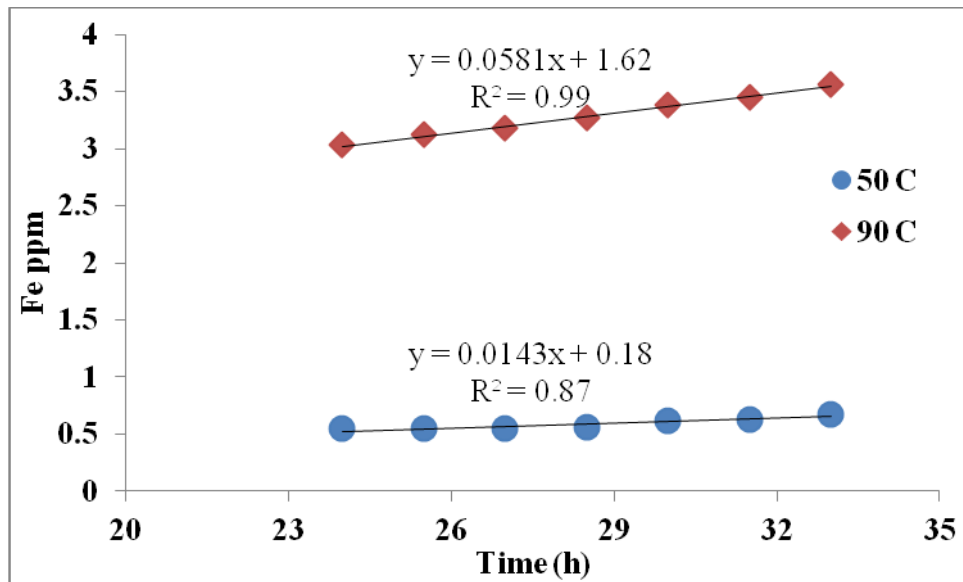


Figure 2-23: Plot of Fe concentration versus time at 50 and 90 °C.

2.4 Low concentration H₂A, lab temperature experiments

2.4.1 Will low concentration H₂A reduce sandstone oxides measurably at low temperatures?

The experiments described above were undertaken at high temperature as preliminary experiments had indicated insignificant reductive dissolution of hematite at lab temperature in low rock water ratio range between 0.002 to 0.02 g/ml. However, shaking was not possible in water baths needed for higher temperatures. So a few experiments were undertaken to see

if using a high rock-water ratio with shaking would release measurable Fe and Mn at lab temperature. 0.04 litre samples of H_2A solutions at concentrations from 10 to 100 ppm were used with 10 g of sandstone (rock water ratio 250 g/ml). The samples were shaken for 2 hours at 300 rpm, then centrifuged for 10 minutes at 4500 rpm before analysis by FAAS. Replicate samples were filtered through 0.2 μm filters.

The pH of H_2A solution with sst range from 4.8 to 4.41 for 10 to 100 ppm of H_2A respectively. The results, which shown in Figure 2.24 and appendix 2.13, show that measurable amounts of Fe and Mn (concentrations > 0.1 ppm) are released using this method. The filtering is not needed as the results from filtered and unfiltered samples are the same. Variation of replicates indicated a variation of about 10% of the mean value indicating that the sandstone is heterogeneous. This is even though a large quantity of sandstone was crushed and thoroughly mixed before being taken for the reaction vessels. In addition, this method results for the first time in Mn concentrations being greater than Fe concentrations, but this could be because the experiments have short contact times (see later).

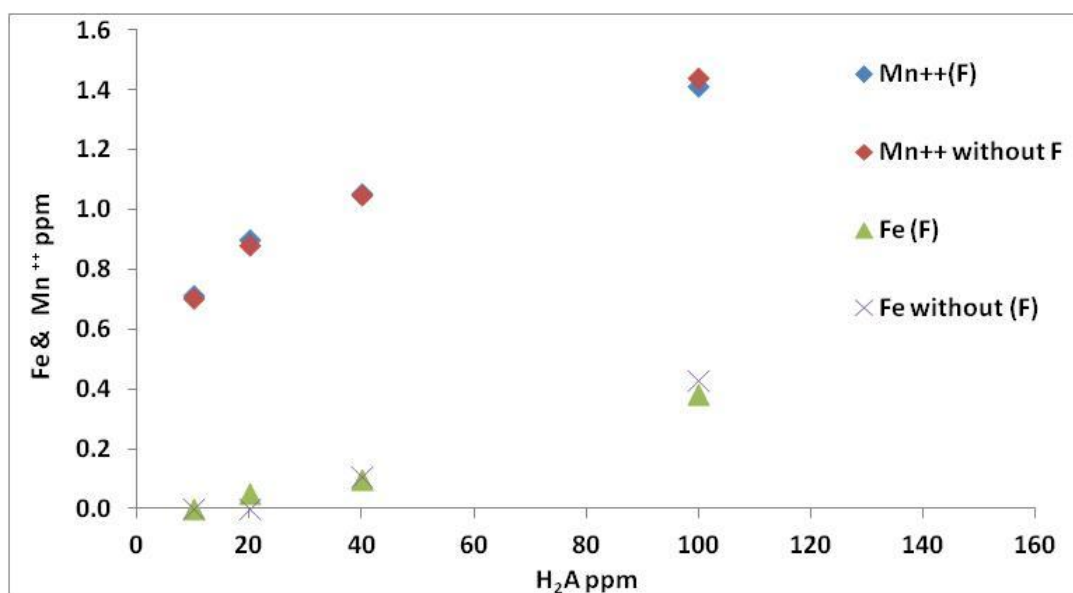


Figure 2-24: Fe and Mn^{++} concentrations as a function of H_2A concentration at lab temperature. 10 g sandstone with 0.04 l of H_2A solutions, shaken for 2 hours. “(F)” is with filtering, “without F” is without filtering.

2.4.2 Does filtering and shaking affect dissolution at low H_2A concentrations and low temperatures

Following the successful preliminary experiments with high rock-water ratios and shaking, further experiments were undertaken to determine the effect of the shaking at lab temperature. 10 g samples of red sandstone were put in 50 ml centrifuge tubes, then 0.04 l of various concentrations of ascorbic acid, (vary from 10 to 100 ppm) were added and reacted for 4 hours. One group of samples was put in a (slow to avoid particle damage) shaker at 300 rpm and the other was not shaken. All samples were centrifuged for 10 minutes at 4500 rpm and then filtered using 0.2 μm filters.

Figure 2.25 shows the results (see also Appendix 2.14). The significant effect of shaking is confirmed. Previous release rates may therefore be associated with diffusive transport of reaction products rather than rates at the mineral surfaces. Therefore it is important to include the shaking when designing the final experimental procedure. In these experiments again the Mn^{++} concentrations are greater than the Fe concentrations. This could be because of the shaking or because the time of contact is much shorter. The pH range from 4.25 to 4.79 for 100 and 10 ppm of H_2A with sandstone respectively.

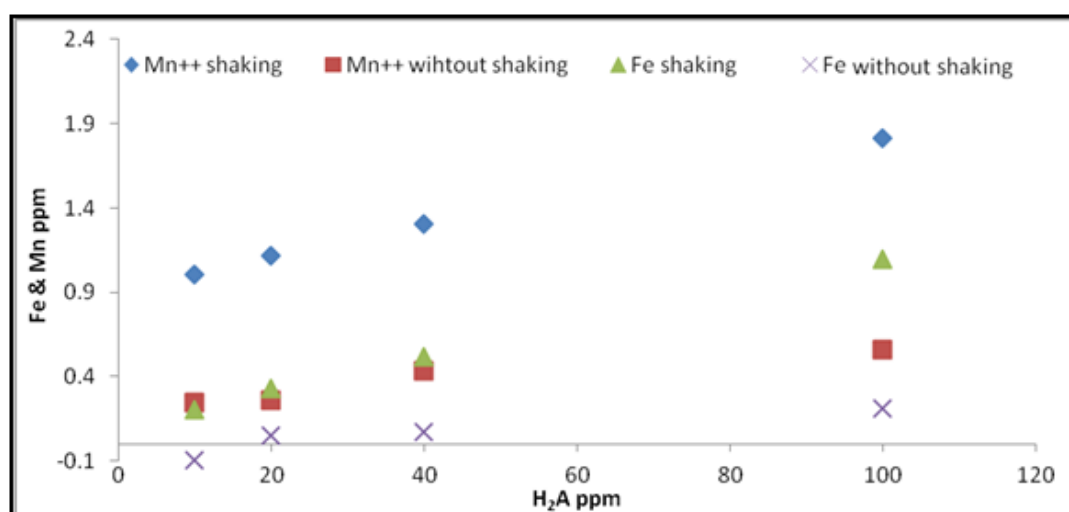


Figure 2-25: The effect of shaking on the rate of reductive dissolution of Fe and Mn oxides in 10g sandstone samples in 0.04 l of H_2A solutions at lab temperature after 4 h reaction.

2.4.3 Effect of shaking at lab temperatures and without shaking at higher temperatures

To determine whether the experiments undertaken at elevated temperatures were also affected by lack of shaking, the amount of Fe and Mn^{++} released using the same rock /water ratio and time but under different temperature and shaking conditions was determined. One group of samples was placed in a shaker at lab temperature while a second group was put in a water bath under higher temperatures without shaking (as cannot use shaker in the water bath). Both groups of samples have the same mass of sandstone and concentration of ascorbic acid and also were run for the same period of time. 10 ± 0.01 g samples of sandstone were put in 50 ml centrifuge tubes and 0.04 l of H_2A solution added. One group of centrifuge tubes was put in a shaker for 2 h under 300 rpm at lab temperature and after that put in centrifuge at 4500 rpm for 10 min before analysis. The second group was put in a water bath at 73°C for 2 h without shaking, and then centrifuged for 10 min at 4500 rpm. In addition, a standard solution was treated as a sample.

Figure 2.26 and appendix 2.15, shows the results. pH was 4.3 to 4.9. The shaking has a larger effect than the temperature increase. It is concluded that high temperature experiments are not required, just shaking needed.

Figure 2.25 indicates that again Mn^{++} concentrations are greater than Fe concentrations. solution under lab temperature, compared with release at high temperature without shaking. In general, comparing all the results of relevant experiments in this chapter (Table 2.1), Mn concentrations are greater than Fe concentrations when concentrations are low (<100 ppm), temperature is lab temperature, or water rock ratio is high (10g/40ml rather than $<10\text{g}/500\text{ml}$). The reason for this is not known.

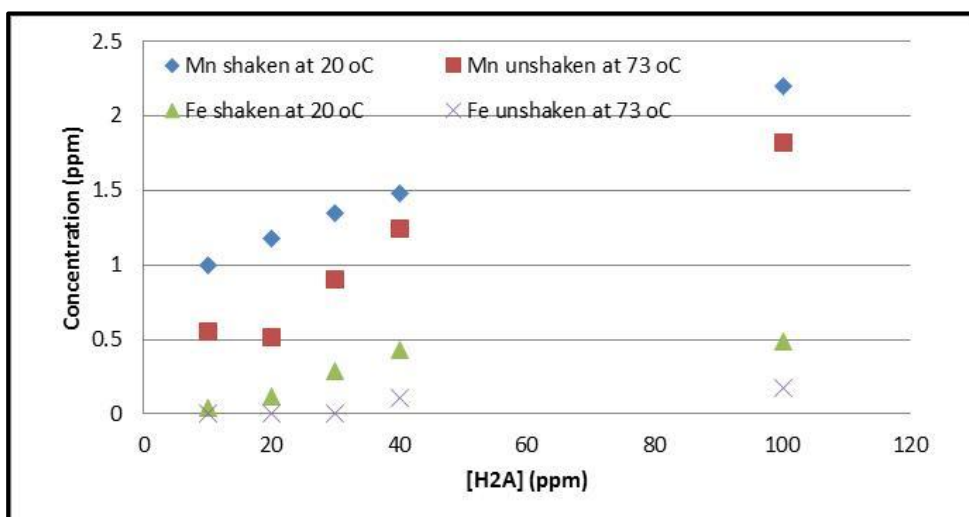


Figure 2-26: Fe and Mn release after 2 hours of shaking and without shaking for 10 g sandstone in 40 ml H₂A

Table 2-1: The relative concentration of Fe and Mn⁺⁺ in all comparable experiments.

Concentrations	Shaken	Time (hours)	Temperature (°C) [g:ml]	Figure number	H ₂ A concentration
Fe>Mn	No	24-33	50-90 [1:500]	2.4, 2.7	10mM
Fe>Mn	No	1-6	60 [1:500]	2.9	25-75mM
Fe>>Mn	No	150-400	80 [1,5,10:500]	2.13, 2.14	10 mM
Mn>Fe	Yes	2	20 [10:40]	2.24	10-100ppm (0.06-0.6 mM)
Mn>Fe	Yes	4	20 [10:40]	2.25	10-100 ppm
Mn>Fe	No	2	20 [10:40]	2.26	10-100ppm

2.5 What is the effect of initial conditions on dissolution at low H₂A concentrations and low temperatures?

2.5.1 *The release of Fe and Mn⁺⁺ from sandstone by HCl*

The purpose of this experiment was to compare the amount of Fe and Mn released from sandstone by H₂A with that released by an inorganic acid, in this case HCl.

HCl was prepared at various concentrations (2 to 0.00625 M). Also several concentrations of ascorbic acid was prepared (0.56 – 0.14M, 100 to 25 ppm). 10 g of red sandstone was weighed and put in each of 22 centrifuge tubes. Then 40 ml of each inorganic and organic acid was added to each centrifuge tube separately (low HCl experiments (0.05 to 0.00625M) were done in duplicate). All samples were shaken for 4 hours at 300 rpm and afterwards centrifuged for 10 minutes at 4500 rpm. Ascorbic acid samples were acidified by adding 100 µl (1-2 drops) of 0.5 M of HNO₃, which dropped the pH from 4.7 to 2.4. The results are shown in Figure 2.27 and Appendix 2.16.

The H₂A released more Mn than Fe as is usual for lab temperature experiments (Table 2.1). Though no release of Fe was seen with deionised water, there was quite a lot of Mn. This might be because of colloids that were not retained during the centrifuging but subsequently dissolved during acidification before analysis. However, any Fe(II) release might result in MnO₂ reductive dissolution.

The HCl experiment results are very different. The pH is much lower and therefore the comparison is not direct. Fe concentrations are higher than Mn (and Mn higher than for the H₂A experiments especially for higher than 0.05 M of HCl). As pH falls Fe becomes dominant over Mn at pH lower than 1 (Figure 2.28). It is clear that dissolution by strong acids is much more rapid than by reductive dissolution by weaker organic acids.

Another experiment was carried out to compare the amount of Mn and Fe released from sandstone by very dilute HCl but at higher pH values (around 3.85 and 4.75). As in previous experiments, 10 g of sandstone were accurately weighed and put in each of four centrifuge tubes to which were added 40 ml of 0.162 and 0.00064 mM of HCl with two replicates for each concentration. Each reactor was put into a shaker for 16 h at 300 rpm, then centrifuged for 10 min and filtered using 0.2 μm filter before analysis using FAAS.

Results (appendix 2.17) revealed that using extremely dilute HCl alone, at pH 3.8 and 4.6, no measurable iron was released from sandstone. On the other hand, very dilute HCl was able to release Mn^{++} . The concentrations are slightly higher than concentrations obtained using deionised water in the previous experiment (0.75 ppm). There is a slight rise in pH after interaction with sandstone. These results are interesting because there is no obvious reductant in the system. One possibility is that H^+ is sorbed, raising the pH, and this results in release of Mn(II) from sorption sites on the hematite. The change in pH is equivalent to about 10^{-5} M for both the higher and lower concentrations of HCl, but change in Mn is respectively 10^{-4} M and 10^{-5} M. Without further investigation the mechanism cannot be determined for sure. In conclusion very low pH can result in significant increase in Fe concentrations without H_2A being present. But at pHs of the H_2A experiments the release of Fe is very little. For Mn^{++} there was much released at low pH and even some released with deionised water and at higher pHs (lower concentration of HCl experiments). So Fe and Mn^{++} can be released without H_2A , but it is only Mn^{++} concentrations that need to be considered in terms of H_2A -independent dissolution.

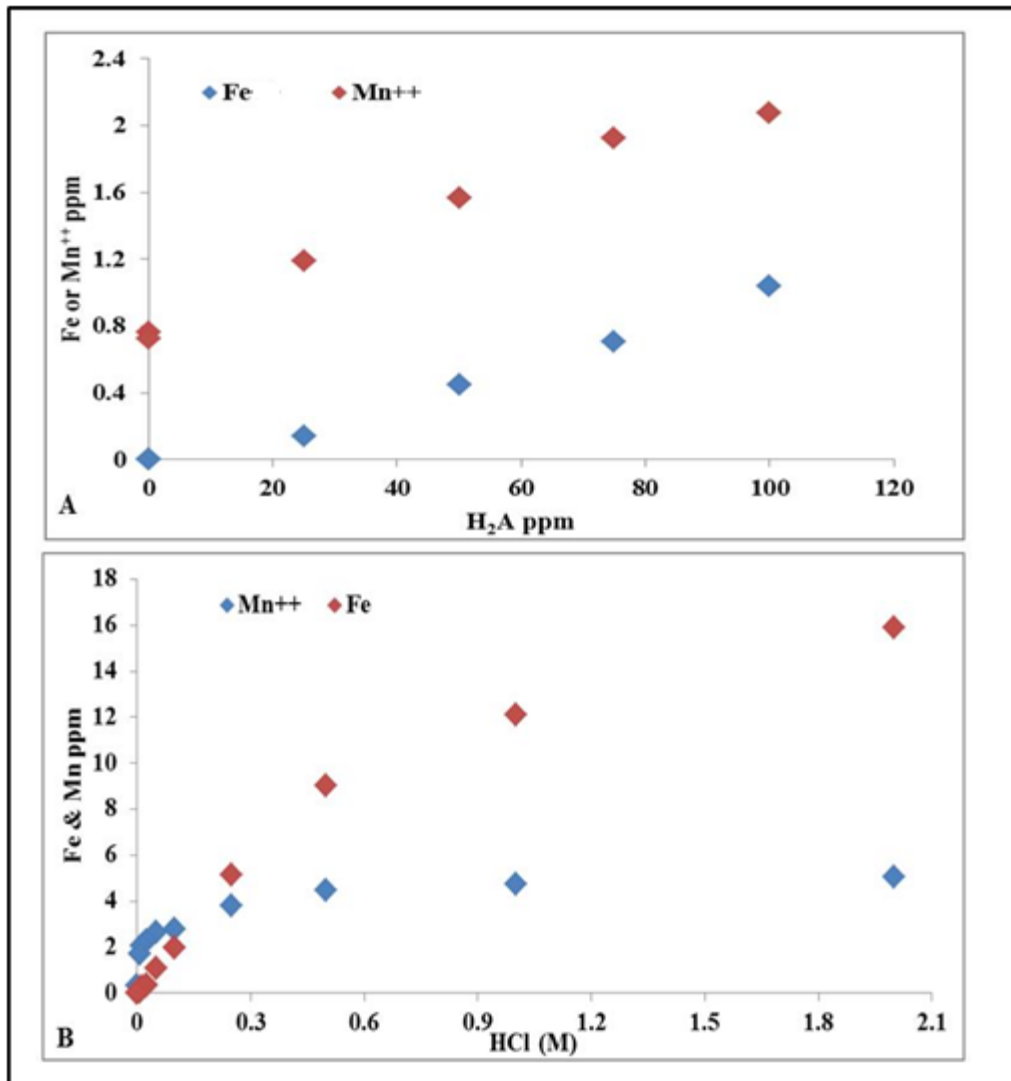


Figure 2-27: Fe and Mn release from 10 g sandstone at lab temperature A) by ascorbic acid at pH 4.5 to 4.75. B) by various concentrations of HCl at very low pH.

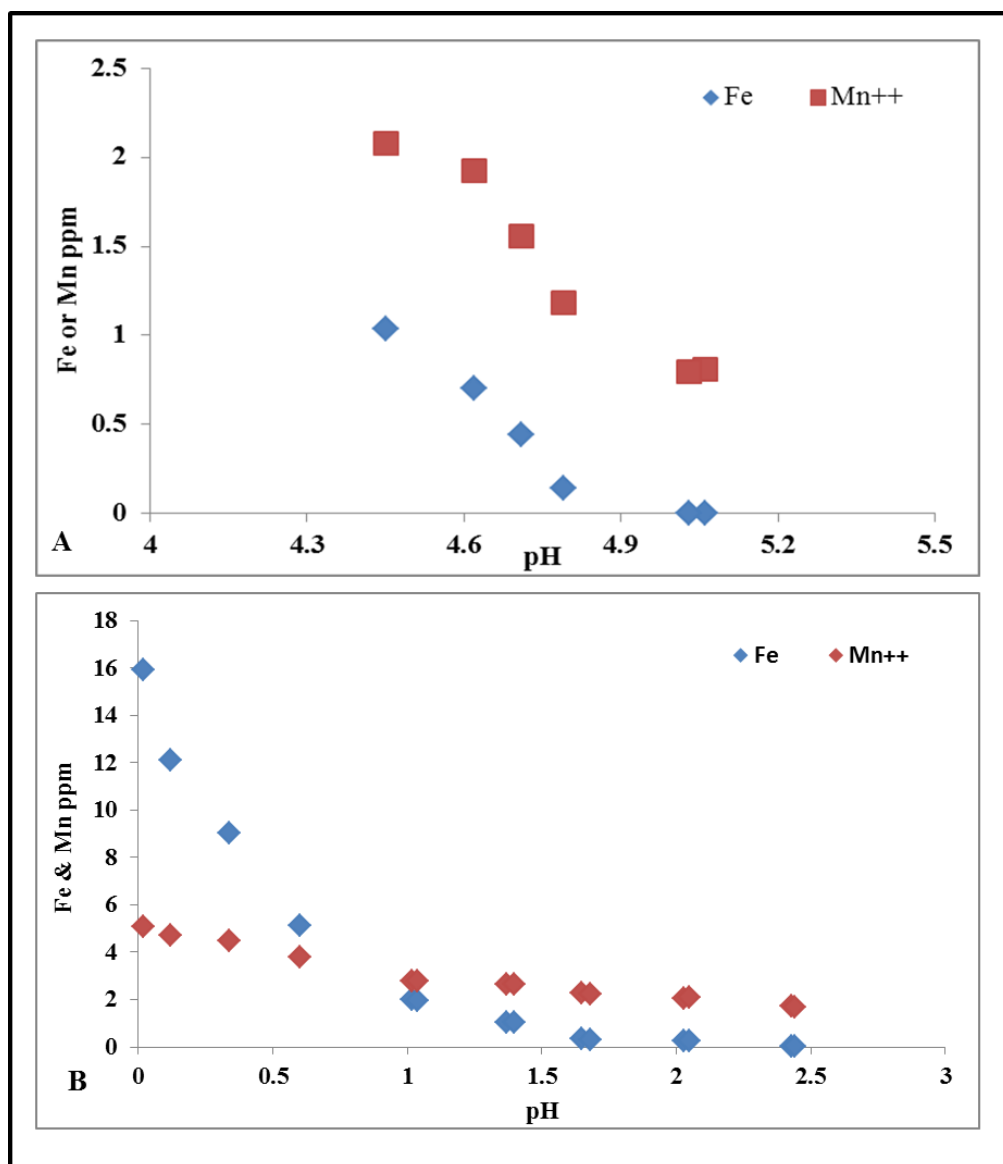


Figure 2-28 The relationship of [Fe] and [Mn] with pH. A) Using ascorbic acid. B) using [HCl].

2.5.2 The effect of washing sandstone with dilute HCl on the reductive dissolution of oxides by H_2A

The initial condition of the surface of a solid may affect the reactions seen when H_2A is added. In the case of previous work, e.g. Suter et al. (1991)'s work, the solid was synthetic and its surface had been in contact only by ascorbic acid and Fe solutions. So this experiment was planned to see if changing the surface composition has any effect on reaction with H_2A .

Sediment samples were washed by dilute HCl (12.5 mM). The reason for choosing this concentration was that at this concentration the average pH was the same as that of ascorbic acid after acidification by 1-2 drops of 0.5 M nitric acid. 10 g samples of red sandstone were put into six 50 ml centrifuge tubes and 40 ml of dilute HCl (12.5 mM, pH ~ 2) was added. The tubes were then put in a shaker for 2 h at 300 rpm, then centrifuged for 10 min at 4500 rpm. The HCl supernatant was then discarded. 3-4 ml still filled the pore space of the sandstone samples and the sandstone sediment remained attached to the bottom of centrifuge tube, even if turn the tube upside down. Then 40 ml of H₂A (15,25,50 ,75 and 100 ppm) solution was added to each sample, and also to unwashed sediment and to two samples without ascorbic acid (just deionised water with sediment). The samples were then placed in the shaker for 16 h, centrifuged for 10 min, and 15 ml aliquots were filtered through 0.2 µm filters. 10 ml of this filtrate was used for analysis by FAAS after acidifying using 150 µL of nitric acid.

Figure 2.29 a (and Appendix 2.18) compares the results from washed and unwashed samples. All washed and unwashed samples had pH values of 2.1 ± 0.1 ppm. From these results it is obvious that washing samples with dilute HCl results in the release of higher amounts of iron.

In general there is about 3 to 6 times greater iron release after washing the sediment.

May be the reason for more iron release is that the HCl makes the surface of the iron oxide saturated with hydrogen ions (H⁺). Zinder et al. (1986) and Suter et al. (1991) point out that protonation of the surface of oxides leads to broken and weakened metal – oxygen bonds and hence easier release of iron. In both washed and unwashed samples there is an increased release of iron with increase of H₂A concentration.

The opposite result was true for Mn (Figure 2.29 b). The amount of Mn released into solution from the washed sediment was lower than the amount released from unwashed samples by

more than 1.5 times. It is possible that the HCl-washed sediment may have led to dissolution of Mn oxide resulting in little Mn oxide still in present in the washed sediment when the ascorbic acid was added. In the zero H₂A unwashed sample about 0.75 ppm of Mn was present in samples.

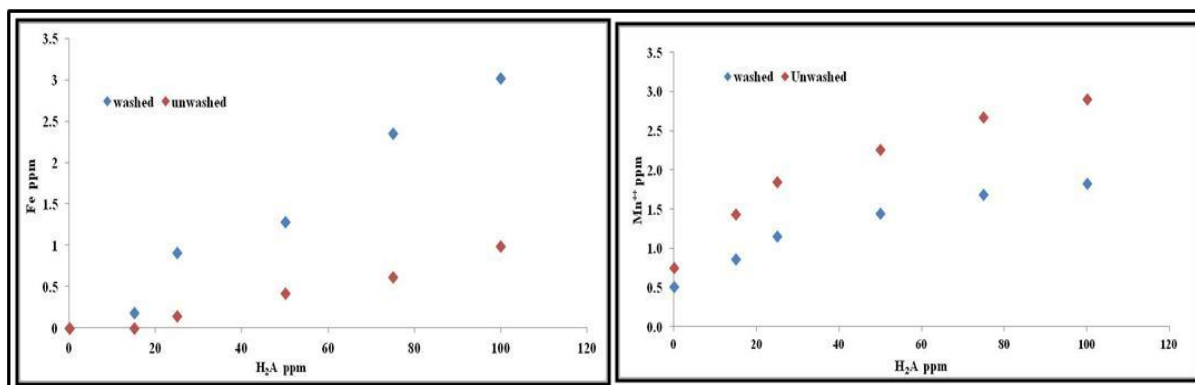


Figure 2-29: The amount of Fe and Mn released from 10 g of sandstone washed with dilute HCl and unwashed using ascorbic acid after 16 h shaking at lab temperature. pH~2 in all cases.

To investigate the release of Fe and Mn in more detail, a further experiment was undertaken where the sandstone was washed with HCl and then twice more with DIW and each washing analysed, before finally reacting it with H₂A. The idea is that the washing removes the HCl in the pore water but retains the H⁺ on the sorption sites of the oxide surfaces. Firstly 10 g samples of sandstone were weighed and put into each of 12 centrifuge tubes. 0.04 l of 12.5 mM HCl (pH~2) was then added to each of the six centrifuge tubes.

These were then shaken for 1 h at 300 rpm and centrifuged for 10 min at 4500 rpm. 30 ml of the dilute HCl supernatant was removed by pipette and 10 ml kept for analysis of Mn and Fe. Then 30 ml of DIW (in order to keep the same volume of 40 ml) was added to the centrifuge tubes containing the sandstone and the latter centrifuged for 5 minutes. Again 30 ml of the DIW supernatant were removed by pipette and 10 ml kept to analyse for Fe and Mn. Another 30 ml of DIW was then added to the centrifuge tubes containing the sandstone. These were

put in a centrifuge for 5 minutes and around 36 ml were removed. This washing procedure means that the dilute HCl was diluted by 16 times, each sample containing around 4 ml of fluid in the pore space of the sediment. Finally 40 ml of various concentrations of H_2A (100, 75 and 50 ppm) were added to the washed and unwashed sandstone samples with two replications for each concentration. The very diluted HCl in the pore volume of the sediment will mean that the concentration of H_2A will be reduced by about 8% compared with unwashed samples. Finally all samples were put in a shaker for 15 h at 300 rpm, then centrifuged for 10 min at 4500 rpm, and the 10 ml samples filtered using 0.2 μm syringe filters. pH was measured for each sample in contact with sediment before acidification and after acidification for both washed and unwashed sandstone .

Finally each sample was acidified by using 150 μl of 0.5 M HNO_3 to drop the pH from around 3.8 to around 2. The washings samples for HCl and DIW were not acidified because they already had a low pH value.

Results showed (Figure 2.30 and Appendix 2.19) that the amount of Mn released from unwashed sandstone samples was higher by a factor of about 2.5 to 3 times than the washed samples. As explained above, washed samples dissolved significant amounts of Mn oxides which leads to a drop in concentration after washing. For Fe, washed samples had slightly higher concentrations than unwashed samples in spite of the washed samples having about 8% lower ascorbic acid concentrations (see below) (Figure 2.30). This indicates that the HCl-washed samples underwent slightly enhanced reductive dissolution of iron oxides. This was not as much as for the experiments of Figure 2.29 as the latter retained more acid as there was no DIW flushing. It suggested that H^+ enhances the reductive dissolution but that only at lower pHs is there direct dissolution of hematite by H^+ .

Analysis of the washing supernatant (Figure 2.31; Appendix 2.20) revealed that: the average Mn in the diluted HCl was 2.9 ppm; the first washing with deionised water contained 0.37 ppm; and the second washing contained no detectable Mn. No detectable Fe was present in either the HCl or the DIW washings. This means that this dilute concentration of HCl was not able to dissolve the iron oxides, but that attachment of H^+ on the surface of the oxides slightly accelerated the rate of reductive dissolution by H_2A suggesting that H^+ was retained on the oxide surfaces throughout the washings. Figure 2.32 compares washed and unwashed results in terms of Fe and Mn concentrations and pH. Despite much care the pH values were different between the washed and unwashed samples, the former being about one unit lower. Fe concentrations remain constant but Mn drop probably because of the initial dissolution during the washings.

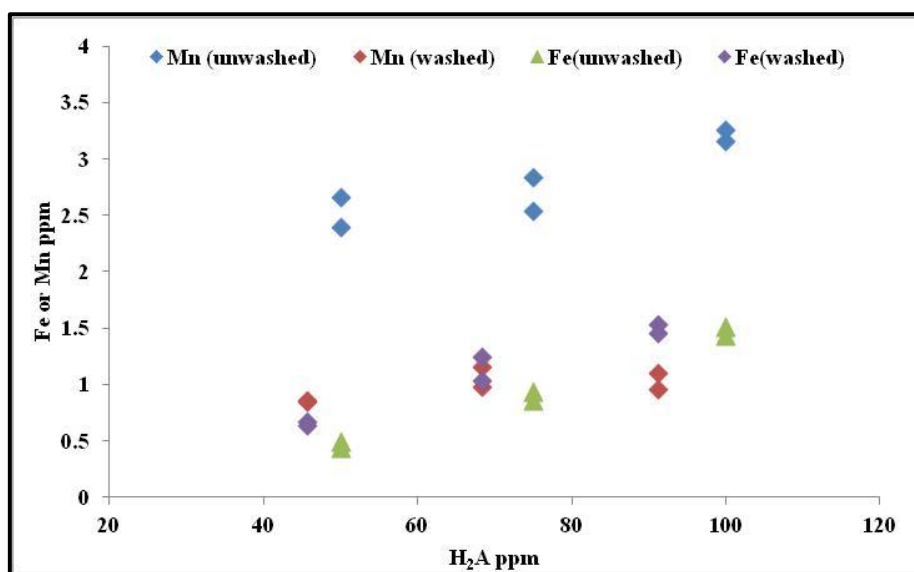


Figure 2-30: The amount of Fe and Mn released from unwashed and dilute HCl -washed sandstone by ascorbic acid.

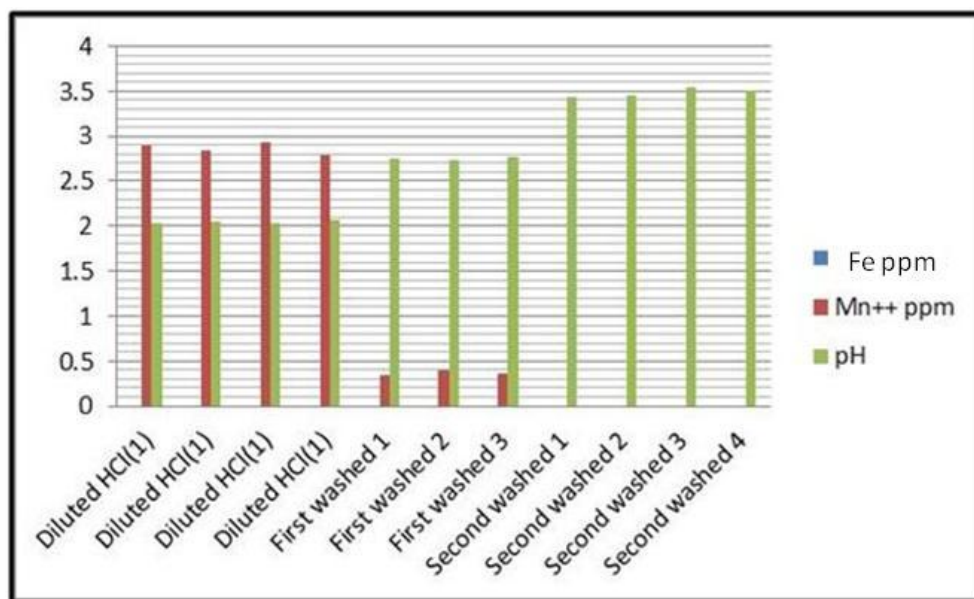


Figure 2-31: The variation of Fe and Mn concentration and pH in the washing supernatants.

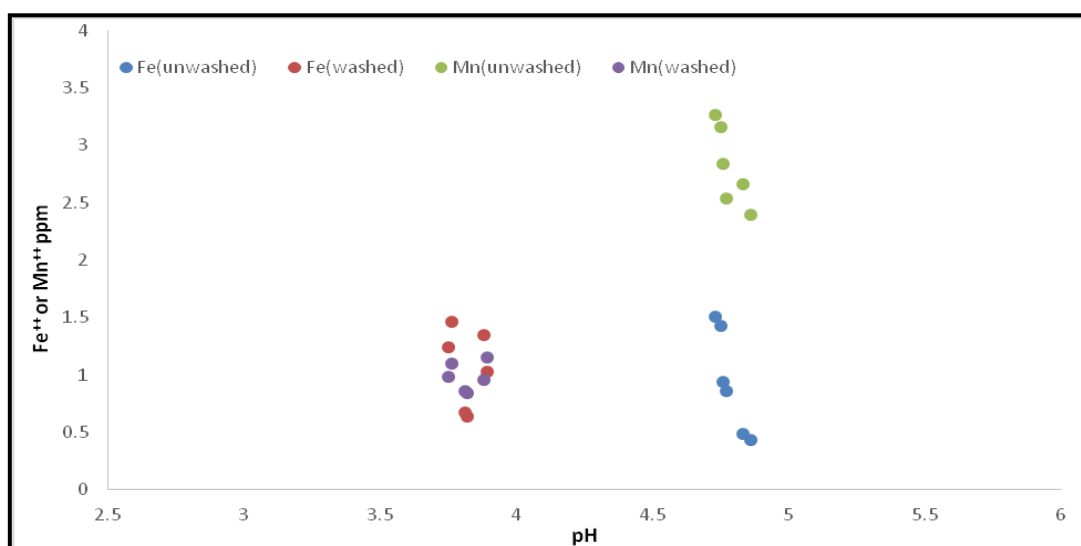


Figure 2-32: The relationship between pH and the concentration of Fe and Mn after H_2A contact with the sandstone for unwashed and HCl-washed sandstone samples.

2.5.3 Effect on reductive dissolution of saturation of the surface of the oxides with Ca^{++}

A final experiment on washing was carried out using $CaCl_2$. This was to see how much Ca^{++} sorption to the oxide surface would affect dissolution by H_2A . The same double DIW washing procedure was used as described above.

10 g mass of sandstone was weighed and put into each of six centrifuge tubes, then 40 ml of 4.12 mM calcium chloride (from $\text{CaCl}_2 \cdot 2\text{H}_2\text{O}$) solution was added to each tube. All samples were shaken for 1 h at 300 rpm to saturate the surface of oxides with Ca^{++} . Then the reactors were centrifuged for 10 minutes at 4500 rpm, and 30 ml of the supernatant removed keeping 10 ml for Fe and Mn analysis. Then 30 ml of DIW was added to keep the volume to 40 ml, centrifuged for 5 minutes, 30 ml of supernatant removed and a sample kept for analysis of Fe and Mn^{++} content. Then another 30 ml of DIW was added and centrifuged for 5 minutes. Then 36.5 ml of supernatant was removed and H_2A solution added to the 40 ml mark. The concentrations of H_2A were 100, 75 and 50 ppm each in duplicate. Both washed and unwashed samples were shaken for 16 h, and then centrifuged for 10 min at 4500 rpm, and aliquots of 10 ml filtered using 0.2 μm filters before analysing.

The Fe and Mn concentrations after contact with the H_2A are shown in Figure 2-33 (data in Appendix 2.21). It is clear that washing with Ca^{++} solution has an effect on both Fe and Mn^{++} concentrations. Fe concentrations in the washed samples are very low. Presumably the Ca^{++} sorbed to the oxide surface reduces the interaction of the H_2A with the surface. However the washed samples ended up with higher pHs so may be this is the main effect. For unwashed samples much more Fe is released. No measureable Fe was released in the washings (see appendix 2.22). The same general relationship is seen with Mn, but this has been the case in previous experiments and is explained by the washing removing the finite amount of Mn^{++} available. This is supported by the data on washing concentrations shown in Figure 2.34 as they decrease a lot with each washing and are undetectable in the final washing. Figure 2.35 shows the relationship between pH and concentrations of Mn^{++} and Fe. It is clear that there is a close similarity of range of pH between washed and unwashed sandstone samples, the variation between them not exceeding 0.5 pH units.

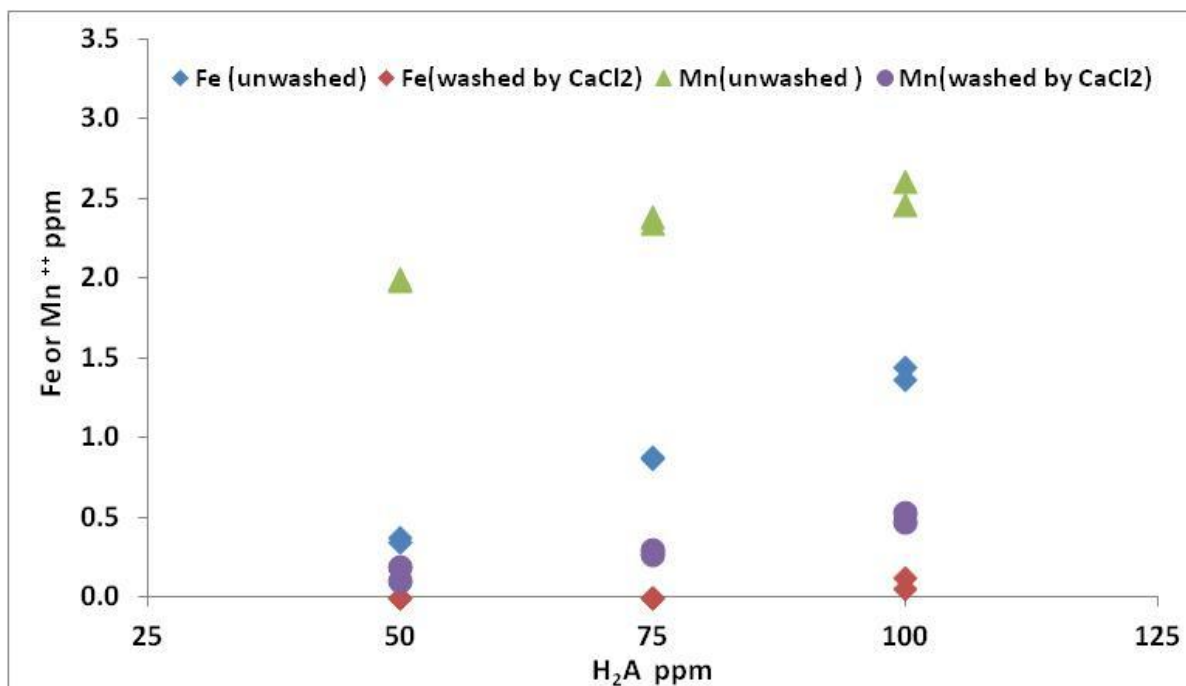


Figure 2-33: Concentrations of Fe and Mn⁺⁺ released by contact of ascorbic acid with unwashed sandstone samples and CaCl₂-washed sandstone samples.

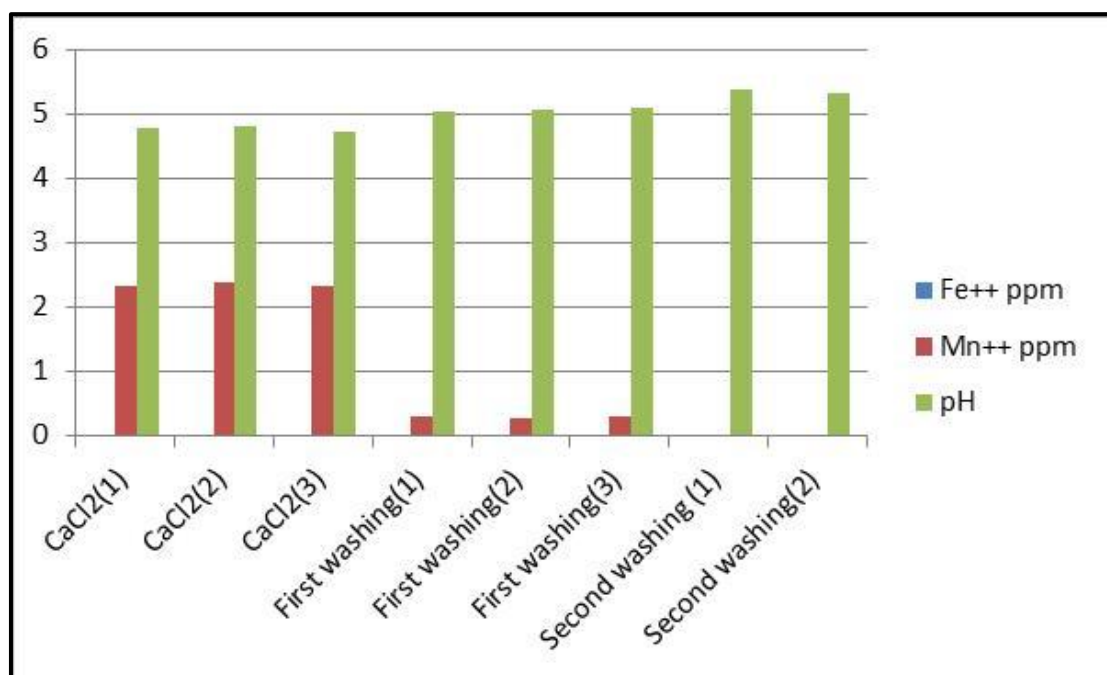


Figure 2-34: The variation of Fe and Mn⁺⁺ concentration and pH in the washing supernatants. All Fe concentrations are below detection limit.

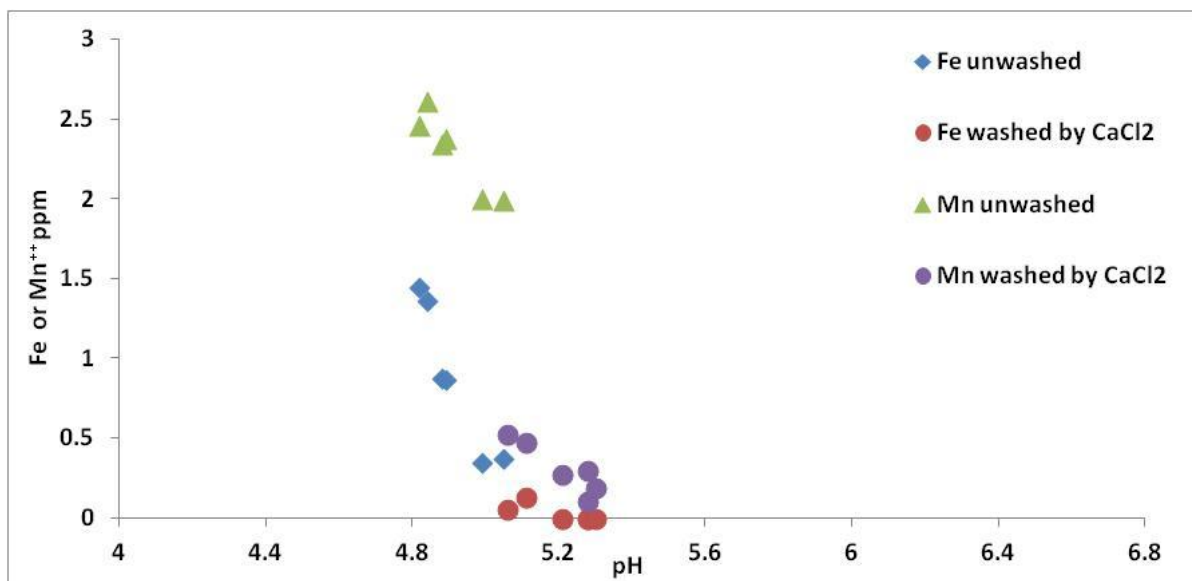


Figure 2-36: Concentrations of Fe and Mn^{++} as a function of pH for unwashed and CaCl_2 -washed sandstone.

2.6 Summary and Conclusion

At high $[\text{H}_2\text{A}]$ and high temperatures, H_2A appears to dissolve Fe and Mn oxides reductively, as both $[\text{Fe}]$ and $[\text{Mn}]$ rise during the experiments. Also the results revealed filtering and acidifying have a negligible effect on Fe and Mn^{++} concentrations. Fe concentrations are greater than Mn^{++} concentrations in low water rock ratio (500ml / 1 or 10 g). It was found that Fe and Mn^{++} concentrations increased with increased temperature, sandstone mass, and H_2A concentration and decreased with increased O_2 and increased pH. The rate of rise of concentration of Fe decreases slowly with time where there is limiting sandstone mass or H_2A concentration especially, but over limited time intervals the rate can appear linear. The rate can be related to temperature using the Arrhenius equation, but the results are specific to the conditions of the experiment and cannot be applied elsewhere. Rise in Mn^{++} concentrations appears to flatten off earlier than Fe. TOC measurements suggest a small amount of degradation of H_2A occurs.

At low $[H_2A]$ experiments at lab temperature shaking the reactors considerably increases the concentrations measured. With appropriate water/rock ratio (e.g. 40 ml/10g) and time, low (<0.6 mM) concentration H_2A reductive dissolution of sandstone Fe and Mn oxides can be measured even over short periods (e.g. 2 h) with shaking. Under these conditions Mn^{++} concentrations are measurable even in the absence of H_2A . Mn concentrations are greater than Fe concentrations at least for short times. Concentrations change with $[H_2A]$ concentration, pH and initial condition (protonated, Ca-rich) of the sandstone surface, but it is difficult to distinguish Ca effects and pH effects. Also HCl in the absence of H_2A resulted in some dissolution.

In summary H_2A reductively dissolves Fe and Mn oxides from the sandstone samples, but the final experiments should have appropriate water/rock ratio (e.g. 40 ml/10g), have $[H_2A]$ of up to 0.6 mM, be anaerobic, be shaken, do not need filtering and consider initial sandstone surface composition and pH.

Chapter Three

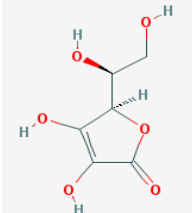
The Analysis of Ascorbic Acid Using the Reduction of KMnO_4

3.1 Introduction

The main goal of this project was to determine the oxidising capacity and mechanisms of red sandstone. Therefore a method must be found to quantify the dissolved concentration of the organic carbon compound, and this is the subject of this chapter. The aim of the work described in this chapter is therefore to develop an analysis method for ascorbic acid.

Ascorbic acid (also generally known as vitamin C) ($\text{C}_6\text{H}_8\text{O}_6$) is an organic acid and an important reducing agent (Elmagirbi et al., 2012). It is essential for humans, lack of ascorbic acid resulting in serious diseases like scurvy (Ball, 2006). There are several reasons for choosing ascorbic acid to represent dissolved organic carbon in this project. Firstly, it is a simple organic carbon compound, which is easily dissolved in water; secondly, it has types of functional groups present in humic acids (carboxyl, hydroxyl); thirdly, experiments have previously been carried out on ascorbic acids using synthetic iron oxides, showing that there is a strong interaction and also providing a baseline against which to test the experiments involving geologically ancient iron oxides; fourthly, it is cheap, environmentally friendly, and does not impose any significant hazards during lab work (Elmagirbi et al., 2012). Table 3.1 gives some details of the general chemical properties of ascorbic acid.

Table 3-1: Some chemical and physical properties of ascorbic acid

Properties		Sources
Molecular Formula	$C_6H_8O_6$	(Ball,2006)
Molecular Weight	176.12 g/mol	
Structure		
Physical Description	White to slightly yellow powder	(Ball, 2006)
<u>Melting Point</u>	190 °C	(Ball, 2006)
<u>Solubility in water</u>	330 g/l at 25°C	(Kuellmer and Othmer, 2001) and (Ball, 2006)
<u>Density</u>	1650 kg/m ³	(Lide, 2007)
pH	pH = 3 (5 g/l); pH = 2 (50 g/l)	(Crawford and Crawford,1980), (Ball, 2006)
<u>pK_a</u>	pK ₁ =4.17 ,pK ₂ = 11.79 pK ₁ = 4.17 and pK ₂ = 11.57	(Ball, 2006) (O'Neil, 2006)

H₂A is used here as the symbol for ascorbic acid. Bhagavan (2001) points out that there are three main factors that enhance the oxidation of ascorbic acid: rise in temperature; presence of cations; and exposure to high intensity light.

There are various methods and techniques for determination of ascorbic acid concentration, for instance: spectrophotometrically (Güçlü et al., 2005; Fadhel, 2012); using liquid chromatography (Kall and Anderson, 1999; Iwase and Ono, 1998); using cyclic voltammetry (while Pisoschi et al, 2008); using oxidant titration (Mussa and El Sharaa, 2014).

Most of the methods listed above were not available for the current study and so several alternative methods were initially trialled. Several unsuccessful trials were made to analyse ascorbic acid using total organic carbon (TOC) determination. Fluorescence measurements

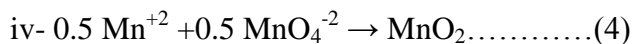
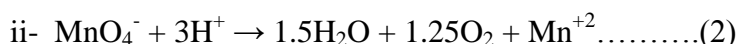
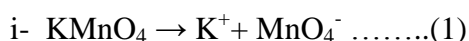
were also unsuccessfully attempted. Finally, uv sepectrophometry gave promising results when the decrease in absorption of potassium permanganate (KMnO₄) solutions was measured in the presence of ascorbic acid, essentially the method of Güçlü et al. (2005) and Fadhel (2012).

The rest of this chapter gives more explanation and detail of the development and testing of the spectrophotometric KMnO₄ method used to measure the concentration of ascorbic acid.

3.2 KMnO₄ solutions at equilibrium

The spectrophotometric method relies on the measurement of Mn(VII) in solution. As H₂A is oxidised by Mn(VII), the absorbance of Mn(VII) drops, and this can be calibrated to determine the amount of H₂A initially present. Details are provided later. Mn(VII) has a characteristic sorption wavelength of 530 nm (Fadhel). If in solution KMnO₄ gradually breaks down to produce Mn species of other oxidation states, absorbance will change in the absence of H₂A. So it is needed to look at the chemistry of KMnO₄ in solution at equilibrium.

When KMnO₄ is dissolved in water, various reactions may occur, including (Zumdahl and Zumdahl (2014):



The phreeqc program (Parkhurst and Appelo, 1999) has been set up to check the dissolution of KMnO₄ in water at equilibrium at a wide range of fixed pH values varying from 3 to 8.5, in order to find out which Mn species are dominant when dissolution of KMnO₄ takes place. The calculations assumed 0.31 mol/kg H₂O KMnO₄, and a P_{O_2} of 0.2 bar to be similar to lab

analysis. The results are shown in Figure 3.1. They reveal that Mn(II) concentration decreases rapidly with increase in the pH. This means at equilibrium Mn (VII) would be present at extremely low concentrations at acidic pHs (see Appendix 3.1).

Preliminary measurements of KMnO_4 solutions gave significant absorbances (e.g. 1.5 the absorbance value for 100 ppm of KMnO_4). According to the phreeqc calculations, the KMnO_4 solutions used in the experiments had not reached equilibrium as the absorbance measured at the wavelength associated with Mn(VII) would have been extremely low.

To look at this in more detail, other experiments were carried out to measure the absorbance of KMnO_4 as a function of pH.

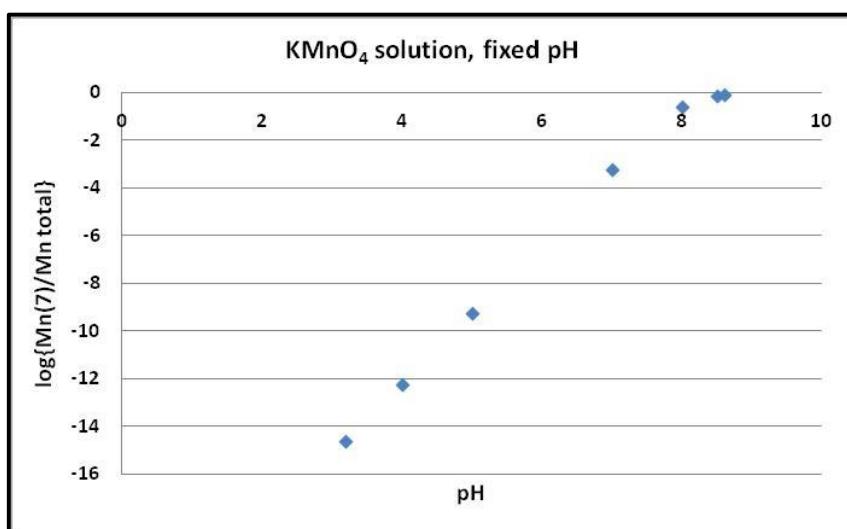


Figure 3-1: Modelling of KMnO_4 solutions at equilibrium using phreeqc.

3.3 The absorbance (A) as a function of pH in pure KMnO_4 solutions

The main aim of this experiment was to check the effect of variation of pH on the absorbance of KMnO_4 solutions. A 0.5 M solution of HNO_3 and a 76.25 Mm solution of NaOH were prepared and used to adjust the pH of the 100 ppm solution of KMnO_4 (see Appendix 3.2).

Results showed that pH has no effect on the absorbance of pure KMnO_4 solution, see Figure 3.2. This result confirms that reaction 2 does not occur significantly under the conditions

present during use in the laboratory. This result shows that corrections need not be made for pH when using KMnO_4 in the analysis of H_2A .

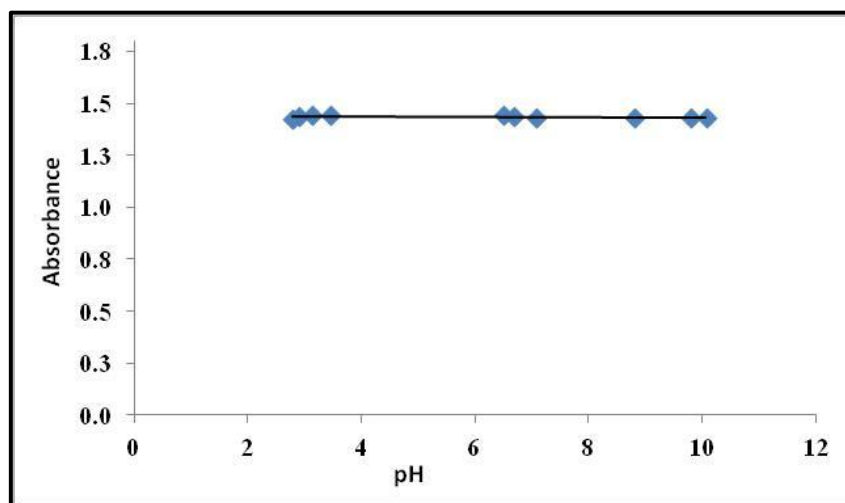


Figure 3-2: The absorbance of a 100 ppm solution of KMnO_4 at different final pH values.

3.4 The absorbance of KMnO_4 solutions as a function of concentration

The absorbance of KMnO_4 was measured from 20 to 200 ppm (see Appendix 3.3). The 200 ppm solution of KMnO_4 has a dark purple colour, the intensity of which decreases linearly ($r^2=0.99$) with concentration as shown in Figure 3.3. Also the intercept of this plot goes through zero as expected by Beer's Law. The result is broadly similar to that obtained by Fadhel (2012), but with a slope lower than that obtained by Fadhel (2012). The absorptivity ($\epsilon=A/(bC)$, where b is cell length, C is concentration, A is absorbance (Swinehart, 1962) agrees well with values from the literature (Table 2.2). Interestingly, Fadhel (2012) reports a similar $\epsilon_{530\text{nm}}$.

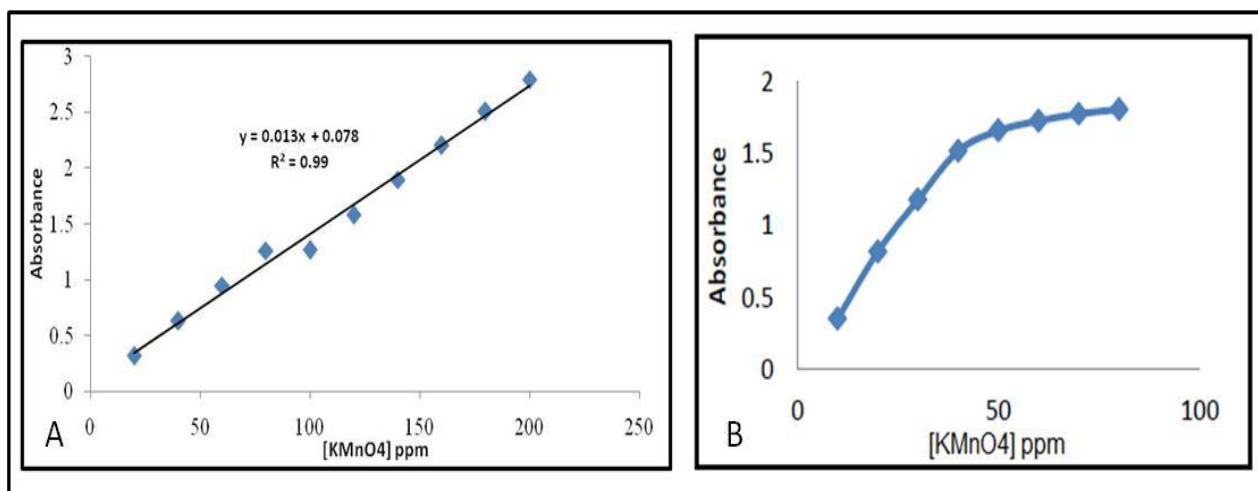


Figure 3-3: (A) Dependence of absorbance on $[\text{KMnO}_4]$ this study. (B) the relationship between $[\text{KMnO}_4]$ and absorbance obtained by Fadhel (2012).

Table 3-2: Values for absorptivity for KMnO_4 from the literature and this study.

No.	Absorptivity ϵ (L/mol/cm)	ϵ (nm)	Authors
1	2192	546	Ganesh et al. (2012)
	2279	526	Ganesh et al. (2012)
2	2356	530	Fadhel (2012)
3	2038	520	Bohman (2006)
4	2380	546	Stewart (1965) as cited in Gauger & Hallen (2012)
4	2400	526	Stewart (1965) as cited in Gauger & Hallen (2012)
4	1800	311	Stewart (1965) as cited in Gauger & Hallen (2012)
5	2100	530	This study

3.5 Reaction between KMnO_4 and H_2A

Based on the method of Fadhel (2012), 5 ml of different concentration solutions of H_2A (100 to 20 ppm) were mixed with 5 ml of 100 ppm of KMnO_4 . Within 1 minute the absorbance of the mixture was measured at 530 nm with three replicates for each sample. The absorbance values for the $\text{H}_2\text{A}+\text{KMnO}_4$ mixtures increased linearly with decline of ascorbic acid concentration as expected from Beer's Law with an excellent correlation coefficient ($r^2 = 0.99$), as shown in Figure 3.4 a & b. The slope of the calibration plots are around 25% of those obtained by Fadhel (2012) (Figure 3.4 (C)), but it has been noted above that there is a discrepancy between Fadhel's (2012) data and absorptivity values. The precision of this method for example for 100 ppm of H_2A is ± 1.69 mg/L and for 20 ppm is ± 0.61 mg/l, based on the standard deviation of repeat measurement data on standards before and after experiments.

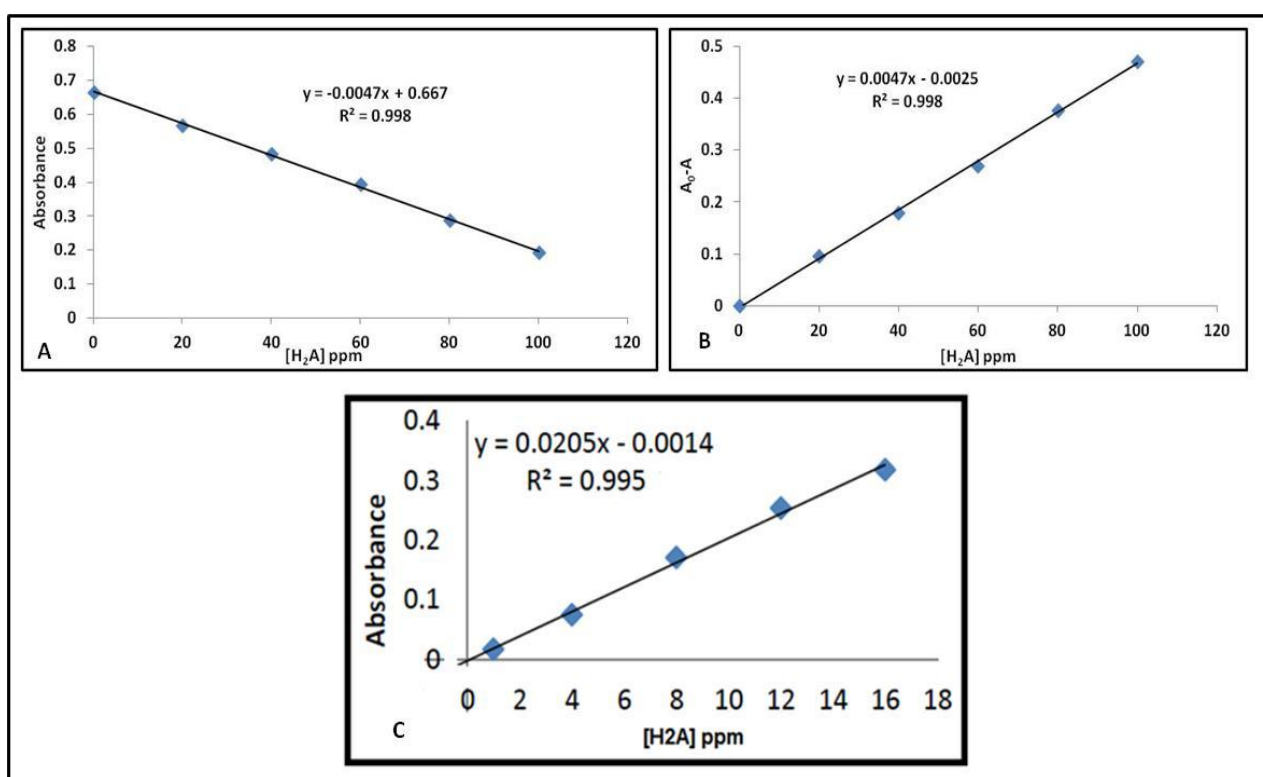


Figure 3-4: (A) absorbance against $[\text{H}_2\text{A}]$; (B) absorbance change against $[\text{H}_2\text{A}]$; (C) calibration curve from Fadhel (2012).

The reaction between ascorbic acid and KMnO_4 suggested by Babatunde (2008) is:



In order to investigate if the above reaction took place, KMnO_4 / absorbance (A) and $[\text{H}_2\text{A}]$ / absorbance relationships have been compared (Figures 3.3 a & 3.4 a).

The plots show that the absorbances are linearly related:

$$A=m_1[\text{KMnO}_4]_{\text{ppm}}+C_1; A=m_2[\text{H}_2\text{A}]_{\text{ppm}} +C_2$$

where m is a gradient and C an intercept.

$$\therefore dA/d[\text{KMnO}_4]_{\text{ppm}} = m_1; dA/d[\text{H}_2\text{A}]_{\text{ppm}} = m_2$$

$$\therefore d[\text{KMnO}_4]_{\text{ppm}} /d [\text{H}_2\text{A}]_{\text{ppm}} = m_2/m_1 ,$$

From the data, slope $m_1= 0.0133/ \text{ ppm}$, and slope $m_2= 0.0047$

$$\therefore d[\text{KMnO}_4]_{\text{ppm}}/d[\text{H}_2\text{A}]_{\text{ppm}} = 0.0047/0.0133= 0.353$$

$$\therefore d[\text{KMnO}_4]/d [\text{H}_2\text{A}] \text{ (i.e. ratio in molar terms)} = 0.353(176.1/158.1)=0.394$$

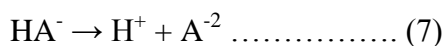
The expected ratio is $2\text{MnO}_4^-/5\text{H}_2\text{A}$ (Reaction (5)) $=2/5= 0.4$.

Hence the experimental results are consistent with Reaction 5.

In addition, measurement the pH of each H_2A solution before and after adding KMnO_4 was made, and the change of $[\text{H}^+]$ calculated (see Table 3.3). Figure 3.5 shows the relationship between $[\text{H}_2\text{A}]_{\text{ppm}}$ and change of $[\text{H}^+]$. The drop in $[\text{H}^+]$ is much less than predicted by Reaction (5)($d[\text{H}^+]/d[\text{H}_2\text{A}] = 1.2$ compared with observed value of 0.14). This may be because H_2A buffers the pH change by dissociating to HA^- as follows (Benelli, 2015):



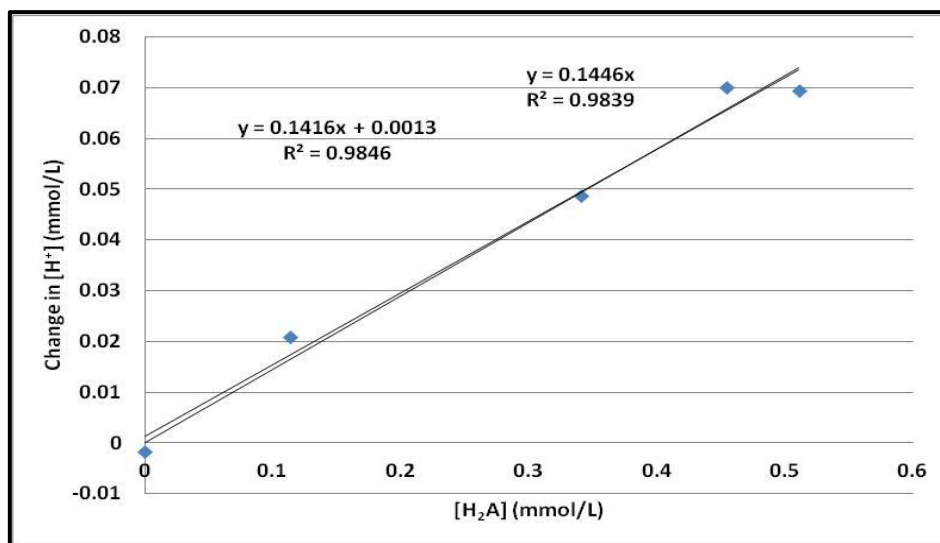
($\text{pK}_1 = 4.17$; Domitrović, 2006)



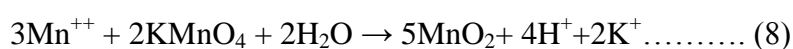
($\text{pK}_2 = 11.8$ so less important; Domitrović, 2006)

Table 3-3: pH of [H₂A] solutions before and after adding KMnO₄

H ₂ A ppm	pH before adding KMnO ₄	pH after adding KMnO ₄	Δ [H ⁺] mmol/l
90	3.8	4.05	0.06936
80	3.82	4.09	0.07007
60	3.94	4.18	0.04874
20	4.21	4.39	0.02092
0	5.6	5.37	-0.00175

**Figure 3-5:** H⁺ change (positive is rise) after adding KMnO₄ as a function of [H₂A] initially present in solution.

After taking the measurement of absorbance of ascorbic acid with KMnO₄, the solutions were left for one day. It was found that a brown or black precipitate formed especially in the cases of higher [H₂A] like 90 and 100 ppm. This indicates MnO₂ precipitation has occurred. No precipitate was visible for the initial hours of reaction or for the lower H₂A concentrations even if left for long time (more than 24 h) (see Table 3.4). It is assumed that the reaction is as follows (Kawamura (1991) as cited in USEPA (2001)):



This precipitation was insufficient to identify visibly other than in the most concentrated H_2A solutions and was not enough to spoil the relationship between H_2A and $KMnO_4$, presumably because there was insufficient time for the precipitation to occur (all the measurements were carried out no longer than 2 minutes after adding $KMnO_4$ to the ascorbic acid containing sample).

Table 3.4: Observations on particle formation in H_2A after addition of $KMnO_4$ and leaving for 24 h.

Samples $[H_2A]$ ppm	Form of precipitation of colloid in brown colour
90	yes
80	no
60	no
20	no
0	no

3.6 Effect of different $[KMnO_4]$ on the absorbance of ascorbic acid

The aim of this experiment was to find out the best $[KMnO_4]$ to measure the ascorbic acid concentration in range between 0 and 100 ppm. A range of H_2A solutions were prepared (100, 80, 60, 40, 20, 0 ppm) along with two $KMnO_4$ solutions (100 and 40 ppm). 5 ml of each H_2A solution were added to 5 ml of the 100 ppm $KMnO_4$ solutions, and the mixtures then shaken by hand for less than 30 seconds before measuring the absorption at 530 nm. The results (Figure 3-6; Table 3-5 and appendix 3.4) demonstrated that there is an increase of absorption with decline of $[H_2A]$ for both $KMnO_4$ concentrations, but the slopes are identical (both have the same value = -0.0047 /ppm). As long as $KMnO_4$ is in excess, i.e. there is enough to oxidise the H_2A present, the concentration of $KMnO_4$ is not important, as might be expected: the slope is a direct function of the stoichiometry of the reaction, so the reaction appears to remain the same independent of the initial $KMnO_4$ concentration. In conclusion the reaction is independent of $[KMnO_4]$, but it is better to use the higher $[KMnO_4]$ (100 ppm)

concentrations of H_2A up to 100 ppm are to be used. Also to avoid lower absorbance values when using 40 ppm of KMnO_4 especially with relatively high concentration of ascorbic acid.

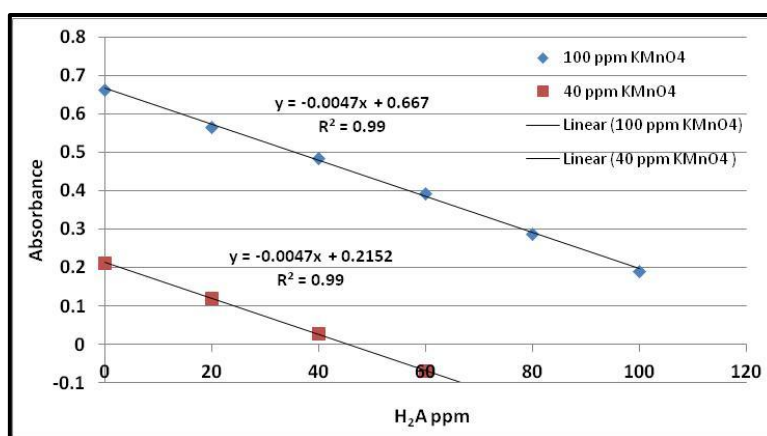


Figure 3-6: Measurements of the absorbance of H_2A using 100 ppm of KMnO_4 and using 40 ppm KMnO_4 .

Table 3-5: Variation in colour for different $[\text{H}_2\text{A}]$ in presence of 40 and 100 ppm of KMnO_4

$[\text{H}_2\text{A}]$ ppm	Colour of mixture using 40 ppm KMnO_4	Colour of mixture using 100 ppm KMnO_4
100	colourless	colourless
80	colourless	Very pale yellow
60	colourless	Pale yellow
40	pale yellow	Dark yellow
20	pink	Pink
0	pink	Pink

3.7 Effect of Fe on the measurement of $[\text{H}_2\text{A}]$

3.7.1 Effect of adding Fe(III) to KMnO_4

Fe was expected to be released when H_2A is placed in contact with sandstone, and therefore it is appropriate to determine if Fe affects the measurement of H_2A . Both Fe(III) and Fe(II) are examined because Fe(III) could be present if low pH experiments are undertaken and if Fe(III) is initially released from the haematite. The aim of this experiment therefore was to find out if there was any effect of the presence of Fe(III) on the reaction between KMnO_4 in the absence of H_2A . Ferric iron solutions were prepared from Fluka Fe standard solutions, added to both 100 and 40 ppm solutions of KMnO_4 and the absorbance measured at 530 nm.

The results from both KMnO_4 concentrations showed (Figure 3.7) that there is insignificant difference in absorbance between control samples free from ferric iron and samples containing various Fe(III) from 1 to 10 ppm (see Appendix 3.5 a & b). This result is as expected, as KMnO_4 cannot oxidise Fe(III) as the latter is already in its most oxidised form.

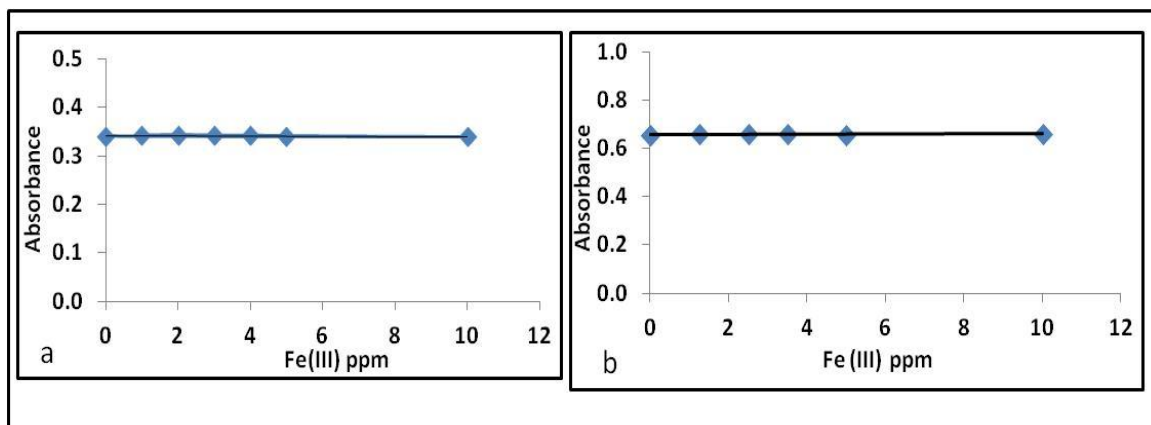


Figure 3-7: The effect on absorbance of KMnO_4 solutions by various concentrations of Fe(III) . (a) 40 ppm of KMnO_4 ; (b) 100 ppm of KMnO_4 .

3.7.2 $\text{KMnO}_4 + \text{Fe(III)} + \text{H}_2\text{A}$

Another Fe(III) experiment was also carried out, this time in the presence of ascorbic acid (see Appendix 3.6). The absorbance of various $\text{H}_2\text{A}/\text{KMnO}_4$ solutions was measured in the presence of 0 and 4 ppm Fe(III) . The results (Figure 3.8) showed that ferric iron has no effect.

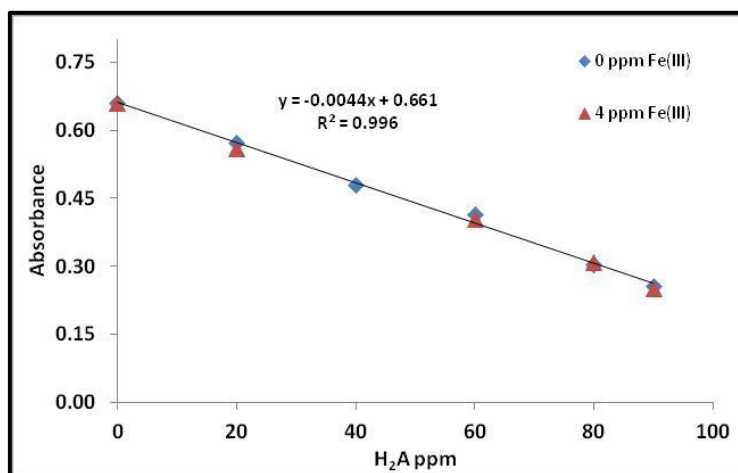
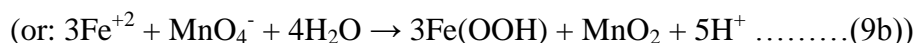


Figure 3-8: The effect of addition of 0 and 4 ppm of Fe(III) on absorbance of $\text{KMnO}_4 / \text{H}_2\text{A}$ solutions.

3.7.3 $\text{KMnO}_4 + \text{Fe (II)}$

The aim of this experiment was to study effect of the presence of ferrous iron (FeII) on the absorbance of KMnO_4 solutions. The ferrous solutions were prepared from ferrous chloride tetrahydrate salt ($\text{FeCl}_2 \cdot 4\text{H}_2\text{O}$) (Appendix 3.7).

Results of this experiment (Figure 3-9) revealed that there is a slight drop of absorbance with increase of Fe(II) in solution. This means that there is a reaction between KMnO_4 and ferrous iron, thus reducing the absorbance of KMnO_4 at 530 nm. The likely reaction is (EPA, 2001):



The maximum measure amount of Fe released during the sandstone/ H_2A reduction experiments did not exceed 4 ppm (see Chapter 6). Therefore the effect of Fe(II)/ KMnO_4 reaction on the interpreted H_2A would be less than, and mostly much less than, 4% in terms of H_2A concentration.

Because absorbance falls, it seems that colloidal $\text{Fe}(\text{OH})_3$ (or other FeIII oxide or hydroxide – similar stoichiometry) (and colloidal MnO_2)(Reaction 9) does not seem to be causing an increase in absorbance; in addition, the excellent repeatability of the measurements of the absorbance (replicates R_1 , R_2 , R_3) suggests that colloidal particles are not involved.

Measured pHs show that there is a drop of pH after adding the Fe^{++} , as shown in Figure 3.9 b. The relationship between change in H^+ and (change in) Fe^{++} concentration is linear with a high correlation coefficient ($r^2=0.97$). This result would be surprisingly well for a reaction that involves precipitation. Also it is observed that the pH falls during this reaction as

expected from Reaction 9, but by less than this reaction would suggest (observed $d[H^+]/d[Fe] = 0.8-0.9$, expected rate from Reaction 9 = 1.67).

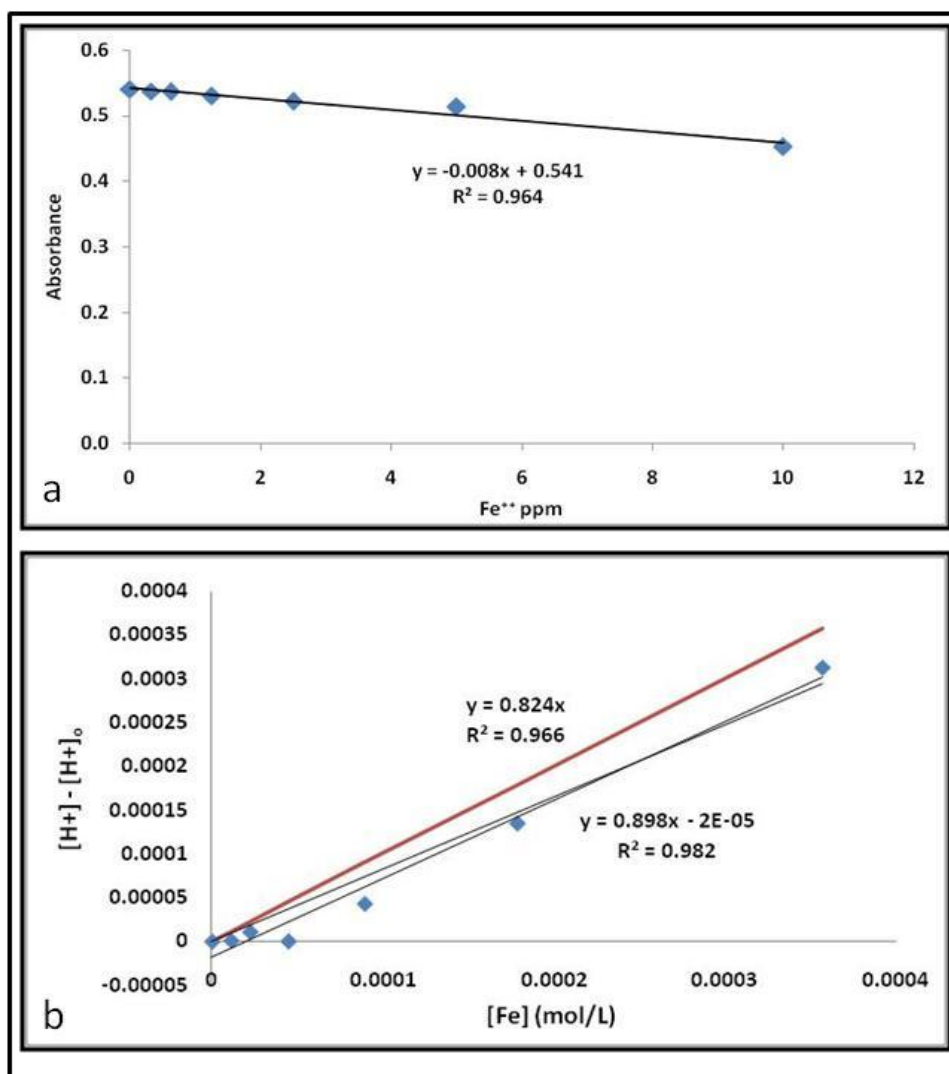


Figure 3-9: Effect of ferrous iron on $KMnO_4$ solution absorbance. a) Plot of absorbance against $Fe(II)$ concentration. b) Change in $[H^+]_{mol/L}$ plotted against $[Fe^{++}]_{mol/L}$. Red line is 1:1 line.

Looking at the $Fe/KMnO_4$ stoichiometry of Reaction 9 using the experimental data (Figure 3-9), it is possible to express on absorbance in presence of ferrous iron with this equation

$$A = -0.008[Fe]_{ppm} + 0.5416$$

and from previous experiments (Figure 3-3) absorbance as a function of $[KMnO_4]$ can be expressed as

$$A = 0.013 [\text{KMnO}_4]_{\text{ppm}} + 0.078$$

Assuming that all added Fe^{+2} reacts with KMnO_4 , a given addition of Fe^{+2} will cause a change in absorbance ($=\Delta A$) of $-0.008\Delta[\text{Fe}]_{\text{ppm}}$, where $\Delta[\text{Fe}]$ is the amount of Fe added. This ΔA is caused by a change in $[\text{KMnO}_4]$, and this $\Delta[\text{KMnO}_4]$ can be calculated knowing that $\Delta A = 0.0133 \Delta[\text{KMnO}_4]_{\text{ppm}}$.

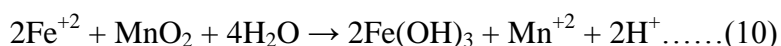
$$\text{Hence } \Delta[\text{KMnO}_4]_{\text{ppm}} = \Delta A / 0.013 = -0.0083\Delta[\text{Fe}]_{\text{ppm}} / -0.013.$$

$$\text{Hence } \Delta[\text{KMnO}_4]_{\text{ppm}} = 0.624 \Delta[\text{Fe}]_{\text{ppm}}, \text{ or}$$

$$\Delta[\text{KMnO}_4] = 0.624 \times 56/158 \Delta[\text{Fe}] = 0.221 \Delta[\text{Fe}].$$

Hence $[\text{Fe}]:[\text{KMnO}_4]$ (molar) ratio from this experiment, assuming all Fe reacts, is 4.5:1 ($=1/0.221:1$). However, according to Reaction 9 the ratio should be 3:1. The implication is that not all the added Fe^{+2} reacts with KMnO_4 . Thus the stoichiometry does not seem to agree with Reaction 9, either from the $\text{Fe}:\text{KMnO}_4$ or $\text{Fe}:\text{H}^+$ point of views.

However, Fe^{+2} is also likely to react with MnO_2 quickly, according to the following reaction (Thornton et al., 2011):



In this case the $\text{Fe}:\text{KMnO}_4$ ratio rises to 5:1, which may be close enough to explain the calculated 4.5:1 ratio. This would also mean less colloidal MnO_2 , agreeing with the lack of experimental evidence for colloids production. With Reaction 10 also occurring, the predicted $d[\text{H}^+]/d[\text{Fe}]$ becomes $7/5 = 1.4$. Presumably the Mn^{+2} does not then react significantly with the MnO_4^- , or else the ratio would go back down to 3:1. The observed $d[\text{H}^+]/d[\text{Fe}]$ is still too low (0.8-0.9) suggesting that Reactions 9 and 10 are not the complete story, and again may be $\text{H}_2\text{A}/\text{HA}^-$ adjustment is occurring.

Presumably Reaction 8 would also occur given enough time (Section 3.5) .

3.7.4 $\text{KMnO}_4 + \text{H}_2\text{A} + \text{Fe(II)}$

The aim of this experiment was to find out the effect of adding ferrous iron on the absorbance of ascorbic acid in the presence of KMnO_4 , and therefore the effect on interpreted $[\text{H}_2\text{A}]$.

Concentrations of H_2A ranging from 0 to 100 ppm were used, with Fe concentrations of 0, 1 and 4 ppm (see appendix 3.8).

The results are shown in Figure 3.10 (see also Appendix 3.9 & 3.10). It is clear from the results that there is only slight increase of absorbance of all samples in case of the 4 ppm Fe^{+2} experiments in comparison with the absorbance seen in the experiments with $[\text{Fe}^{+2}] = 0$. The average $dA/d[\text{Fe}^{+2}]$ for all H_2A concentrations (Figure 3.10b) is 3.3×10^{-4} /ppm. This is equivalent to a difference in interpreted $[\text{H}_2\text{A}]$ of 0.25 ppm. This is further represented graphically in Figure 3.11.

In conclusion, these experiments have confirmed the conclusion of Section 3.7.3 that the presence of $[\text{Fe}^{+2}]$ has no significant effect on the absorbance of H_2A hence there is no need to correct measurement of $[\text{H}_2\text{A}]$ for the presence of released Fe. In fact the effect of Fe(II) even less in the presence of H_2A than in its absence (compare between the results here with those from Section 3.7.3).

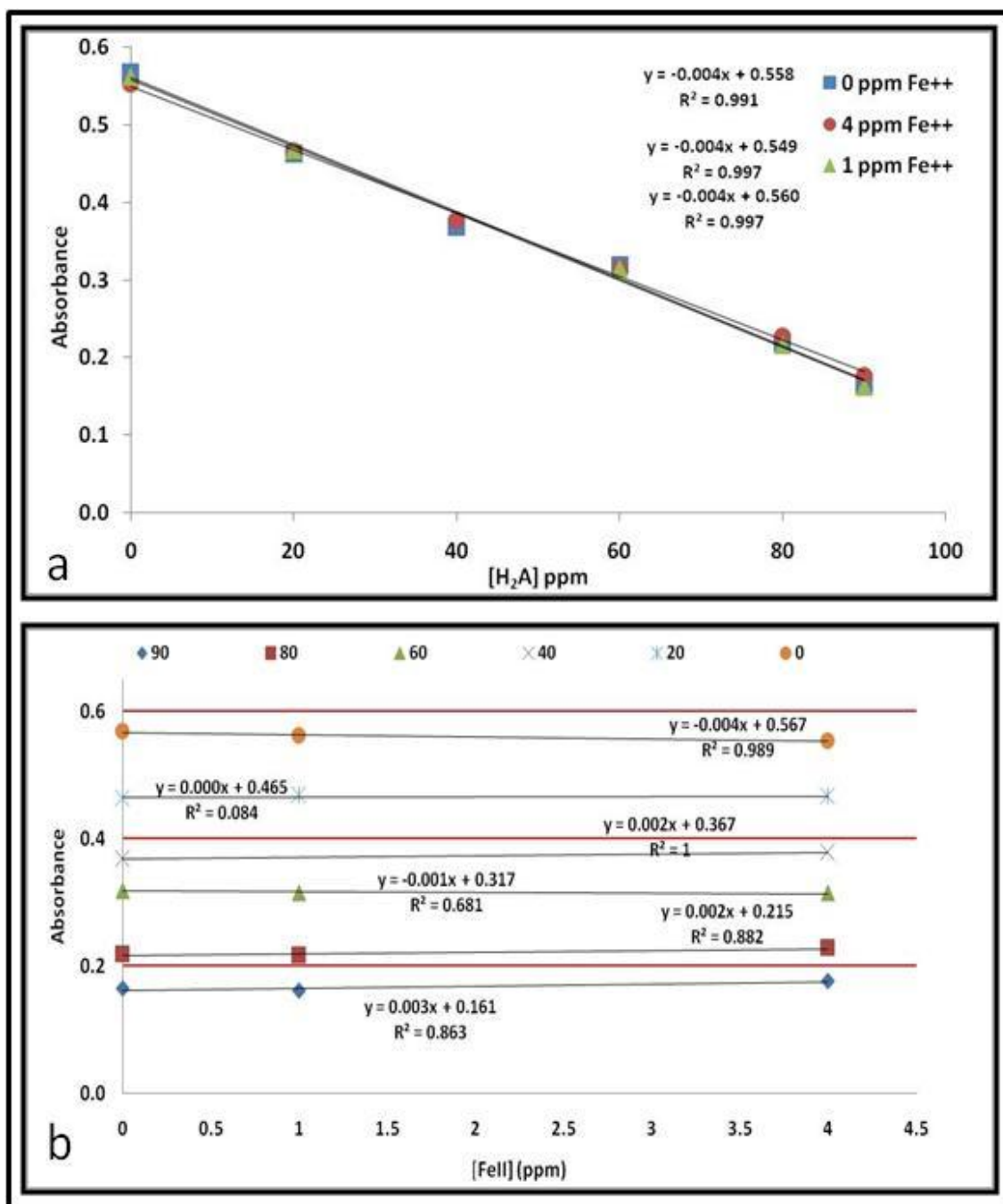


Figure 3-10: Addition of Fe^{+2} to $KMnO_4$ solutions in the presence of H_2A : a) Absorbance against $[H_2A]$ ppm; b) absorbance against $[FeII]$ for each $[H_2A]$.

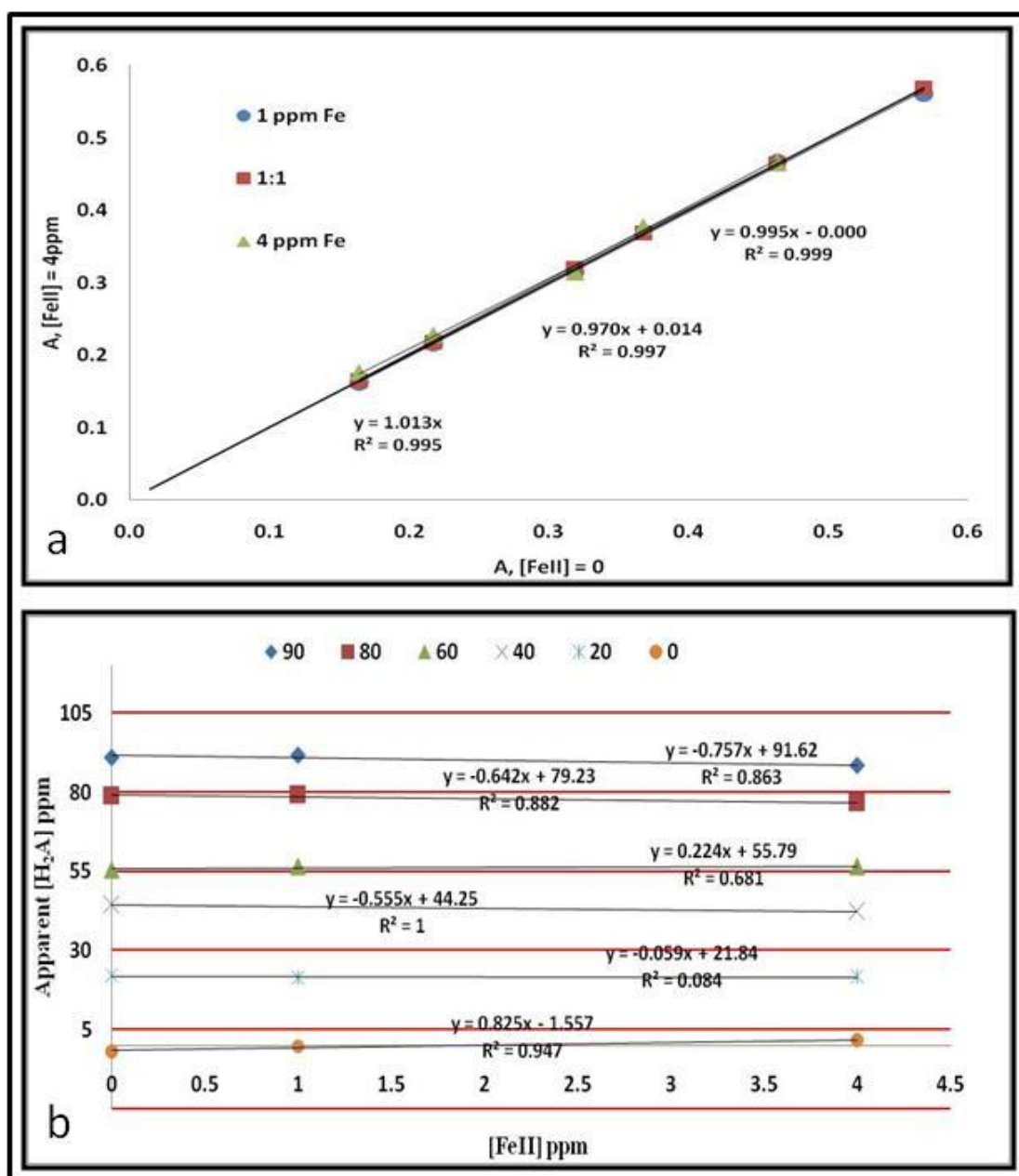


Figure 3-11: Addition of Fe^{+2} to $KMnO_4$ solutions in the presence of H_2A : (a) Absorbance for $[FeII]=0$ against A for $[FeII] = 1$ and 4 ppm; (b) apparent $[H_2A]$ (ppm) against $[FeII]$ (ppm).

3.8 Effect of Mn^{+2} on measurement of $[H_2A]$

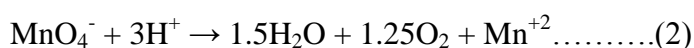
3.8.1 Effect of Mn^{++} on the absorbance of $KMnO_4$

A series of experiments has been carried out to study the effect of presence of Mn^{+2} , varying from 0.625 to 10 ppm, on the absorbance of $KMnO_4$ in the absence of ascorbic acid. The

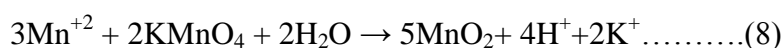
Mn(II) salt used was $\text{MnCl}_2 \cdot 4\text{H}_2\text{O}$ salt. Three replicates were used for each sample, as in previous experiments.

Results showed that there is a consistent and significant linear increase of absorbance with increase of $[\text{Mn}^{+2}]$, as shown in Figure (3.12 a) (see also Appendix 3.11). For example, the presence of 10 ppm of Mn led to a 22 % increase the absorbance in comparison with the absorbance of KMnO_4 in solutions free from Mn^{++} . The measurements are stable over the period of determination of the three measured values.

The most important observation here is that absorbance (A) increases with initial $[\text{Mn}^{+2}]$. A rise in absorbance might be caused by either a rise in MnO_4^- or by a rise in colloidal MnO_2 . These represented by Reaction 2 (in reverse direction)



and by Reaction 8



(Kawamura (1991) as cited in USEPA (2001)).

Though under the conditions of the experiments the theoretical equilibrium for Reaction 2 should be to right hand side, it has been shown that this reaction does not occur to any significant extent in the time length of the experiments. Calculations indicate that increase in Mn^{+2} does not reverse the direction of the reaction. It is therefore concluded that Reaction 8 is more likely. Harish and Manisha (2013) find that MnO_2 NPs have an absorption peak at 340nm, but Balan et al. (2013) find a large increase in absorbance over a range including 530nm as MnO_2 NPs form. Though takes 5-10 mins at $\text{pH} > 7$, may be still fast enough at the conditions here.

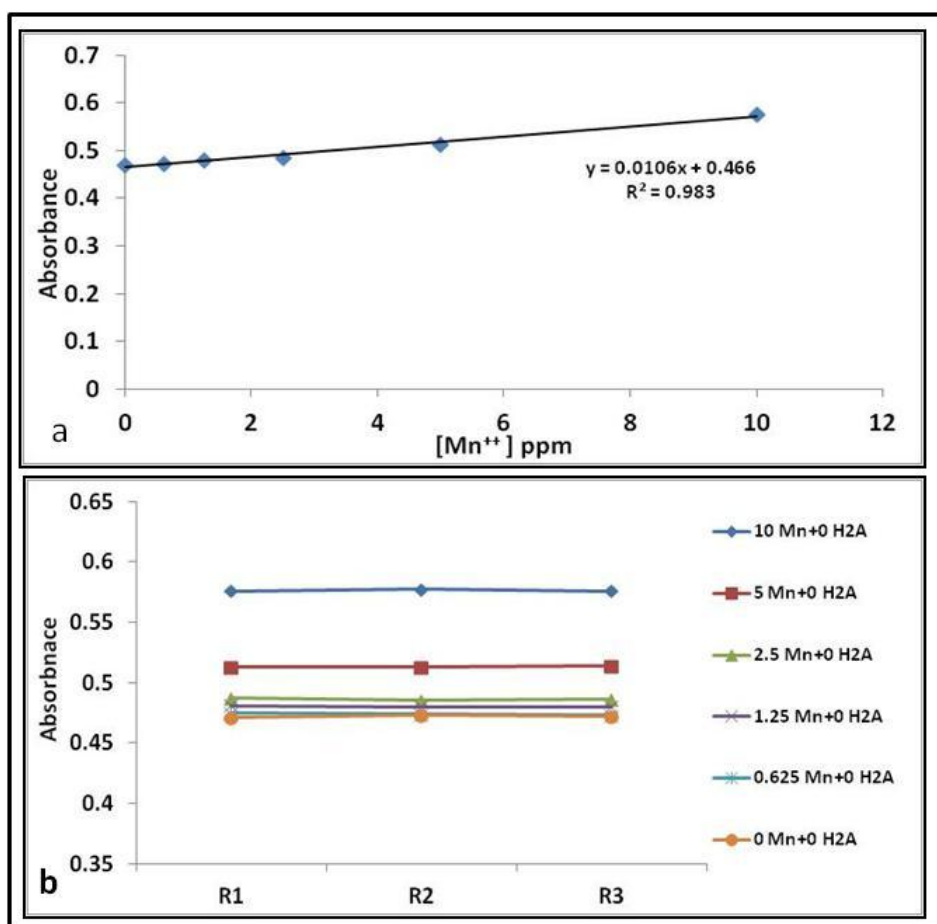


Figure 3-12: Addition of Mn^{+2} to $KMnO_4$ solutions. a) Absorbance against $[Mn^{+2}]$; (b) replicate absorbance measurements.

It is concluded that Mn increases absorbance by a rate defined by $dA/d[Mn] = 0.0106$ /ppm (Figure 3.12a). Need next to see if same relationship happens when there is H_2A in the solution.

3.8.2 Effect of $KMnO_4 + H_2A + Mn^{++}$

The goal of this experiment was to determine the effect of added Mn^{+2} on the absorbance of ascorbic / $KMnO_4$ solutions (see Appendix 3.12). The absorbance in the presence of 0, 1 and 4 ppm concentrations of Mn^{++} was measured. This range of concentrations covers the likely range of Mn released during the final sandstone leaching experiments, as indicated by preliminary test runs. The salt used was $MnCl_2 \cdot 4H_2O$.

It was found that the addition of Mn^{++} makes a significant difference to the absorbance as shown in Figure 3.13a (Appendix 3.13). As in the case of the H_2A -free solutions (Section 3.8.1), the absorbance are increased. Figure 3.13b (and Appendix 3.13) indicate the equivalent apparent decrease in interpreted H_2A as a result of the added Mn^{++} present. Figure 3.14 shows the relationship between absorbance change and added Mn^{++} concentration. Though there is some scatter (Figure 3.14a), the averaged relationship (Figure 3.14b) is very close to that seen in the absence of H_2A (Figure 3.12) as indicated also by Figure 3.15.

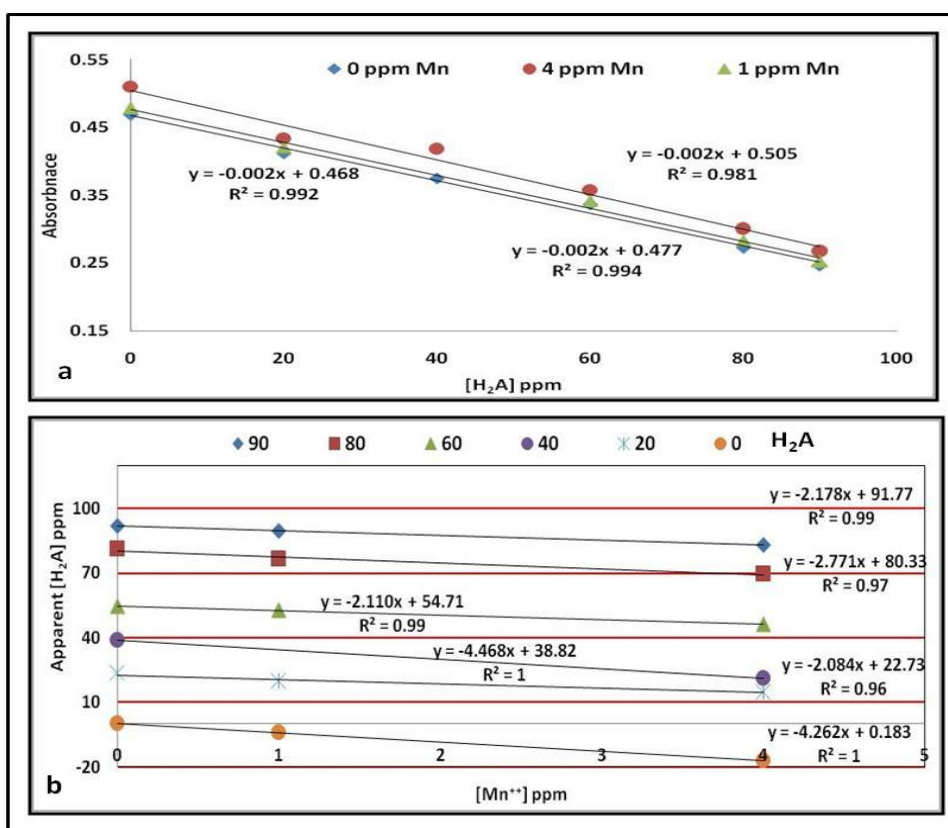


Figure 3-13: The effect of the addition of Mn^{++} on A. (a) the relationship between A and $[\text{H}_2\text{A}]$ for 0, 1 and 4 ppm $[\text{Mn}^{++}]$ under oxic conditions; (b) replotted in terms of interpreted $[\text{H}_2\text{A}]$ as a function of $[\text{Mn}^{++}]$.

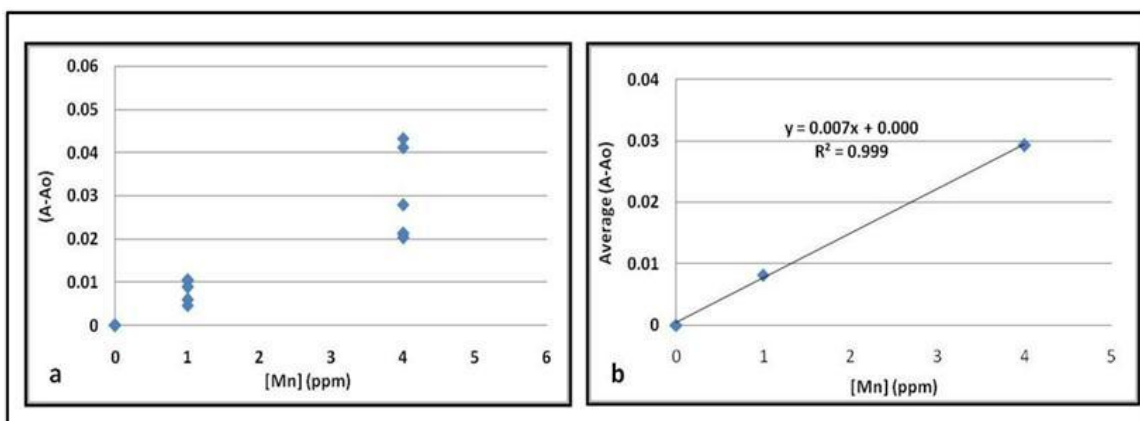


Figure 3-14: The dependence of $\{A_{[Mn]>0} - A_{[Mn]=0}\}$ for H_2A solutions in the presence of Mn (II) under oxic conditions. (a) all data; (b) data averaged for each $[Mn]$.

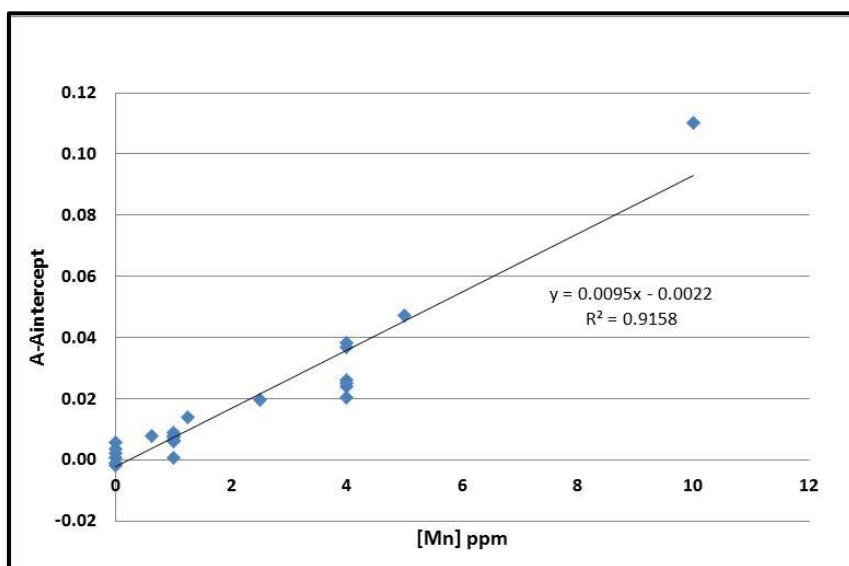


Figure 3-15: The dependence of A for all H_2A solutions investigated in the presence of Mn (II) under oxic conditions.

There was no significant difference in pH before and after adding $KMnO_4$, which ranged from 3.8 to 4.3 (see Appendix 3.14), except for the samples free from H_2A .

Leaving the mixture for about 24 h led to the formation of observable colloids of brown colour especially for the higher H_2A concentrations in the presence of 4 ppm of Mn, as shown in Table 3.6. This is consistent with the idea that MnO_2 is forming, the reason suggested in Section 3.8.1 for the increase in Absorbance.

Table 3.6: Observations on particle formation in H₂A solutions after adding 4 and 1 ppm of Mn⁺² after the solutions have been left for 24 h.

Samples [H ₂ A] ppm	1 ppm	4 ppm
	Form of precipitation of colloid in brown colour	
90	yes	yes
80	No	yes
60	No	yes
20	No	No
0	No	No

It concluded that Mn(II) in the test solution will give MnO₂ precipitation in colloids form, at first invisible but later aggregating enough to become visible. This causes the measured absorbance to be higher than expected, resulting in an apparently lower H₂A concentration.

2.8.3 Correcting H₂A Measurements for the Presence of Mn⁺⁺

Figure 3.15 shows the relationships between [Mn] and absorbance for all concentrations including [Mn]=0. This figure indicates that the rate of change of absorbance with [Mn] is similar for all [H₂A]. This hence suggest that correction for [Mn] can be done using the correlation equation indicated on Figure 3.15. The method used for correcting the data for the presence of Mn is

$$dA/d[Mn] = 0.0095 \text{ /ppm (Figure 3.15)}$$

$$dA/d[H_2A] = -0.0024 \text{ /ppm (Figure 3.13)}$$

$$\text{hence } d[H_2A]/d[Mn] = 0.0095/-0.0024 = -3.96 \text{ (ppm/ppm)}$$

i.e. when [Mn]=1ppm the measured value of [H₂A] will be decreased by 3.96 ppm.

It is noted that in this series of measurements that all the results have lower slopes for the A/[H₂A] plots than usually found. However, they are consistent across all experiments in the study of the effect of Mn (4, 1 and 0 ppm) and another experiment produced more usual

slopes with a final value of -3.58 ppm/ppm. So it concluded that -3.96 ppm/ppm, is the value for correction of presence of Mn on the concentration of H₂A .

3.9 The stability of ascorbic acid

The purpose of this experiment was to determine the apparent stability of ascorbic acid, as indicated by absorbance, over times comparable with experiments conducted later with sandstones under anaerobic conditions.

2 x 100 ml of H₂A were prepared at each of six concentrations (100, 80, 60, 40, 20, 0 ppm) and then split into two groups. Group one samples were put into an anaerobic chamber ('Glove Box' manufacture by Laboratory Products INC), while the second group of samples were retained under aerobic conditions. 5 ml samples were then collected from both groups at 4.5, 28, 52, and 126 hours. There was a slight difference of temperature between the experiments: the aerobic experiments were carried out under 21 °C, while the anoxic experiments were carried out at 24 °C. All experiments were done in triplicate. The times recorded were experimental time, but in reality times were about 2 hours greater because of preparation time for setting up experiments and analysis.

The results are shown in Figure 3.16 (see also Appendix 3.15). There is a slight increase of absorbance over time under both oxic and anoxic conditions for all H₂A concentrations. The solution free from H₂A (just KMnO₄) did not show any increase of absorbance over time, in fact a possible very small decrease.

Figure 3-16 shows the variation with time for aerobic conditions plotted as absorbance against time for each H₂A concentration and as absorbance against H₂A concentration for each time. There is little change with time. There is no pattern to change in slope with time or

concentration. However, overall averages indicate possibly a slightly increase in absorbance with time and therefore a slightly decrease in concentrations with time (Figure 3-17).

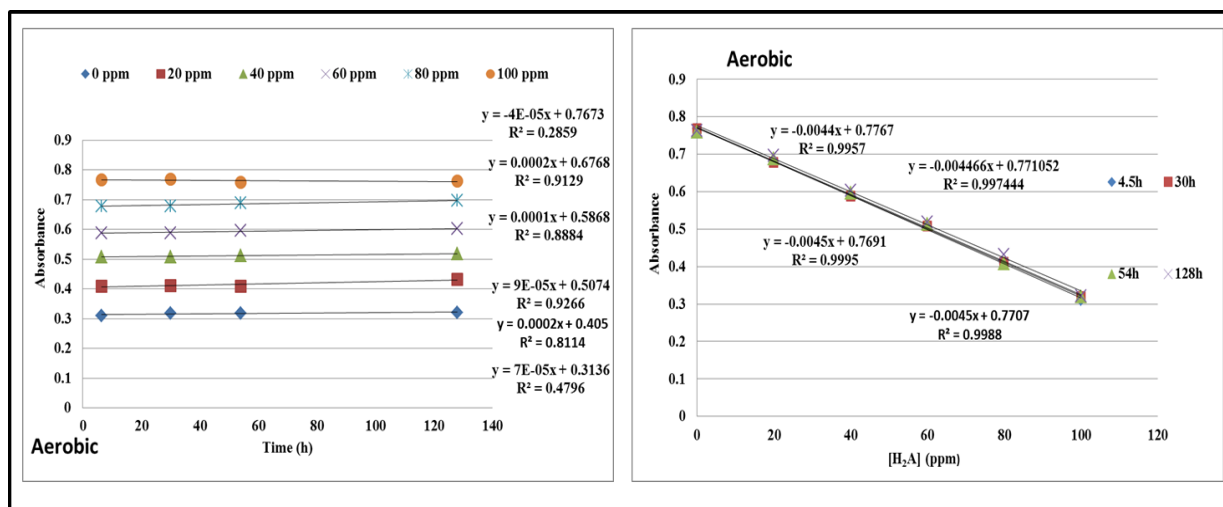


Figure 3-16: Change of absorbance under oxic conditions over time.

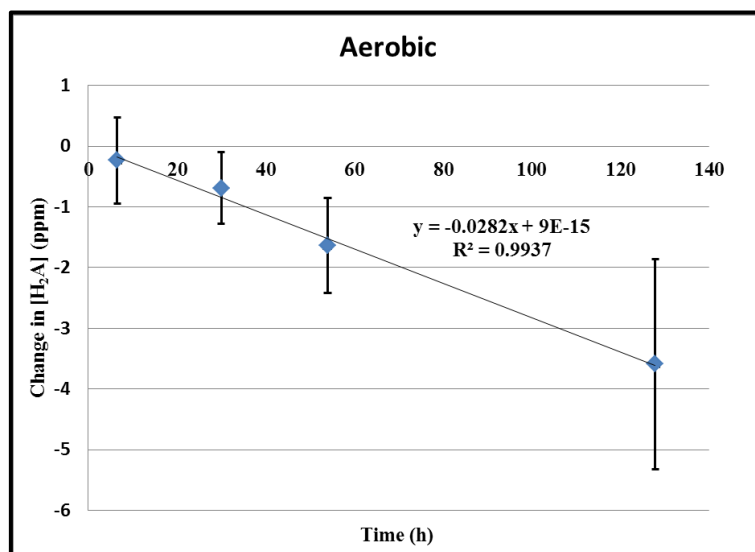


Figure3-17: Change of H_2A under oxic conditions over time. Each point is the average change for each time. Error bars indicate plus and minus one standard deviation.

Similar plots are given for anaerobic systems in Figure 3.18 and 3.19. Main difference seen is that the data for 100ppm H_2A appear anomalous (Figure 3-18). Removing the 100ppm data indicates much more consistency of absorbance with H_2A concentration (last plot Figure 3.18). Calculating the change in interpreted H_2A concentration with time the result is in

Figure 3.19. Left hand plot shows all data and indicates a greater drop but with large uncertainty. Right hand plot has no 100 ppm data and shows much less change in concentration and less uncertainty (though still significant). These plots assume that there is no change in decay rate with initial concentrations as this is indicated by there being no obvious variation in slopes in Figure 3.18 (top plot left).

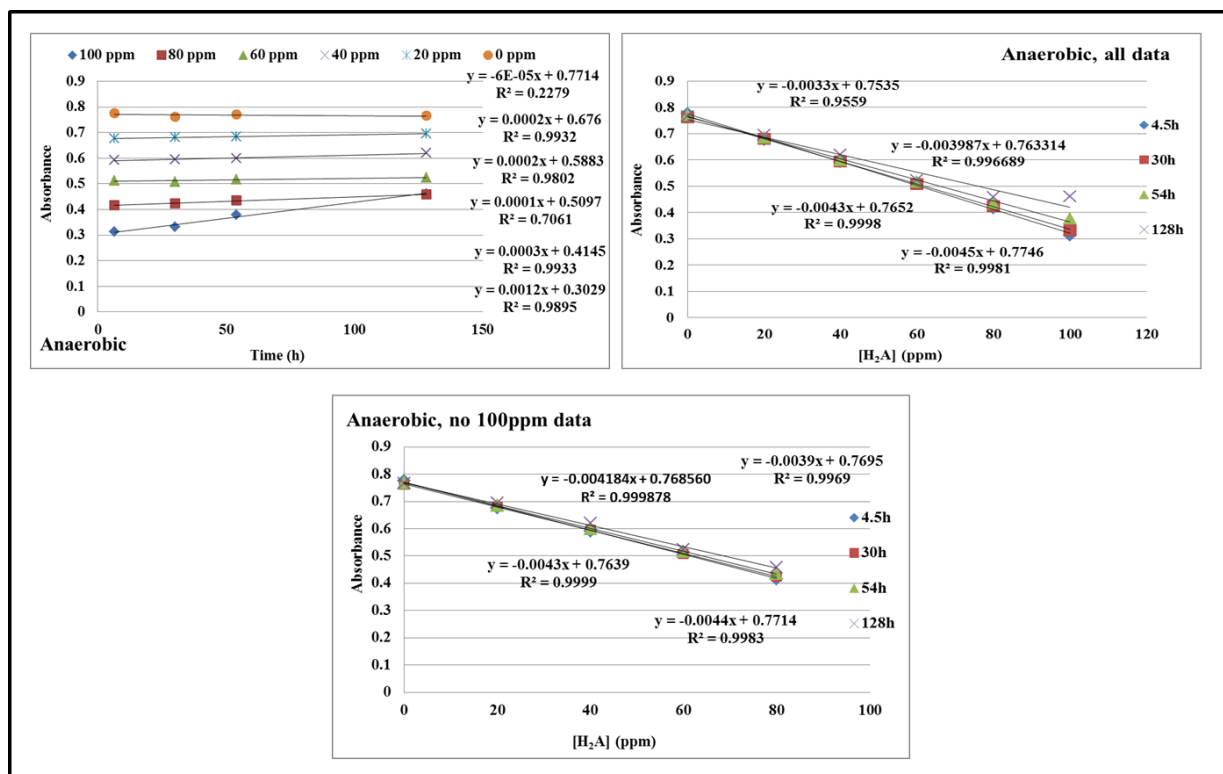


Figure 3-18: Change of absorbance under anaerobic conditions over time.

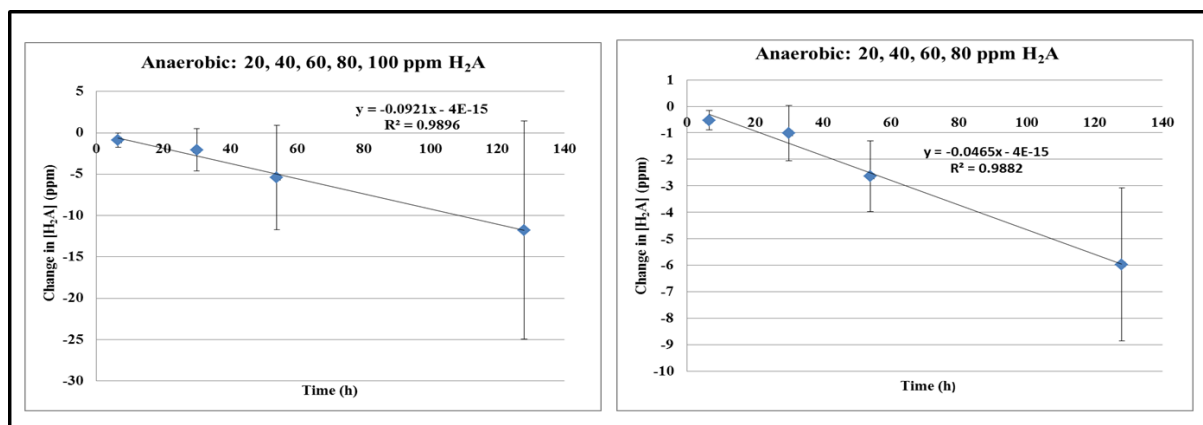


Figure 3-19: Change of H_2A under anaerobic conditions over time. Each point is the average change for each time. Error bars indicate plus and minus one standard deviation. Left is all data. Right is without the anomalous 100ppm data.

The anoxic experiments indicate greater degradation of H_2A (i.e. higher absorbance values) than the oxic experiments. Tannenbaum et al. (1985) observed that the degradation of H_2A can occur under anoxic conditions, the product being diketogulonic acid. Also Ball (2006) found out that under acidic conditions at pHs between 3 and 4, degradation rates of H_2A were higher under oxygen-free conditions. Kennedy et al. (1992) observed that though the main pathway of degradation of ascorbic acid took place under oxic conditions, when the dissolved oxygen was eliminated the degradation continued, though was markedly impacted by temperature. To account for the change in time of H_2A concentrations in the final experiments of Chapter 6 the correlations of Figure 3.17 and Figure 3.19 can in principle be used. In case of Figure 3-19 there are two possible corrections. However, without more certainty the H_2A degradation rate obtained using all data has been used in Chapter 6. The difference would be up to about 2ppm in the longer time experiments if the correlation excluding the 100ppm data were used.

The degradation reactions are probably biotic and therefore corrections may not be required for experiments undertaken under sterile conditions.

3.10 Recommendations for H_2A Analysis Using $KMnO_4$

The $KMnO_4$ spectrophotometric method provides good results for the determination of H_2A concentrations. A correction is needed for H_2A degradation with time, and this is slightly different depending on whether the experiment has been undertaken in oxic or anoxic conditions (Section 3.9).

In the final experiments using sandstone, it is expected that $Fe(II)$ and $Mn(II)$ will be in solution, and both of these species could potentially be oxidised by $KMnO_4$ during the

analysis of H_2A , and hence be recorded incorrectly as H_2A . As a result, the effects of Fe(II) and Mn(II) have been investigated.

Fe(II) concentrations were found not to affect absorbance to any significant amount at relevant pHs (Section 3.7) but Mn(II) concentrations increase absorbance by enough that a correction should be considered and this was proposed in Section 3.8.

However, in all experiments using sandstone, Fe(II) and Mn(II) were both found to be present. As deduced in Section 3.7, Fe^{2+} reacts quickly with colloidal MnO_2 , and therefore the rise in absorbance due to the presence of colloidal MnO_2 is likely to be removed if there is enough Fe . Thus corrections to absorbance due to colloidal MnO_2 should only be done on $[\text{Mn}] - [\text{Fe}]/2$, and not on total $[\text{Mn}]$.

The measurement of H_2A using the KMnO_4 / spectrophotometer method therefore requires care but was the only practicable method available and has the advantages of quickness and cheapness. Its application in the interpretation of the final sandstone experiments will use the discussions and results of this chapter.

Chapter four

Sorption of ascorbic acid on sandstone

4.1 Introduction

The aim of this chapter is to determine the ability of sandstone to sorb ascorbic acid from solution as this is expected to be one of the necessary steps in oxidation of organic carbon . It is assumed that the sorption will mainly involve the iron and manganese oxides grain coatings but could also involve clay minerals.

4.2 Sorption

4.2.1 Introduction

Sorption is considered a key geochemical process (*Bencala et al.*, 1984; Harvey and Fuller, 1998). In aquifer systems, sorption plays a key role in delaying the arrival of contaminants at receptors (*Chiou et al.*, 1983; Pignatello, 1998; Delle Site, 2001). However, in the present context sorption is important in that it is thought to be first stage in reductive dissolution of hematite (*Suter et al.*, 1998) and so it needs to be quantified if possible if reductive dissolution is to be understood.

4.2.2 The distribution coefficient (K_d) and Isotherms

The ratio representing the distribution of ions (organic or inorganic) between liquid and solid phases is called the K_d , generally expressed in l/g or ml /g. The K_d value has a significant variation from extremely high (e.g. in fine grained sediment which contains a high percentage of organic matter it may reach around 1000 ml/g) to nonsorbent material when the K_d value equals zero (*Freeze and Cherry*, 1979). This distribution coefficient (K_d) is obtained from specific lab experiments undertaken under a specific range of concentrations. However, such

experiments are expensive to undertake and leading to use in practice of K_d values for field conditions very different from the lab experiment conditions. This may produce invalid results (Gillespie et al., 2000).

In general in a batch experiment the mass sorbed on the surface of a solid can be calculated using equation (4-1) (Domenico and Schwartz ,1990).

$$S = (C_0 - C) \times V / S_m \quad (4-1)$$

C_0 = initial concentration of solute (e.g. mg/l)

C = concentration of solute after equilibrium within the solid medium is reached (e.g. mg/l)

V = volume of samples (e.g. litres)

S_m = mass of the sediment (e.g. g)

S = sorbed concentration (mass of contaminant per mass of solid, e.g. mg/g).

A plot of S values against C values represent a sorption isotherm. The slope of this curve represents the partition coefficient K_d (L/g), of most use if the sorption follows a linear sorption model which considered the simplest kind of sorption.

In batch sorption experiments to determine K_d values for sediments, there are so many factors potentially affecting K_d values, including temperature of reaction, pH, non-sorption reactions, the ratio between the solid and solution, other species present in the solution competing for sorption sites, grain size / surface area of sediment and which kind of minerals are present (Moody, 1982, (cited in Domenico and Schwartz ,1990)); Linge, 2008). It is therefore possible to get significantly different K_d values depending on the precise conditions of the experiment (Domenico and Schwartz ,1990).

One advantage of determining K_d values of sediment, to use this value to estimate the retardation factor (R_f) (Freeze and cherry, 1979)

$$R_f = 1 + \frac{\rho_b}{\theta} K_d$$

where R_f represents retardation factor (dimensionless), θ represents the water content of sediment, ρ_b represents the bulk density of sediment (g/cm^3), and K_d distribution coefficient ml/g.

The importance of R_f is to estimate the ability of sediment to attenuate transport of organic or inorganic chemicals in an aquifer system via sorption. R_f values are the ratio of the average linear velocity to the apparent velocity of a sorbing contaminant. So an R_f of 2 means that the sorbing contaminant will take twice as long to reach an observation point than a non-sorbing contaminant. The Retardation Equation is a formula that is suited to modelling hydrophobic sorption of organic chemicals. The limitations of the equation are that it assumes ideal, linear, instantaneous equilibrium sorption and may, therefore, not be appropriate for all dissolved organic carbon compounds.

4.2.3 Speed of Sorption Reactions, K_d Values and relevant controlling factors.

Generally most sorption reactions take place within very short times to reach equilibrium, within a time scale range between a few hours to several minutes (Morel and Hering, 1993).

There is wide variation in K_d with different type of organic compounds and type of geological sorbent material. For instance, K_d varies from 0.11, 1.7 and 94 ml/g for sorption of toluene on the London Clay, Merica Mudstone and Oxford Clay respectively (Gillespie et al., 2000).

This indicates that even for fine grain sediments the K_d of sorption toluene on the clay surface varies considerably. It is clear from literature review that the K_d value significantly varies

amongst geological materials and chemical composition of organic fraction (Beaven et al., 2009).

Though both sorption and desorption commonly can occur in soil -water systems (Marschner and Kalbitz 2003), hydrophobic organic compounds are much more likely to be associated with the sorbed phase than hydrophilic compounds, i.e. they are unsurprisingly more sorbed. Sorption of organic compounds can be affected by change in pH, for example Jardine et al. (1989) report that lower pH soil solutions favour greater sorption of dissolved organic carbon. Many reported lab experiments demonstrate that considerable amounts of dissolved organic matter can be sorbed on the surface of different kinds of synthetic iron oxides and hydroxides (Schwertmann 1966; Sibanda and Young 1986). Jardine et al. (1989) observed considerable decline in sorption capacity of soil for dissolved organic matter (DOM) after eliminating iron oxide / hydroxide from the soil. Tipping (1981) compared the sorption of different molecular weight humic substances on synthetic hematite and goethite and found out that with decrease in molecular weight of humic substances there is a decrease of adsorption capacity, which indicate that higher molecular weight and more complex structures of organic compounds have more potential to sorb to synthetic iron oxides.

4.2.4 Mechanisms of Sorption Reactions

At low pHs, protons (H^+) attach to hydroxyl groups on mineral surfaces, leading to increase in net positive charge on the surface of metal oxide. This attracts negatively charged ions including anionic organic species which then form complexes on the mineral surface. With increase in pH, removal of protons (deprotonation) leads to a significant decline in net positive charge of mineral oxides and the oxide surface becomes more negatively charged hence more attractive of cations and metals. As a consequence of this, organic matter (OM) release into the solution is often observed as a result of pH rise (Parfitt et al., 1977; Sibanda

and Young, 1986; Loganathan et al., 2014). For example, Avena and Koopal (1998, cited in Grybos et al., 2009) found out that there is considerable sorption of humic acid (HuA) on the surface of iron oxide at lower pH values, but with pH rise the reverse process took place and a considerable proportion of the HuA desorbed from the iron oxide surface. This means that there is a considerable drop of adsorption capacity for HuA on the surface of iron oxide under higher pHs.

The net charge on solid phase surfaces plays a significant role in the sorption process. There are four main factors controlling the net charge on the surface of a solid (e.g. Essington 2003). Firstly, the fixed charge of the particle independent of pH variation and due to substitution within the crystal lattice. Secondly net protonation charge. Thirdly charge due to the presence of sorbed inner sphere complexes. Finally charge due to the presence of sorbed outer sphere complexes. All these factors vary as a function of pH change with the exception of the first parameter. Oxyhydroxides are considered to have predominantly variable surface charges (i.e. pH dependent) while 2:1 clay minerals are considered to have a much greater permanent, pH-independent charge (fix charge) (Eby, 2004). Change of pH therefore plays a critical role with altering surface charge of particles (Eby, 2004).

Table 4.1 shows the zero point charge (ZPC) for some minerals, if the pH of the solution equals the pH of the mineral at ZPC, then the surface of the solid has a net zero charge, (i.e. its negative and positive charges are equal). For example, for quartz, the net zero point is very low at pH =2. This means that if the pH is higher than 2, the surface charge of silica will be dominated by negative surface charge and will attract dissolved cations while at pH less than 2 the surface charge will be dominated by positive charge and will attract anions to attach to the silica surface. Another example is hematite. The net zero point of charge lies between 5 and 9. This means that if the pH is higher than 9, its surface charge will be dominantly negative, while at pH lower than 5 it will be dominantly positive.

Table (4-1): Values of net zero point charge for some natural mineral and materials. Data from Stumm (1992), Drever (1982) and Kehew (2001).

Mineral or material	Symbol	ZPC
Quartz	SiO ₂	2
Feldspars	KAlSi ₃ O ₈ – NaAlSi ₃ O ₈ – <u>Ca</u> Al ₂ Si ₂ O ₈	2-2.4
Birnessite	δ. MnO ₂	2.8
Magnetite	Fe ₃ O ₄	6.5
Goethite	α FeOOH	6-7
hematite	αFe ₂ O ₃	5-9
Amorphous iron(III)hydroxide	Fe(OH) ₃	8.5

In addition to the effect of surface charge, specific reactions also occur between the ion and the surface. So an organic ion might react to form a surface complex even if it has the same charge as the surface. So sorption is combination of these processes though in practice the two are usually considered as one “sorption” process (e.g. Essington, 2003).

Also temperature affects sorption reaction, for instance MacIntyre et al. (1991) who studied the sorption of naphthalene on the surface of sediment samples collected from the Columbus alluvial aquifer. They investigated temperature and found out that rise of temperature led to decrease of sorption capacity of alluvial sediment because the sorption mechanism was exothermic.

Generally the sorption capacity for organics of sandstones is not high as they often contain little organic matter. Kaiser and Zech (1997) mention that binding sites of iron oxides in mineral soils are less preferred for the hydrophilic (dissolved) fraction of dissolved organic matter than the hydrophobic fraction of dissolved organic matter DOM.

4.2.5 Implications from Literature for Experiments on Sandstone

From previous studies it is concluded that experiments need to be undertaken with care to make the conditions the same. All experiments were undertaken at relatively low temperatures, i.e. lab temperature (20-24°C), the temperature of the final reductive dissolution experiments, but above UK groundwater temperatures (about 10°C). From the literature it is seen that most sorption is completed within a few hours and so all experiments were conducted for 120 minutes. At 120 minutes there is very limited release of Mn and Fe from the sandstone using lower concentrations of ascorbic acid (40 ppm and below) so this suggests that by this time very little H_2A reaction has occurred so change in H_2A concentration is mainly because of sorption. These low Fe and Mn concentrations also mean that no correction for H_2A concentrations need be made (see Chapter 3) but may be the correction for the effect of [Mn] on the ascorbic acid concentration also needs to be done to compare between both cases (see below). Other implications of sorption experiments will be discussed in the results section below.

4.3 Sorption Batch Experiments

4.3.1 Initial sorption experiment with higher mass of sandstone: (Experiments E_1 & E_2)

The detail of the first two sorption experiments, E_1 and E_2 , is explained in this section. The following H_2A concentrations were prepared: 40, 30, 25, 20, 15, 10, and 0 ppm and measure the absorption for each standard solution, (see appendix 4.1). Then 20 g masses of sandstone were weighed and put in 50 ml centrifuge tubes. Then 40 ml of the following [H_2A] (30, 25, 20, 15, 10 and 0) ppm were added to each centrifuge tube, all in duplicate. All samples were then put in a shaker for 120 min at 300 rpm. 2 h was chosen as redox reactions at this time were likely to be very limited (very low Mn^{++} and Fe concentrations, see Chapter 2), but

sorption was likely to be nearly complete (Morel and Hering, 1993). The samples were then centrifuged for 10 min at 4500 rpm. Samples were then analysed using UV-vis spectrometer. The sorbed concentration (S) was calculated using equation (4-1), see appendix 4.2. No corrections were undertaken for decay (Chapter 3) as the experiments were so short (correction would be equals about 0.2ppm).

Figure (4.1) shows the isotherm obtained, which gave a reasonable linear correlation coefficient of $r^2 = 0.78$, but is probably better fitted using a Langmuir isotherm (see below). However, it is possible to get this type of isotherm if Mn^{++} was present in solution. Though little Mn^{++} would be expected experiments in Chapter 6 later indicated that perhaps might get up to at most 1ppm Mn initially due to non- H_2A reactions. Correction for Mn at concentrations of about 1 ppm would mean for data of Figure (4.1) that the intercepts could be reduced to close to zero.

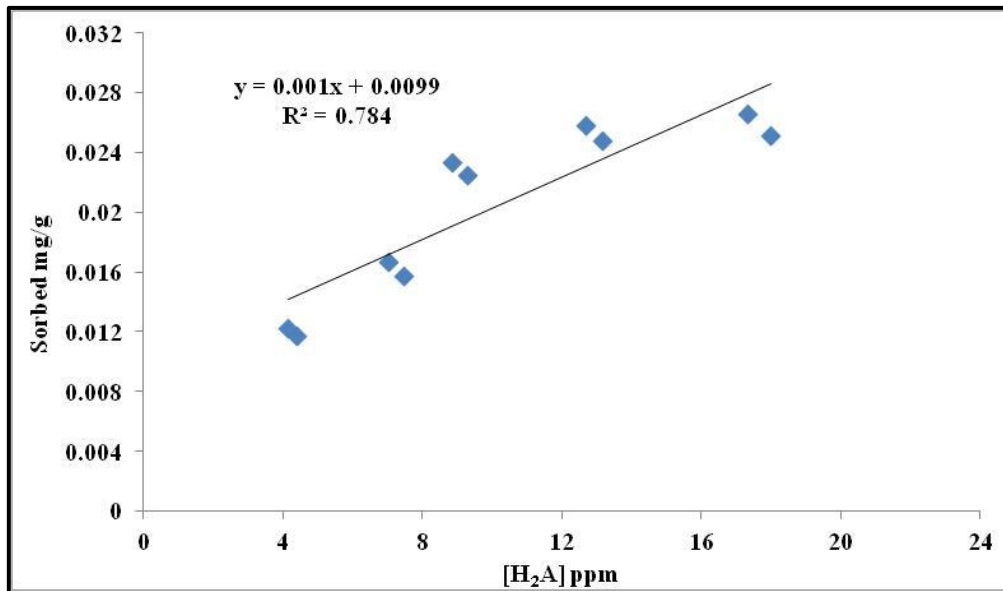


Figure (4-1) Sorption isotherm for E₁ various [H₂A] with 20 g mass of sandstone.

Another sorption experiment has been carried out using the same procedures and time for previous experiment, but using a lower mass of sandstone - 15 g. The absorbance of

sandstone sample free from ascorbic acid (0 ppm of H_2A) gave 1.63 ppm, therefore the data were corrected by subtracting this value. Appendix 4.3 and Figure (4.2) shows the isotherm which is very similar to that for E_1 . Figure (4.3) includes both sets of data, E_1 and E_2 .

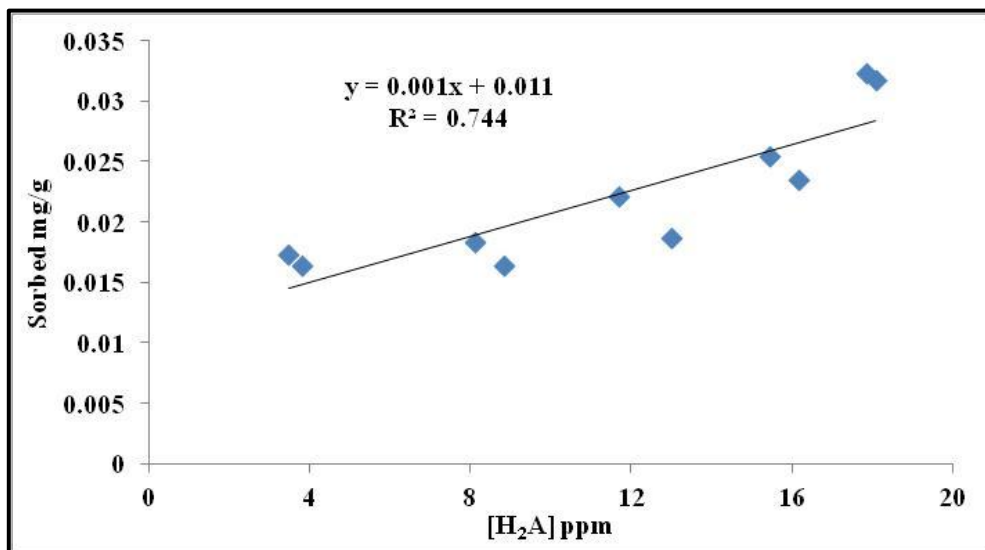


Figure (4-2) Sorption isotherm for E_2 various $[H_2A]$ with 15 g mass sandstone.

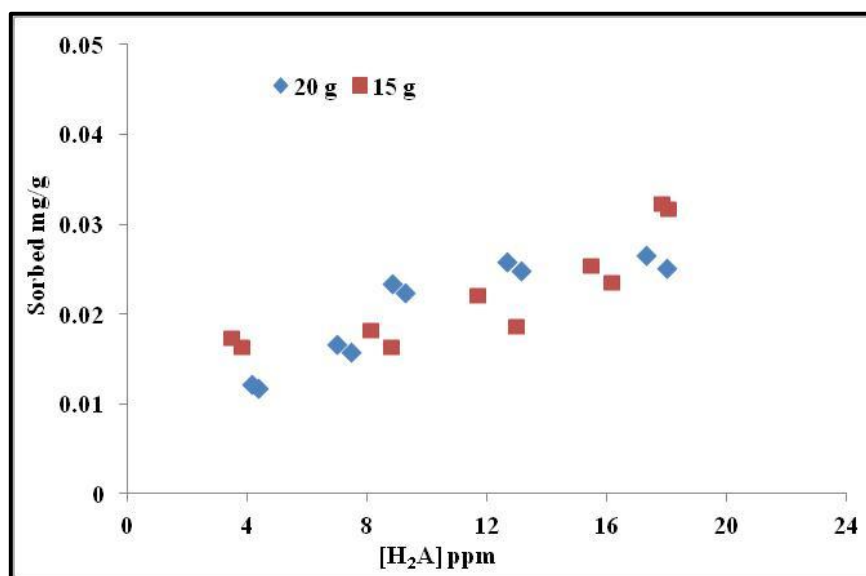


Figure (4-3) Sorption isotherm for various concentrations of ascorbic acid with 20 and 15 g sandstone (E_1 and E_2).

The most common sorption isotherm for organic compounds on the surface of natural solid material (sediment) is nonlinear, like Langmuir and Freundlich (Schwarzenbach, 1993). In this kind of sorption isotherm plot, the K_d value varies according to the change in the concentration (C), not like the linear sorption isotherm, when distribution coefficient (K_d) has unique value. Also in the Langmuir sorption model the sorbed concentrations (S) do not continue to increase with the rise in concentration like in the linear sorption isotherm model, but reach a maximum sorbed concentration (S_{max}).

The Langmuir equation can be express as below equation

$$S = \frac{C_{max} KC}{1 + KC} \dots \dots \dots (4-4)$$

S = sorbed (mg/g)

C_{max} = the maximum concentration of H_2A that can be adsorbed on the sandstone (mg/g)

K= an coeffiecent constant (l/mol)

C = equilibrium concentration of H_2A ,

Excel was used to fit a Langmuir isotherm to the data. This done in the following way.

$$S = \frac{C_{max} KC}{1 + KC}$$

From a mass balance,

$$SM + CV = C_o V$$

where V represents the volume of solution, M represents the mass of sandstone, and C_o is the initial concentration of H_2A . Combining these two equations gives

$$VKC^2 - C(VKC_o - V - MC_{max}K) + VC_o = 0$$

Solving this to get concentration:

$$\therefore C = \frac{(VKC_o - V - MC_{max}K) \pm [(VKC_o - V - MC_{max}K)^2 + 4V^2KC_o]^{0.5}}{2VK}$$

By trial and error the fit indicated in Figure (4.4) was obtained.

Attempting the fitting for E₁ gave the results shown in Figure (4.4) (a). Figure (4.4)(b) shows the isotherm obtained by adding Mn⁺⁺ until the isotherm passes through the origin. The final Mn concentration, 1.07 ppm, is slightly higher than would be expected from result from Chapter 6.

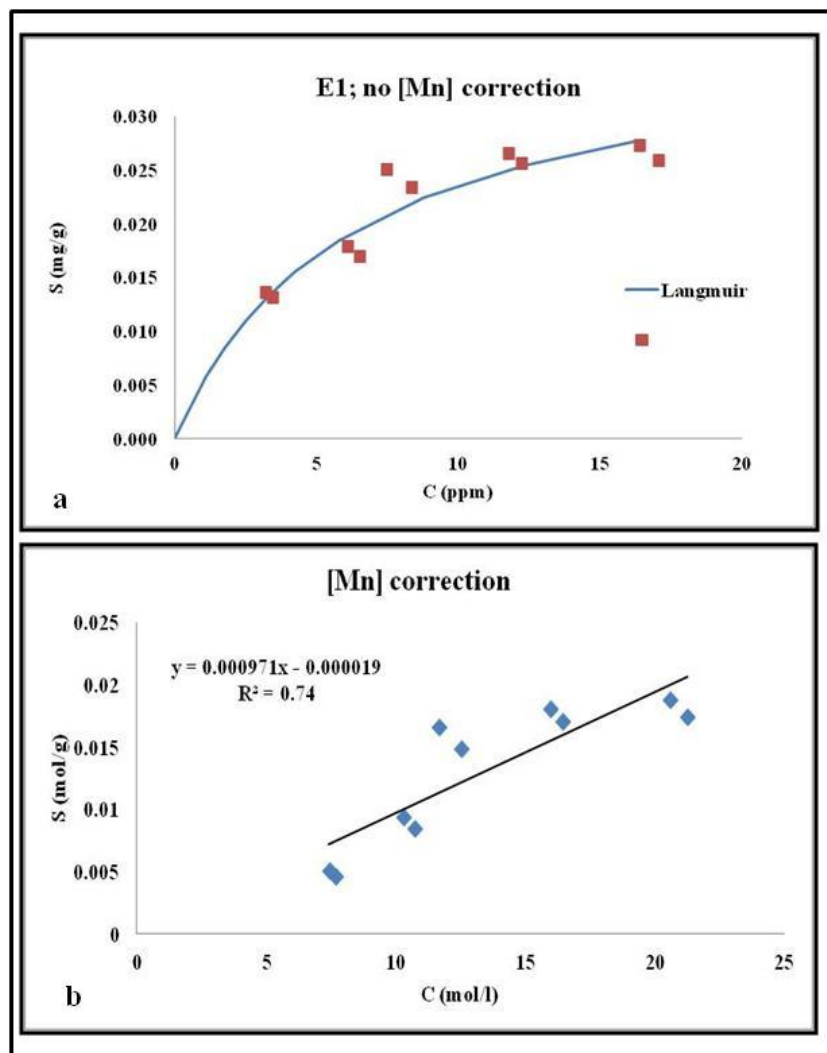


Figure (4-4). Experiment E1. (a) Langmuir fit ($K = 28561$ l/mol; $s_{max} = 2.17 \times 10^{-7}$ mol/g). (b) corrected for [Mn] so that passes through origin ([Mn] = 1.07ppm)($K_d = 0.0097$ l/g).

Attempting the fitting for E₂ gave the results shown in Figure (4.5). Figure (4.5) (b) shows the isotherm obtained by adding Mn⁺⁺ until the isotherm passes through the origin. The final Mn⁺⁺ concentration is too big (3.6 ppm) suggesting that Mn⁺⁺ cannot explain all isotherms with apparent intercepts. Figure (4.5) (c) shows the results of not having 10ppm points (as these appear like outliers on a linearized Langmuir plot (1/S against 1/C)). The result is not a very good fit.

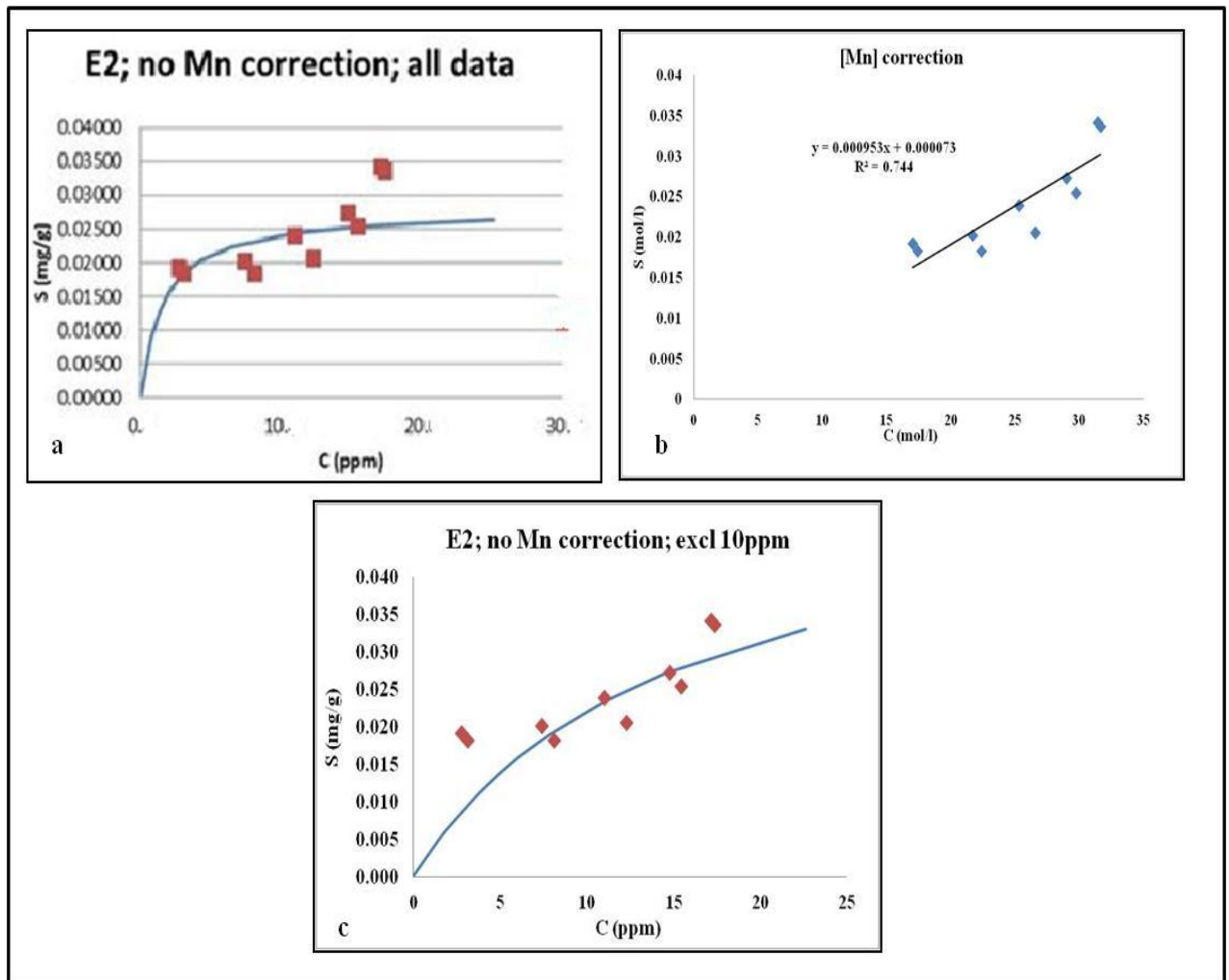


Figure (4-5). Experiment E₂. (a) Langmuir fit ($K = 106016$ l/mol; $s_{\max} = 1.6 \times 10^{-7}$ mol/g). (b) corrected for [Mn] so that passes through origin ([Mn] = 3.6 ppm) ($K_d = 0.0095$ l/g). (c) 10ppm points excluded as they appear as outliers on linearized Langmuir plot ($1/C$ v $1/S$) ($K = 11997$ l/mol; $s_{\max} = 3.09 \times 10^{-7}$ mol/g)

4.3.2 Sorption of ascorbic acid using a higher concentration range of H_2A (E_3)

The main purpose of this experiment was to investigate sorption at a higher range concentrations of ascorbic acid (20-120 ppm), but using a lower mass of sandstone (10 g). The method was the same as for E_1 and E_2 . All standard solutions were stable within no more than 2% difference over the experiment time period, except for one standard sample (100 ppm) that gave an absorbance about 4% greater at the end of experiment. This was because of instrument drift that developed during time of these experiments and methods to correct are discussed in following sections where experiment results were affected significantly. See appendix (4.4).

Appendix 4.5 and figure (4.6)(a) shows the isotherm. Highest concentration point is very low. It is not know why this was the case so the point has been removed and the isotherm shown in Figure (4.6)(b) used. In all other work using concentrations of H_2A above 100ppm has been avoided as it may be that at this concentration all the $KMnO_4$ is used up.

The isotherm of Figure (4.6) is very similar to that of Figure (4.3). Applying the Langmuir trial and error fit method resulted in the fit shown in Figure (4.7).

Figure (4.7) (a) shows an attempted Langmuir fit. This is not a very good fit. Using Mn concentration resulted in the isotherm passing through the origin but the amount of Mn that had to be added was too large (3.35ppm).

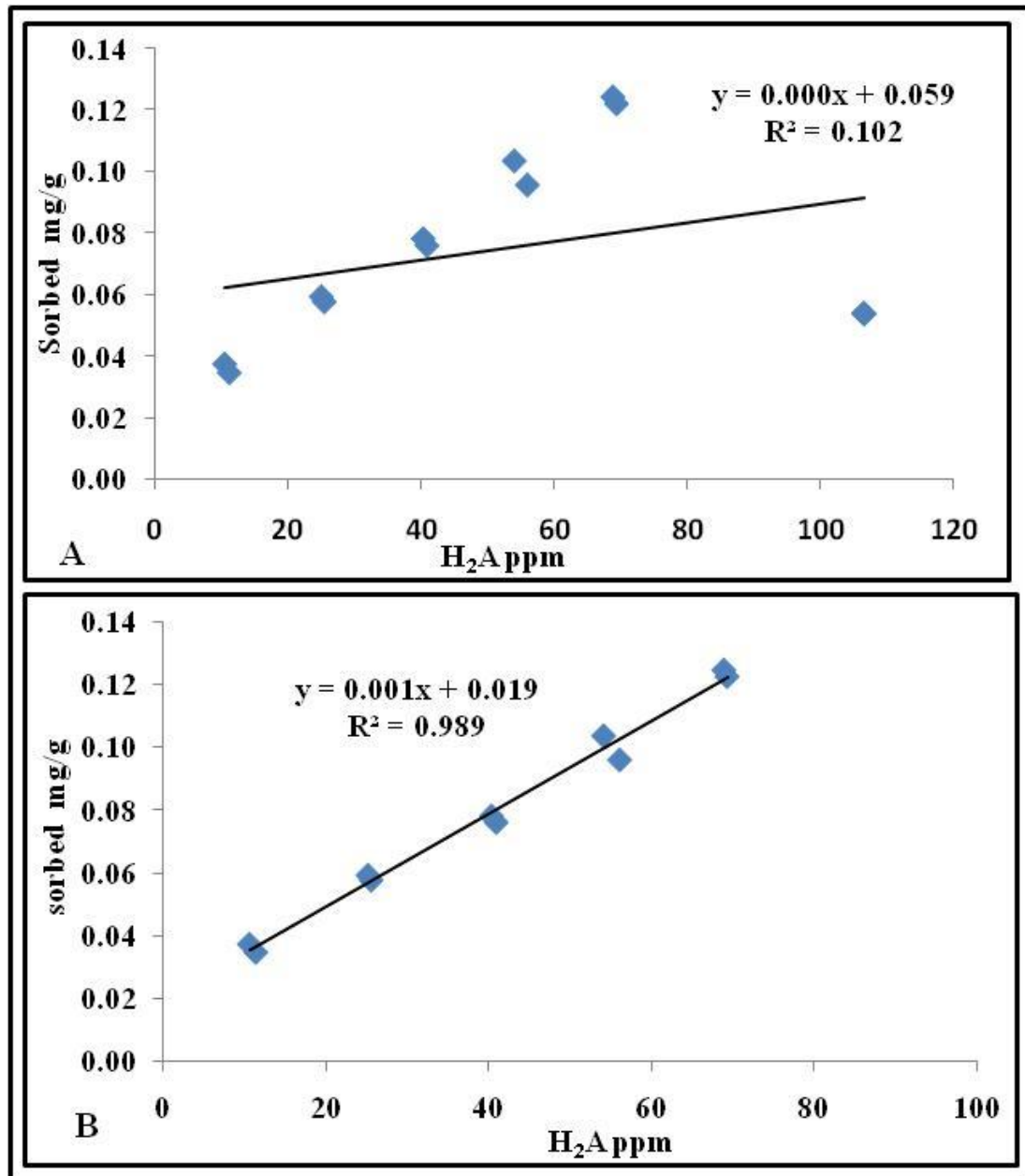


Figure (4-6) Sorption isotherm plot for experiment E₃ A) [H₂A] range from 20 – 120ppm. B) [H₂A] range from 20-100ppm after excluding the 120 ppm point.

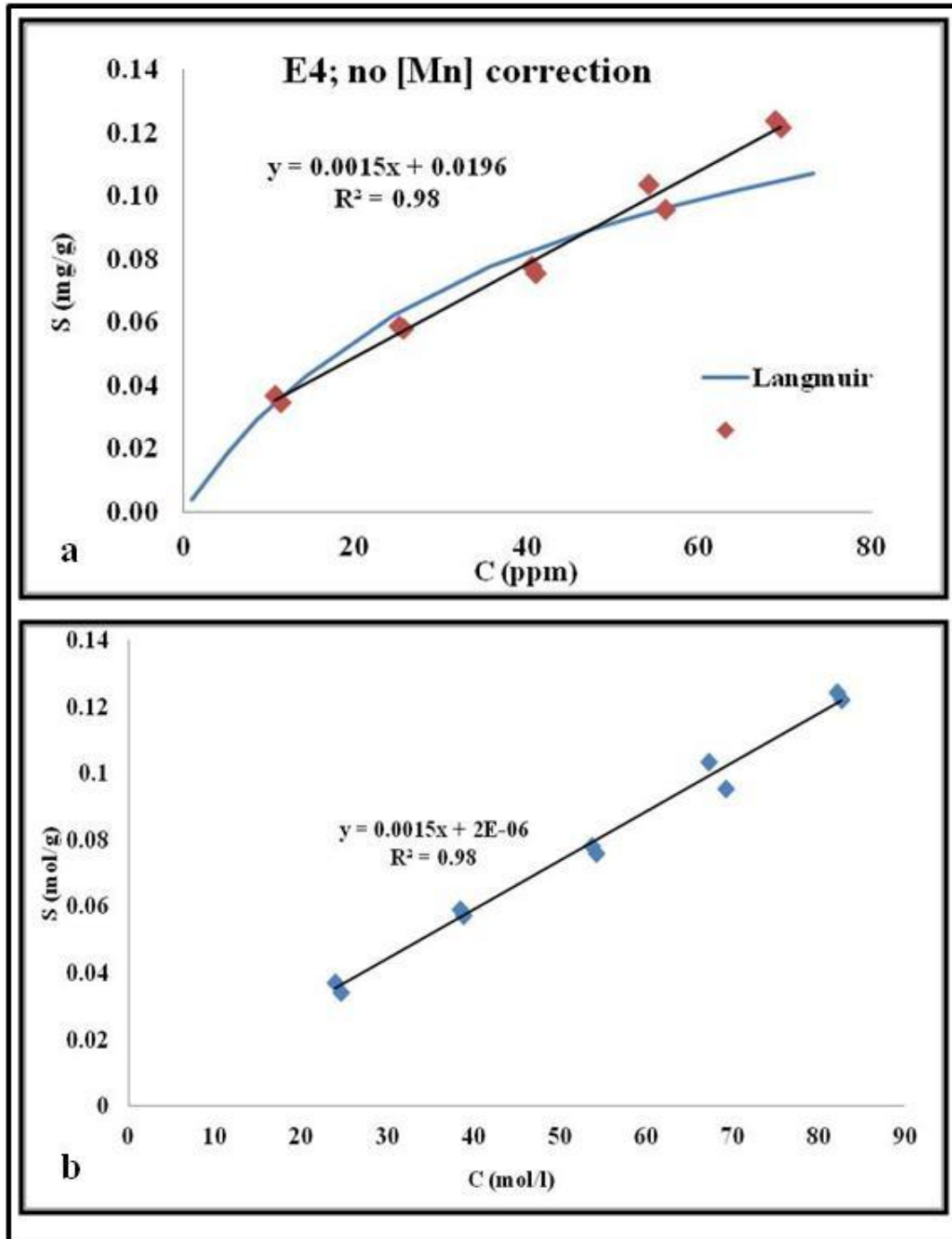


Figure (4-7). Experiment E₃. (a) Langmuir fit ($K = 4313 \text{ l/mol}$; $s_{\text{max}} = 9.46 \times 10^{-7} \text{ mol/g}$). (b) corrected for [Mn] so that it passes through origin ($[\text{Mn}] = 3.35 \text{ ppm}$) ($K_d = 0.0015 \text{ l/g}$).

4.3.3 Sorption of ascorbic acid using a lower mass of sandstone and lower concentration range of $[H_2A]$ (E_4)

The purpose of this experiment was to measure the sorption of H_2A on the surface of smaller masses of sandstone (2 and 5g) and with a moderately low range of initial $[H_2A]$ (30, 25, 20, 15 and 10 ppm). As the same procedure of previous sorption experiments was then completed. However, in this experiment machine drifted, (see appendix 4.6 a&b). There was an increase in the absorbance between the calibration at the start of the experiment and at the end. A time-dependent linear correction was applied assuming each sample took the same amount of time to analyse and knowing what the order of the analysis was.

Appendix 4.7 and figure (4.8) shows the isotherms for 2 and 5 g. The experiment with the smaller mass did not work well for an unknown reason. However, the results for 5g were similar to those for previous experiments.

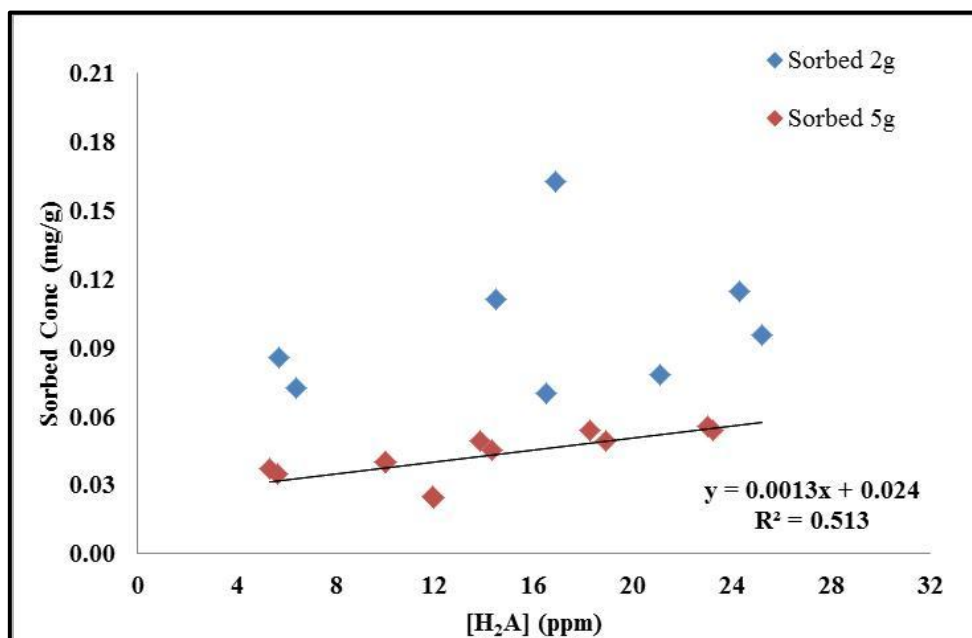


Figure (4-8) Sorption isotherms for E_4

Figure (4.9) shows the fitted model isotherms to data. The Langmuir model is possible. A linear isotherm can be fitted if the Mn^{++} concentration is set at 0.815ppm which is reasonable.

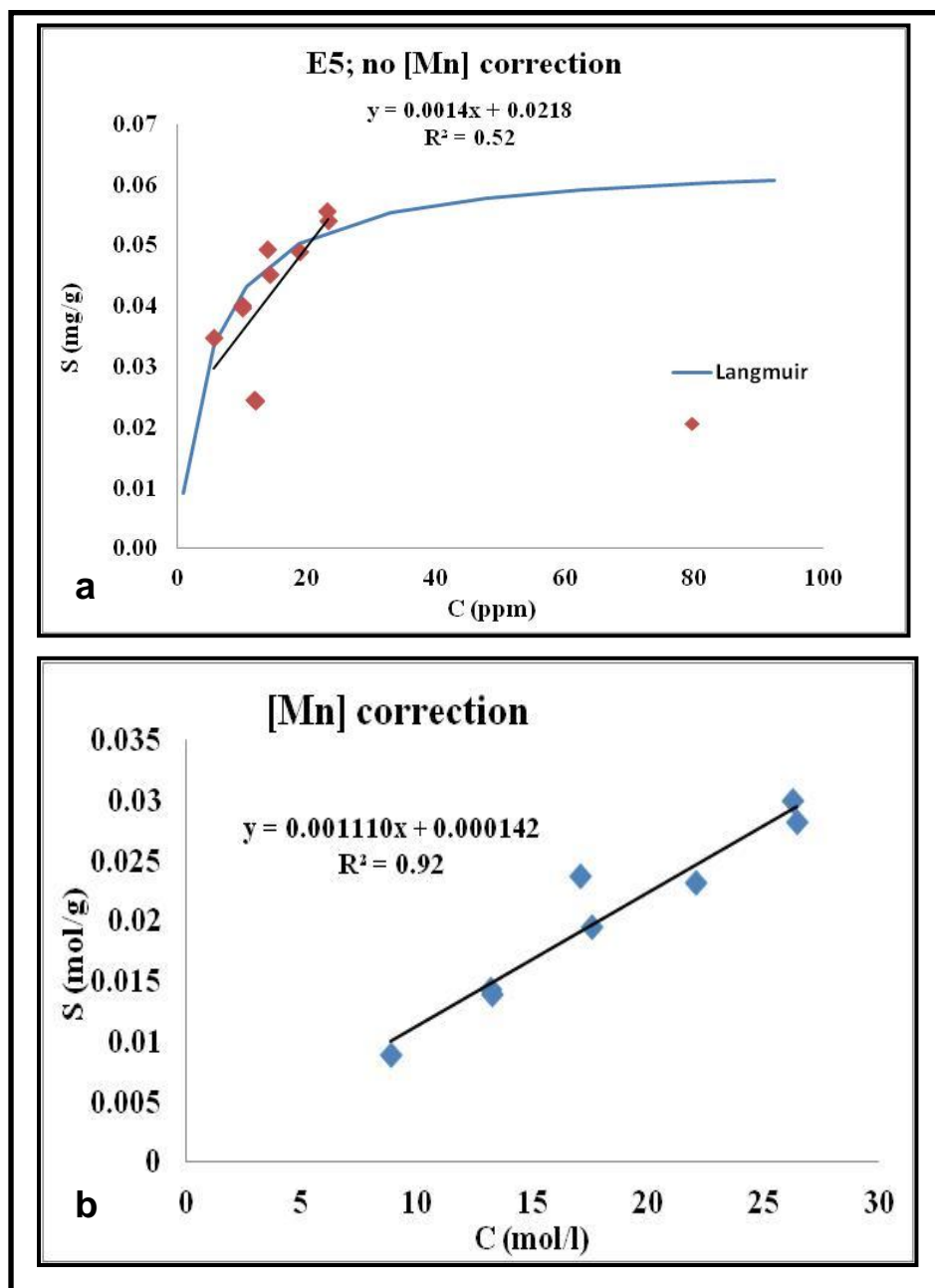


Figure (4-9). Experiment E4. (a) Langmuir fit ($K = 34129 \text{ l/mol}$; $s_{\text{max}} = 3.64 \times 10^{-7} \text{ mol/g}$). (b) corrected for [Mn] so that it passes through origin ($[\text{Mn}] = 0.815 \text{ ppm}$) ($K_d = 0.0011 \text{ l/g}$).

4.3.4 Confirming the drift of the UV-vis spectrophotometer

Recording time was very important to correct the drift of absorbance of UV-vis machine, due at the time of analysis there being a slight drift occurring. Therefore small experiment has been carried out to measure the absorbance of 40 and 80 ppm KMnO_4 alone (after adding 5 ml of KMnO_4 to 5 ml of diw) at 530nm wavelength in the absence of H_2A for about 50 min at 5 min intervals. The reason for choosing this time (50 min) is that almost sorption experiments are conducted within no more than 1 hour. The results (Figure 4.10 and appendix 4.8) confirmed the drift and that it was linear. Drift was only important from E_5 onwards as there was no observable drift before and after the set of sorption experiments reported in this chapter the machine was repaired.

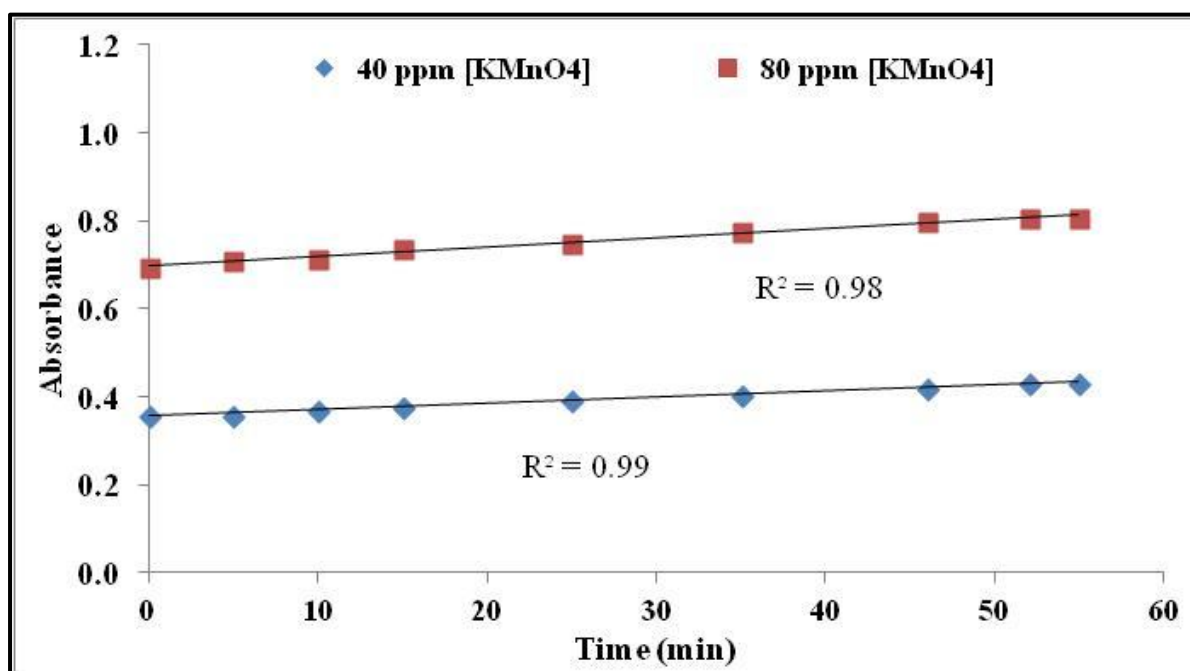


Figure (4-10) Monitoring the absorbance of different $[\text{KMnO}_4]$ over time.

4.3.5 Sorption of ascorbic acid using 10g sandstone and a moderate range of concentrations of H_2A (E_5)

In this final sorption experiment the time each analysis was done has been recorded in order to correct the drift of the absorbance of the uv -vis spectrophotometer accurately. The absorbance of some control samples (without sandstone) was also made in between run samples, to check the accuracy of the correction technique.

The experiment was otherwise undertaken in the same way as before, with 10g sandstone and concentrations of 30, 25, 20, 15, 10 ppm. The concentrations were again interpreted using a linearly varying calibration, but this time knowing the exact times of the analyses, see appendix 4.9.

The pH of the H_2A standards and samples revealed the pH of samples vary very slightly (4.82 to 4.90), while the pH of the standards vary from 4.21 to 4.92, with increasing pH with decrease of $[H_2A]$ (Figure (4.11)).

The absorbance measurement revealed there is an increase of absorbance for the same $[H_2A]$ over time, and therefore several steps have been done to correct the absorbance drift depending on the recorded time for each sample. The correction was based on subtracting the initial absorbance value for each $[H_2A]$ from the intercept for the same $[H_2A]$, appendix 4.10 & 4.11. The resulting plot against time (Figure 4.12) gave an excellent linear relationship ($r^2=0.96$), the slope of which was used as a basis to correct the rise of absorbance over time. Figure (4-13) and appendix 4.12 shows the matching of absorbance after correction.

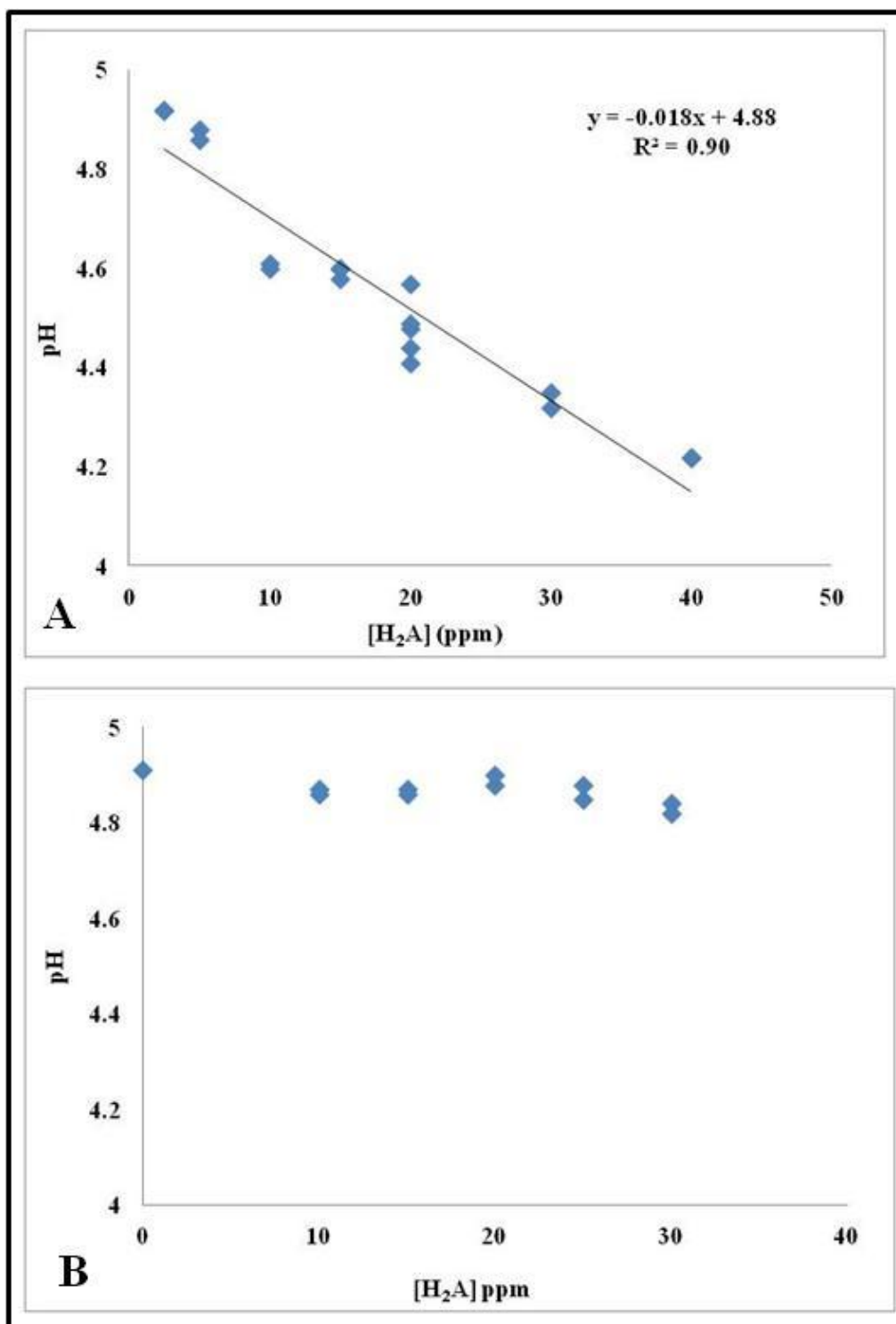


Figure (4-11) Relation between $[H_2A]$ and pH. A) H_2A standards B) samples in contact with sandstone.

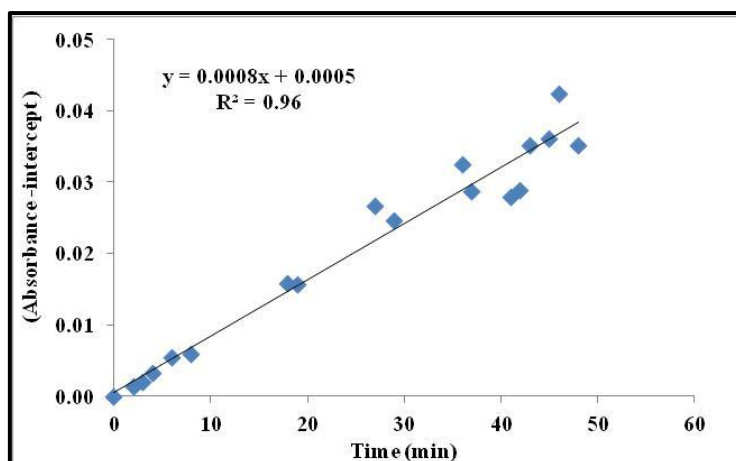


Figure (4-12). A plot of the (absorption –intercept) for [H₂A] analysis against time.

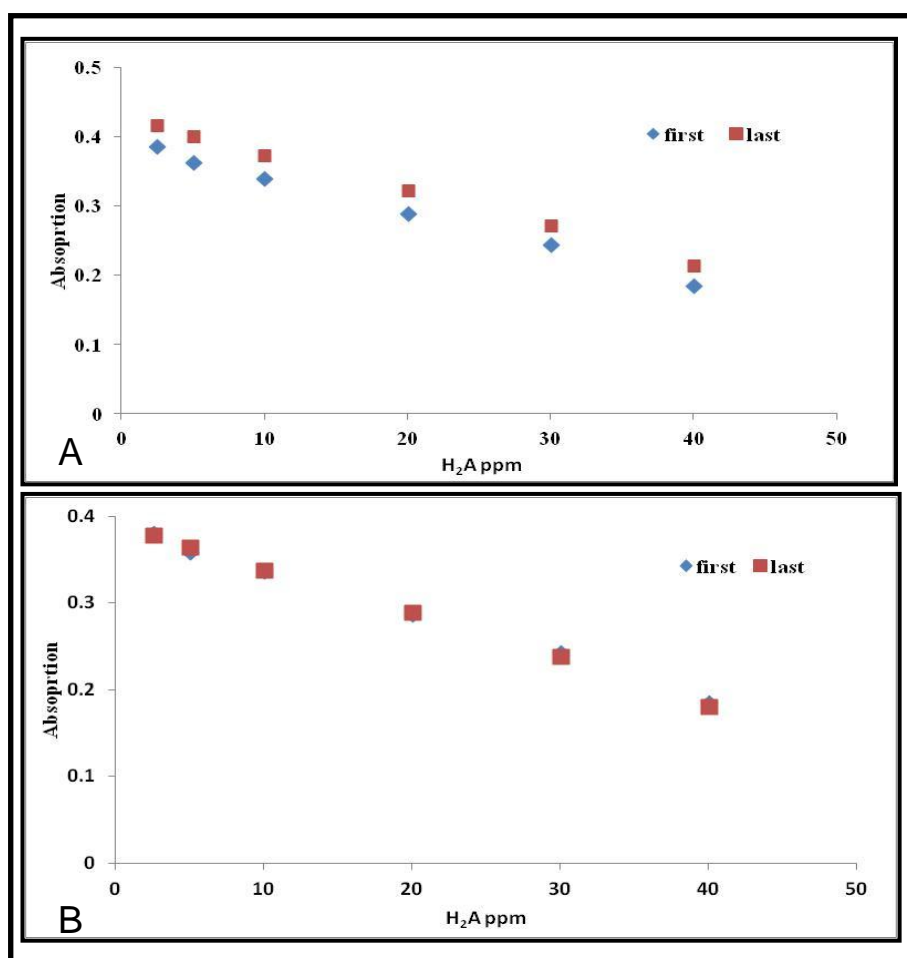


Figure (4-13) The relationship between the absorbance and [H₂A] A) before correction B) after correction for both first and last standard solutions.

The resulting isotherm is shown in Figure (4.14) and appendix 4.13. Again the shape suggests a possible Langmuir model if the high intercept is to be explained.

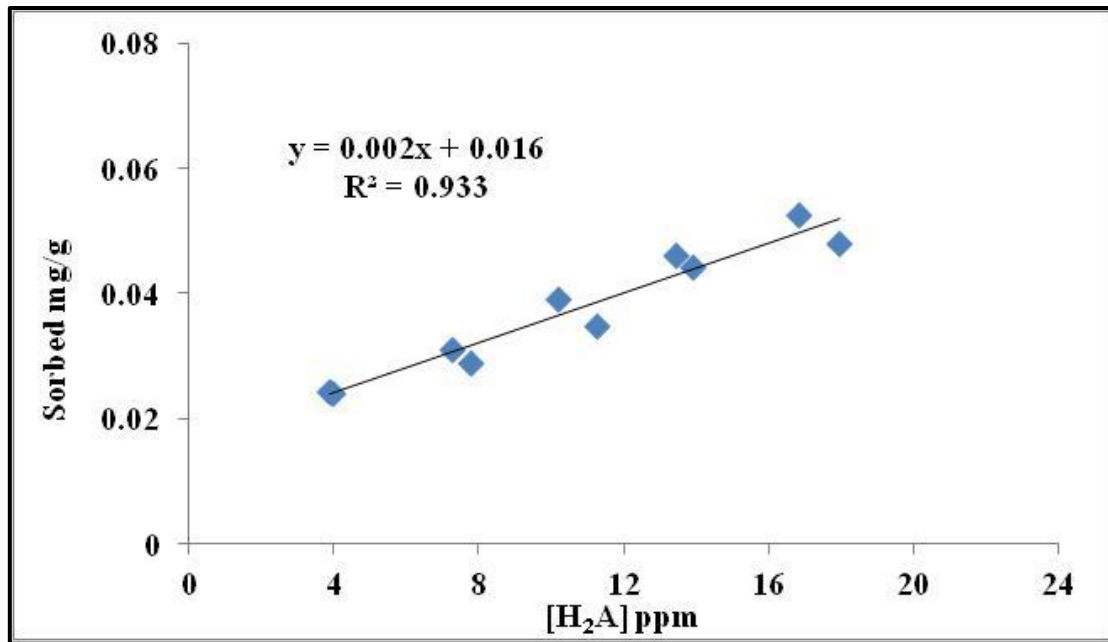


Figure (4-14) The sorption isotherm plot for E₅ for a range of ascorbic acid with 10 g sandstone, after correction.

Figure (4.15) shows the isotherm model fits. Figure (4.15) (a) indicates that the Langmuir isotherm flattens off at lower values than the experimental data. A linear isotherm model is possible (Figure (4.15)(b)) if Mn concentrations are set at 1.15ppm which is too big.

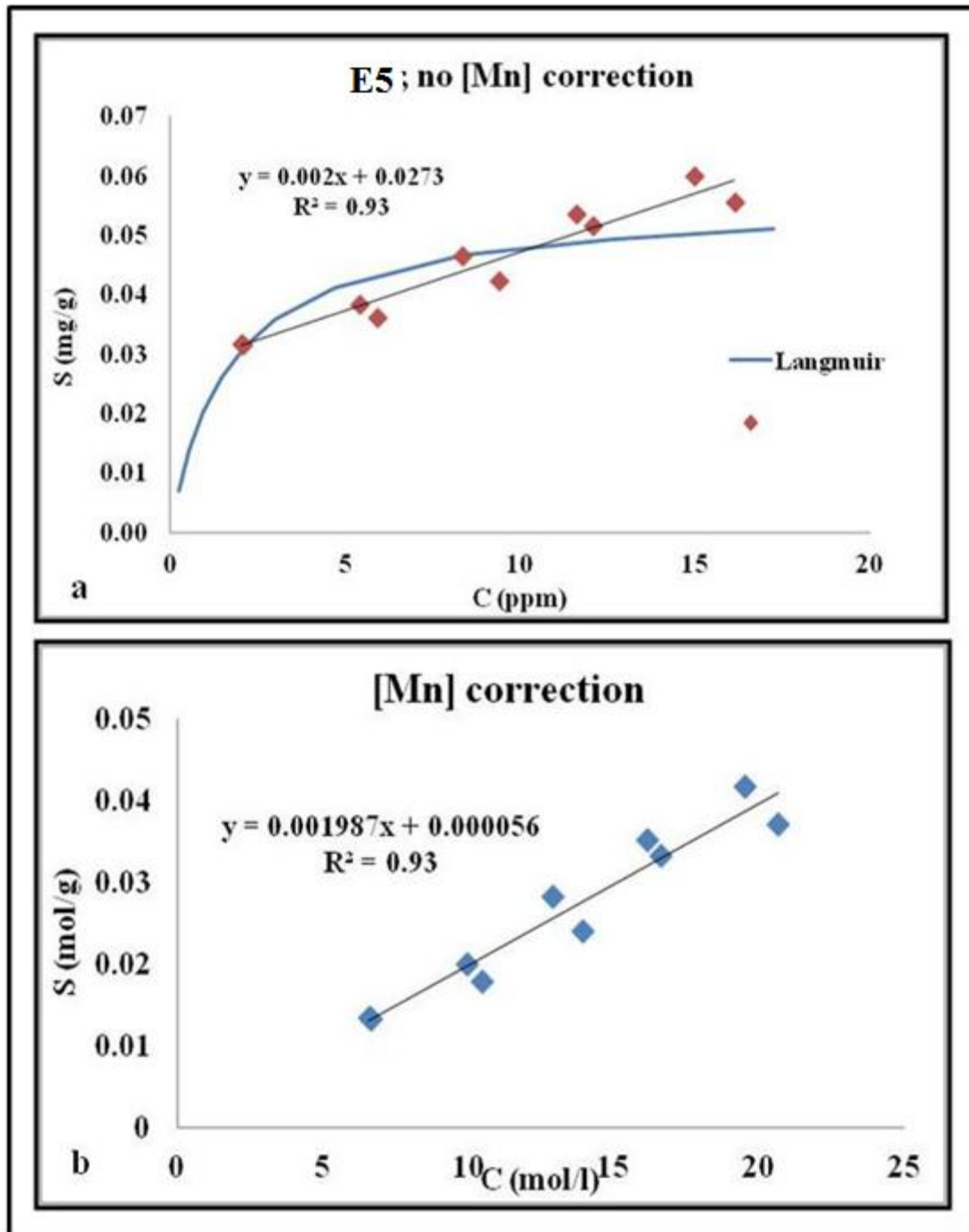


Figure (4-15). Experiment E₅. (a) Langmuir fit ($K = 103912$ l/mol; $s_{\max} = 3.18 \times 10^{-7}$ mol/g).

(b) corrected for [Mn] so that passes through origin ($[Mn] = 1.15$ ppm) ($K_d = 0.0020$ l/g).

4.4 Discussion and Conclusion

Figure (4.16) shows all the data plotted together as one isotherm. It is obvious there is consistency among all the results as isotherm slope was almost same but with a slight variation in the intercept may be due to pH difference.

Table (4.2) lists the fits obtained using Langmuir and linear with intercept and linear isotherms (last with initial Mn^{++} concentrations chosen to make intercept zero) in this chapter. Neither Langmuir or linear isotherms are really good fits. For two experiments a linear fit with an initial Mn^{++} concentration is impossible so this suggest that the linear isotherm is not correct. The Langmuir isotherms are also generally not good fitting and there are a big range in parameter values.

The general shape of the uncorrected (no account of possible initial Mn^{++}) isotherms is a quick rise to a flatter linear increase (Figure (4.16)). Afonso et al. (1990) (Figure (4.17)) and Banwart et al. (1989) also found this. These studies just use Langmuir isotherms without further comments. It probable that the isotherm is not Langmuir and may even be a two site sorption. It is probable that by combining small Mn corrections and fitting Langmuir isotherms less variability of the isotherm shape would be seen, but even then the shape is not proper Langmuir. However any of the fits listed in Table (4.2) below would be appropriate as empirical equations for estimating sorption in the range of dissolved concentrations for which the experiments were undertaken (generally 5-30 ppm after reaction).

Table (4-2) Summary of sorption isotherm parameters for all sorption experiment. Slope and intercept are for a least squares linear fit to the uncorrected data. Fit: > means better, < means worse. Mn: means an initial concentration of Mn^{++} needed to be assumed to get the isotherm to pass through the origin.

Exp code	Isotherm slope l/g	Intercept mg/g	Zero [H ₂ A] data	Sst mass & conc range (g, ppm)	Langmuir K (l/mol)	Langmuir smax mol/g	Fit	K _d l/g	Mn ppm
E ₁	0.001	0.011	Yes	15 10-30	28561	2.17×10^{-7}	>	0.009 7	1.07
E ₂	0.001	0.009	Yes	20 10-30	106016 11997	1.6×10^{-7} 3.09×10^{-7}	< <	(0.009 5)	3.6
E ₃	0.001	0.019	No	10 20-100	4313	9.46×10^{-7}	<	(0.001 5)	3.35
E ₄	0.0013	0.024	No	5 10-30	34129	3.64×10^{-7}	>	0.001 1	0.815
E ₅	0.002	0.016	Yes	10 10-30	103912	3.18×10^{-7}	<	0.002 0	1.15

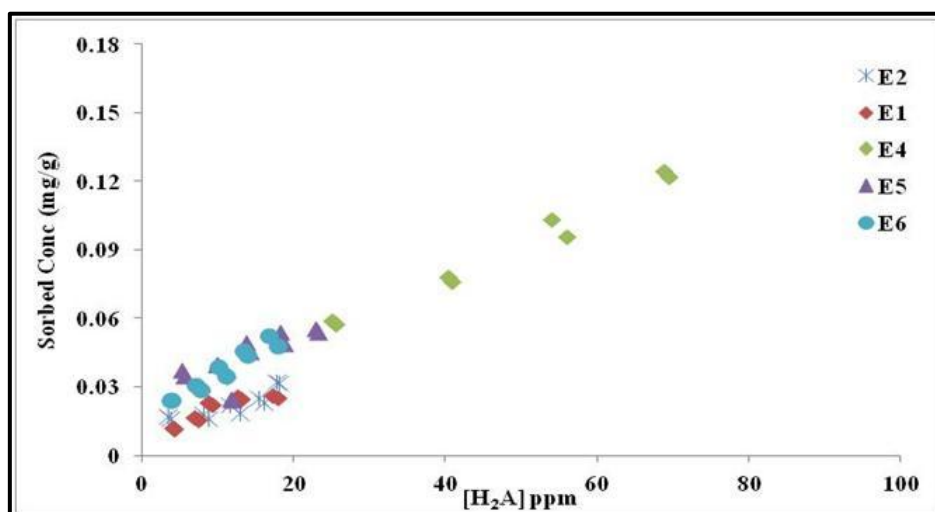


Figure (4-16) All experimental isotherms plotted together

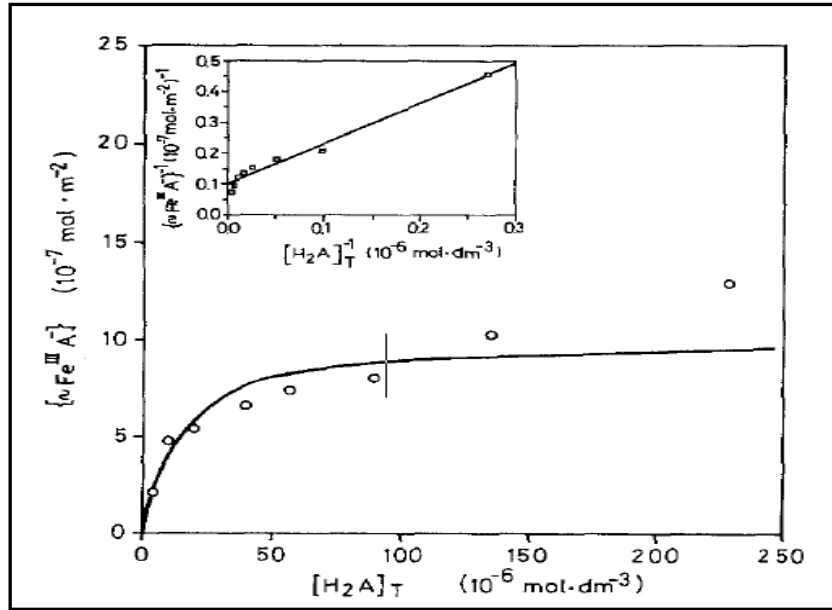


Figure (4-17) Langmuir sorption isotherm for ascorbic acid on the surface of synthetic hematite (α Fe_2O_3) at 25°C from (Afonso et al., 1990).

In conclusion different sorption experiments revealed that red sandstone was able to sorb ascorbic acid from solution, at pHs of 4.5-5, and that the sorption isotherm did not follow either linear or Langmuir sorption types properly but either might be used to obtain an estimate of the sorption over the range of concentration used in the experiments. The isotherms were the same shape as previous researchers obtained for synthetic hematite.

Chapter 5

Cation Exchange

5.1 Introduction

When Fe and Mn^{++} are produced by reductive dissolution of haematite by ascorbic acid some of the produced Fe and Mn^{++} will probably be taken up following ion exchange. This means concentrations of Fe and Mn^{++} may be underestimated. Therefore determining cation exchange capacity (CEC) and selectivity coefficients is important to correct the concentration of Fe and Mn^{++} . The goal of the studies described in this chapter was to determine CEC and selectivity coefficients for Fe and Mn^{++} on the red sandstone.

5.2 Cation Exchange

Cation exchange capacity is the capacity of sediment or soil to adsorb cations present in solution at aqueous phase (Gillespie et al. 2000). It is measure of the total concentration of cations attached by ion exchange (mainly charge attraction) and may be some other sorption (includes bonding) processes to the mineral surfaces. The most common unit to express CEC values is meq/100 g dry mass or centi-mol /kg dry mass (cmol_c/kg) (Essington, 2004).

Cation exchange capacity is a fundamental parameter for many sciences, for example in soil sciences this parameters can be used as an indicator for evaluating the degree of soil fertility (Alyabina, 2009). In environmental sciences, CEC plays a considerable role in determining the capacity of sediment for natural attenuation of various contaminants (Fetter, 1994).

Determining CECs is also very important in groundwater studies in order to estimate retardation of contaminant movement from landfill site to pristine aquifers (Gillespie, et.al 2000). Ceazan et al. (1989) studied a sand aquifer with <0.1% clay, but found that even with this tiny fraction of clay, the sediment was capable of causing a considerable drop of $[\text{NH}_4^+]$ and $[\text{K}^+]$ in a leachate plume coming from a landfill site.

CEC values vary with many factors including grain size of sediment, the kind of cations involved in the reaction and the competition among them, and pH (Essington, 2004). Not surprisingly, particle size has a big effect on cation exchange capacity. For instance, Kennedy (1965) found that with the decrease in the fraction size of selected stream sediments from 60-1000 μm to $<4 \mu\text{m}$ that CEC increased from (0.3-13) meq/100g to (14-65) meq/100g. Another example is MacIntyre et al. (1991) who report that alluvial aquifer material passing through 2mm sized sieves has higher CEC values of around (0.6 to 0.9 meq/100g) than the unsieved alluvial aquifer sediment. Figure (5.1) indicates typical ranges of CEC from some clay minerals, oxides and soils of various grain sizes. The highest range of CEC belongs to montmorillonite clay, while the lowest range of CEC belongs to sandy soils.

pH also affects CEC values. CEC represents the total amount of negative charges actually existing on the surface of sediment (clay + oxides in sediment) (Camberato, 2001). El-Ghonemy (1997) points out that pH at zero point of charge (ZPC) can be considered the boundary between cation exchange and anion exchange being dominant. At pHs of higher than ZPC, cation exchange is dominant while at pHs lower than ZPC was anion exchange is dominant. In groundwater systems, the majority of cation exchange reactions take place on the surface of clay minerals, and this is almost certainly the case for the English Triassic sandstones (El-Ghonemy, 1997; Tellam et al., 2002). As long as pH is greater than the ZPC for clay minerals which is about 3 cation exchange will dominate. The reaction is considered very quick and reversible (Parker, 2005).

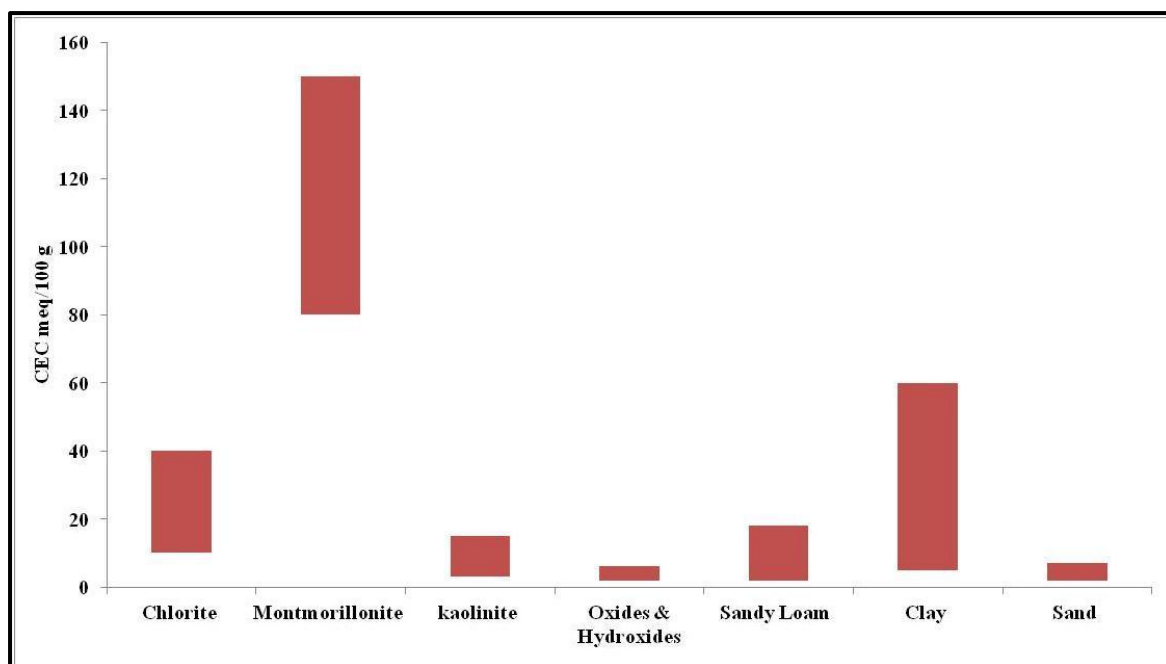


Figure (5-1) Typical ranges of values for cation exchange capacities of different soil texture and clay minerals (data from Dragun, 1988)

Physical and chemical properties of sediments and soils can result in a significant variation of CEC. In some sediments, organic matter (OM) can contribute significantly to cation uptake (El-Ghonemy, 1997; Aprile and Lorandi, 2012), but the Triassic Sandstone studied here contains only a tiny amount of organic matter. There is sometimes a positive correlation between CEC and pH, because of changes in surface charge particularly on oxides but also on clay edge sites (Aprile and Lorandi, 2012). CEC values for iron oxides depend on the pH value, for example the CEC of iron oxide may reach 100 meq/100 g, if the pH is bigger than 8.3 (Appelo and Postma, 2005). However, in general the CEC is much lower for oxide minerals (McBride, 1995).

Sandy soil and sandy loam soil have relatively small CEC values which range between 5 to 1 meq/100 g (Soil Chemistry, 2011). Boguslavsky (2000) found that in glacial sand sediment about 3 % of the CEC came from quartz and other non-clay silicates, while the remaining 97 % came from clay minerals, organic matter and oxides coating the sand grains. This suggests that the vast majority of CEC in sandstone will come from the small fractions of clay and

oxides. Batty (2015) has shown that the majority of the CEC in the sandstones used in the present study are not pH-dependent and this suggests that most of the CEC is from clays as usually assumed. Jaweesh (In Prep) has investigated the heterogeneity of CEC variation in a 65m length of English Triassic sandstone and found that from 129 samples the matrix sandstone excluding mudstones and mudclasts varies from 1 to 11 meq/100g with average, median and geometric means around 2.1 meq/100g.

In terms of reaction time Ogwada and Sparks (1986)(cited in Pandey et al. 2014) and Gillespie et al. (2000) state that very short time scales are needed for ion exchange reactions to occur in sediments, usually in time frames not exceeding 5 minutes, though Sparks (1989) indicates that ion exchange reactions take several seconds to 24 hours to get to equilibrium. Longer time periods are possibly associated with diffusion into inter-layer locations in clay structures.

5.3 Measurement of Cation Exchange Capacity of Sandstone Samples Using Strontium Chloride

The CEC of the sandstones was measured using a SrCl_2 flushing method of a type common in CEC estimation (e.g. Schäfer and Steiger (2002) who use the same concentration of SrCl_2 to determine CEC in sandy sediment). The method is to add Sr^{++} at concentrations great enough to displace effectively all other cations from the sandstone surfaces and then measure the Ca^{++} , Mg^{++} , Na^+ and K^+ released, the sum of these being the CEC estimate (other cations are assumed to be present in only negligible amounts). There is no need to correct for carbonate dissolution (Jaweesh, In Prep) as the sandstones contain no carbonate mineral.

The following steps explain the procedure to determine CEC for sandstone samples

1. Disaggregate about 400 g of red sandstone and mix well to make it homogeneous.
Then weigh 10 ± 0.002 g masses of sandstone and put them in each of four centrifuge tubes.
2. Dissolve 33.550 g of strontium chloride ($\text{SrCl}_2 \cdot 6\text{H}_2\text{O}$) in 500 ml of deionised water to prepare 0.25 M of $\text{SrCl}_2 \cdot 6\text{H}_2\text{O}$, then add 40 ml of this solution to each centrifuge tube containing the 10 g mass of sandstone. (This water-rock ratio will be the same as that used in the final ascorbic acid/sandstone experiments.)
3. Repeat the experiment but using deionised water instead of strontium chloride.
4. Measure the pH of the solution with sediment before separating the supernatant from the sediment.
5. Analyse the solutions for Ca^{++} , Mg^{++} , Na^+ , K^+ , Fe^{++} and Mn^{++} using FAAS
6. Put the all centrifuge tubes in a shaker and shake for 1 h under gentle speed (300 rpm) and then centrifuge for 15 min at 4500 rpm in order to settle the sediment in the bottom of the tubes (the fine fraction (clay) settled on the top of sand grains). Remove around 25 ml of supernatant and filter using a $0.2 \mu\text{m}$ pore size filter.
7. Analysis for potassium, magnesium, manganese and iron was carried out without dilution, while calcium and sodium samples were diluted. The Mn^{++} and Fe samples were acidified by nitric acid after separating from the sediment in order to stop the oxidation of Mn^{++} and Fe^{++} which could have led to decline in concentration.

All the samples have pHs in the range from 4.98 to 4.18. The pH of the samples with strontium chloride have pHs lower than those with deionised water by about 0.5 pH units. The pH values in the final experiments described in Chapter 6 have a minimum value of about 4.4 so this suggest that the CEC values obtained in this chapter are appropriate.

These pHs also confirm that there is negligible carbonate in the sandstone. This is good as carbonate will affect CEC measured using SrCl_2 as the presence of carbonate minerals leads

to increase in the apparent CEC value (Gillespie et al. 2000;cited in Aprile and Lorandi, 2012). Jaweesh (in preparation), working with carbonate-containing English Triassic sandstones and correcting for carbonate dissolution used different concentrations of CsCl ranging from 0.1 M to 4 M to determine CEC. Jaweesh (in preparation) found that there is no significant correlation between CEC and concentration of CsCl with a shaking time in the range from 10 min to 100 min and water/rock ratio.

The CEC results are listed in Table (5.1). Because the deionised water experiments resulted in small but significant release of ions possibly from precipitated pore water salts as well as existing mineral dissolution, the concentrations from the deionised water experiments have been subtracted from the concentrations from strontium chloride experiments to obtain the CEC estimates. The results are given in Table (5.2).

Table (5-1): The concentrations in solution obtained after contact of deionised water and strontium chloride solutions with the sandstone. Calcium ions dominate. Iron was not detectable using FAAS.

Samples	Ca ⁺⁺	Mg ⁺⁺	Na ⁺	K ⁺	Fe ⁺⁺	Mn ⁺⁺	pH
	ppm						
diw (1)	21.50	3.72	13.29	5.93	b.d.l.	1.13	4.98
diw(2)	21.47	3.63	13.47	6.0	b.d.l.	1.12	4.88
diw(3)	20.80	3.50	13.58	6.19	b.d.l.	1.18	4.86
diw(4)	20.48	4.10	13.39	6.34	b.d.l.	1.20	4.78
min	20.48	3.50	13.29	5.93	b.d.l.	1.12	4.78
max	21.47	4.10	13.58	6.34	b.d.l.	1.20	4.98
average	21.04	3.74	13.43	6.12	b.d.l.	1.16	
SrCl ₂ .6H ₂ O (1)	141.50	7.95	13.65	9.75	b.d.l.	2.85	4.19
SrCl ₂ .6H ₂ O (2)	147.80	8.22	13.50	10.43	b.d.l.	2.73	4.31
SrCl ₂ .6H ₂ O (3)	145.90	8.27	13.24	10.35	b.d.l.	2.52	4.35
SrCl ₂ .6H ₂ O (4)	136.30	8.12	13.47	9.97	b.d.l.	3.04	4.32
min	136.30	7.95	13.24	9.75	b.d.l.	2.52	4.19
max	147.80	8.27	13.65	10.43	b.d.l.	3.04	4.35
average	142.87	8.14	13.47	10.12	b.d.l.	2.78	

Mn^{++} and Fe may be released at low concentrations by desorption from hematite, especially at low pH values. In addition there will be some dissolution of hematite and MnO_2 especially at low pH. The release is shown by ascorbic acid free experiments (Table (5-1)) . The concentrations are small in comparison with the release in the presence of ascorbic acid and have been taken into account during the processing of the experimental data. In addition, both Fe and Mn^{++} will also be involved in ion exchange reactions and the experimental data were processed to try and take the exchange processes into account. However, the significant effect of the presence of ascorbic acid on both Mn^{++} and Fe concentrations strongly suggests that reductive dissolution has occurred and dominates.

The CEC values for the sandstone samples using 0.25 M of $\text{SrCl}_2 \cdot 6\text{H}_2\text{O}$ ranged from 2.5 to 2.74 meq/100 g with an average of 2.64 meq/100g. This is close to the average CEC (2.1 meq/100g) obtained by Jaweesh (In Prep) mentioned above. Tellam et al. (2002) found similar CEC values for the analysis of 12 samples of English Triassic sandstone. They found values ranging from 0.6 to 2.3 meq/100 g with an average value of 1.2 meq/100g. Variation in CEC may be caused by differences in the amounts of clay present or the type of clay (Shafie et al. 2013; El-Ghonemy 1997). Gillespie et al (2000) found a mean value for CEC using SrCl_2 of Permo-Triassic Sherwood Sandstone Group rocks where they measured grains bigger than $0.2\mu\text{m}$ was 2.41meq/100 g with a 0.11 meq/100g standard deviation, while the same sediment but looking at the grain size “ $< 0.2 \mu\text{m}$ ” (may be means $<2\mu\text{m}$?) was CEC 14.46 meq/100 g (0.61 meq/100g standard deviation). Similarly Reardon et al. (1983) determined CEC for calcareous sands in Ontario, Canada, and found that the average CEC value was about 0.51 meq/100 g.

Ca^{++} was the dominant cation on the exchange sites. Bjerg and Christensen (1993) also found this for their sandy aquifer sediments but also observed H^+ was important under acidic pH conditions.

Table (5-2): Concentration of cations corrected for concentrations from deionised water experiments and resulting total CEC for the sandstone samples. (b.d.l. = below detection limit.)

samples	Ca^{++}	Mg^{++}	Na^+	K^+	Fe^{++}	Mn^{++}	CEC
	meq/100 g dry sandstone						
1	2.39	0.13	0.006	0.039	b.d.l.	0.025	2.606
2	2.52	0.15	0.0006	0.045	b.d.l.	0.023	2.741
3	2.49	0.15	0.004	0.042	b.d.l.	0.019	2.720
4	2.31	0.13	0.001	0.037	b.d.l.	0.026	2.509
min	2.31	0.13	0.0006	0.037	b.d.l.	0.019	2.509
max	2.52	0.15	0.006	0.045	b.d.l.	0.026	2.741
average	2.43	0.14	0.003	0.040	b.d.l.	0.023	2.644

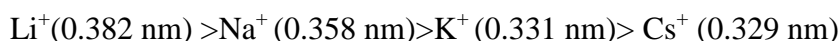
5.4 Selectivity Coefficients

The simple definition of selectivity coefficient is the relationship between the dissolved cations in aqueous phase and cations on the exchange sites (sediment surface) under equilibrium. The selectivity of cations rises with increase in cation charge and declines with hydrated ionic radius (McBride, 1995; Essington, 2004; Dube et al., 2001; Appelo and Postma, 2005). The sequence below indicates the order from more favoured to less favoured on the exchange surfaces (Fetter, 1999), though the actual composition on exchange sites is also dependent on the ions's activity in solution:



In low ionic strength solutions, many exchangers prefer multivalent cations rather than monovalent cations, whereas in elevated ionic strength solutions the exchange phase on the solid surface prefers monovalent cations (Drever, 1997; Essington, 2004).

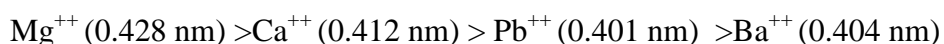
To see the dependence on hydrated radius sequences of cations from lower to higher likeliness to attach to a surface have been put together by Essington (2004) for monovalent and divalent cations. For monovalent cations (hydrated ion radius)



More replaceable

Less replaceable

and for divalent cations



More replaceable

Less replaceable

Ion exchange is usually modelled using equations based on the equilibrium constant equation and this is the formal definition of the selectivity coefficient. A straightforward example to explain the method is to take the example of exchange between Ca^{++} and K^+ :



$$K_s = \frac{(CaX_2)(K^+)^2}{(KX)^2(Ca^{++})} \dots\dots\dots (5-1)$$

K_s = selectivity coefficient (dimensionless)

(K^+) = aqueous activity (dimensionless)

(KX) = activity of ion on the exchange site (dimensionless).

The main problem is that there is no generally accepted method for estimating the activity of the sorbed ions. However, there are various approximate ways to do this named after people who proposed it. For example Vanselow, and Gaines and Thomas. There are also other methods (the Rothmund-Kornfeld method modifies the equation by raising one of the concentration ratios by a power and the Gapon method changes the reaction so that only single charges are transferred (e.g. Essington, 2004)). In this chapter the Gaines-Thomas method (Gaines and Thomas, 1953) will be used as this is the most common in hydrogeology (El-Ghonemy 1997; Bolt, 1982; Evangelou and Phillips, 1988).

The Gaines-Thomas convention approximates the exchanged activities by using equivalent fractions (Vanselow uses mole fractions):

$$K_{Ca/K} = \frac{X_{Ca}(K^+)^2}{X_K^2(Ca^{++})} \dots\dots\dots (5-2)$$

where

X_{Ca} represents the equivalent fraction of cation on the exchange site, i.e. the concentration in meq/100g of the ion divided by the CEC:

$$X_{Ca} = \frac{Ca \text{ on exchange sites in meq per } 100 \text{ g}}{CEC} \dots\dots\dots (5-3)$$

(Ca^{++}) represents the dissolved activity (from multiplying the concentration in mol/l by the activity coefficient for that ions).

So in the case of the six cations concerned in the present results (Ca, Mg, Na, K, Fe and Mn) this means

$$X_{Ca} + X_{Mg} + X_{Na} + X_K + X_{Fe} + X_{Mn} = 1 \dots\dots\dots (5-4)$$

Because the sorbed activities are approximations, the K value is not really an equilibrium

constant and is therefore called a selectivity coefficient. It was shown by El-Ghonemy (1997) to vary with composition of the exchange sites for Triassic sandstone. Table (5-3) lists the definitions of the selectivity coefficients used in this study.

Table (5-3) Equations used to determine selectivity coefficient for different pairs of cations using the Gaines - Thomas convention used in this study.

$K_{Ca/Mg} = \frac{X_{Ca} (Mg^{++})}{X_{Mg} (Ca^{++})}$	$K_{Ca/Na} = \frac{X_{Ca} (Na^+)^2}{X_{Na}^2 (Ca^{++})}$
$K_{Ca/K} = \frac{X_{Ca} (K^+)^2}{X_K^2 (Ca^{++})}$	$K_{Ca/Mn} = \frac{X_{Ca} (Mn^{++})}{X_{Mn} (Ca^{++})}$
$K_{Ca/Fe} = \frac{X_{Ca} (Fe^{++})}{X_{Fe} (Ca^{++})}$	

To calculate the selectivity coefficients, dissolved phase activity coefficients were calculated using the extended Debye-Huckel equation:

$$-\log \gamma_i = \frac{A Z_i \sqrt{I}}{1 + a_i B \sqrt{I}} \dots \dots \dots (5-5)$$

γ_i = activity coefficient (molality⁻¹)

m = concentration (mol/kg H₂O)

I = the ionic strength of the solution (mol/kg H₂O).

A and B = constants dependent on temperature of solution (e.g. Fetter, 1994)

a_i = the ion size parameter which varies between 3 and 11 x 10⁻¹⁰ m according the type of ion (e.g. Fetter, 1994). In the absence of anion concentration data the ionic strength was estimated using Reardon et al. (1983) and Carlyle (1991):

$$I = \sum_1^n m_i z_i^2 \dots \dots \dots (5-6)$$

m_i = molality of cation

z_i = the charge of cation i

n = number of cations.

The activities were calculated using the total concentrations observed in solution. The exchanged ion concentrations were calculated by correcting the observed concentrations using the deionised water experiment results as described above. Calculations are provided in Appendix (5.1).

The results are shown in Table 5.4. Table (5.5) lists Gaines-Thomas selectivity coefficients from the literature for sandstones and sandy sediments. The values obtained here are generally within the range found elsewhere though $K_{Ca/Mg}$ values are a little higher in this study.

Table (5-4) Gaines-Thomas selectivity coefficient values

Samples No.	$K_{Ca/Mn}$	$K_{Ca/Mg}$	$K_{Ca/K}$	$K_{Ca/Na}$
1	1.44	1.61	0.08	1.74
2	1.49	1.57	0.07	10.78
3	1.59	1.56	0.07	14.74
4	1.37	1.57	0.07	1.69
average	1.47	1.58	0.07	1.71
standard deviation	0.092	0.022	0.005	6.57

Table (5-5) Gaines-Thomas selectivity coefficients from the literature for sandstones and sandy sediments.

References	$K_{Ca/Mg}$	$K_{Ca/K}$	$K_{Ca/Na}$	$K_{Ca/Mn}$	$K_{Ca/Fe}$
Appelo & Postma (2005)			2.5	1.4	1.5
Carlyle (1991) English Triassic Sandstone	1.27	0.2			
Reardon et al. (1983)	1.3	0.001			
Tellam et al. (2002) English Triassic Sandstone	0.96	0.2			
El-Ghonemy (1997)		0.28-0.6			
The present study	1.58	0.07	1.71	1.47	

5.5 Experiments on Fe (II) Exchange

Iron was not released in measureable amounts from the treatment of the sandstone samples with $SrCl_2$ during the determination of CEC. Therefore separate experiments were carried out to determine the selectivity coefficients for Fe (II) exchange.

20, 15, 10, 5, 2.5, 0 ppm Fe^{++} solutions were made up from a $FeCl_2$ stock solution. Then 40 ml of these ferrous iron solutions were added to 10 g of sandstone (similar rock water ratio for final experiment, Chapter 6) in duplicate. Ca^{++} , Mg^{++} , Na^+ , K^+ , Mn^{++} and Fe^{++} concentrations were measured after shaking for 1 h at 300 rpm and centrifuging for 15 min at 4500 rpm. All samples were filtered using 0.2 μm filters before analysis. pH was also measured on each sample.

All the data are provided in Appendix (5.2). As can be seen from Figure (5.2), there is considerable increase of Ca^{++} with increase in ferrous iron concentration in solution and a slight increase of the concentrations of the other cations except sodium. In all cases the initial iron concentration dropped after interaction with the sandstone, consistent with sorption taking place. Though oxidation of Fe^{++} by oxygen is possible it will be assumed insignificant. The drop in Fe concentration was greater than the increase in Mn^{++} which might

have been the result of reductive dissolution of MnO_2 by Fe (II). For instance the initial 20 ppm of Fe dropped to 11.3 ppm after interaction with the sandstone, while the total amount of Mn present was 1.7 ppm. And the initial concentration of Fe of 5 ppm dropped to 2.2 ppm after interaction with sandstone, while the amount of Mn^{++} present was 1.3 ppm. In other words the amount of Fe decline was higher than amount of Mn^{++} increase even taking into account the fact that 2 moles of Fe are required to reduce one mole of Mn. This does not mean that no MnO_2/Fe reaction occurred just that this did not control the Fe concentrations. Even if some oxidation of Fe had occurred it would not necessarily mean that all Fe was removed from the system by precipitation as a ferric oxide. However this is still uncertain.

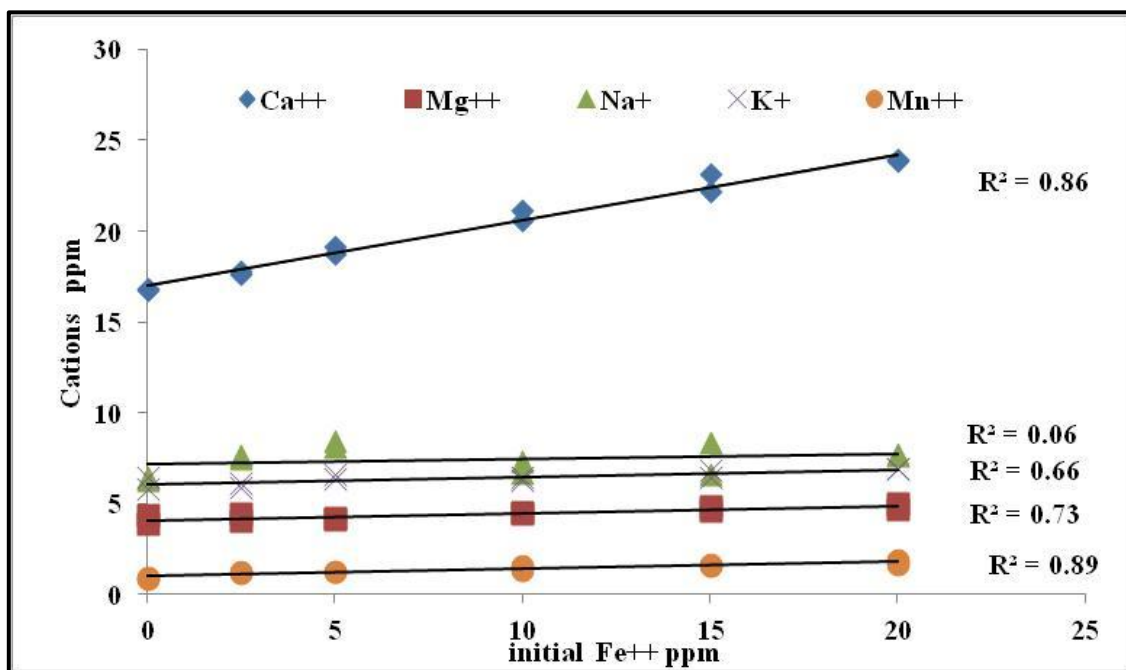


Figure (5-2) Concentrations of cations released from 10 g sandstone in contact with various initial concentrations of ferrous iron solutions.

To calculate the selectivity coefficient for Ca/Fe exchange,

a hydrochemistry numerical model (Phreeqc) has been used. The rock was equilibrated with the composition of the solutions after DIW was added and assuming Fe concentration was 0.4 ppm. The CEC and selectivity coefficients used were those from the previous analysis but $K_{\text{Ca/Fe}}$ was used as a calibration variable. Then FeCl_2 was added in same amounts as in the lab

experiment. $K_{Ca/Fe}$ was varied until the observed data were matched by the model. The best match was judged by eye.

The results are plotted in Figure (5.3) and appendix (5.3). The match of the model to the lab data seem good though perhaps Ca^{++} and Mg^{++} are a bit low. From the results it looks like the calibrated selectivity coefficient of $K_{Ca/Fe}$ was very low ,around 0.01. This is much lower than Appelo and Postma's (2005) value of 1.5.

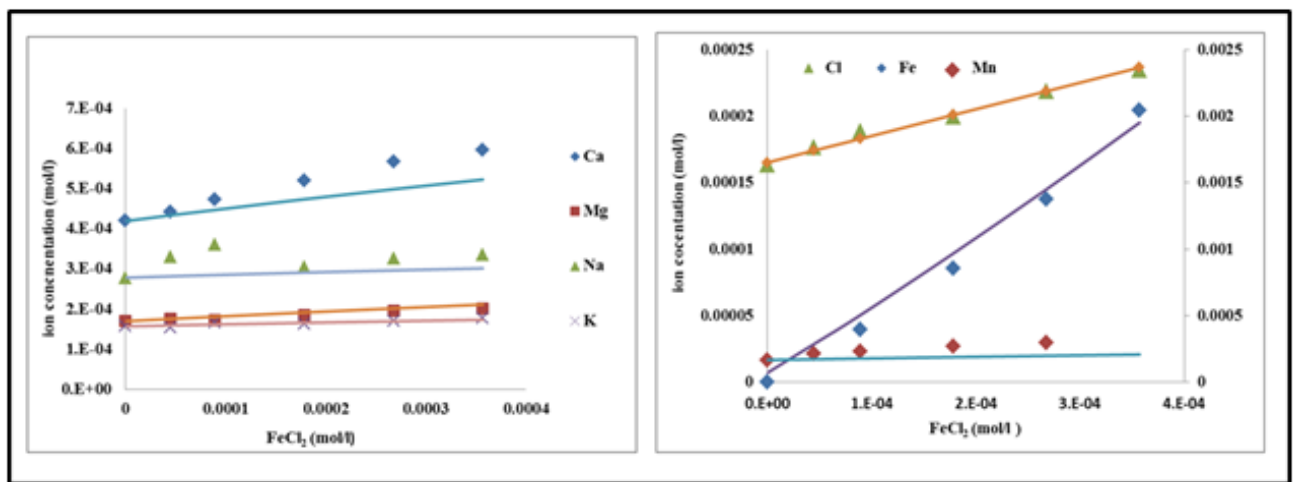


Figure (5-3) Results of Phreeqc modelling of the $FeCl_2$ experiments.

5.6 Sorption of Mn^{++}

A further experiment was undertaken using Mn^{++} . Concentrations of 20, 15, 10, 5, 2.5, and 0 ppm were prepared and 40 ml of each was added to 10g of sandstone in duplicate. The procedure of this experiment was the same as for the Fe experiments described in the previous section.

The results are shown in Figure (5.4) and appendix (5.4). The sorbed concentrations have been corrected using the average concentrations measured in the two 0 ppm Mn experiments. It is clear that they cannot be correctly interpreted just as a sorption isotherm. The negative sorption concentrations suggest that there is Mn^{++} supplied from another source. This may be

just for the two negative sorption value results but also may be for the other values.

Insufficient time was available to repeat the experiments.

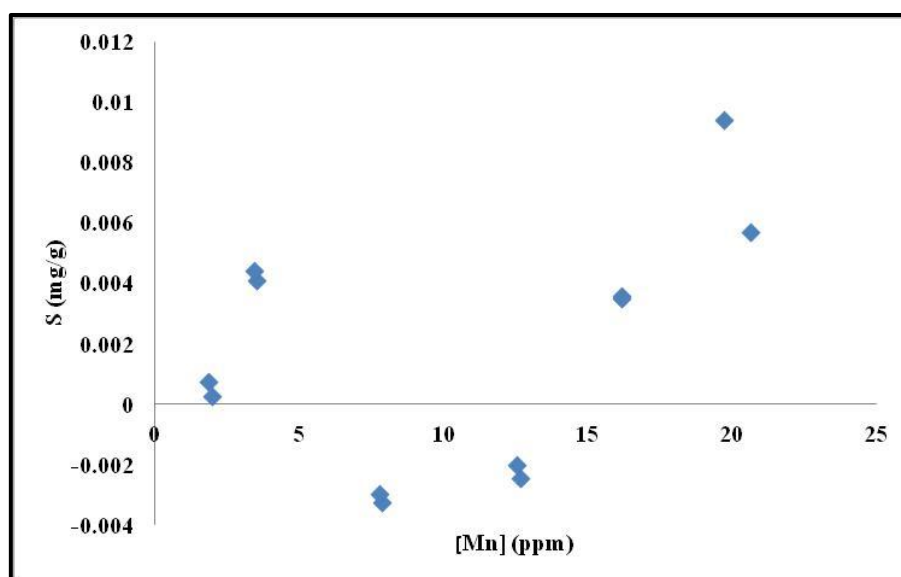


Figure (5-4): The isotherm for the Mn experiments.

So we rely on the Mn selectivity coefficient values obtained during the ion exchange experiments though even these are not certain for the same reasons as given here. However, they are very similar to values from the literature.

5.7 Conclusions

The reason to investigate the ion exchange reactions was to find out the effect on the Fe and Mn^{++} concentrations following ascorbic acid being added to sandstone. Without correction the measured values of Fe and Mn^{++} would be underestimated, due to adsorption on the surface of oxides and clay.

Many batch experiments have been carried out to determine cation exchange capacity of the sandstone samples. The results revealed that CEC varies from 2.50 to 2.74 meq/100 g with good repeatability among samples. This value is relatively low in comparison with CEC values for other kinds of sediment like clay.

Selectivity coefficients have been determined for Mn and Fe and the value for Mn was significantly higher than for Fe ($K_{Ca/Mn}=1.47$ while for $K_{Ca/Fe}=0.01$). The values interpreted are not precise and depend on the models used (Gaines-Thomas) and the other assumptions made (initial concentrations for example). The final Mn experiments indicate possible problems. However the models used were able to reproduce acceptably the concentrations observed in the experiments. The Mn selectivity coefficient agreed very well with the value obtained from literature but the Fe one was much less. However as Mn^{++} concentrations are greater in the experiments of Chapter 6 than the Fe concentrations the main effect of corrections depends on the Mn selectivity coefficient. The results will be used in Chapter 6.

Chapter 6 Reaction of Ascorbic Acid and English Triassic Sandstone

6.1 Introduction

From experiments carried out by previous authors on synthetic hematite it was thought that ascorbic acid may be able to reductively dissolve natural hematite and may provide insights into the oxidation of dissolved organic matter by hematite coated surfaces of the English Triassic Sandstone (Chapter 1). In Chapter 2 it was shown that ascorbic acid was capable of reductively dissolving hematite and Mn oxides from sandstone samples from the English Triassic Sandstones. In Chapter 3 a method for the analysis of ascorbic acid was developed. In Chapter 4 the sorption of ascorbic acid in the sandstones was investigated as this was assumed to be the first stage of the reductive process. In Chapter 5 ion exchange was investigated as it was expected that any Fe and Mn⁺⁺ released by reductive dissolution may be taken up in part by exchange sites. In this chapter the final experiments on the reaction of ascorbic acid and sandstone are undertaken under both unsterile (biotic) and sterile (abiotic; Benelli, 2015) conditions. Both set of experiments are in anaerobic box.

6.2 Methods

The method used is listed below.

- 1- Preparation of sandstone samples. Samples were collected from sandstone outcrop close to Quatt, Shropshire (National Grid Reference SO75528823). Samples were disaggregated using a pestle and mortar, to convert the slightly cemented sandstone to sand. The sand was then mixed well together to make them homogeneous. Then 10 g \pm 0.001g subsamples of the crushed sand were put in 50 ml centrifuge tubes (Corning CentristartTM).

- 2- Preparation of H₂A. 100 ppm stock solution of H₂A was prepared and diluted to 80, 60, 40 20 and 0ppm under aerobic conditions. Then these solutions were put inside the anaerobic chamber. The chamber was purged with N₂ gas which was also used to purge each standard solution for 5 min to remove dissolved oxygen from it.
- 3- Preparation of the anaerobic box. All the equipment (pipette, pH & Eh meter, shaker, syringe and 0.5 M of HNO₃) for the experiment and all samples were placed inside the anaerobic box.
- 4- Preparation of reactions. 40 ml of 100, 80, 60, 40, 20 and 0 ppm ascorbic acid solution were added to each centrifuge tube which contained the 10 g sandstone samples. Replicates were as indicated in Table (6-1).

Table (6-1) Replication of samples

[H ₂ A] ppm	Number of replicates
100	3
80	1
60	3
40	1
20	3
0	1
Total	Σ12

- 5- Reaction. All the centrifuge tubes were put in a shaker inside the anaerobic box, and shaken at 300 rpm for different times: 4.5, 16, 24, and 49 h.
- 6- Sample preparation. After shaking measure the pH and Eh for each sample in presence of the sediment, then filter 15 ml of each solution using a 0.2 μm syringe filter (Acrodisc syringe filters).
- 7- Analysis of Mn⁺⁺ and Fe. 10 ml of filtered sample was used to determine the concentrations of Fe and Mn by FAAS, after acidification by 150 μl of 0.5M of HNO₃

to maintain low pH and prevent precipitation of ferric iron, and Mn^{+4} oxides during exposure of samples to the oxygen during analysis.

- 8- Analysis of H_2A . 5 ml of KMnO_4 was added to 5 ml of ascorbic acid sample, then shaken by hand for less than 1 min and put in a cuvette to measure the absorbance at 530 nm with three replicates using UV-vis spectrophotometry.

The same above lab procedure was repeated by Benelli (2015) under the author's supervision using heat-treated samples and all equipment used in this experiment was sterilized.

Many previous researchers suggest using autoclaves to sterilize sandstone core samples (Jang et.al 1983; Jenneman, 1985, 1986). Therefore, dry heating has been used to prepare abiotic sandstone samples. Each sample was put in an oven at 90 °C for 48 h. NEB (2015) state that at around 60 °C most microorganisms will be killed and this was confirmed by Handley-Sidhu (pers. comm., 2015). Higher temperatures were not used because of possible damage to the sandstone mineral surfaces. To test how well this worked, microbiology plate tests were carried out for heat-treated and unsterilized sandstone samples. From Figure (6.1) it is clear that most bacteria are killed off though may be not all. The sandstone may not be completely sterilised, but it is likely from the observed results that biotic activity will be significantly inhibited using this method. All equipment was washed first with 5% HCl, and then rinsed with deionised water several times before placing in an autoclave at 120 °C for about 20 minutes. The inside surfaces of the anaerobic box were wiped using an antibacterial solution. Solutions used were all filtered.

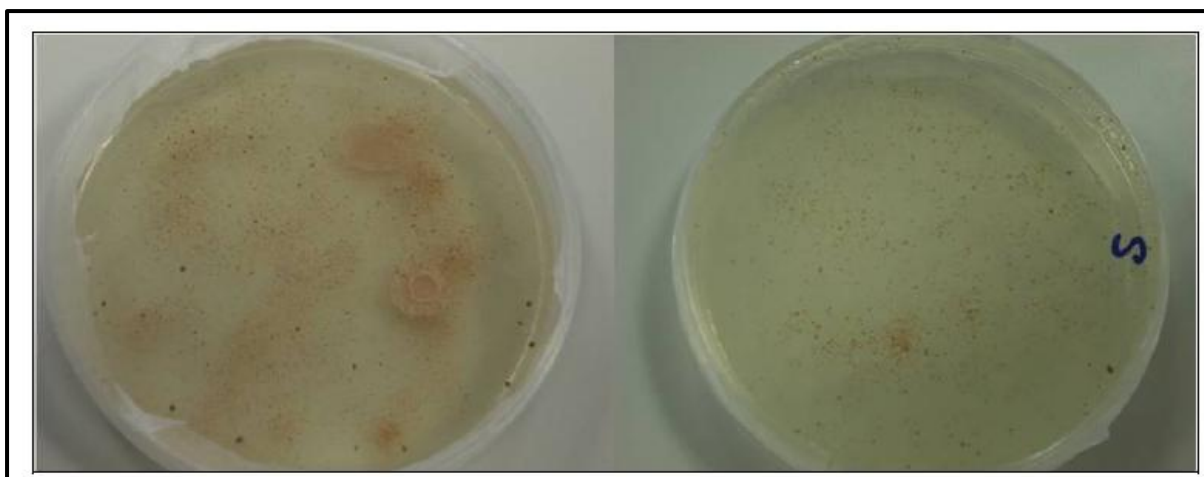


Figure (6-1) Agar plates after 3 weeks of incubation of untreated sandstone (left) and heat-treated sandstone (right). High bacteria population growth in the left plate, which represents sandstone without any treatment (unsterilized), while there are many less bacteria in the right plate sample which represented an attempt at providing an abiotic control condition (Benelli, 2015).

There are three steps to correct the raw data: correct the apparent H_2A analytical concentration for the effect of Mn; correct for the degradation observed in experiments without sandstone (Chapter 3) over time; and correct for Fe and Mn concentration as a result of ion exchange uptake of these metals.

For the Mn^{++} correction, the below equation has been used to carry out this correction for all the concentrations of ascorbic acid

$$[H_2A]_c = [H_2A]_{dissolved} - (-3.96) \times ([Mn] / 55 - [Fe] / 56 / 2) \times 55$$

$[H_2A]_c$ = the concentration of H_2A after correction for the concentration of Mn in the sample

-3.96 constant is derived from the data in Chapter 3. The main effect (Chapter 3) was due to MnO_2 colloids forming due to oxidation of Mn^{II} by the permanganate. This causes rise in absorbance. But Fe^{II} reacts with MnO_2 colloids to produce Mn^{II} so reducing the effect of the

colloids. It is possible that the produced MnII reacts again with permanganate to produce more MnO₂ colloids within the time of the analysis. But checks on including and excluding the Fe correction indicate that there is only a slight effect.

After applying this correction to the raw data, the corrected H₂A concentration was a higher than the raw concentration value. The effect of correction increased with the rise in [Mn⁺⁺] in the solution. For example the average H₂A after 4.5 h was 73 ppm before correction but increased to 82 ppm after correction, (see appendices 6.1 to 6.5).

The effect of degradation of H₂A was corrected for using the equation below (Chapter 3).

$$[\text{H}_2\text{A}]_{\text{deg}} = 0.0921 \times (\text{time in hours} + 2)$$

where 0.0921ppm /hour is the constant derived in Chapter 3. The 2 hours was added to the reaction time for preparation and analysis.

$[\text{H}_2\text{A}]_{\text{deg}}$ = the concentration of H₂A corrected for degradation.

The correction effect of degradation was minor. For example after 4.5 h in one biotic experiment the 82 ppm increased to 82.6 ppm after correction, while after 49 h 30 ppm increased to 34.9 ppm, the effect of degradation increasing over time, (see appendices 6.1 to 6.5).

Fe and Mn will be up taken on exchange surfaces and the selectivity coefficients and cation exchange capacities were determined in Chapter 5. The corrections were done in the following way. A Phreeqc model was set up that equilibrated the sandstone with the measured cation exchange capacities and Gaines-Thomas selectivity coefficients with a water with concentrations obtained from analysis of DIW in contact with sandstone. Fe and Mn⁺⁺ were then added by trial and error in amounts that produced the observed concentrations in solution. The total added Fe and Mn⁺⁺, i.e. the increase in solution and the increase in sorbed

concentration, were the predicted amounts of Fe and Mn^{++} added through reductive dissolution.

The amount of increase was significant for the [Mn] and minor for Fe. For example in a biotic experiment after 4.5 h the average of Mn released was 2.68 ppm but after ion exchange was taken into consideration using Phreeqc it increased to 5.1 ppm, while in the case of Fe the ion exchange correction changed the concentration from 1.13 to 1.28 ppm. (see appendices 6.1 to 6.5).

6.3 Results and Initial Observations

This section presents the results of the experiments and commenting on the data. Following sections present an interpretation of the data based on the initial observations made in Section 6.3.

Appendices (6.1) to (6.5) and figures (6.2) to (6.12) summarize the results of the data after correction. The H_2A measurements have been corrected for Mn concentrations and degradation using the methods suggested in Chapter 3. The correction for ion exchange have been undertaken on the Fe and Mn values. A number of preliminary observations can be made by referring to these plots.

For the biotic experiments there is an increase in the release of Mn^{++} and Fe over time and a sharp drop of $[\text{H}_2\text{A}]$ from its initial concentration with time. For all concentrations of H_2A , Mn released was significantly higher than Fe release as found for low temperature and concentrations and high water rock ratios in Chapter 2. Besides the increase release of Mn and Fe over time for given initial $[\text{H}_2\text{A}]$, also there is a rise of release of Mn^{++} and Fe with rise in the initial $[\text{H}_2\text{A}]$. pH values showed a decrease with greater initial H_2A concentrations as expected. They also increased a small amount through each biotic experiment, and Eh fell.

In the abiotic experiments (Benelli, 2015) there was a similar pattern. Increase in Fe and Mn^{++} concentrations (except for 49h, see below), the latter being greater than the former, with both time and initial $[\text{H}_2\text{A}]$, and a decrease in $[\text{H}_2\text{A}]$ with time. However the Fe and Mn^{++} concentrations were generally lower and the H_2A concentrations were higher than for the biotic experiments. In all abiotic cases the change in concentration in Fe and Mn^{++} between the 24 and 49hour samples appeared not consistent with the previous rise and in many cases there was a fall in concentration. pH showed similar relationship with initial H_2A concentration as with the biotic experiments with pH linearly decreasing with increasing $[\text{H}_2\text{A}]$, but the pH value for abiotic was higher. Similar with Eh, but here abiotic Eh was lower than biotic (Figure 6.12). In summary in all cases there is a drop of H_2A over time for biotic and abiotic experiments, though the amount of decline was higher in biotic experiments than in abiotic experiments. In general these results confirm the ability of red sandstone to oxidise the dissolved organic carbon.

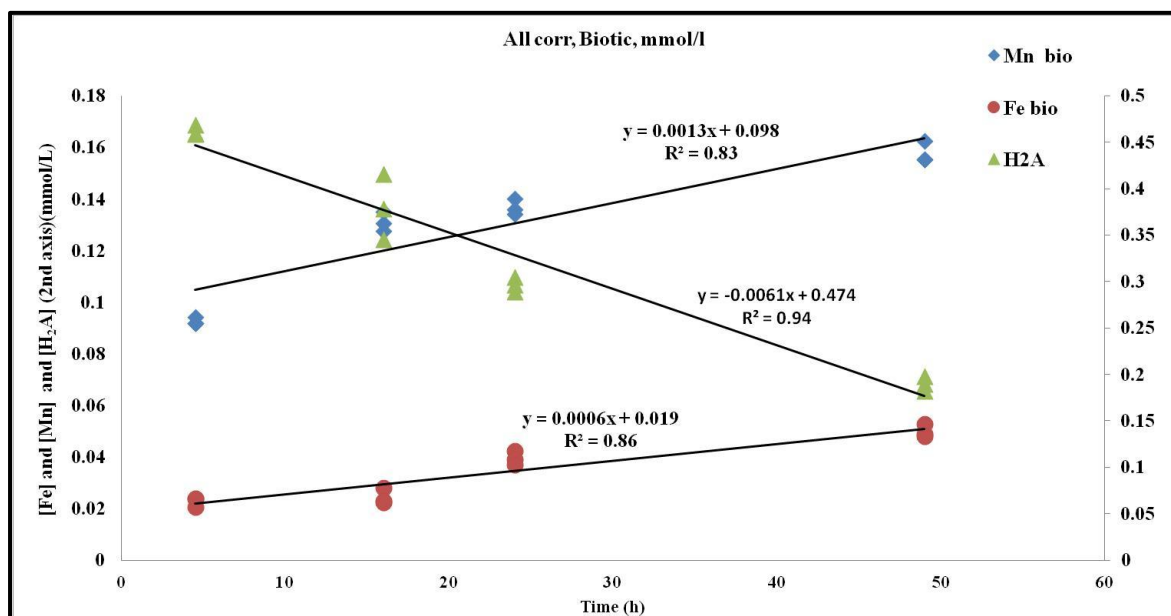


Figure 6-2 Amount of Fe and Mn^{++} released into the solution and concentration of H_2A for biotic experiments using an initial H_2A of 100 ppm.

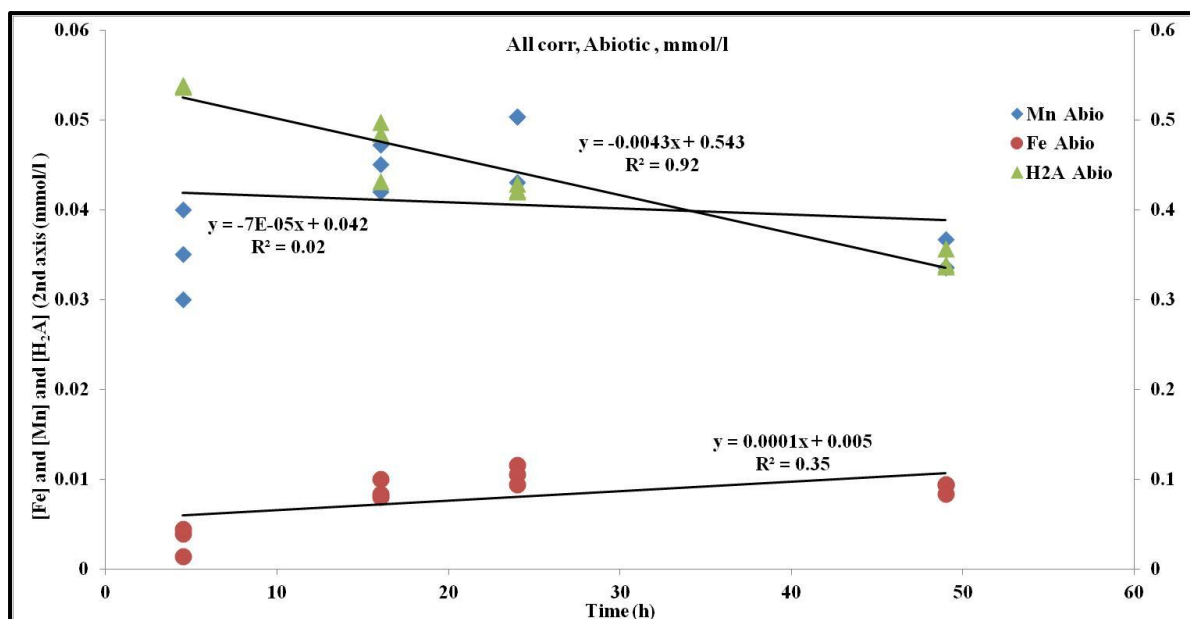


Figure 6-3 Amount of Fe and Mn^{++} released in the solution and concentration of H_2A for abiotic experiment using initial H_2A of 100 ppm.

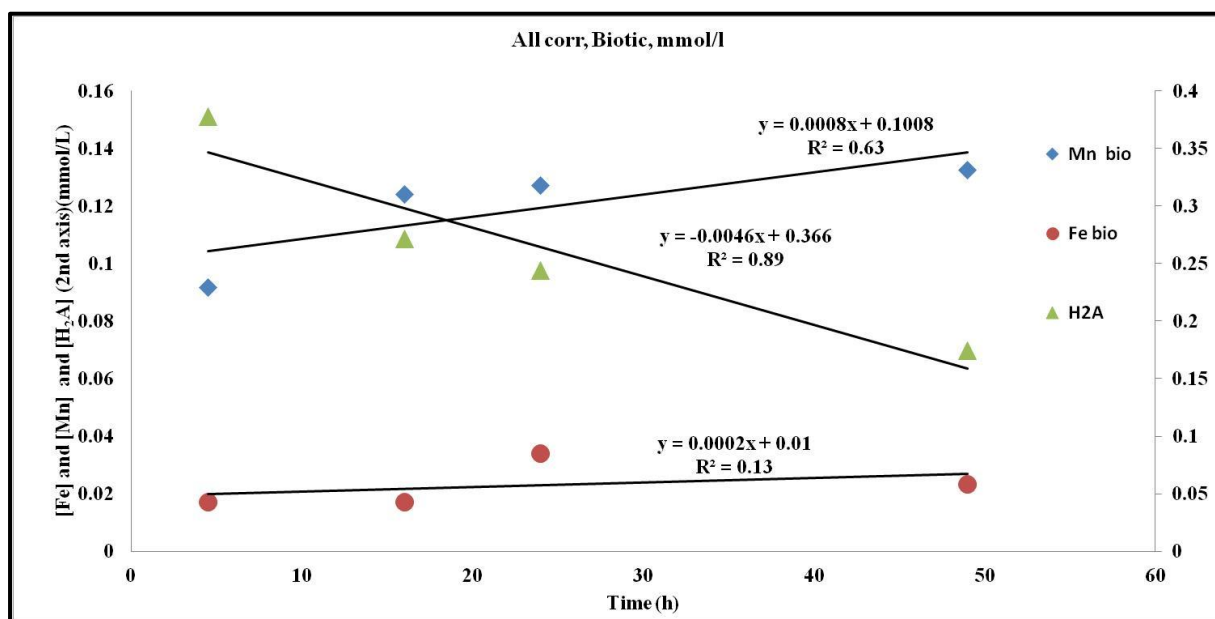


Figure 6-4 Amount of Fe and Mn^{++} released in the solution and concentration of H_2A for biotic experiment using initial H_2A of 80 ppm.

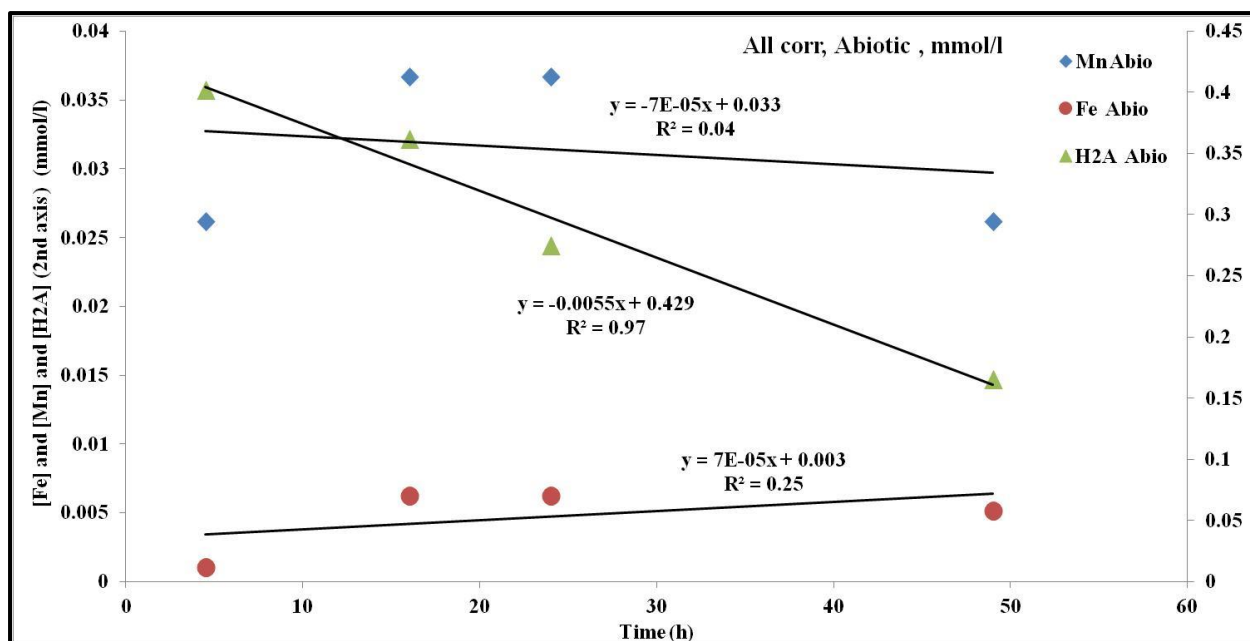


Figure 6-5 Amount of Fe and Mn^{++} released in the solution and concentration of H_2A for abiotic experiment using initial H_2A of 80 ppm.

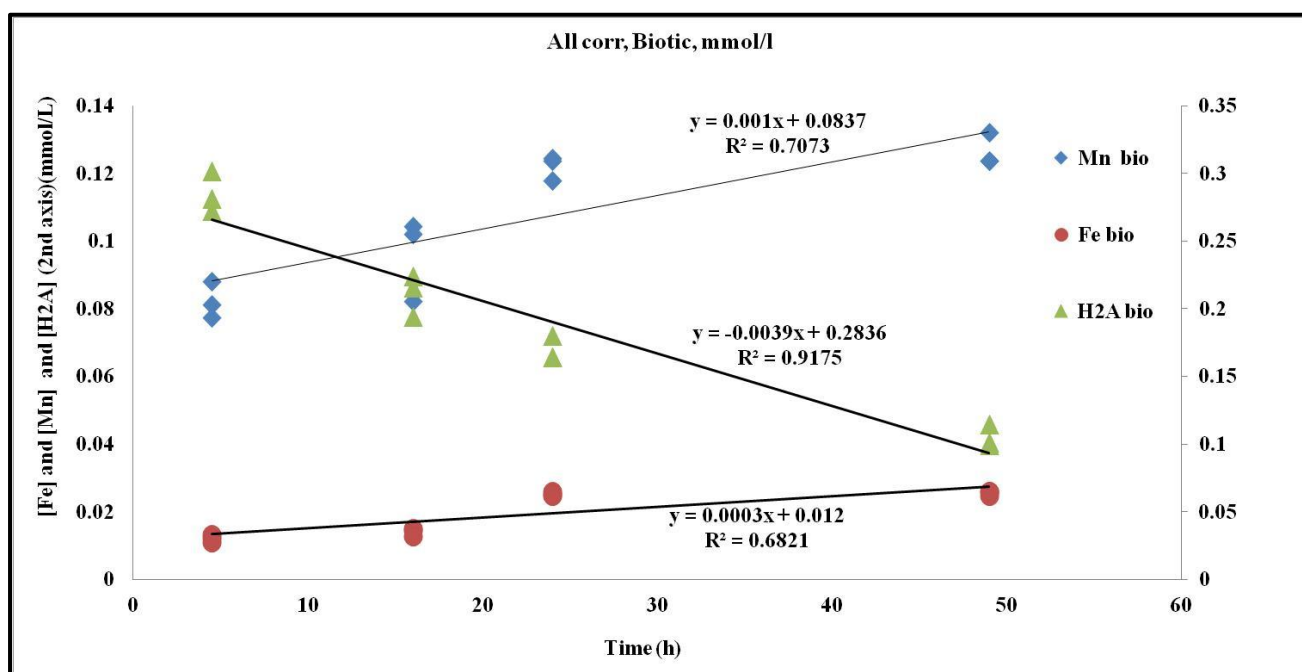


Figure 6-6 Amount of Fe and Mn^{++} released in the solution and concentration of H_2A for biotic experiment using initial H_2A of 60 ppm.

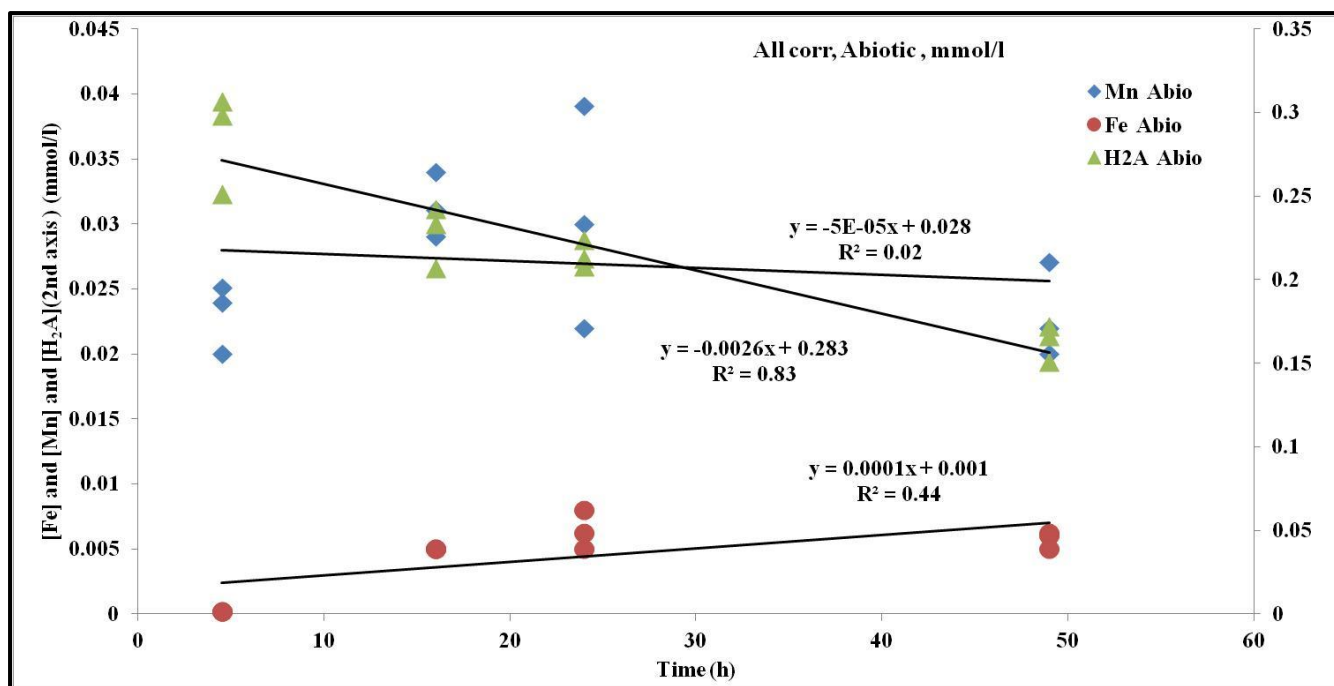


Figure 6-7 Amount of Fe and Mn^{++} released in the solution and concentration of H_2A for abiotic experiment using initial H_2A of 60 ppm.

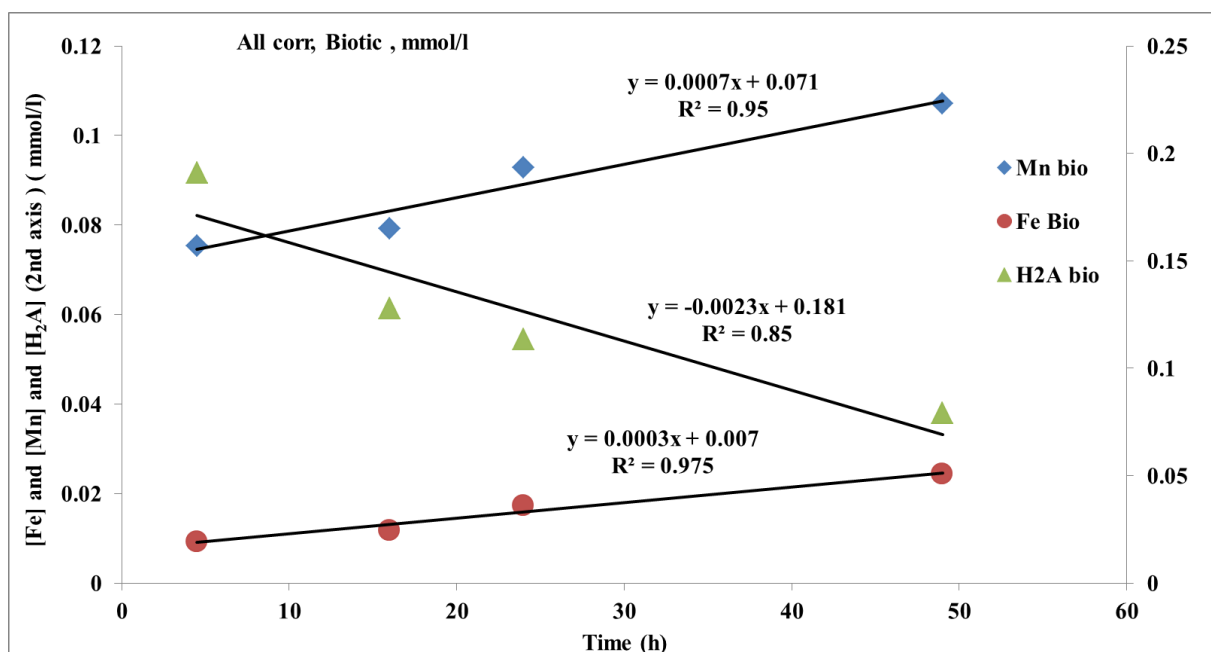


Figure 6-8 Amount of Fe and Mn^{++} released in the solution and concentration of H_2A for biotic experiment using initial H_2A of 40 ppm.

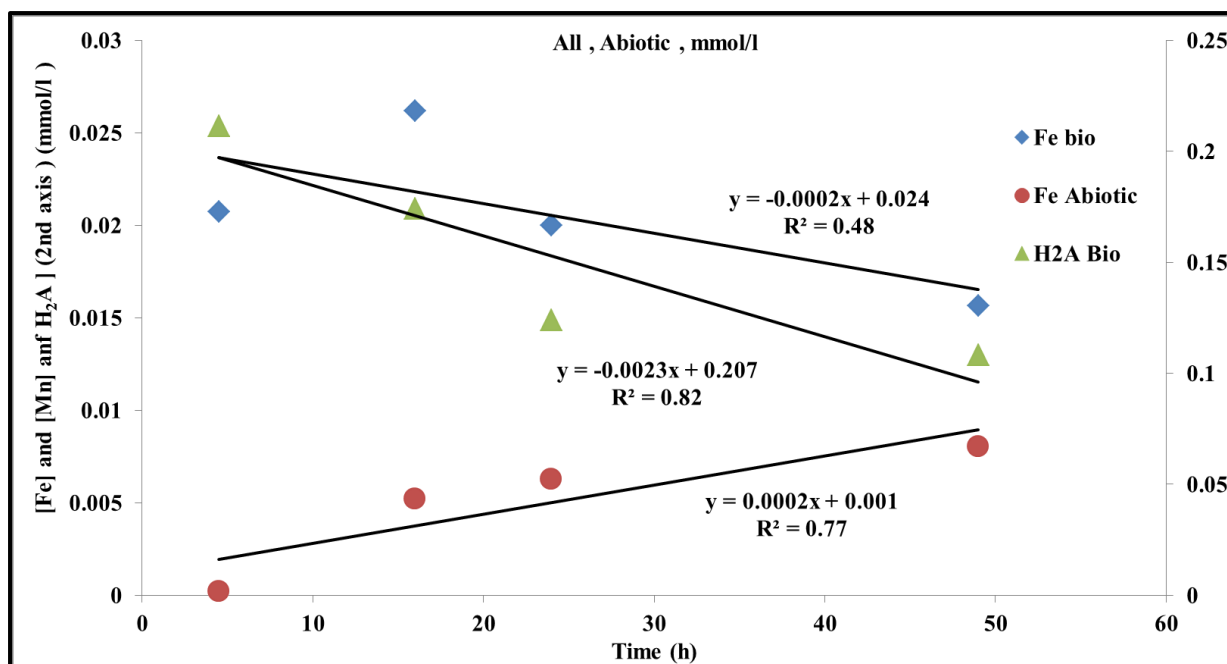


Figure 6-9 Amount of Fe and Mn^{++} released in the solution and concentration of H_2A for abiotic experiment using initial H_2A of 40 ppm.

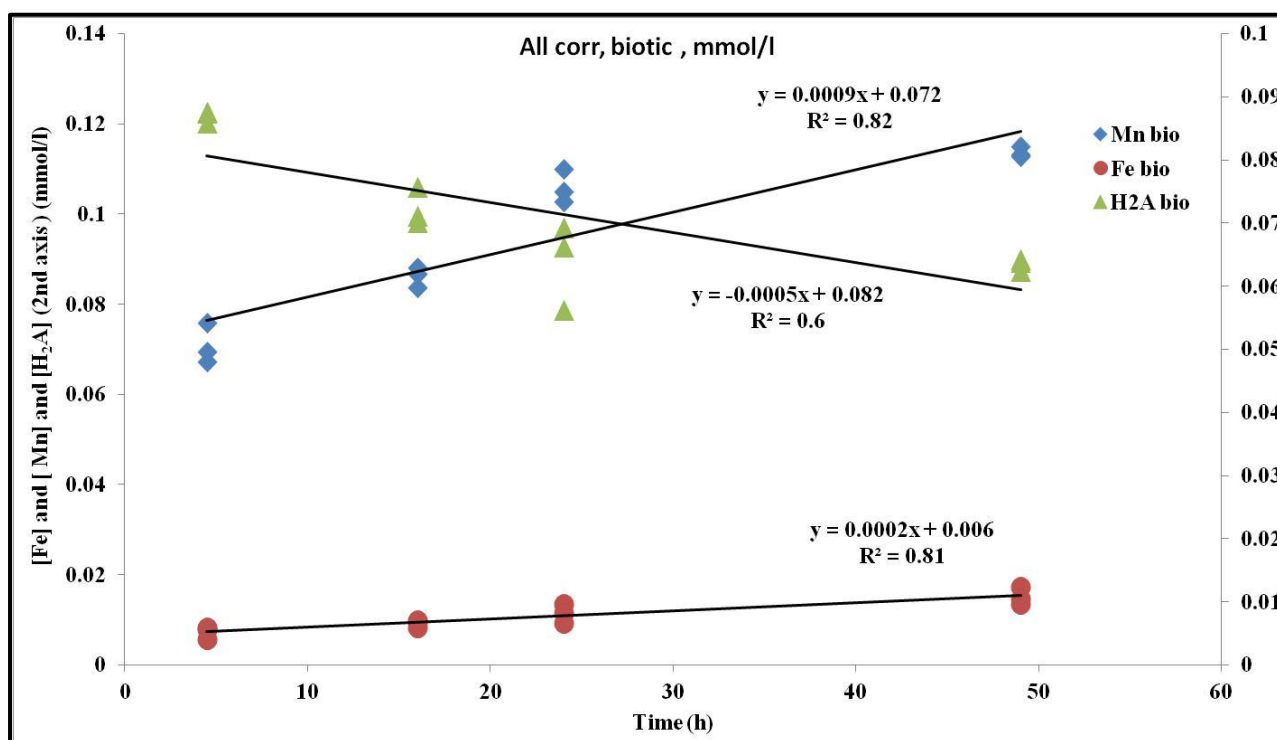


Figure 6-10 Amount of Fe and Mn^{++} released in the solution and concentration of H_2A for biotic experiment using initial H_2A of 20 ppm.

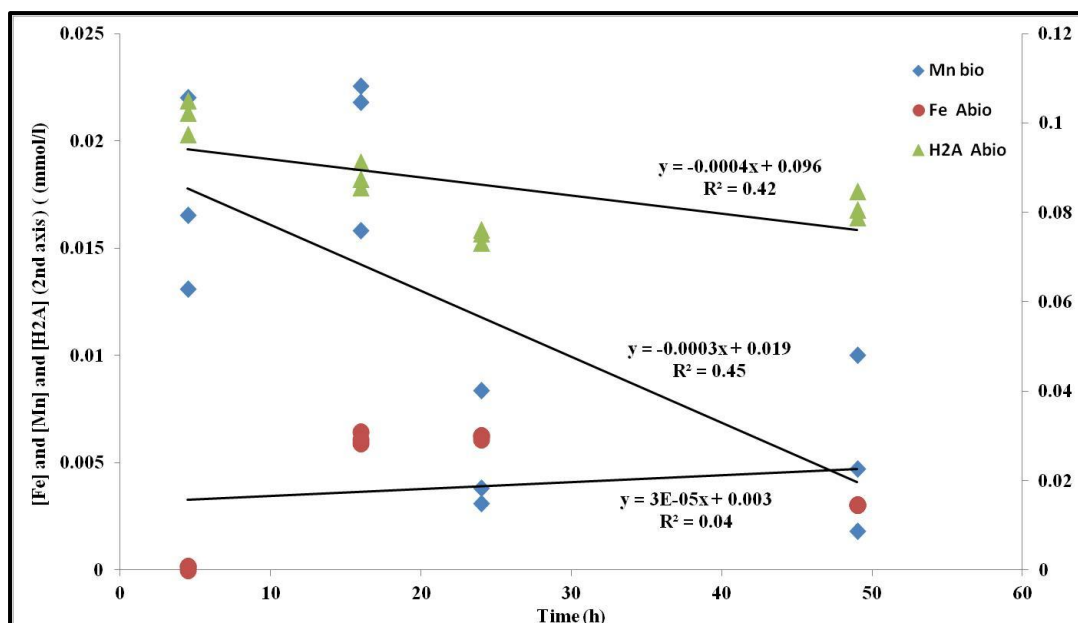


Figure 6-11 Amount of Fe and Mn^{++} released in the solution and concentration of H_2A for abiotic experiment using initial H_2A of 20 ppm.

The results from the biotic and abiotic measurements are different (e.g. Figures (6-2) and (6-3)). In all case, the Fe and Mn concentrations are greater in the biotic (unsterilized) than abiotic experiments (e.g. Figures (6.2) and (6.3)). Also the H_2A concentrations fall more in the biotic experiments. This is expected because if bacteria are involved there is likely to be faster reactions. Another possible explanation is that the biotic experiments have lower pHs (Figure (6.12)) and this was found to speed up the reactions in synthetic systems by Suter et al. (1991). Suter et al (1991) did not say anything about sterilizing their experiments but they used newly prepared hematite that may be did not contain appropriate environmental bacteria.

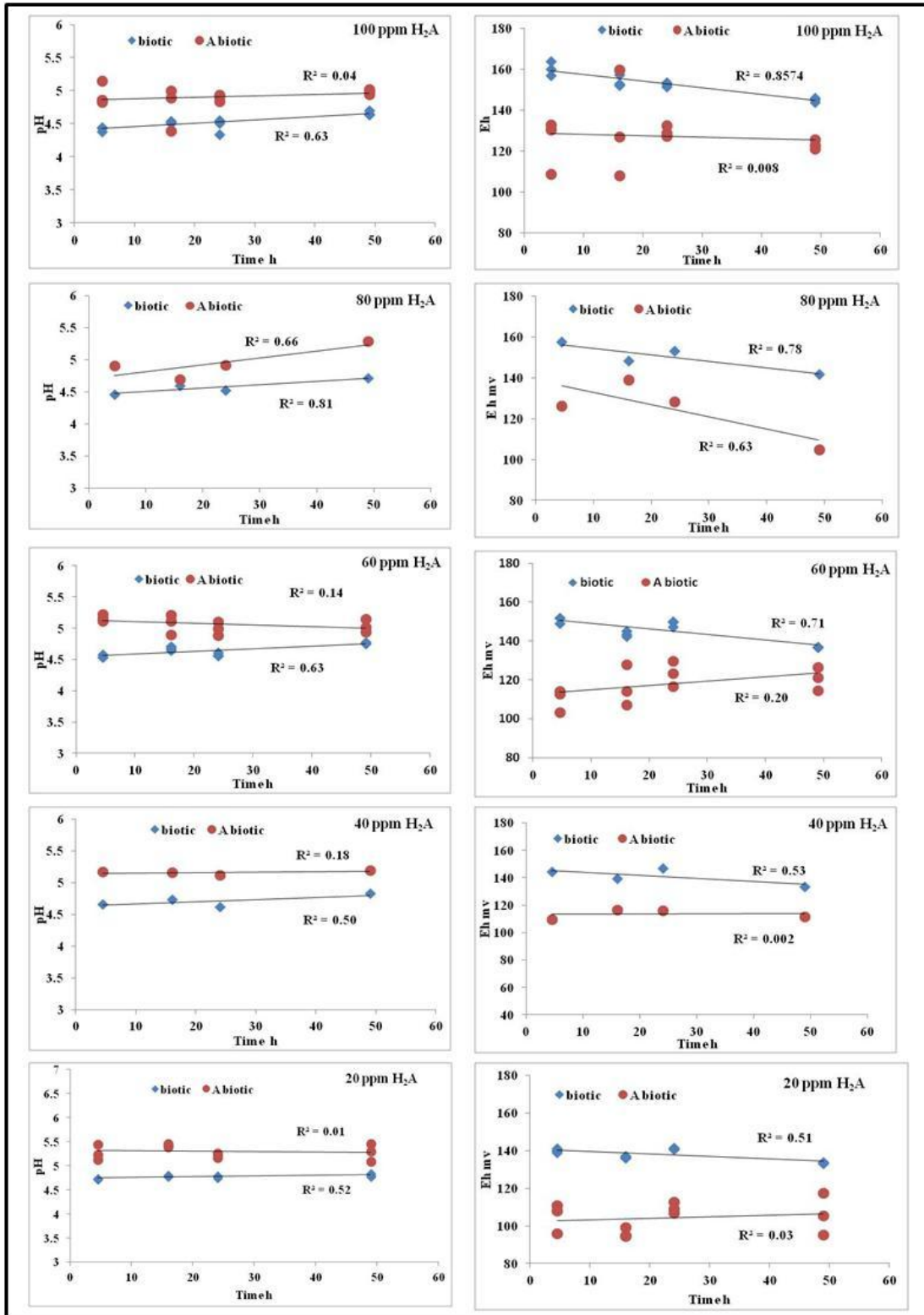
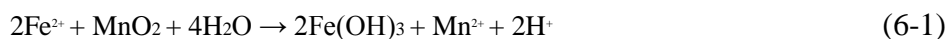


Figure (6-12) Plot of pH and E_h against time for all experiments, appendix (6.6 A&B).

In all cases the Fe concentrations are smaller than the Mn^{++} concentrations despite Fe oxides being much greater in the sandstone. This has nothing to do with bacteria as the same is seen for both biotic and abiotic experiments. This could suggest that Mn oxides are more quickly reactive than the Fe oxides. But could also mean that Fe is produced and then reacts with MnO_2 to release Mn into solution and precipitating Fe(III) oxides. E.g.



(e.g. Postma, 1985; Thornton et al., 2001). This reaction suggests reduction in pH and this is what is seen in the experiments (Figure (6.3)).

Mn concentrations reach a maximum at low initial H_2A concentrations and at high times (e.g. Figure 6.7). At low H_2A it is clear that the H_2A is nearly used up in some cases (e.g. Figure (6.11)) as though concentration does not reach zero the fall has stopped. Perhaps the maximum Mn concentrations seen at slightly higher H_2A and longer times (e.g. Figure 6-7) are because the source of Mn is used up. The Fe concentrations continue to rise for higher times at higher H_2A and may be this supports the idea that Fe dissolution by H_2A is driving Mn oxide dissolution, but the rates of rise are less and in some abiotic cases the rise does not occur (e.g. Figure 6.11).

6.4 Rates of Apparent Reductive Dissolution

In order to determine the rate of apparent reductive dissolution of hematite and Mn oxides and compare it with previous studies, all the data for Mn^{++} and Fe concentrations were plotted against time for biotic experiments (Figure 6.13). The plot shows how the concentration of the sum of half the Fe concentration and the Mn concentration in mmol/l ($=M$), varies with time. This sum is calculated because each H_2A can reduce two Fe(III) to two Fe(II) and reduce one Mn(IV) to one Mn(II).

As we can see from Figure (6.13a) in general the higher the initial $[H_2A]$ the higher metal $[M]$ released into solution and metal concentrations increase roughly linearly with time. The slopes of the plots are similar, unlike the case for Suter et al. (1991) who have slopes increasing with increasing initial $[H_2A]$. The intercepts however increase with increase in initial $[H_2A]$.

Figure (6.13b) is a plot of the same data but with averaged metal M values and with the average of the 4.5 hour data subtracted from each value as was done by Suter et al. (1991). The reason for subtracting the results obtained for the first 4.5 hours is that during this early period of reaction there will be processes occurring additional to those being studied, in particular sorption / desorption and may be even some dissolution. In addition, it may take a finite time for the different reduction reactions to adjust to a constant set of rates. This was done in order to see the relative rates of change in concentrations more clearly. There is a range of slopes and 100ppm is the steepest but there is no other pattern in the other slope values and they are all very similar. The subtraction of the initial 4.5 hour experiment results does not make much difference to the gradients.

Figure (6.14) shows a plot of average pH against the intercept on the $[M]$ /time plot of Figure (6.13a) but with also the results from the less than 49h abiotic experiments added (see below). This shows that there is a negative linear relationship between the intercepts and pH indicating that even slightly lower pHs are associated with greater release of Fe and Mn^{++} .

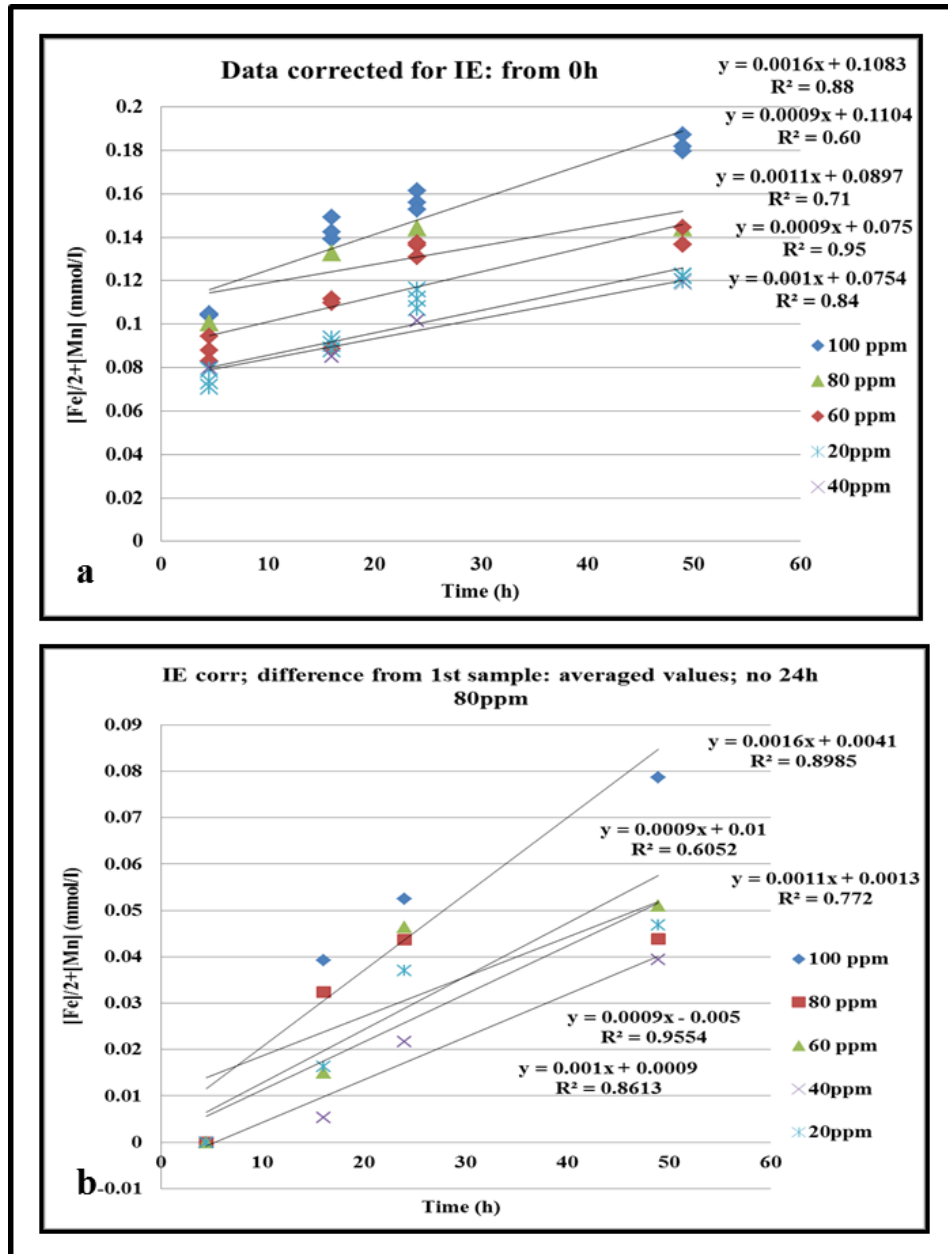


Figure 6-13. Variation of the sum of $Fe/2$ and Mn^{++} concentrations as a function of time in the biotic experiments. (a) is the plot of total concentrations corrected for ion exchange. (b) is plot of same data but using averaged values for each point and with the 4.5hour results subtracted from each value as was done by Suter et al. (1991).

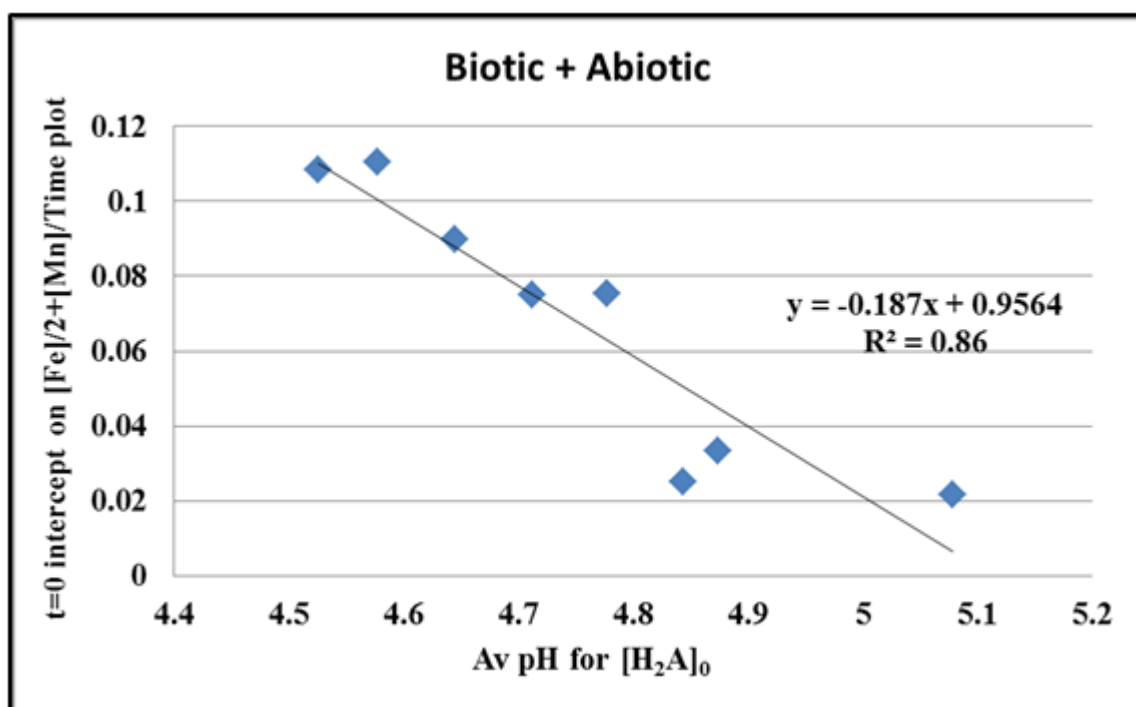


Figure 6-14. Plot of average pH for each initial $[H_2A]$ against the intercept on a time = 0 on a $[Fe]/2 + [Mn]$ against time plot (i.e. Figure 6.13(a)) for both biotic and abiotic experiments. 49h data are not included for the abiotic data (see Section 6.2).

As shown in Figure (6.15), the drop of $[H_2A]$ as a result of reaction with the sandstone ($[H_2A]_{initial} - [H_2A]_{aq}$) plotted vs $[Fe]/2 + [Mn]$ shows a positive relationship, the drop of H_2A leading to more release of metal (Mn^{++} and Fe) in the solution. But the drop in $[H_2A]$ is greater than the rise in $[M]$ indicating that some other process is involved. We would have expected a gradient of 1 if the decrease in $[H_2A]$ is all due to interaction with Fe and Mn oxides. Similar relationships are also seen for the experiments at lower initial H_2A concentrations.

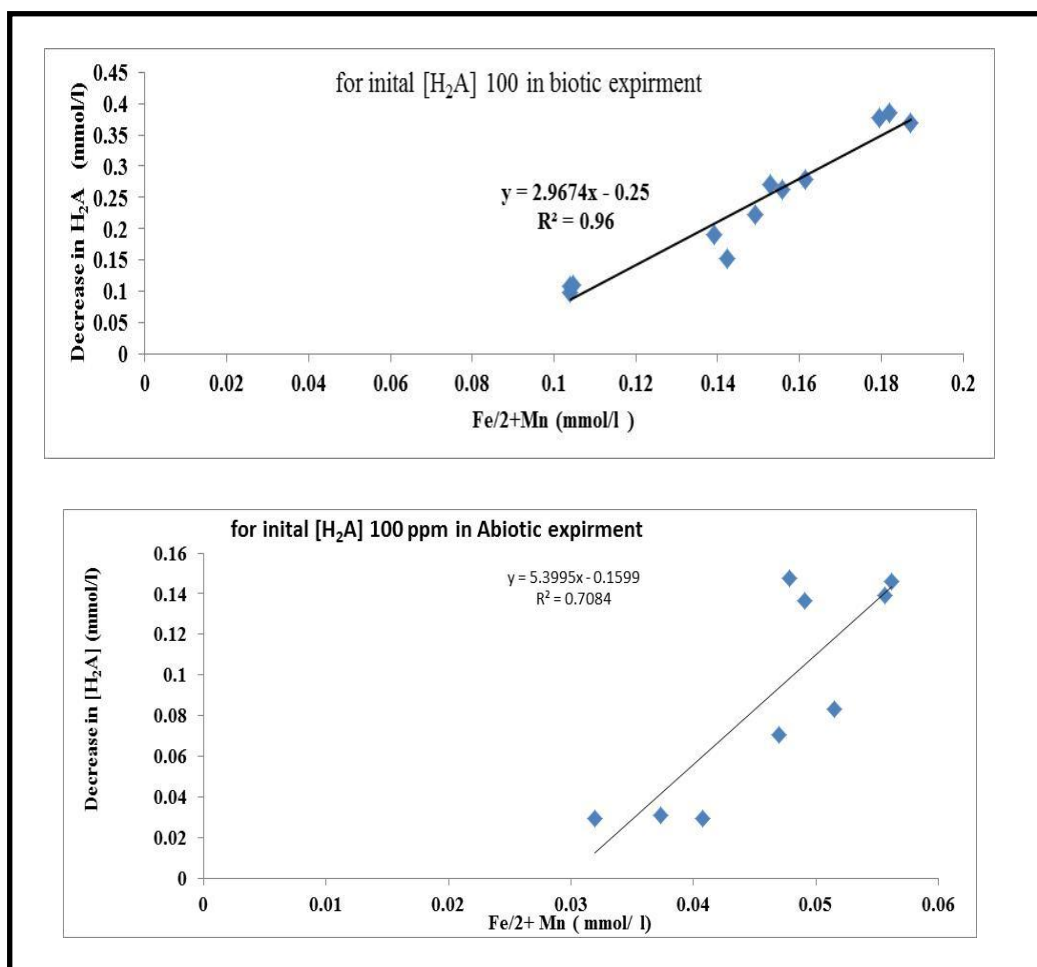


Figure (6-15) Decrease in $[H_2A]$ plotted against increase in metal concentration for (a) biotic and (b) abiotic conditions (excluding 49 hour results). All results for 100 ppm initial concentration of H_2A .

Comparing the rates of dissolution with the results of Suter et al. (1991), the data from a present study indicate rates ($d[M]/dt$) of about $1 \mu\text{mol/l/h}$ (Figure (6.13)) in the biotic experiments, and Figure 6.16 indicates that the rate of change of metal concentrations with time in the case of the sandstone is larger than Suter et al. (1991) saw with synthetic hematite and at the same pH but they are of the same magnitude. Suter et al. (1991) do not comment on sterilizing but it is likely that the procedure they used with synthetic hematite would have contained many less numbers of relevant environmental bacteria than the natural sandstone used here so may be best comparing their data with the abiotic data here. Though the abiotic

rates are lower as seen in Figure (6.16) they are still higher than the rates seen by Suter et al. (1991) at lower pHs.

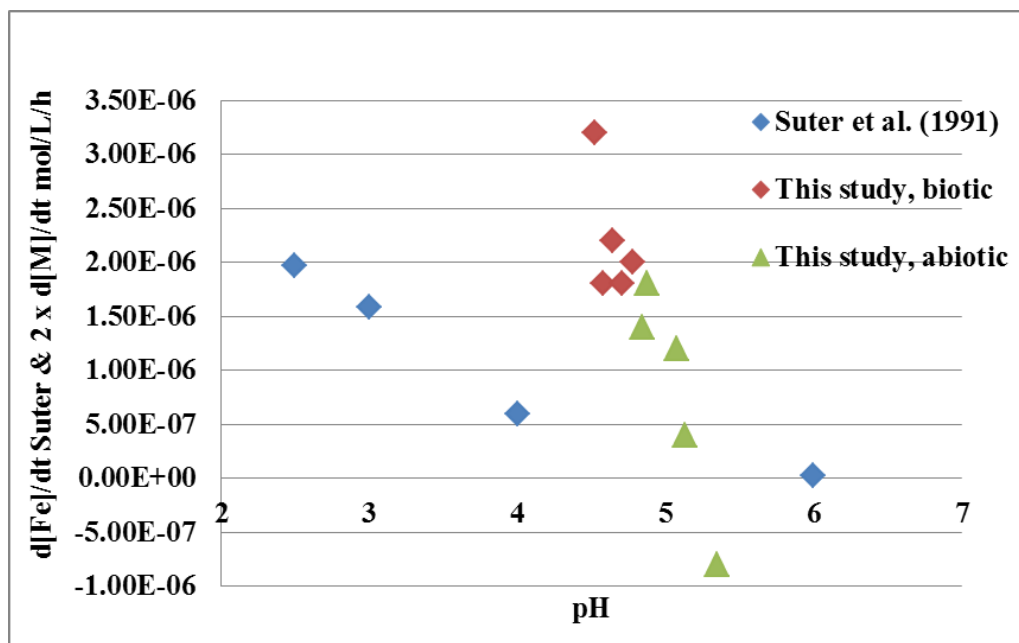


Figure 6-16. Comparison of rates of dissolution of Fe and 2M ($2 \times \{[\text{Fe}]/2 + [\text{Mn}]\}$). 2M is used as Suter et al. (1991) data is in terms of moles of Fe.

6.5 Mass balance and Surface Interactions

Suter et al. (1991) used the equation to determine the amount of H_2A attached to the surface of hematite $[\text{H}_2\text{A}]_{\text{sur}}$:

$$[\text{H}_2\text{A}]_{\text{T}} = [\text{H}_2\text{A}]_{\text{aq}} + [\text{H}_2\text{A}]_{\text{sur}} + 0.5 [\text{Fe}^{++}]$$

In principle, in this study all the components of the system have been measured so that a mass balance can be done rather than simply calculating $[\text{H}_2\text{A}]_{\text{sur}}$ by difference:

$$[\text{H}_2\text{A}]_{\text{T}} = [\text{H}_2\text{A}]_{\text{aq}} + [\text{H}_2\text{A}]_{\text{sur}} + [\text{H}_2\text{A}]_{\text{deg}} + [\text{H}_2\text{A}]_{\text{hae}} \dots\dots\dots(6-1)$$

$$[\text{H}_2\text{A}]_{\text{T}} = [\text{H}_2\text{A}]_{\text{aq}} + [\text{H}_2\text{A}]_{\text{sur}} + [\text{H}_2\text{A}]_{\text{deg}} + \{[\text{Fe}]/2 + [\text{Mn}]\}$$

where

$$[\text{H}_2\text{A}]_{\text{T}} = \text{initial } [\text{H}_2\text{A}] \text{ before reaction with sandstone in } [\text{M}]/[\text{L}^3]$$

$[H_2A]_{aq}$ = concentration of H_2A measured in the solution after reaction with sandstone in $[M]/[L^3]$

$[H_2A]_{deg}$ = mass per unit volume of H_2A degraded/decayed in $[M]/[L^3]$

$[H_2A]_{sur}$ = concentration of $[H_2A]$ attached to the rock surfaces in $[M]/[L^3]$

$[H_2A]_{hae}$ = mass per unit volume of $[H_2A]$ that has reacted with hematite in $[M]/[L^3]$.

If take for example the 100 ppm case to determine the mass balance, we get the result in Figure (6.17). In this plot all values have been expressed in mmol rather than mmol/l as in the balance equation above. The red line represents the initial mass of H_2A added. The blue diamond represents the total mass calculated using equation (6-1) where $[H_2A]_{sur}$ is estimated using the results from Chapter 4 (Sorption). Initially the values are greater than $[H_2A]_T$, but then they fall to less than $[H_2A]_T$ over time. Following Suter et al. (1991) and taking the concentrations as differences from the first measurement (4.5hours), gets rid of the problem of the initial overestimate, but of course still underestimates the total mass at later times. Of the mass balance components ($[H_2A]_{aq} + [H_2A]_{sur} + [H_2A]_{deg} + \{[Fe]/2 + [Mn]\}$) the least well constrained is the reaction with hematite. However, it is not obvious what process would result in removal of Fe and Mn other than ion exchange which has been taken into account. Looking at $[H_2A]_{sur}$ it is possible that the sorption may be different in this system compared with the system of Chapter 4 because there are other reactions occurring here and the pH is different and changing. Assuming this is correct, if the calculated sorption is removed from the balance, the balance is as shown in Figure 6.17 with green triangles (i.e. all H_2A components added together except for sorption). The missing mass in this case is indicated by the difference between the green triangles and the red line.

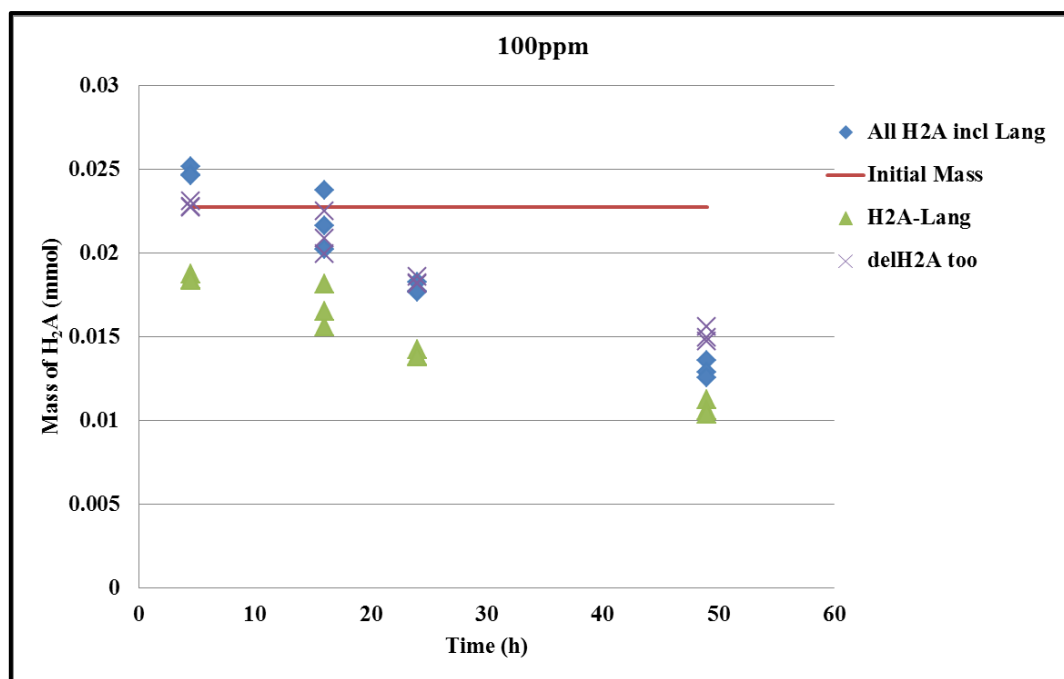


Figure (6-17) Mass balance variation with time for the 100ppm H₂A case.

Figure 6.18 shows the relationship between this missing mass (i.e. $[H_2A]_T - [H_2A]_{aq} - [H_2A]_{deg} - \{[Fe]/2 + [Mn]\}$) and $[H_2A]_{aq}$ and pH for an example experiment (100ppm). It is observed that the missing mass increases with increases in the pH value and with decreases in $[H_2A]_{aq}$. If the missing mass is all due to, following Suter et al. (1991), to sorption, then the result is surprising as sorption then increases with a decrease in $[H_2A]_{aq}$, which is not expected in theory or from the results of Chapter 4. To get an increase in sorption despite decreasing dissolved concentration suggests that the sorption capacity increases with time (and hence with pH). One possibility may be is that dehydroascorbic acid (DHA), the final product of the oxidation of H₂A, sorbs onto the hematite and that HA⁻ sorbs onto the DHA. To model this it was assumed that

- i. H₂A dissociation was occurring to produce HA⁻ (pK_a = 4.17; Domitrović, 2006)
- ii. DHA concentration was set equal to M ($= [Fe]/2 + [Mn]$)
- iii. activity corrections can be ignored

- iv. HA^- attaches to the hematite by linear sorption, i.e. can be represented by a K_d ($K_{\text{HA}^-/\text{Hae}}$ which represents HA^- sorbing onto hematite)
- v. DHA attaches to the hematite by linear sorption ($K_{\text{DHA}/\text{Hae}}$)
- vi. HA^- attaches to DHA attached to hematite by linear sorption ($K_{\text{HA}^-/\text{DHA}}$)

So,

$$K_{\text{DHA}/\text{Hae}} = [\text{DHA}]_{\text{sur}} / [\text{DHA}];$$

$$K_{\text{HA}^-/\text{Hae}} = [\text{HA}^-]_{\text{sur}} / [\text{HA}^-];$$

$$K_{\text{HA}^-/\text{DHA}} = [\text{HA}^-]_{\text{sur}} / [\text{DHA}]$$

Hence

$$\begin{aligned} \text{sorbed } [\text{HA}^-] &= [\text{HA}^-] K_{\text{HA}^-/\text{Hae}} + [\text{DHA}]_{\text{sur}} K_{\text{HA}^-/\text{DHA}} \\ &= [\text{HA}^-] K_{\text{HA}^-/\text{Hae}} + K_{\text{DHA}/\text{Hae}} [\text{DHA}] K_{\text{HA}^-/\text{DHA}} \end{aligned}$$

This model was then used to fit the lab data for all the experimental results. This was done by trial and error in Excel by varying the K_d values until a good fit with the lab data was obtained as judged visually. The model production were compare against the mass balance estimated for $[\text{H}_2\text{A}]_{\text{sur}}$. The values for the calibrated K_d were kept constant in all the experiments. The results are shown in Figure (6.19) for biotic experiments.

After initial calculations, in all cases the 49h data were excluded. As noted before the 49hour data reduce the slopes of the concentration/time plots for the lower concentrations (e.g. Figure 6.11, 20ppm), but on closer looking this also happens for the higher concentrations though at lesser amounts (e.g. Figure 6.4, 80ppm). In addition, the 24h value for 20 ppm was removed as this seems affected by the low concentration of H_2A .

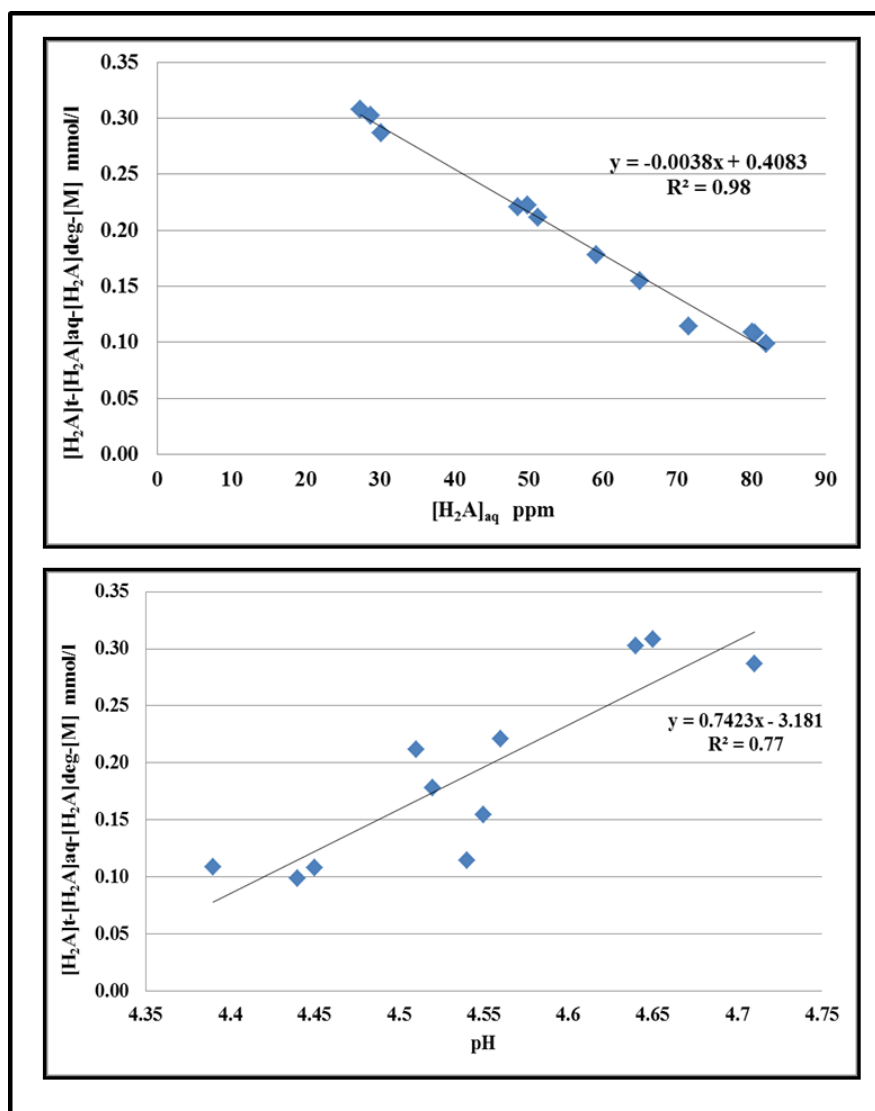


Figure (6-18) Plots of the sorbed HA^- estimated from the mass balance against $[H_2A]_{aq}$ and pH for the 100ppm experiments.

Though the fit shown in Figure (6.19) is not exact the model reproduces roughly the data observed. Possible reasons for a lack of perfect agreement are that the conceptual model is not right and that using a simple K_d approach is not appropriate. However, the calculations suggest the conceptual model is a quantitatively possible explanation.

From the model the K_d values can be estimated. Because $K_{DHA/Hae}$ is always multiplied by $K_{HA-/DHA}$ in the model, only the product of these two K_d values can be determined. So the results indicate $K_{DHA/Hae} \times K_{HA-/DHA} = 0.003 \text{ (l/l)}$ and $K_{HA-/Hae} = 0.2 \text{ (l/l)}$.

Figure 6.20 shows the results for fitting the abiotic experiments using the same model. It was not possible to use the same $K_{\text{DHA/Hae}} \times K_{\text{HA-/DHA}}$ value as for the biotic experiments as there was less sorption occurring than in the biotic experiments but the $K_{\text{HA-/Hae}}$ value was held constant. $K_{\text{DHA/Hae}} \times K_{\text{HA-/DHA}}$ was calibrated at 0.01 (l/l).

The use of different K_d for the sorption involving DHA may indicate that the model is not correct. For example, it is possible that as the bacterial community developed during the unsterilized experiments that they provided the extra sorption capacity rather than the sorbed DHA. The higher pH values of the abiotic experiment may have affected the surface sorption sites, though normally it is expected that higher pH to mean less H^+ competition for the sites so more efficient DHA sorption.

The apparent $K_{\text{HA-/Hae}}$ values obtained from Chapter 4 experiments, converted for HA^- from H_2A , range from about 0.3 to 0.6 l/l depending on what assumptions are made (especially what dissolution there may have been of Mn over the experimental period). This is slightly greater than for the current model (0.2), but of the same order.

One question is why does the sorption of HA^- to sorbed DHA happen here but was not observed with synthetic hematite by Suter et al. (1991)? This is unknown, but could relate to the fact that the coatings of hematite are thin and that the minerals underneath have an impact on the sorption or perhaps the dissolution exposed clay surfaces that then sorbed DHA.

It is concluded that one way of explaining the data is that the sorption increases as a result of sorption of DHA. This means that H_2A is removed by sorption and reductive dissolution and the reductive dissolution is indicated by metal released (M) ($=[\text{Fe}]/2+[\text{Mn}]$).

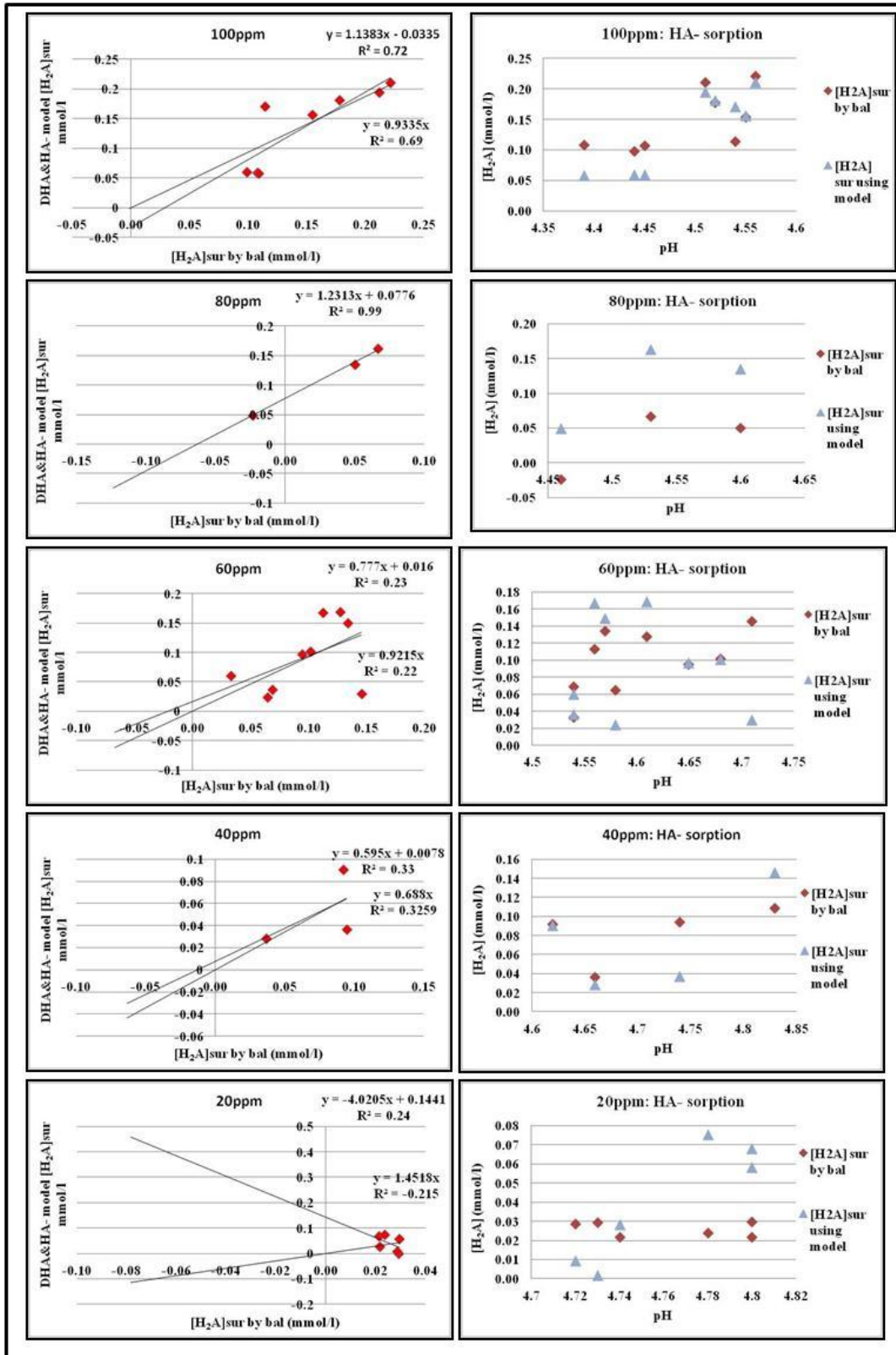


Figure (6-19) Comparison of the DHA sorption model predictions and the lab data for the biotic experiment results

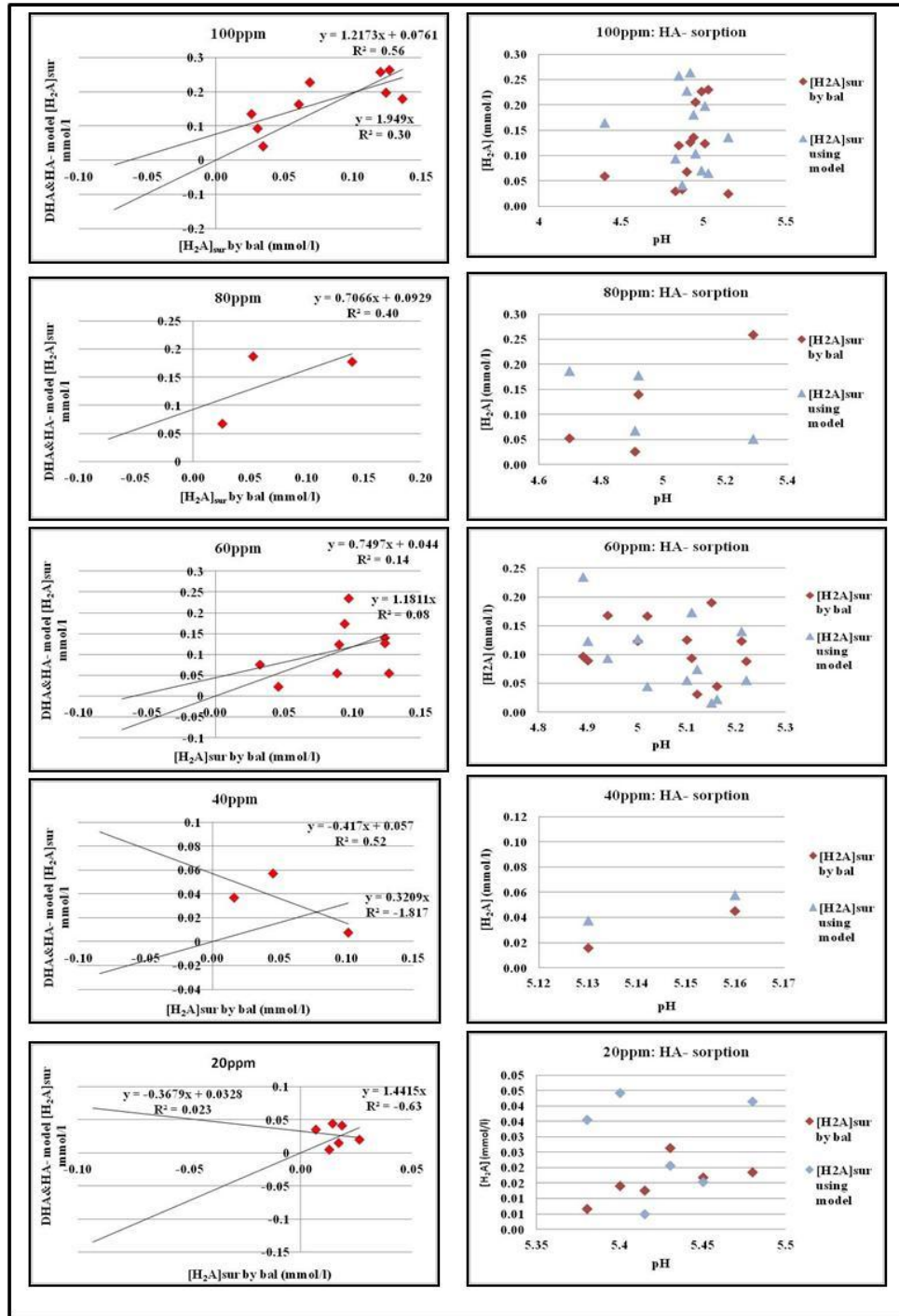


Figure 6-20 Comparison of the DHA sorption model predictions and the lab data for the abiotic experiment results

6.6 Rates of Reductive Dissolution of Sandstone Oxide Coatings

The rate of removal of H_2A from solution is roughly linear with time over the time interval 0-49 hours (24 hours for 20ppm) as seen in Figures 6.2 to 6.11. However the 49h results are below the best fit line, and as result only the earlier results (4.5, 16 and 24h) are included in the following analysis. The drop at 49 hours might relate to the built up of Al as Suter et al. (1991) noted for their experiments where the pH was above 3.

Figure 6.21 plot the rates of change of $[H_2A]$ as a function of average dissolved concentration over the 0-24 hour period for the 100, 80, 60 and 40 ppm experiments, and for 0-16hour for the 20ppm experiment. The plot indicates that there is a rough linear relationship between the rate of decrease in $[H_2A]$ and the average concentration for each experiment, showing that the reaction is approximately first order. The constant of proportionality is more negative for the biotic system, i.e. there is a faster rate of decrease in $[H_2A]$. In both cases forcing a linear relationship through the origin reduces the correlation coefficient only a little suggesting that the relationship passes through the origin as expected. The relationship represents the removal of $[H_2A]$ from solution, including sorption and oxidation by the sandstone (but not any other degradation reaction) and hence it is not representative of oxidation of the $[H_2A]$ or its degradation, these will be less and represented by $d\{Fe\}/2 + [Mn] dt = d[M]/dt$. In other words Figure 6.21 cannot be used to indicate the oxidation of ascorbic acid as it include sorption.

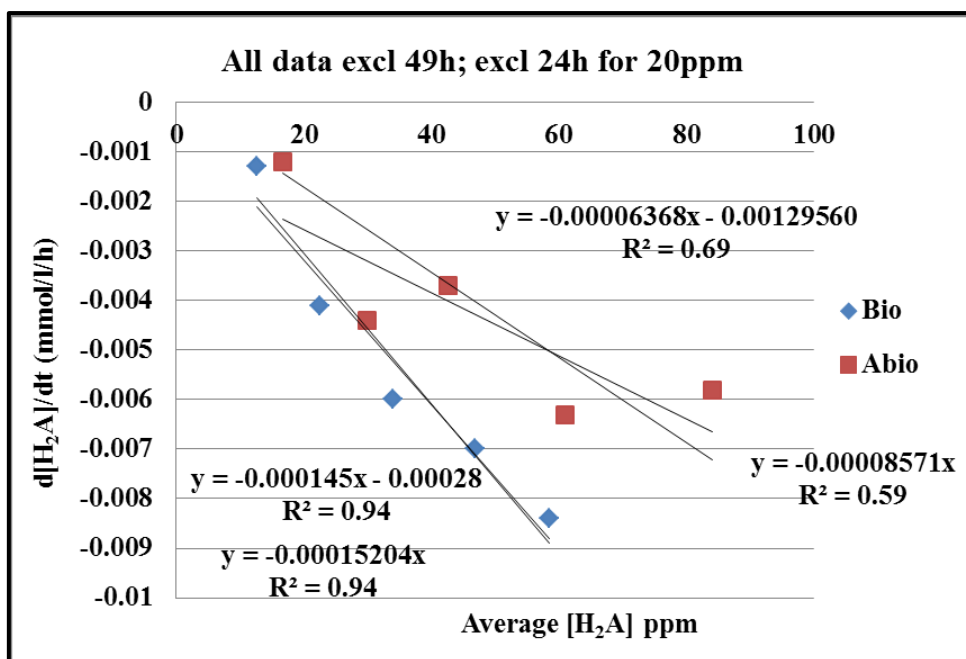


Figure (6-21) the rate of decrease in $[H_2A]$ with time as a relation of $[H_2A]$.

Over the whole time period of the experiments Figure 6.13 indicated that there was no clear relationship between rate of change of metal released (M) with time and H_2A concentration. However, replotting the data without the 49 hour results and without the 24 and 49 hours results for 20ppm gives the plot of Figure 6.22(a). It shows that the rate of $[H_2A]$ oxidation is proportional to the average concentration in each experiment, i.e. is first order in $[H_2A]$.

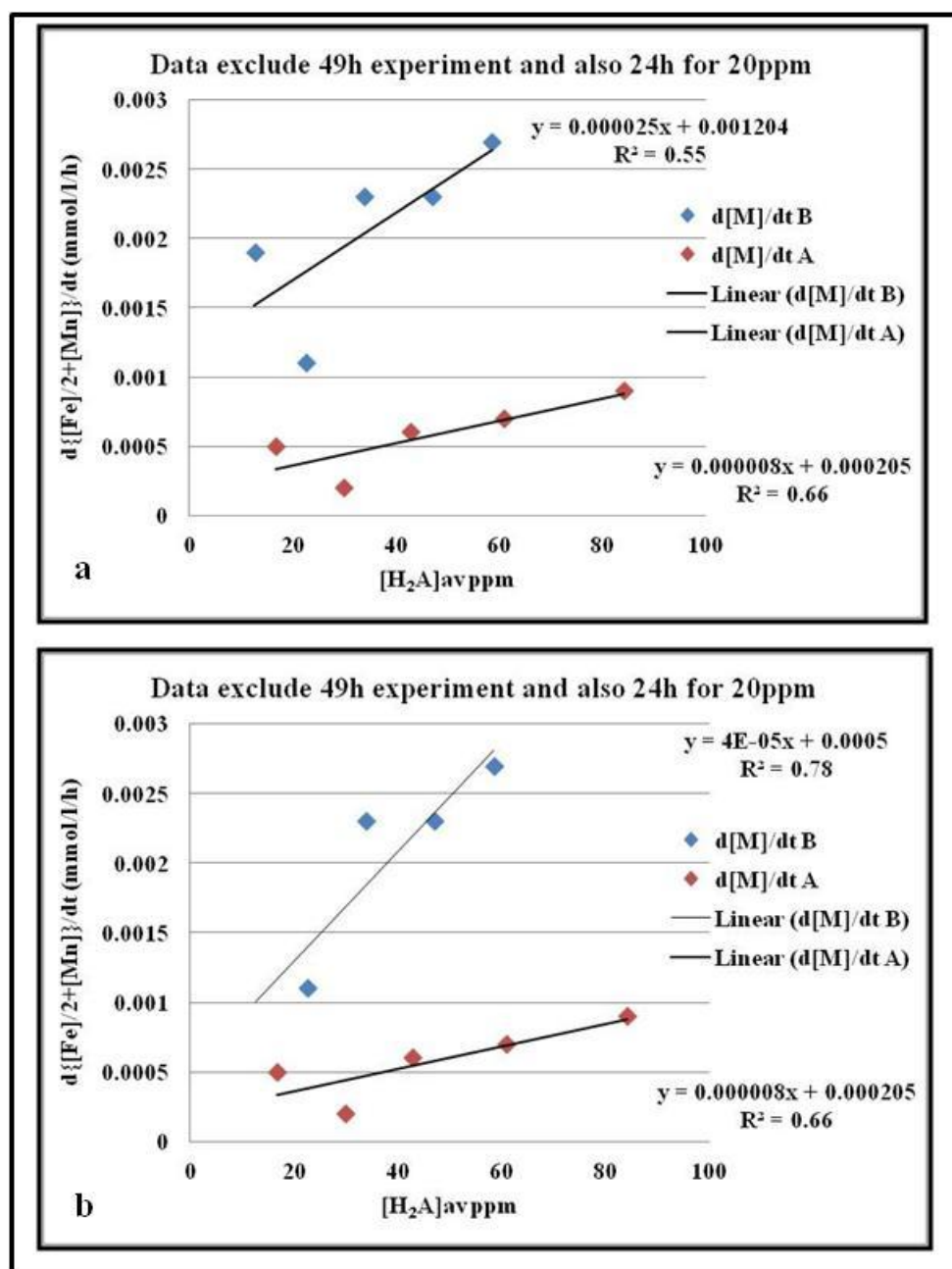


Figure 6-22 The rate of change of $[Fe]/2 + [Mn]$ with time plotted against average $[H_2A]$ for each of 100,80,60,40 and 20ppm experiments. (b) is same as (a) but one point removed for biotic results (see text).

The rate constant for biotic system is about three times the rate constant for the abiotic system and suggests it is faster with bacteria or lower pH. In Figure 6.22(a), the biotic relationship does not pass through the origin. This may be due to non- H_2A dissolution of hematite, may

be dissolution by H^+ . However, remove a possible outlier and the correlation improves and passes through the origin (Figure 6.22(b)).

Another plot, Figure 6.23 shows the relationship between abiotic experiment rate of H_2A oxidation and that for the biotic experiments. The rate for the biotic conditions is as expected from Figure 6.22 about three times that for the abiotic conditions.

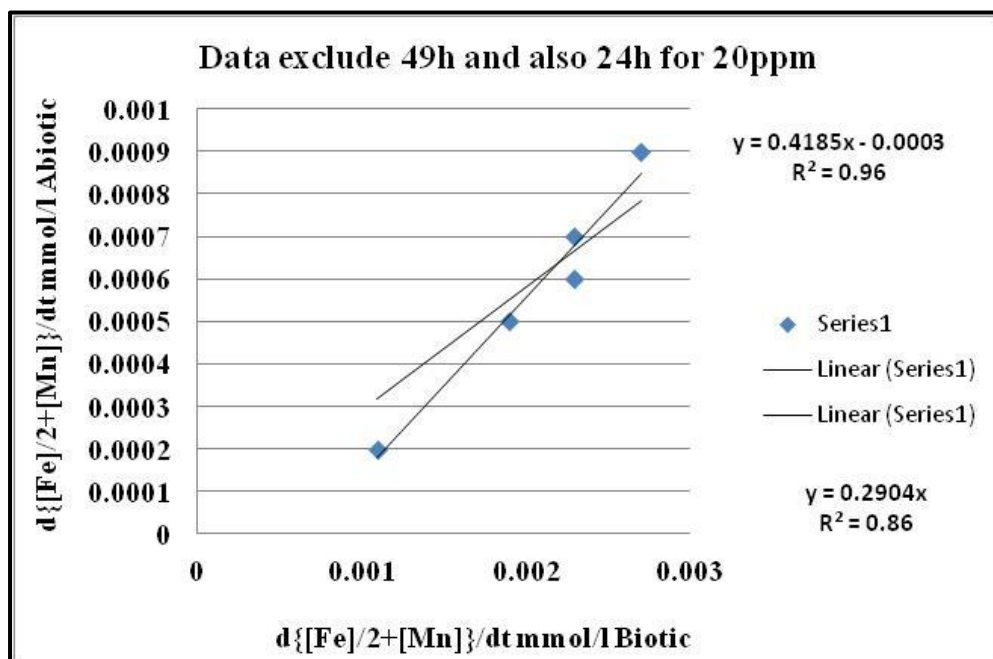


Figure (6-23) Comparing the rates of reductive dissolution for biotic and abiotic experiments

Figure 6.24 (a) and (b) shows the relationship between the rate of H_2A oxidation and the amount of HA^- sorbed on the hematite according to the model used for biotic and abiotic conditions respectively. There appears to be a relationship between the sorbed HA^- and the rate of oxidation of H_2A , as Suter et al. (1991) found too. Figure 6.24 (c) and (d) shows the relationship between the rate of H_2A oxidation and the total amount of HA^- sorbed onto hematite directly and sorbed onto DHA which itself is sorbed onto hematite directly. This relationship is not very important as DHA does not involved with reduction of the hematite but it does indicate total ascorbate sorption according to the model used.

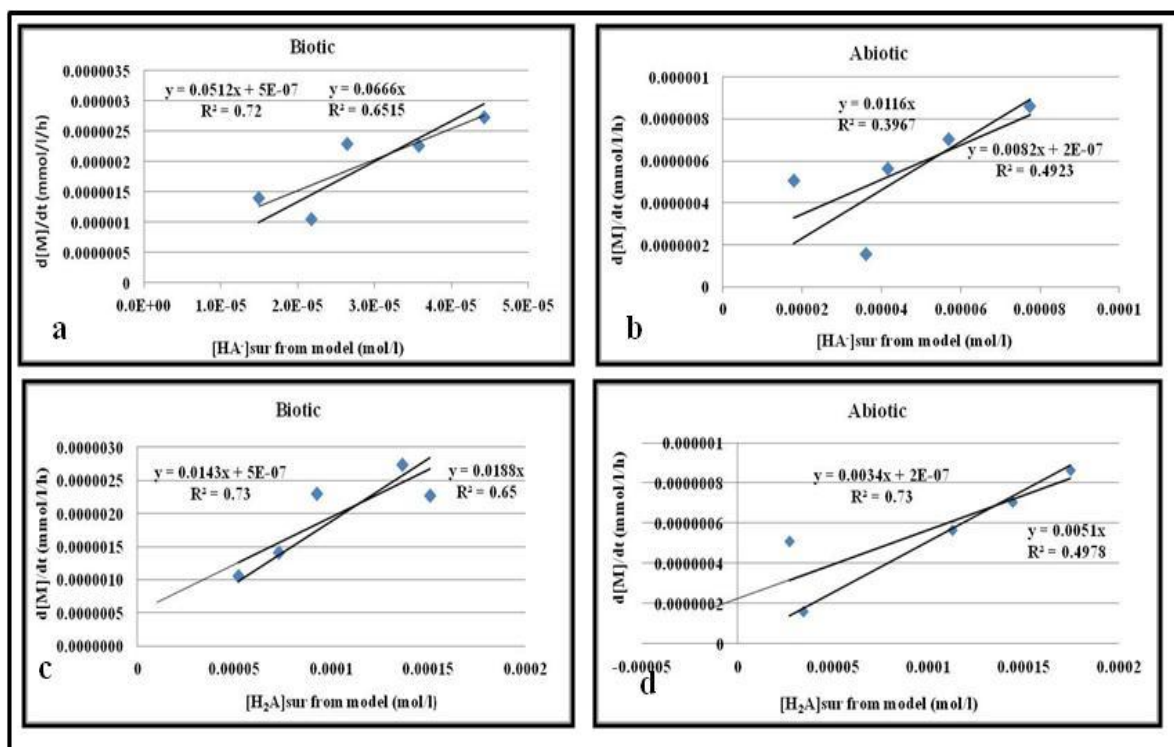


Figure 6-24 The rate of metal reduction versus sorbed concentrations of HA^- . a & b $[HA^-]_{sur}$ on hematite only determined from the model for biotic and abiotic cases. c & d total $[HA^-]_{sur}$ on all surfaces from the model

Figure 6.25 show that the pH of the experiment is related to the rate of oxidation of H_2A . This could be through change in sorption reactions or change in protonation of sites. The same relationship seen with biotic and abiotic suggests that possibly it is pH differences rather than the presence of bacteria that affect the rates.

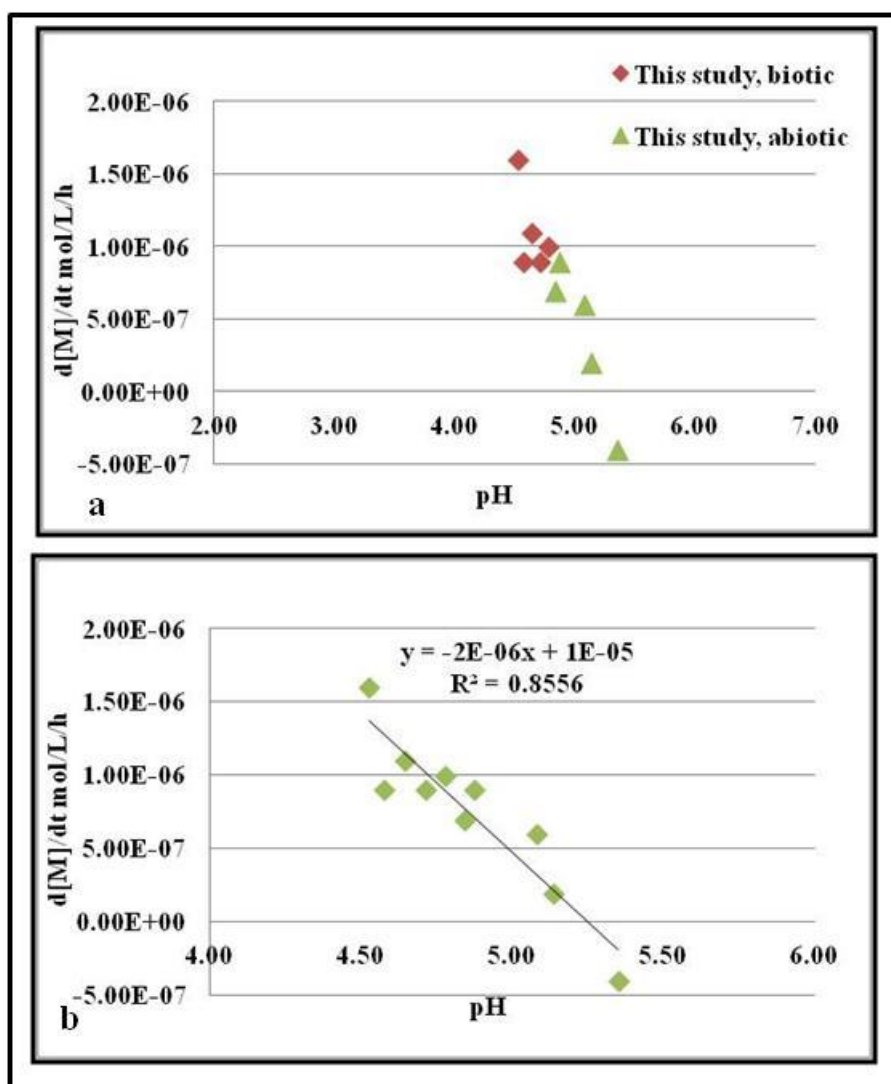


Figure 6-25. The relationship between pH and oxidation rate of H_2A for all experiments (a) data separated into biotic and abiotic. (b) biotic and abiotic together.

Suter et al. (1991) present rate constants (k_e) defining them as $d[Fe]/dt = k_e[H_2A]_{sur}$. Figure 6-26 compares their values with the equivalent values obtained here ($2 \times d[M]/dt$) as Suter et al. (1991) have used Fe change rather than Fe/2 change, and M is defined as $[Fe]/2 + [Mn]$. conclusion from this figure (6.26 a and b) is that very roughly the results are similar between the studies. But closer looking, Figure 6.26 c and d show what has already been presented in Figure 6.16 that the rates in the present study are greater even when average values have been plotted.

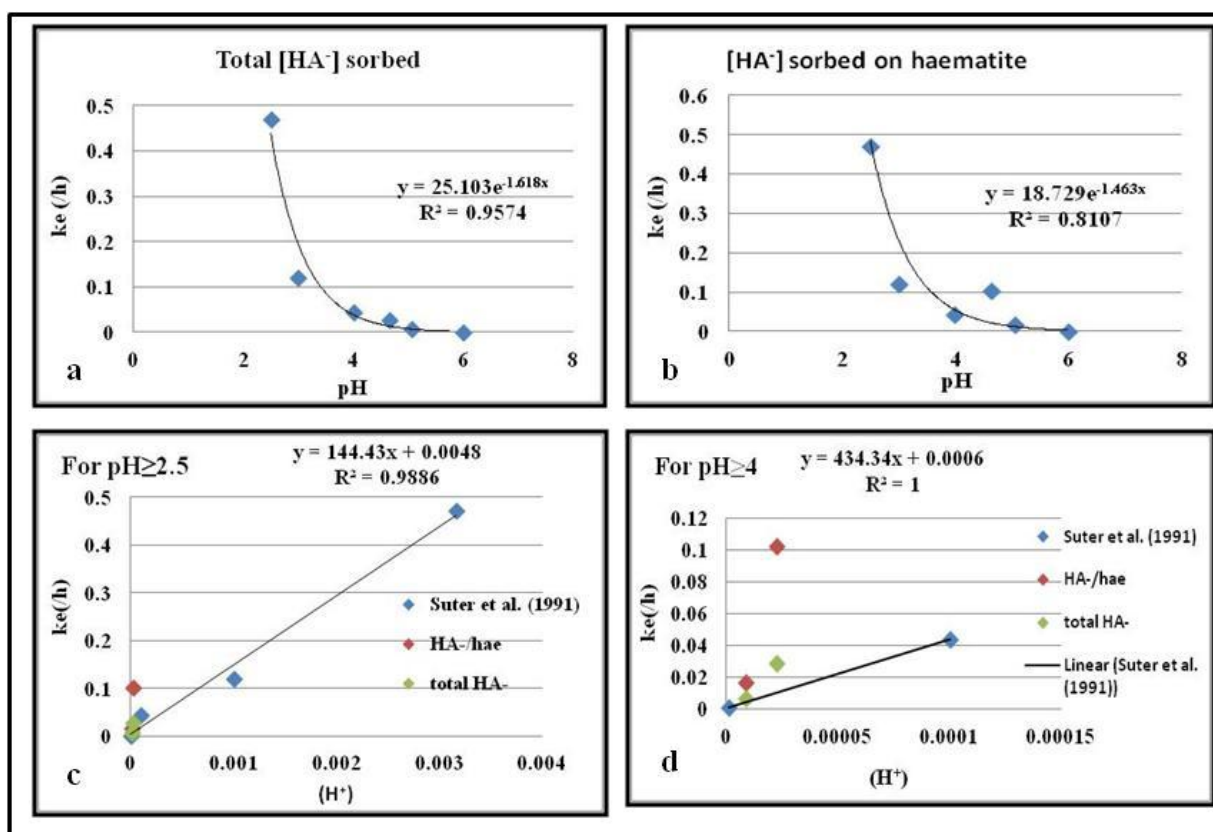


Figure 6-26. (a) Total HA^- sorbed as estimated using the model for this study (biotic and abiotic) and all data from Suter et al. (1991). The data from this study are presented as one average for biotic and one average for abiotic experiments. (b) as for (a) but only HA^- sorbed on hematite. (c) Data plotted against (H^+) for $pH \geq 2.5$. (d) As for (c) but including only $pH \geq 4$ points.

6.7 Conclusions

After setting up the final experiment under anoxic conditions, the concentrations of Fe, Mn^{++} and ascorbic acid have been monitored over time for periods extending up to 49 h. The same experiments have been repeated but under sterile condition (Benelli, 2015).

It is found out over time that there is an increase of released metal (Fe+Mn) and a drop of $[H_2A]$. In the abiotic experiments the concentration of metal released and the drop in $[H_2A]$ was less than in the biotic experiments. This may be ascribed to effect of bacteria, but also

the pH was lower in the abiotic experiments. One of the main and unexpected findings is that the rate of reductive dissolution is slightly greater than has previously been found for synthetic hematite. One possibility is that this is because of the presence of bacteria on the sandstone that are adapted to the sandstone / water conditions and speeds up the reaction. It was meant that the abiotic experiments would determine if bacteria were important but in the end the pH of these experiments was greater than for the biotic experiments and this would have also resulted in a decrease in rate even if the bacteria were not involved. The plot of rate against pH (Figure 6-25) indicates that the relationship between rate and pH for biotic and abiotic experiments lies on the same trend. It might be expected that this would not occur if bacteria were involved, but on other hand may be the bacteria change the pH and in doing so speed up the reaction. Without more experiments the effect of the bacteria cannot be proved. However, the experiments show that the rate is only slightly greater than was found for synthetic hematite and indicate that experiments on synthetic hematite might be used as a guide for what happens in hematite covered sandstones. The drop of H_2A concentration after reacting with sandstone can be ascribed to oxidation by oxides in the sandstone, which is indicated by the rise of Fe and Mn in solution, and to sorption. Mass balance calculations done using the sorption estimation equations from Chapter 4 predict that total H_2A was higher than initial H_2A at early time and over time the total H_2A mass fell below initial H_2A . Assuming this error was due to incorrect sorption estimates, the mass balance was used to determine the H_2A sorption. This calculation showed that the amount of sorption increased with time and therefore with decline of $[H_2A]$, which is not expected from theory or from the results of Chapter 4. In order to determine if the model of sorption to sorbed DHA is correct, various studies could be undertaken including: (i) determine if there is any DHA and diketogulonic acid in the samples; (ii) undertake sorption experiments using DHA; and (iii) undertake sorption experiments on H_2A in the presence of DHA.

One possibility to explain this is that the final product of oxidation of H_2A , dehydroascorbic acid (DHA) adsorbed on the sandstone surface, and then HA sorbed to DHA. Calculations suggest that this might be possible but the mechanism needs further invigation. However, it assumed that this or an equivalent process occurs so that the sum $Fe/2 + Mn$ concentrations is equivalent to the amount of H_2A oxidation. The rate of H_2A oxidation by natural oxides in sandstone is higher than the rate reported for synthetic hematite by Suter et al. (1991), which is very interesting given that it might have been expected that newly precipitated synthetic hematite would be more reactive than old more crystalline hematite.

Chapter seven

Conclusions and Recommendations

7.1 Conclusions

7.1.1 introduction

The principal aim of this project was to determine the capacity and mechanisms of natural oxides (hematite (Fe_2O_3) and Mn oxides) coating sand grains of redbed continental sandstone to oxidize dissolved organic carbon in water under anoxic conditions. Because natural organic matter is so complicated the project has concentrated on studying a relatively simple organic, ascorbic acid.

The method used in the investigation was undertaking a lot of batch experiments to determine rate oxidation of dissolved ascorbic acid by sandstone via reductive dissolution of these oxides. This follows the approach taken previously on synthetic single minerals by various people (e.g. Suter et al., 1991). Because the sandstone is more complicated than a single synthetic mineral the interpretation has involved rather more modelling rather than just calculating parameter values. And comparisons have been made between the rates of reductive dissolution of natural oxides studied here and the rates seen by previous workers for synthetic haematite.

7.1.2 Preliminary batch experiments (Chapter 2)

The aim of the experiments was to provide the data needed to design the final experiments that would be necessary to achieve the aims laid out in Chapter 1. So temperature, concentration of H_2A , aerobic or anaerobic condition, shaking time, filtering and different water rock ratios were investigated. Results of these experiments revealed that H_2A reductively dissolved Fe and Mn oxides from red sandstone. Generally under low water rock ratio it was not possible to measure the released Fe and Mn^{++} using FAAS, but only under higher temperatures (40 °C and above). In these higher temperature experiments the amount of Fe released was higher than Mn^{++} . Mn^{++} did not show a continuing increase in

concentration after long times of reaction, unlike Fe, which indicates, may be that all Mn oxides have been reductively dissolved from the system.

At increased water rock ratios it was possible to measure the released Fe and Mn^{++} under lab temperatures. With high water rock ratios the amount of Mn^{++} released was higher than Fe. Generally there is more released metals in the solutions with higher temperatures, increased mass of sandstone, greater reaction time, and when shaking was used, and anoxic rather than oxic conditions were present. Moreover, changing the initial condition of the surface oxides by protonation (adding H^+) or saturating with Ca has some effect on the rate of reductive dissolution.

7.1.3 Development of methods to analyse ascorbic acid (Chapter 3)

The aim of the next step of the research was to develop a method to measure the concentration of H_2A . After many lab experiments an existing method was development and then adapted to measure the $[\text{H}_2\text{A}]$ in the range from 0 to 100 ppm using KMnO_4 . The method is based on a spectrophotometric technique and produced acceptably repeatable results. However, the method requires corrections to be applied. It is affected by the presence of Mn^{++} which was released via reductive dissolution, though release of Fe did not have any measureable effect. Furthermore there is a minor effect of degradation over time which leads to a slight drop of ascorbic acid concentration over time. New correction methods were developed for these effects.

7.1.4 Sorption of ascorbic acid on the red sandstone (chapter 4)

The aim of this chapter is to determine the capacity of red sandstone to sorb ascorbic acid.

Various sorption experiments were therefore carried out for a short reaction time (2h). The results revealed that at pHs between 4.5 and 5 natural oxides in red sandstone were able to

sorb dissolved ascorbic acid. The sorption isotherms were linear but with an intercept, as has also been found by previous research on synthetic hematite. This previous research used Langmuir isotherms to approximate the observed relationships. The linear-with-intercept fits, and forced Langmuir fits obtained could be used to estimate the amount of sorption under the same range of concentration of ascorbic acid and the same experimental conditions. But it is clear that sorption is not either Langmuir or linear but may be two-site linear. This needs further study.

7.1.5 Cation exchange /total sorption of Fe and Mn^{++} on the red sandstone (chapter 5)

The purpose of carrying out ion exchange experiments was to quantify the sorption of Fe and Mn^{++} on the surface of red sandstone so that uptake of these metals could be taken into account when determining oxidation of ascorbic acid. It was expected that when Fe and Mn were released from the sandstone some of Fe and Mn would be up taken by the sandstone. So ion exchange properties have been investigated to determine the cation exchange capacity CEC and selectivity coefficients for the sandstone. The results give an average CEC value around 2.65 meq/100g with excellent repeatability and consistency with other work. The Fe and Mn selectivity coefficients showed that the selectivity coefficients for Mn were higher than Fe. Applying ion exchange corrections to the final data were much more significant for Mn than for Fe. The results showed that sorption of Fe and Mn released by reductive dissolution is potentially significant. So the correction of $[Mn^{++}]$ and $[Fe]$ is necessary when undertaking measurements of reductive dissolution of hematite and Mn oxides by ascorbic acid.

7.1.6 Reductive dissolution mechanisms (Chapter 6)

The aims of the final set of experiments was to determine mechanisms of reductive dissolution of hematite by ascorbic acid for the first time and to determine if the previously

published work on synthetic hematite could be used when estimating oxidation behaviour of the sandstones, again for the first time. The experiments were designed on basis of the results of the preliminary experiments (Section 7.1.2), used the newly-developed H_2A analysis method (Section 7.1.3), and required data processing that took into account sorption of H_2A (Section 7.1.4) and sorption of Fe and Mn^{++} (Section 7.1.5). All the equipment was set up under anoxic conditions and the amount of Mn^{++} and Fe released from the sandstone and the concentrations of ascorbic were measured for a range of different time intervals up to 49 hours. This was to estimate the rate of Fe and Mn^{++} production and rate of removal of ascorbic acid. The same experiment was repeated but using heat –treated red sandstone samples, filtered solutions and equipment –treated with sterilizing solutions (Benelli, 2015) to find out the effect of bacteria on the rates of reaction. It is found that release of metals (Fe and Mn) increased over time, that $[H_2A]$ decreased with time and decreased at a greater rate with higher initial values of $[H_2A]$, and the $[H_2A]$ decrease was higher in biotic than abiotic experiments. Some of the decrease in $[H_2A]$ can be accounted for by oxidation by Fe and Mn^{++} oxides as indicated by rise in $[Fe]$ and $[Mn^{++}]$ corrected for ion exchange using the approach developed in Chapter 5, and the rest of the decrease is assumed to come from sorption of ascorbic acid. However, mass balances including the predicted sorption from Chapter 4 overestimated the total H_2A mass at early times and underestimated the total mass at later times. Using the mass balance to estimate the sorption, it was found that amount of sorption increases with time and therefore with decrease in $[H_2A]$ and with the (small) increase in pH during the experiments. This is odd because it does not agree with theory that suggests that sorption should decrease with decrease in dissolved concentrations. One possible explanation was found to be that the dehydroascorbic acid (DHA, the oxidised form of ascorbic acid) sorbed to the sandstone surface and then HA^- sorbed to the DHA. Calculations show that this may be possible but the suggestion is speculative and the

mechanism not defined. However, if we take this as an explanation, oxidation rates can be estimated from the increase in Fe and Mn corrected for ion exchange. The oxidation rates seen are greater than found for experiments on synthetic oxides by Suter et al. (1991). This is surprising as it is normally assumed that better crystalline solids produced a long time ago would have less sorption ability than newly made lab minerals. This may indicate that the hematite in the rock is something that is possibly being continuously remade. XRD results for the sandstones usually do not indicate very well crystalline Fe oxides (J. Tellam, Pers. Comm., 2016). The rate of oxidation is a function of concentration of H_2A and specifically the concentration of H_2A on the surfaces of the oxide(s) (first order) and pH. Rates were also faster for biotic experiments than abiotic ones though this may be because the abiotic experiments were at higher pHs.

Though the rates were found to be faster than for synthetic hematite, the results are consistent with the basic mechanisms proposed following the studies by Suter et al. (1991) on synthetic hematite, i.e. that sorption occurs (Section 7.1.4), an electron is transferred, the ascorbate radical is released, then the FeII is released. In broad terms the results from the previously published synthetic hematite experiments are similar to the results obtained from the sandstones, but in the case of the sandstones the rates determined are greater. In addition, the more complex mineral composition of the sandstone means that Mn oxide play a significant role and that on release both Fe and Mn^{++} can be significantly sorbed.

7.2 Review of objectives

The primary aim of the research was to determine the mechanism and capacity of the sandstone to oxidise organic matter. The secondary aim was to determine if synthetic hematite is a suitable model system for investigating hematite coated sandstone. This is the first time, as far as author aware, that the results of such synthetic hematite studies have been compared in detail with hematite coated rock behaviour.

The mechanism proposed by ascorbic acid studies on synthetic hematite (Suter et al 1991) includes three stages: sorption, electron transfer, FeII release.

There is direct evidence for sorption from the sorption experiments of Chapter 4. The isotherms are very similar to those obtained from synthetic hematite (Afonso et al., 1989). Though not commented on before these isotherms are neither Langmuirian or linear and suggest possibly two sorption sites. That sorption is important is also indicated by the need to include a sorption model in the interpretation of final experiments (Chapter 6).

Electron transfer cannot of course be seen. However the increase of Fe release with increase in ascorbic acid concentration strongly suggests that dissolution of hematite is promoted by the ascorbic acid and the simplest explanation is reductive dissolution. The mass balances work when reductive dissolution is included (Chapter 6). More confirms come from the fact that the rates of inferred reductive dissolution are dependent on the same factors as for the synthetic hematite. However in the rock system there are other mechanisms occurring too in particular Mn oxide dissolution (by ascorbic acid or FeII) and sorption of Fe and Mn^{++} . The synthetic hematite model includes no explicitly allowance for bacteria and the experiments undertaken here following heat treatment of the rock, filtering of solutions and cleaning of equipment result in inferred dissolution rates that lie on the same relationship with pH as the experiments that have been undertaken without attempt to sterilize. So this again suggests that there is consistency with the previous synthetic hematite experiment derived reductive dissolution models.

With regards to capacity it is possible that there may be some protection of remaining hematite if the sorption model proposed involving DHA is correct. However at least at high temperature all the hematite can be removed so at high temperature any protection of the surface by sorbed unreacting organic daughter compounds does not seem to occur. This suggest that the capacity is limited only by the total amount of hematite and Mn oxide present.

This has been evaluated by Jaweesh (In Prep) and using his data there would be 0.3-0.7 mol Fe + Mn / litre groundwater available.

With regards to the applicability of the results on synthetic hematite dissolution to rock coating hematite it is clear that though there are other additional reactions occurring (Mn oxides, sorption of Fe and Mn) the mechanisms identified by the synthetic experimentst appear to be also seen in the red sandstone experiments. The rates seen in the rock are greater than in the synthetic experiments so that latter cannot be used direct in prediction but the factors that the rates depend on appear to include those identified by the synthetic experiments. So the synthetic experiment results should not be used directly but are a very good basis for developing a conceptual understanding of the mechanisms involved.

7.3 Implications

The rates of oxidation observed is promising in terms of the ability of natural oxides in sandstones to oxidise dissolved organic carbon in groundwater, and possibly have a significant effect on the attenuation of contaminants in pristine and polluted aquifers.

However it should be borne in mind that the studies on synthetic minerals indicate that the effects become much less as pH rises from the low values studied in the present study. The capacity of the sandstone for oxidation is limited to the amount of oxide present. This is probably about 0.2% of the rock mass in total (Jaweesh, In Prep) and this would be about 0.5 mol Fe + Mn /litre groundwater and this is a lot.

Preliminary work in Chapter 2 indicates that may be some oxidation also occurs in oxic conditions for instance found in the unsaturated zone.

The study has given results that are similar to the results of previous research on synthetic minerals. This suggests that the reaction mechanisms are similar and that gives

encouragement that we can use synthetic mineral experiments to help interpret field data in general. The surprising result is that rates are greater than for synthetic hematite, though this may be partly because of Mn oxides.

If ascorbic acid reduces the oxides because it has some functional groups like humic substances the humic substances might also reduce the oxides in a similar way. Other functional groups in humic substances need to be investigated. Also needs to be investigated is other mechanisms of promoting hematite dissolution including complexation of Fe by organic ligands (see Section 7.4).

The results have indicated sorption is significant. The mechanisms are not very clear as the isotherms are not linear or Langmuir. They may indicate two sorption sites and this needs to be investigated. The model suggested here for sorption to sorbed organic matter might be an important process for other organics and contaminants.

In conclusion the oxidation of organic matter by reaction with oxides may be an important mechanism for removal of organic material from soils in aquifers and an explanation of the drop of TOC with depth seen in the sandstone aquifer (Stagg et al., 1998; recent unpublished analysis undertaken by author for MSc project work of R.Bradford and H.Prosser).

7.4 Recommendation and future research

The following works are recommended:

1. Look at the effect of organic ligands, e.g. oxalic acid, using the same batch experiment method.
2. Look at other organics that are relevant to the various humic functional groups present in the natural environment.

3. Having completed the previous studies, look at humic interactions with sandstone and link to the mechanisms found out in points 1 and 2 above.
4. Look at the different roles of Mn and Fe oxides by using a sequential extraction technique to remove Mn oxides without removing iron oxides, then carry out the same experiments to find out the effect hematite alone on the rate of oxidation of ascorbic acid.
5. Use different type of sandstone. May be sandstone collected from outcrop as in this study, it gives higher oxidising rates than samples collected from cores either because of less Mn oxides with depth or because of reduction of Fe oxides with depth (as Massmann et al. (2004) found for sandstones in Germany). The main difference may be related to the position in relation to the water table.
6. The effect of other cations and anions present in the groundwater and present on the oxide surfaces needs to be evaluated.
7. Other environmental factors must be considered in future lab work, including temperature and higher pH values.
8. Confirm the importance or otherwise of bacteria in the reactions.

Only when all this work is put together can a full picture of organic compound/sandstone interaction be quantified.

References:

- Afonso, M.D.S., Morando, P.J., Blesa, M.A., Banwart, S. and Stumm, W., 1990. The reductive dissolution of iron oxides by ascorbate: The role of carboxylate anions in accelerating reductive dissolution. *Journal of Colloid and Interface Science*, 138(1), pp.74-82.
- Allen, D. J., Brewerton, L. J., Coleby, L. M., Gibbs, B.R., Lewis, M.A., MacDonald, M., Wagstaff, S. J., and Williams, A.T., 1997. The physical properties of major aquifers in England and Wales. British Geological Survey Technical Report WD/97/34. Environment Agency R&D Publication 8.
- Alyabina , I. O., 2009. Database Processing for Studying the Mechanisms of Cation Exchange Capacity Development. *Moscow University Soil Science Bulletin*, Vol. 64, No. 4, pp. 145–153.
- Apello CAJ, Postma D ,2005. *Geochemistry, groundwater and pollution*, 2nd edn. CRC/Balkema, Rotterdam.
- Aprile, F. and Lorandi, R., 2012. Evaluation of cation exchange capacity (CEC) in tropical soils using four different analytical methods. *Journal of Agricultural Science*, 4(6), p.278.
- Avena, M.J., Koopal, L.K., 1998. Desorption of humic acids from an iron oxide surface. *Environmental Science & Technology*. 32, 2572–2577.
- Balan L., Ghimbeu C.M., Vidal L., and Guterl C.V., 2013. Visible light assisted synthesis of manganese oxide nanoparticles at room temperature. *Electronic Supplementary Material (ESI) for Green Chemistry*, The Royal Society of Chemistry .
- Ball, G.F., 2006. *Vitamins in foods: analysis, bioavailability, and stability*. CRC Press, Taylor and Francis Group.

- Banwart, S., Davies, S., and Stumm, W., 1989. The role of oxalate in accelerating the reductive dissolution of hematite ($\alpha\text{-Fe}_2\text{O}_3$) by ascorbate. *Colloids and surfaces*, 39,303-309.
- Barker, R.D. and Tellam, J.H. eds., 2006. Fluid flow and solute movement in sandstones: the onshore UK Permo-Triassic red bed sequence. Geological Society of London.
- Batty, T.A., 2015. Examining the use of the partition coefficient in quantifying sorption of heavy metals in Permo-Triassic sandstone aquifer. PhD thesis, the university of Birmingham, 291p.
- Beaven, R., Potter, H., Powrie, W., Simoes, A., Smallman, D. and Stringfellow, A., 2009. Attenuation of organic contaminants in leachate by mineral landfill liners. Environment Agency, Integrated Catchment Science programme, Science report SC020039/SR5. 58p.
- Bencala, K. E., V. C. Kennedy, G. W. Zellweger, A. P. Jackman, and R. J. Avanzino, 1984. Interactions of solutes and streambed sediments, 1, An experimental analysis of cation and anion transport in a mountain stream. *Water Resources Research*, 20(12), pp.1797-1803.
- Benelli, P., 2015. Organic compounds/sandstone interactions: assessing the reduction of iron and manganese oxides in the English Permo-Triassic Sandstone by ascorbic acid and the impact of bacteria. MSc Thesis, university of Birmingham.
- Berbenni, P., Pollice, A., Canziani, R., Stabile, L. and Nobili, F., 2000. Removal of iron and manganese from hydrocarbon-contaminated groundwaters. *Bioresource technology*, 74(2), pp.109-114.
- Bertino, D.J. and Zepp, R.G., 1991. Effects of solar radiation on manganese oxide reactions with selected organic compounds. *Environmental science & technology*, 25(7), pp.1267-1273.

- Bhagavan N.V. ,2001. Medical Biochemistry, Elsevier, Amsterdam, The Netherlands, 4th edition.
- Bittell, J.E. and Miller, R.J., 1974. Lead, cadmium, and calcium selectivity coefficients on a montmorillonite, illite, and kaolinite. *Journal of Environmental Quality*, 3(3), pp.250-253.
- Bjerg, P.L. and Christensen, T.H., 1993. A field experiment on cation exchange-affected multicomponent solute transport in a sandy aquifer. *Journal of contaminant hydrology*, 12(4), pp.269-290.
- Black,F.J, Gallon. And Flegat, A.R ,2008. Sediment retention and release. *Encyclopaedia of Ecology*, volume (4), pp3172-31 87.
- Blaser, P., 1994. The role of natural organic matter in the dynamics of metals in forest soils. In: Senesi, N., Miano,T.M. (Eds.), *Humic Substances in the Global Environment and Implications on Human Health*. Elsevier,Amsterdam, pp. 943– 960.
- Boguslavsky, S., 2000. Organic Sorption and Cation Exchange Capacity of Glacial Sand, Long Island. Thesis of MS, State University of New York at Stony Brook, NY.
- Bolt, G.H., 1982.soil chemistry, B.Physico –chemical models. Elsevier, Amsterdam, 527pp.
- Bose, P., & Sharma, A. ,2002. Role of iron in controlling speciation and mobilization of arsenic in subsurface environment.*Water Research*, 36, pp.4916–4926.
- Burdige ,D.J.,1993. The biogeochemistry of manganese and iron reduction in marine sediments. *Earth-Science Reviews*, 35 ,pp. 249-284.
- Burdige, D.J., Dhakar, S.P. and Nealson, K.H., 1992. The role of manganese oxide mineralogy on microbial and chemical manganese reduction. *Geomicrobiology Journal*, 10(1), pp.27-48.

Camberato JJ ,2001. Cation exchange capacity—everything you want to know and much more. First printed in South Carolina Turfgrass Foundation News, October–December, 2001. <http://ebookbrowse.com/cation-exchange-capacity-pdf-d19788599>.

Canfield, D.E., Thamdrup, B., Hansen, J.W., 1993. The anaerobic degradation of organic matter in Danish coastal sediments: Iron reduction, manganese reduction, and sulfate reduction. *Geochimica et Cosmochimica Acta*, 57(16), pp.3867-3883.

Carlyle ,H.F.,1991, The hydrochemical recognition of ion exchange during sea water intrusion at widnes, Merseyside ,UK . Unpublished Ph.D. thesis, university of Birmingham.

Ceazan, M.L., Thurman, E.M. and Smith, R.L., 1989. Retardation of ammonium and potassium transport through a contaminated sand and gravel aquifer: the role of cation exchange. *Environmental science & technology*, 23(11), pp.1402-1408.

Champ, D.R., Gulens, J., Jackson, R.E., 1979. Oxidation–reduction sequences in groundwater flow systems. *Canadian Journal of earth sciences*, 16(1), pp.12-23.

Chapelle, F.H. ,1993. Ground water Microbiology and Geochemistry. J. Wiley & Sons , Inc., New York .

Chiou, C.T., Porter, P.E. And Schmedin, D.W., 1983. Partition equilibria of nonionic compounds between soil organic matter and water. *Environmental Science & Technology*, 17(4), pp.227-231.

Cornell, R.M., Schwertmann, U., 2003. The Iron Oxides: Structure, Properties, Reactions, Occurrence and Uses, Second ed. VCH Verlagsgesellschaft mbH.

Crawford, T.C. and Crawford, S.A., 1980. Synthesis of L-ascorbic acid. *Advances in carbohydrate chemistry and biochemistry*, 37, p.79.

Davidson, W., Seed, G., 1983. The kinetics of the oxidation of ferrous iron in synthetic and natural waters. *Geochimica et Cosmochimica Acta*, 47(1), pp.67-79.

Davranche, M. and Bollinger, J.C., 2000. Heavy metals desorption from synthesized and natural iron and manganese oxyhydroxides: effect of reductive conditions. *Journal of Colloid and Interface Science*, 227(2), pp.531-539.

DeLaune RD, Smith CJ., 1985. Release of nutrients and metals following oxidation of freshwater and saline sediment. *Journal of Environmental Quality*, 14(2), pp.164-168.

Dellesite, A., 2001. Factors affecting sorption of organic compounds in natural

Domenico, P A and Schwartz, F W;(1990) ; *Physical and Chemical Hydrogeology*; John Wiley & Sons, Inc.

Domitrovic, R., 2006. Vitamin C in disease prevention and therapy. *Biochemia Medica*, 16(2), pp.89-228.

Dragun , J. 1988. *The soil chemistry of hazardous materials* .silver spring , MD :Hazardous materials Control Research Institute ,458p.

Drever J. I. ,1982. *The Geochemistry of Natural Waters*. Prentice-Hall, 388 p.

Drever, J. I. ,1997. *The Geochemistry of Natural Waters: Surface and Groundwater Environments*. 3rd ed., Prentice Hall, Englewood Cliffs, 480 pp.

Dube A, Zbytniewski R, Kowalkowski T, Cukrowska E, Buszewski B (2001) Adsorption and migration of heavy metals in soil. *Polish journal of environmental studies*, 10(1), pp.1-10.

Eby, G.N., 2004. *Principle of environmental Geochemistry*. Brooks / cole, Cengage Learning, USA, 514pp.

Ehrlich, H.L., 1981. *Geomicrobiology*. Marcel Dekker, Inc., New York.

El-Ghonemy ,H.M.R., 1997. Laboratory experiments for quantifying and describing cation exchange in the UK Triassic sandstone. Ph.D. thesis ,University of Birmingham .

- Elmagirbi, A., Sulistyarti, H. and Atikah, A., 2012. Study of Ascorbic Acid as Iron (III) Reducing Agent for Spectrophotometric Iron Speciation. *The Journal of Pure and Applied Chemistry Research*, 1(1), pp.11-17.
- Essington, M.E., 2004. *Soil and Water Chemistry: An Integrative Approach*. CRC Press.
- Evangelou, V.P. and Phillips, R.E., 1988. Comparison between the Gapon and Vanselow exchange selectivity coefficients. *Soil Science Society of America Journal*, 52(2), pp.379-382.
- Fadhel, D.H., 2012. Spectrophotometric determination of ascorbic acid in aqueous solutions. *Journal of Al-Nahrain University*, 15(3), pp.88-94.
- Fetter, C.W., 1994. *Applied Hydrogeology*, Prentice Hall. New Jersey, NJ, p.691.
- Fetter, C.W., 1999. *Contaminant hydrogeology*, second edition. Waveland press, INC. Long Grove, Illinois, 500p.
- Fischer, W.R., in (1972) in *Pseudogley and Gley* (Schlichting, E., Schwertmann, U., eds. Weinheim: Verlag Chemie.
- Freeze, R.A. and Cherry, J.A., 1979. *Groundwater*. Prentice Hall, Englewood Cliffs, 606pp.
- Froelich, P.N., Klinkhammer, G.P., Bender, M.L., Luedtke, N.A., Heath, G.R., Cullen, D., Dauphin, P., Hammond, D., Hartman, B., and Maynard, V., 1979. Early oxidation of organic matter in pelagic sediments of the eastern equatorial Atlantic: suboxic diagenesis. *Geochimica et Cosmochimica Acta*, 43(7), pp.1075-1090.
- Gaines, G.L. and Thomas, H.C., 1953. Adsorption studies on clay minerals. II. A formulation of the thermodynamics of exchange adsorption. *The Journal of Chemical Physics*, 21(4), pp.714-718.

Ganesh, S., Khan, F., Ahmed, M.K., Velavendan, P., Pandey, N.K. and Mudali, U.K., 2012. Developed New Procedure for Low Concentrations of Hydrazine Determination by Spectrophotometry: Hydrazine-Potassium Permanganate System. Journal of Analytical Sciences, Methods and Instrumentation, 2(02), p.98.

Gauger, A.M. and Hallen, R.T., 2012. Individual Reactions of Permanganate and Various Reductants. Student Report to the DOE ERULF Program for Work Conducted May to July 2000 (No. PNNL-21728). Pacific Northwest National Laboratory (PNNL), Richland, WA (US). Geoderma 154, 13–19.

Gillespie, M. R., Leader, R. U., Higgo, J. J.w, Harrison, I., Hards, V. L., Gowing, C. J.B., Vickers, B.P., Boland ,M.P. and Morgan D.J. ,2000. CEC & Kd Determination in Landfill Performance Evaluation . A review of methodologies and preparation of standard materials for laboratory analysis. Environment Agency R&D technical Report p.340 .

Glasauer, S., Weidler, P.G., Langley, S., Beveridge, T.J., 2003. Controls on Fe reduction and mineral formation by a subsurface bacterium. Geochimica et Cosmochimica Acta, 67(7), pp.1277-1288.

Gonzalez-Gil, G., Amonette, J.E., Romine, M.F., Gorby, Y.A., Geesey, G.G., 2005. Bioreduction of natural specular hematite under flow conditions. *Geochimica et cosmochimica acta*, 69(5), pp.1145-1155.

Gotoh S, Patrick Jr WH. ,1972. Transformation of Manganese in a waterlogged soil as influenced by redox potential and pH. Soil Science Society of America Journal, 36(5), pp.738-742.

Gotoh, S.; Patrick, W.H., 1974. Transformation of iron in a waterlogged soil as influenced by redox potential and pH. Soil Science Society of America Journal, 38(1), pp.66-71.

Grybos, M., Davranche, M., Gruau, G., Petitjean, P. and Pédrot, M., 2009. Increasing pH drives organic matter solubilization from wetland soils under reducing conditions. *Geoderma*, 154(1), pp.13-19.

Güçlü K., Sözgen K., Tütem E., Özyürek M., and Apak, R. ,2005. Spectrophotometric determination of ascorbic acid using copper(II)-neocuproine reagent in beverages and pharmaceuticals,” *Talanta*, vol. 65, no. 5, pp. 1226–1232.

Hansel, C.M., Benner, S., Nico, P., Fendorf, S., 2004. Structural constraints of ferric (hydr)oxides on dissimilatory iron reduction and the fate of Fe(II). *Geochimica et Cosmochimica Acta*, 68(15), pp.3217-3229.

Harish, K. and Manisha, P.S., 2013. Synthesis and Characterization of MnO₂ Nanoparticles using Co-precipitation Technique. *International Journal of Chemistry and Chemical Engineering*, 3, pp.155-160.

Harvey JW, Fuller CC, 1998. Effect of enhanced manganese oxidation in the hyporheic zone on basin-scale geochemical mass balance. *Water Resources Research*, 34(4), pp.623-636.

Heron, G. and Christensen, T.H., 1995. Impact of sediment-bound iron on redox buffering in a landfill leachate polluted aquifer (Vejen, Denmark). *Environmental Science & Technology*, 29(1), pp.187-192.

Heron, G., Christensen, T.H. and Tjell, J.C., 1994. Oxidation capacity of aquifer sediments. *Environmental Science & Technology*, 28(1), pp.153-158.

Hiscock, K.M., Grischek, T., 2002. Attenuation of groundwater pollution by bank filtration. *Journal of Hydrology*, 266(3), pp.139-144.

Hussain, Z. and Islam. M. , 2010. Leaching of heavy metals from contaminated soils using inductively coupled plasma optical emission spectrometer (ICP-OES) and atomic absorption spectrometer (AAS). *Journal of Scientific Research* 40:pp.47-53.

Iwase H. and I. Ono I. 1998.Determination of ascorbic acid in food by column liquid chromatography with electrochemical detection using eluent for pre-run sample stabilization, *Journal of Chromatography A*, vol. 806, no. 2, pp. 361–364.

Jang, L.-K., P. W. Chang, J. E. Findley, and T. F. Yen. ,1983. Selection of bacteria with favorable transport properties through porous rock for the application of microbial-enhanced oil recovery. *Applied and environmental microbiology*, 46(5), pp.1066-1072.

Jardine, P. M., McCarthy, J. F., & Weber, N. L. ,1989. Mechanisms of dissolved organic carbon adsorption on soil.*Soil Science Society of America Journal*, 53(5),pp. 1378-1385.

Jaweesh, M. (In Preparation). The importance of correlation between lithofacies, within sandstone sequences and geochemical properties in groundwater contaminant transport. PhD thesis (in Preperation), University of Birmingham.

Jenneman, G. E., M. J. McInerney, and R. M. Knapp. 1985. Microbial penetration through nutrient-saturated Berea sandstone. *Applied and Environmental Microbiology*, 50(2), pp.383-391.

Jenneman, G.E., McInerney, M.J., Crocker, M.E., and Knapp, R.M., 1986. Effect of sterilization by dry heat or autoclaving on bacterial penetration through Berea Sandstone. *Applied and environmental microbiology*, 51(1), pp.39-43.

Joseph, S., Visalakshi, G., Venkateswaran, G., & Moorthy, P. N. ,1996. Dissolution of hematite in citric acid-EDTA -ascorbic acid mixtures. *Journal of nuclear science and*

technology, 33(6), pp.479-485. Journal of Physical and Chemical Reference Data, 30, 1, pp.187-439.

Kaiser, K. and Zech, W., 1997. Competitive sorption of dissolved organic matter fractions to soils and related mineral phases. Soil Science Society of America Journal, 61(1), pp.64-69.

Kall M. A. and C. Andersen, C. 1999. Improved method for simultaneous determination of ascorbic acid and dehydroascorbic acid, is ascorbic acid and dehydroisoascorbic acid in food and biological samples," Journal of Chromatography B, vol. 730, no. 1, pp. 101–111.

Kehew, A.E., 2001. Applied chemical hydrogeology. Upper saddle river, NJ: prentice Hall, Inc, 368pp.

Kenndey, V.C., 1965. Mineralogy and cation exchange capacity of sediment from selected streams. U.S. Geological survey professional paper 433-D.

Kennedy, J.F., Rivera, Z.S., Lloyd, L.L., Warner, F.P. and Jumel, K., 1992. L-Ascorbic acid stability in aseptically processed orange juice in TetraBrik cartons and the effect of oxygen. Food Chemistry, 45(5), pp.327-331.

Kueller V and Othmer, K. 2001. Encyclopedia of Chemical Technology. (2001). New York, NY: John Wiley & Sons; Ascorbic Acid. Online Posting Date: Apr 16, 2001.

Larsen, O., and Postma, D., 2001. Kinetics of reductive bulk dissolution of lepidocrocite, ferrihydrite and goethite. Geochimica et Cosmochimica Acta, 65(9), pp.1367-1379.

Larsen, O., Postma, D. and Jakobsen, R., 2006. The reactivity of iron oxides towards reductive dissolution with ascorbic acid in a shallow sandy aquifer (Rømø, Denmark). Geochimica et cosmochimica acta, 70(19), pp.4827-4835.

Larsen, O., Postma, D. and Jakobsen, R., 2006. The reactivity of iron oxides towards reductive dissolution with ascorbic acid in a shallow sandy aquifer (Rømø, Denmark). *Geochimica et cosmochimica acta*, 70(19), pp.4827-4835.

Lee, E. Y., Cho, K. S., Ryu, H. W., & Chang, Y. K. ,1999. Microbial removal of Fe (III) impurities from clay using dissimilatory iron reducers. *Journal of bioscience and bioengineering*, 87(3), pp.397-399.

Lee, R. W., & Bennett, P. C.,1998. Reductive Dissolution and Reactive Solute Transport in a Sewage-Contaminated Glacial Outwash Aquifer. *Ground Water*, 36(4), 583-595.

Levy, D. B., Barbarick, K. A., Siemer, E. G., & Sommers, L. E. ,1992. Distribution and partitioning of trace metals in contaminated soils near Leadville, Colorado. *Journal of Environmental Quality*, 21(2), 185-195.

Lide, D.R. ,2007. *Handbook of Chemistry and Physics 88TH Edition 2007-2008*. CRC Press, Taylor & Francis, Boca Raton, FL p. 3-28.

Lindsay, W.,1991. Iron oxide solubilization by organic matter and its effect on iron availability, p. 29–36. In: *Iron Nutrition and Interactions in Plants*, edited by Y. Chen and Y. Hadar, Kluwer Academic Publishers, Dordrecht .

Linge, K.L., 2008. Methods for investigating trace element binding in sediments. *Critical Reviews in Environmental Science and Technology*, 38(3), pp.165-196.

Loganathan, P., Vigneswaran, S. , Kandasamy ,J. and Bolan ,N.S., 2014. Removal and recovery of phosphate from water using sorption . *Critical Reviews in Environmental Science and Technology*, 44(8), pp.847-907.

- Lohmayer, R., Kappler, A., Lösekann-Behrens, T. and Planer-Friedrich, B., 2014. Sulfur species as redox partners and electron shuttles for ferrihydrite reduction by *Sulfurospirillum deleyianum*. *Applied and environmental microbiology*, 80(10), pp.3141-3149.
- Lovley, D., Anderson, R., 2000. Influence of dissimilatory metal reduction on fate of organic and metal contaminants in the subsurface. *Hydrogeology Journal*, 8(1), pp.77-88.
- Lovley, D.R., M.J. Baedeker, D.J. Lonergan, I.M. Cozzarelli, E.J.P. Phillips, and D.I. Siegel, 1989. Oxidation of aromatic contaminants coupled to microbial iron reduction. *Nature*, 339(6222), pp.297-300.
- Lovley DR, Holmes DE, Nevin KP, 2004. Dissimilatory Fe(III) and Mn(IV)
- Lovley, D. R., & Anderson, R. T., 2000. Influence of dissimilatory metal reduction on fate of organic and metal contaminants in the subsurface. *Hydrogeology Journal*, 8(1), pp.77-88.
- Lovley, D. R., & Phillips, E. J., 1988. Novel mode of microbial energy metabolism: organic carbon oxidation coupled to dissimilatory reduction of iron or manganese. *Applied and environmental microbiology*, 54(6), pp. 1472-1480.
- Lovley, D.R., 1987. Organic matter mineralization with the reduction of ferric iron: a review. *Geomicrobiology Journal*, 5(3-4), pp.375-399.
- Lovley, D.R., 1991. Dissimilatory Fe (III) and Mn (IV) reduction. *Microbiological reviews*, 55(2), pp.259-287.
- Lovley, D.R., 1992. Microbial oxidation of organic matter coupled to the reduction of Fe (III) and Mn (IV) oxides. *Catena, Supplement*, (21), pp.101-114.
- Lovley, D.R., Phillips, E.J.P., 1986. Availability of ferric iron for microbial reduction in bottom sediments of the freshwater tidal Potomac River. *Applied and Environmental Microbiology*, 52(4), pp.751-757.

- MacIntyre, W. G., Stauffer, T. B., & Antworth, C. P. 1991. A comparison of sorption coefficients determined by batch, column, and box methods on a low organic carbon aquifer material. *Ground Water*, 29(6), pp.908-913.
- Marschner, B. and Kalbitz, K., 2003. Controls of bioavailability and biodegradability of dissolved organic matter in soils. *Geoderma*, 113(3), pp.211-235.
- Massmann, G., Pekdeger, A. and Merz, C., 2004. Redox processes in the Oderbruch polder groundwater flow system in Germany. *Applied geochemistry*, 19(6), pp.863-886.
- McBride, M.B., 1994 : Environmental chemistry of soils. 1st Edition; Oxford University Press, , 416 p
- McBride, M.B., 1987. Adsorption and oxidation of phenolic compounds by iron and manganese oxides. *Soil Science Society of America Journal*, 51(6), pp.1466-1472.
- Miao, S., DeLaune, R. D., & Jugsujinda, A. ,2006. Influence of sediment redox conditions on release/solubility of metals and nutrients in a Louisiana Mississippi River deltaic plain freshwater lake. *Science of the Total Environment*, 371(1), pp. 334-343.
- Moody, J.B., 1982. Radionuclide migration/retardation: research and development technology status report (No. ONWI-321). Battelle Memorial Inst., Columbus, OH (USA). Office of Nuclear Waste Isolation, 61p.
- Morel, F.M. and Hering, J.G., 1993. Principles and applications of aquatic chemistry. John Wiley & Sons.
- Mulvaney, P., Cooper, R., Grieser, F. and Meisel, D., 1988. Charge trapping in the reductive dissolution of colloidal suspensions of iron (III) oxides. *Langmuir*, 4(5), pp.1206-1211.
- Munch J. C. and Ottow J. C. G. ,1983. Reductive transformation mechanism of ferric oxides in hydromorphic soils. *Ecological Bulletins*, pp.383-394.

Munch, J.C., Ottow, J.C.G., 1980. Preferential reduction of amorphous to crystalline iron oxides by bacterial activity. *Soil Science*, 129(1), pp.15-21.

Mussa, S.B. and El Sharaa, I., 2014. Analysis of Vitamin C (ascorbic acid) Contents packed fruit juice by UV-spectrophotometry and Redox Titration Methods. *IOSR Journal of Applied Physics*. Volume 6, Issue 5 Ver. II, pp.46-52.

Myers, C.R. and Nealson, K.H., 1988. Microbial reduction of manganese oxides: Interactions with iron and sulfur. *Geochimica et Cosmochimica Acta*, 52(11), pp.2727-2732.

Neal, A.L., Rosso, K.M., Geesey, G.G., Gorby, Y.A., Little, B.J., 2003. Surface structure effects on direct reduction of iron oxides by *Shewanella oneidensis*. *Geochim. Cosmochim. Acta* 67, 4489– 4503.

Nealson, K. H., and Myers, C. R., 1992. Microbial Reduction of Manganese and Iron: New Approaches to Carbon Cycles. *Applied and Environmental Microbiology*, 439-443.

Nealson, K.H. and Saffarini, D., 1994. Iron and manganese in anaerobic respiration: environmental significance, physiology, and regulation. *Annual Reviews in Microbiology*, 48(1), pp.311-343.

Nealson, K.H., Rosson, R.A., Myers, C.R., 1989. Mechanisms of oxidation and reduction of manganese, in: Beveridge, T.J., Doyle, R.J. (Eds.), *Metal ions and Bacteria*. Wiley, New York, NY, pp. 383–411.

New England Biolabs (NEB), Inc., 2015. Heat Inactivation. <https://www.neb.com/tools-and-resources/usage-guidelines/heat-inactivation>. Accessed 05/06/2016

- Ogwada, R.A., Sparks, D.L., 1986. Kinetics of ion exchange on clay minerals and soil: I. Evaluation of methods. *Soil Science Society of America Journal*, 50(5), pp.1158-1162.
- O'Neil, M.J. (ed.), 2006. *The Merck Index - An Encyclopedia of Chemicals, Drugs, and Biologicals*. Whitehouse Station, NJ: Merck and Co., Inc., p. 136
- Ottow, JCG, 1981. Mechanism of bacterial iron reduction in flooded soils. *Proc Symp Paddy Soils*, Institute of Soil Science, Academia Sinica. Science Press, Beijing, pp. 330-343 .
- Gounot, A.M., 1994. Microbial oxidation and reduction of manganese: consequences in groundwater and applications. *FEMS Microbiology Reviews*, 14(4), pp.339-349.
- Pandey, S.C., Pollard, A.M., Viles, H.A. and Tellam, J.H., 2014. Influence of ion exchange processes on salt transport and distribution in historic sandstone buildings. *Applied Geochemistry*, 48, pp.176-183.
- Parker, K.E., 2005. calculation ion exchange parameters from pure clay assemblages . Ph.D thesis, university of Birmingham, UK.
- Parkhurst, D.L. and Appelo, C.A.J., 1999. User's guide to PHREEQC (Version 2): A computer program for speciation, batch-reaction, one-dimensional transport, and inverse geochemical calculations.
- Patrick Jr WH, Jugsujinda A., 1992. Sequential reduction and oxidation of inorganic nitrogen, manganese and iron in flooded soil. *Soil Science Society of America Journal*, 56(4), pp.1071-1073.
- Petrunic B.M., MacQuarrie K.T.B ,and Al, T.A ,2005. Reductive dissolution of Mn oxides in river recharged aquifers:a laboratory column study.*Jouranl of Hydrology* 301, 163-181pp.

Piccolo, A., 1994. Interactions between organic pollutants and humic substances in the environment. In: Senesi, N., Miano, T.M. (Eds.), *Humic Substances in the Global Environment and Implications on Human Health*. Elsevier, Amsterdam, pp. 961–979.

Pignatello, J.J., 1998. Soil organic matter as a nanoporous sorbent of organic pollutants. *Advances in Colloid and Interface Science*, 76, pp.445-467.
Pisoschi, A.M., Danet, A.F. and Kalinowski, S., 2009. Ascorbic acid determination in commercial fruit juice samples by cyclic voltammetry. *Journal of Analytical Methods in Chemistry*, 2008.

Pignatello, J.J., 1998. Soil organic matter as a nanoporous sorbent of organic pollutants. *Advances in Colloid and Interface Science*, 76, pp.445-467.

Plant, J.A., Jones, D.G. and Haslam, H.W. eds., 1999. *The Cheshire Basin: Basin evolution, fluid movement and mineral resources in a Permo-Triassic rift setting* (p. 263). Nottingham, UK: British Geological Survey.

Ponnamperuma, F.N., 1972. The chemistry of submerged soils. *Advances in agronomy*, 24, pp.29-96.

Postma, D., 1985. Concentration of Mn and separation from Fe in sediment –I. Kinetics and stoichiometry of the reaction between birnessite and dissolved Fe(II) at 10 C. *Geochimica et Cosmochimica Acta*, 49(4), pp.1023-1033.

Postma, D., 1993. The reactivity of iron oxides in sediments: a kinetic approach. *Geochimica et Cosmochimica Acta*, 57(21-22), pp.5027-5034.

Reardon, E.J., Dance, J.T. and Lolcama, J.L., 1983. Field determination of cation exchange properties for calcareous sand. *Ground Water*, 21(4), pp.421-428.

Reddy, k. R., and Delaune R.D., 2008. *Biochemistry of wetlands sciences and applications*. CRC press ,Taylor &Francics group .774p.

Reeburgh, W.S., 1983. Rates of biogeochemical processes in anoxic sediments. *Annual Review of Earth and Planetary Sciences*, 11, pp. 269-298.

Roden, E.E., 2004. Analysis of long-term bacterial vs. chemical Fe (III) oxide reduction kinetics. *Geochimica et Cosmochimica Acta*, 68(15), pp.3205-3216.

Roden, E.E. and Zachara, J.M., 1996. Microbial reduction of crystalline iron (III) oxides: Influence of oxide surface area and potential for cell growth. *Environmental Science & Technology*, 30(5), pp.1618-1628.

Schäfer, M. and Steiger, M., 2002. A rapid method for the determination of cation exchange capacities of sandstones: preliminary data. *Geological Society, London, Special Publications*, 205(1), pp.431-439.

Schwertmann, U. ,1966. Inhibitory effect of soil organic matter on the crystallization of amorphous ferric hydroxide. *Nature* 212,pp.645-646.

Shafie, N.A., Aris, A.Z. and Puad, N.H.A., 2013. Influential factors on the levels of cation exchange capacity in sediment at Langat river. *Arabian Journal of Geosciences*, 6(8), pp.3049-3058.

Shin, W. T., Garanzuay, X., Yiacoumi, S., Tsouris, C., Gu, B., & Mahinthakumar, G. K. ,2004 . Kinetics of soil ozonation: an experimental and numerical investigation. *Journal of contaminant hydrology*, 72(1), pp.227-243.

Sibanda, H.M. and Young, S.D., 1986. Competitive adsorption of humus acids and phosphate on goethite, gibbsite and two tropical soils. *Journal of Soil Science*, 37(2), pp.197-204.

Smith , J W N. ,2005. Groundwater–surface water interactions in the hyporheic zone. *Environment Agency Science Report*, SC030155/SR1.

- Soil Chemistry ,2011. Section 9—oxidation reduction. <http://lawr.ucdavis.edu/classes/ssc102/Section9.pdf>. sorbent/water systems and sorption coefficients for selected pollutants.
- Sparks, D.L., 1989. Kinetics of soil chemical processes. Academic Press.
- Stagg, K .A , Tellam J H, Barrett M.H., and Lerner D.N., 1998. Hydrochemical variations with depth in a major UK aquifer: the fractured, high permeability Triassic Sandstone. In: Brahana, J.V., Eckstein, Y., Ongley, L.K., Schneider, R., and Moore, J.E. (eds), Gambling with groundwater - physical, chemical, and biological aspects of aquifer-stream relations. American Institute of Hydrology, St Paul, Minnesota, Proc IAH Conference, Las Vegas, 53-58.
- Steventon-Barnes, H., 2001. Solid organic carbon in UK aquifers: its role in sorption of organic contaminants. PhD thesis, University of London.
- Stewart, R.,1965. Chapter 1: Oxidation by permanganate, Oxidation in Organic Chemistry (pp. 1-68). New York: Academic Press.
- Stone, A.T., and Morgan, 1987. Aquatic Surface Chemistry. Edited by (Stumm W.),Wiley ,new York pp.221-254.
- Stumm, W. & Morgan, J. J.,1996. Aquatic Chemistry: Chemical Equilibria and Rates in Natural Waters (John Wiley & Sons, New York).
- Stumm, W., 1992. Chemistry of the solid-water interface: processes at the mineral-water and particle-water interface in natural systems. John Wiley & Son Inc.
- Sulzberger, B., Suter, D., Siffert, C., Banwart, S. and Stumm, W., 1989. Dissolution of Fe (III)(hydr) oxides in natural waters; laboratory assessment on the kinetics controlled by surface coordination. Marine Chemistry, 28(1-3), pp.127-144.

- Suter, D., Banwart, S. and Stumm, W., 1991. Dissolution of hydrous iron (III) oxides by reductive mechanisms. *Langmuir*, 7(4), pp.809-813.
- Suter, D., Siffert, C., Sulzberger, B., & Stumm, W. ,1988. Catalytic dissolution of iron (III)(hydr) oxides by oxalic acid in the presence of Fe (II). *Naturwissenschaften*, 75(11), 571-573.
- Swinehart,D.F.,1962. The beer-lambert law , *Journal of chemical education* 39(7), 333-335.
- Tannenbaum, S.R., Young, V.R. and Archer, M.C., 1985. Vitamins and minerals, in *Food chemistry*, Fennema ,O.R.,Ed.,2nd ed.,Marcel Dekker ,New York ,p.477.
- Taylor, S.W., Lange, C.R. and Lesold, E.A., 1997. Biofouling of Contaminated Ground-Water Recovery Wells: Characterization of Microorganisms. *Ground Water*, 35(6), pp.973-980.
- Tellam,J.H., Carlyle ,H.F., El-Ghonemy,H.,Parker,K.E.&Mrrchener, R.G.R.,2002. Towards quantification of ion exchange in a sandstone aquifer. In: Thangarajan, M., Singh, V.S., and Rai, (eds), *Sustainable development and management of groundwater resources in semi-arid regions with special reference to hard rocks*. Oxford & IBH Publishing C. Pvt. Ltd, New Delhi, 205-214.
- Thomas, N.E., Kan, K.T., Bray, D.I., MacQuarrie, K.T.B., 1994. Temporal changes in manganese concentrations in water from the Fredericton Aquifer, New Brunswick." *Ground Water* 32(4), 650-656.
- Tipping, E., 1981. Adsorption by goethite (α -FeOOH) of humic substances from three different lakes. *Chemical Geology*, 33(1), pp.81-89.

Skinner, H.C.W. and Fitzpatrick, R.W., 1992. Biomineralization, Processes of Iron and Manganese, Modern and Ancient Environments. Catena Verlag, Cremlingen- Destedt, Germany, pp. 101–114.

Torres, R., Blesa, M. A., & Matijević, E. ,1989. Interactions of metal hydrous oxides with chelating agents: VIII. Dissolution of hematite. Journal of colloid and interface science, 131(2), 567-579.

Tuccillo, M.E., Cozzarelli, I.M. and Herman, J.S., 1999. Iron reduction in the sediments of a hydrocarbon-contaminated aquifer. *Applied Geochemistry*, 14(5), pp.655-667.

Vaughan ,K ,Rabenhorst,M. And Needelman ,B. ,2009. Saturation and Temperature Effects on the Development of Reducing Conditions in Soils. Soil Sci. Soc. Am. J. 73:663-667.

Vepraskas, M.J., and. Sprecher S.W ., 1997. Overview of aquic conditions and hydric soils. p. 1–22. In M.J. Vepraskas and S.W. Sprecher (ed.) Aquic conditions and hydric soils: The problem soils. SSSA Spec. Publ. 50. SSSA, Madison, WI.

Viollier, E., Inglett, P.W., Hunter, K., Roychoudhury, A.N., and Van Cappellen, P. (2000) *The ferrozine method revisited: Fe(II)/Fe(III) determination in natural waters*. *Applied Geochemistry*, 15: pp. 785-790.

Wahid, P. A., and Kamalam, N. V.,1993. Reductive dissolution of crystalline and amorphous Fe (III) oxides by microorganisms in submerged soil. *Biology and fertility of soils*, 15(2), pp.144-148.

Weber, K.A., Achenbach, L.A. and Coates, J.D., 2006. Microorganisms pumping iron: anaerobic microbial iron oxidation and reduction. *Nature Reviews Microbiology*, 4(10), pp.752-764.

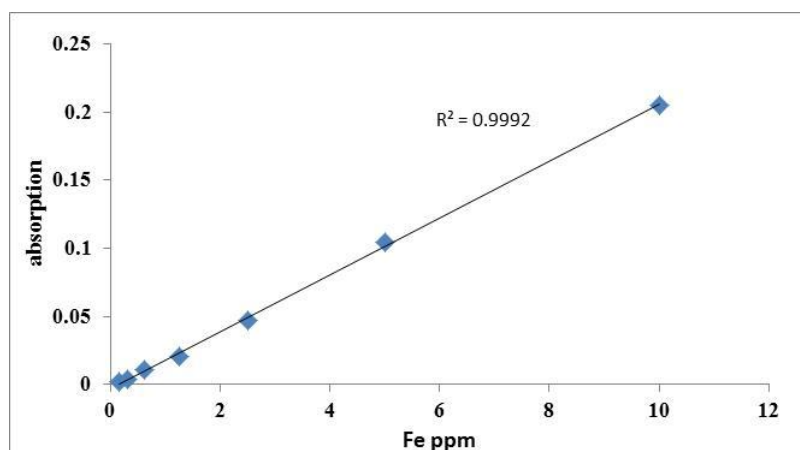
- Weng, H. X., Qin, Y. C., & Chen, X. H., 2007. Elevated iron and manganese concentrations in groundwater derived from the Holocene transgression in the Hang-Jia-Hu Plain, China. *Hydrogeology Journal*, 15(4), pp. 715-726.
- Zaw, M. and Chiswell, B., 1999. Iron and manganese dynamics in lake water. *Water Research*, 33(8), pp.1900-1910.
- Zinder, B., Furrer, G. and Stumm, W., 1986. The coordination chemistry of weathering: II. Dissolution of Fe (III) oxides. *Geochimica et Cosmochimica Acta*, 50(9), pp.1861-1869.
- Zsolnay, A., 1996. Dissolved humus in soil waters. In: Piccolo, A. (Ed.), *Humic Substances in Terrestrial Ecosystems*. Elsevier, Amsterdam, pp. 171– 223.
- Zumdahl, S.S. and Zumdahl, S.A., 2014. *Chemistry*, 20 Davis Drive, Belmont, CA 94002-3098. Brooks/Cole, Cengage Learning: USA. ISBN 13:978-1-133-61109-7.

Appendices

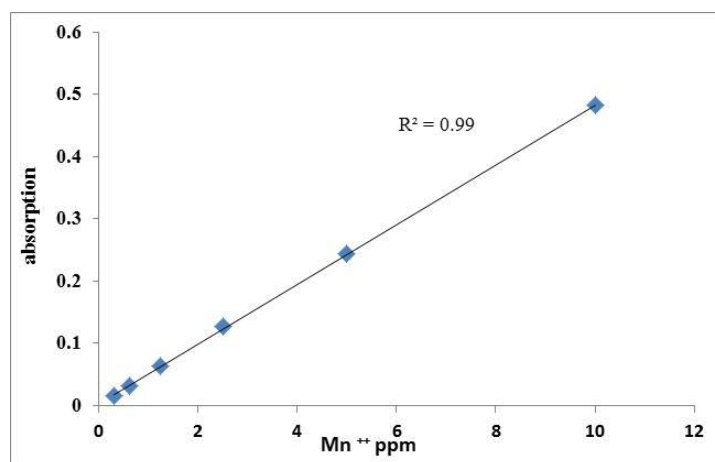
chapter 2

Appendix (2-1) Example calibration data for Fe and Mn using FAAS.

Concentration of Fe or Mn ⁺⁺ ppm	Absorption of iron	Absorption for Mn ⁺⁺
0.156	0.002166	
0.3125	0.003955	0.015559
0.625	0.011057	0.031865
1.25	0.020294	0.063479
2.5	0.046603	0.126799
5	0.10395	0.243912
10	0.205346	0.482276



Plot of [Fe] against the absorption using the FAAS machine



Plot of [Mn⁺⁺] against the absorption using the FAAS machine

Appendix (2-2) Iron released from 1 g sandstone using 10 mM ascorbic acid at 42 °C.

time h	Fe ppm	Fe mmol/l	volume in ml after took samples for each time
2	b.d.l	b.d.l	500
4	0.09	0.0016	495
6	0.088	0.0015	490
21	0.358	0.0064	485
26	0.432	0.0077	480
29	0.451	0.0080	475
45	0.615	0.0110	470
51	0.691	0.0123	465
75	1.202	0.0215	460
95	1.44	0.0257	455
116	2.15	0.0384	450
125	2.494	0.0446	445
142	2.757	0.0493	440
148	2.82	0.0504	435
169	3.057	0.0547	430
195	3.925	0.0702	425

Appendix (2-3) Fe and Mn⁺⁺ released from H₂A reactions with sandstone at different reaction temperatures and different storage conditions for the samples.

Reaction temperature Time h	50 °C Fe (1) Mg/l	50°C Fe (2) Mg/l	60 °C Fe (1) Mg/l	60°C Fe (2) Mg/l	75 °C Fe (1) Mg/l	75°C Fe (2) Mg/l	90 °C Fe (1) Mg/l	90°C Fe (2) Mg/l
24	0.546	0.489	0.987	0.968	1.774	1.608	2.981	2.621
25.5	0.547	0.471	1.096	1.130	1.821	1.671	3.032	2.676
27	0.555	0.541	1.117	1.148	1.928	1.724	3.119	2.729
28.5	0.561	0.494	1.152	1.173	1.966	1.797	3.177	2.846
30	0.622	0.594	1.17	1.211	2.043	1.882	3.274	2.941
31.5	0.625	0.576	1.266	1.303	2.14	1.992	3.384	3.048
33	0.672	0.589	1.345	1.342	2.259	2.099	3.445	3.143
Reaction temperature Time h	50 °C Mn ⁺⁺ (1) Mg/l	50°C Mn ⁺⁺ (2) Mg/l	60 °C Mn ⁺⁺ (1) Mg/l	60°C Mn ⁺⁺ (2) Mg/l	75 °C Mn ⁺⁺ (1) Mg/l	75°C Mn ⁺⁺ (2) Mg/l	90 °C Mn ⁺⁺ (1) Mg/l	90°C Mn ⁺⁺ (2) Mg/l
24	0.038	0.036	0.052	0.047			0.059	0.054
25.5	0.042	0.036	0.051	0.045	0.053	0.047	0.047	0.043
27	0.039	0.035	0.0493	0.044	0.055	0.047	0.049	0.046
28.5	0.040	0.037	0.0477	0.045	0.054	0.047	0.071	0.063
30	0.043	0.040	0.048	0.047	0.055	0.047	0.049	0.048
31.5	0.041	0.043	0.05	0.047	0.055	0.048	0.07	0.062
33	0.040	0.037	0.048	0.046	0.055	0.047		

Fe(1) sample storage at lab temperature , Fe(2) sample storage in the fridge (4 °C)

Appendix (2-4) Fe and Mn⁺⁺ released from reactions of different [H₂A] with sandstone at 60 C , without and with filtering.

	75 Mm H ₂ A					
	Without (F)	with (F)	% different between unfiltered and filtrate samples	without F	with F	% different between unfiltered and filtrate samples
time h	Fe ppm	Fe ppm		Mn ⁺⁺ ppm	Mn ⁺⁺ ppm	
1	0.5915	0.581	1.775	0.061	0.058	4.918
2	0.717	0.695	3.068	0.057	0.056	1.754
3	0.7875	0.774	1.714	0.0529	0.05	5.482
4	0.904	0.89	1.548	0.044	0.0415	5.681
5	0.9835	0.968	1.576	0.04	0.038	5.000
6	1.0725	1.059	1.258	0.044	0.04225	3.977
	50 Mm H ₂ A					
	Without (F)	with (F)	% different between unfiltered and filtrate samples	Without (F)	with (F)	% different between unfiltered and filtrate samples
time h	Fe ppm	Fe ppm		Mn ⁺⁺ ppm	Mn ⁺⁺ ppm	
1	0.449	0.439	2.227	0.04025	0.0403	-0.124
2	0.5395	0.531	1.575	0.0338	0.0358	-5.917
3	0.629	0.609	3.179	0.0785	0.079	-0.636
4	0.692	0.705	-1.878	0.0715	0.074	-3.496
5	0.7935	0.771	2.835	0.0724	0.07	3.314
6	0.837	0.832	0.597	0.06945	0.0709	-2.087
	25 Mm H ₂ A					
	Without (F)	with (F)	% different between unfiltered and filtrate samples	Without (F)	with (F)	% different between unfiltered and filtrate samples
time h	Fe ppm	Fe ppm		Mn ⁺⁺ ppm	Mn ⁺⁺ ppm	
1	0.2515	0.249	0.9940	0.0619	0.0609	1.615509
2	0.3840	0.382	0.5208	0.0605	0.057	5.785124
3	0.4525	0.451	0.3314	0.061	0.058	4.918033
4	0.5705	0.566	0.7887	0.056	0.055	1.785714
5	0.6375	0.626	1.8039	0.052	0.0489	5.961538
6	0.7250	0.717	1.1034	0.047	0.0469	0.212766

with (F)= measured the concentration of Fe or Mn⁺⁺ with filtration

Without (F)= measured the concentration of Fe or Mn⁺⁺ with filtration using 0.45 µm pore size syringe filter.

Appendix (2-5) The concentration of Fe released from 1 g mass sandstone using 500 ml of 1 and 0.75 mM H₂A at 20 and 80 °C.

time h	Fe ppm 1mM H ₂ A	Fe ppm 0.75mM H ₂ A	Fe ppm 1Mm H ₂ A	Fe ppm 1mM H ₂ A
	80 °C	80 °C	20 °C	20 °C
6.5	0.033535	0.002	0.0002	0
25.5	0.108626	0.018462	0.0001	0
47.5	0.152994	0.046664	0.000015	0
55.5	0.153212	0.047259	0.000415	0
72	0.178893	0.050157	0.00004	0.0063

Appendix(2-6 A) Fe released from two replicates (without and with filtering) following reaction of 1,5 and 10 g mass sandstone for 163 to 400 hours with 10Mm[H₂A] at 80 °C.

Samples No.	Filtration using 0.2 µm	time (h)	Iron ppm		
			1g sst	5 g sst	10 g sst
1	NO	163	6.197	14.919	17.863
	Yes	163	5.956	15.203	18.23
2	NO	187	6.195	15.069	18.514
	Yes	187	5.923	15.436	18.529
3	NO	235	6.162	16.083	19.596
	Yes	235	6.091	15.755	18.884
4	NO	259	6.394	16.57	20.034
	Yes	259	6.029	15.788	19.319
5	NO	338	6.701	17.594	20.74
	Yes	338	6.317	16.894	20.059
6	NO	362	6.629	16.674	22.464
	Yes	362	6.421	17.072	21.876
7	NO	378	6.383	17.104	22.638
	Yes	378	6.575	16.722	22.716
8	NO	400	6.801	17.595	26.496
	Yes	400	6.65	17.343	25.976

Appendix (2-6 B) Amount of Mn^{++} released from two replicates (without and with filtering) from reaction of 1,5 and 10 g mass sandstone for 163 to 400 hours with 10Mm[H₂A] at 80 °C.

Samples No.	Filtration using 0.2 µm	time (h)	1g sst	5 g sst	10 g sst
			ppm		
1	NO	163	0.162	0.563	1.021
	Yes	163	0.148	0.616	1.024
2	NO	187	0.154	0.584	1.046
	Yes	187	0.159	0.58	0.955
3	NO	235	0.153	0.65	1.138
	Yes	235	0.173	0.589	1.03
4	NO	259	0.175	0.628	0.977
	Yes	259	0.159	0.583	1.079
5	NO	338	0.169	0.617	1.089
	Yes	338	0.161	0.621	1.09
6	NO	362	0.178	0.624	1.115
	Yes	362	0.174	0.577	1.072
7	NO	378	0.175	0.62	1.099
	Yes	378	0.158	0.573	1.047
8	NO	400	0.175	0.614	0.998
	Yes	400	0.179	0.611	1.096

Appendix (2-7) Amount of iron released from reaction of 1g mass sandstone and 10mM[H₂A] at 90°C

Condition	without filtration	filter by 0.2µm	Acidification of samples by HNO ₃	%different of without and with filter samples	% different between acidification and without acidification samples
Time h	Fe' ppm	Fe ppm	Fe ppm		
19.66	2.133	1.925	2.347	9.75	9.12
41	3.517	3.347	3.645	4.83	3.51
48.5	3.768	3.683	3.977	2.26	5.26
64.5	4.34	4.262	4.674	1.80	7.15

Appendix (2-8) Amount of Fe and Mn⁺⁺ released from reaction of 1g sandstone and 10 mM[H₂A] under aerobic and anaerobic conditions at 21 °C.

time	Fe mg/l anaerobic	Mn ⁺⁺ ppm anaerobic	Fe ppm aerobic	Mn ⁺⁺ ppm aerobic
98	0.429	0.012	0.178	b.d.l
121.5	0.32	0.01	0.209	b.d.l
145.5	0.368	0.045	0.231	b.d.l
168	0.484	0.115	0.259	b.d.l
193.5	0.522	0.107	0.28	b.d.l

Appendix (2-9) Variation of dissolved oxygen concentrations versus time for deionised water with sandstone, and ascorbic acid with and without sandstone for 17 h of monitoring.

Time h	Dissolved oxygen (D.O.) ppm			%the different between (H ₂ A) - (H ₂ A+sst)	Temperature
	DIW+sst	H ₂ A	H ₂ A+sst		
0.0	8.20	8.2	8.16	0.48	21
1.0	8.17	8.2	8.10	1.21	22
2.6	8.08	8.02	7.95	0.87	21
3.2	8.07	8.02	7.90	1.49	21
9.8	7.50	6.75	5.97	11.55	21
13.8	7.50	6.50	5.99	7.84	21
16.8	7.50	6.40	5.75	10.15	21

DIW+sst= deionised water +sandstone, H₂A+sst= ascorbic acid +sandstone , H₂A= ascorbic acid alone

Appendix (2-10) Dissolved oxygen concentration versus time for deionised water with sandstone, and ascorbic acid with and without sandstone for 71 h of monitoring.

time hr	H ₂ A+sst	H ₂ A	Diw +sst	%the different between (H ₂ A) - (H ₂ A+sst)
0	8.46	8.55	8.54	1.05
1	8.3	8.43	8.54	1.54
2	8.12	8.29	8.52	2.05
3	7.91	8.12	8.43	2.58
4	7.66	7.96	8.36	3.76
5	7.41	7.81	8.26	5.12
22	5.51	6.51	7.9	15.36
24	5.56	6.39	7.8	12.98
27	5.6	6.22	7.55	9.96
50	5.55	5.46	6.65	-1.64
71	5.06	5.32	7.11	4.88

DIW+sst= deionised water +sandstone, H₂A+sst= ascorbic acid +sandstone, H₂A= ascorbic acid alone

Appendix (2-11) Dissolved oxygen concentration versus time for deionised water with sandstone, and ascorbic acid with and without sandstone for 30 h of monitoring.

time h	DIW+sst	Temperature °C	[H ₂ A]	Temperature °C	[H ₂ A]+sst	Temperature °C	%the different between (H ₂ A+sst)- (H ₂ A)
0	7.82	24.3	7.56	24.3	7.66	24.3	1.30
0.6	7.84	24.9	7.19	25	7.54	24.8	4.64
1.6	7.88	23.6	6.55	23.8	6.97	23.6	6.02
2.6	7.95	23	5.98	23.2	6.36	23	5.97
3.6	7.97	22.7	5.4	22.8	5.77	22.6	6.41
4.6	8.04	22.4	4.89	22.6	5.19	22.4	5.78
5.6	8	22.9	4.38	22.3	4.7	22.5	6.80
6.6	8.05	22.3	3.93	22.2	4.22	22.1	6.87
7.6	8.08	23.3	3.68	22.1	3.94	22.3	6.59
23.1	8.3	21	2.95	21.2	3.83	21	22.97
28.8	8.29	21.8	2.89	21.4	4.01	21.3	27.93
29.8	8.29	21.3	3.09	21.3	4.21	21.3	26.60

DIW+sst= deionised water +sandstone

H₂A+sst= ascorbic acid +sandstone

Appendix (2-12) Concentration of iron and TOC for 10 mM[H₂A] with 1 g sst at 50 and 90 °C .

Time h	iron Fe mg/l	TOC mg/l for H ₂ A+sst	TOC mg/l for H ₂ A	iron Fe mg/l	TOC mg/l for H ₂ A+sst	TOC mg/l for H ₂ A
	Temperature 50	Temperature 50		Temperature 90	Temperature 90	
24	0.546	726.88	730.95	3.032	703.89	738.76
25.5	0.547	720.47	745.25	3.119	707.52	719.95
27	0.555	719.95	711.26	3.176	698.72	707.85
28.5	0.561	720.28	707.85	3.273	705.93	715.66
30	0.622	714.23	711.59	3.383	684.09	732.6
31.5	0.625	716.32	713.68	3.445	698.61	716.87
33	0.672	716.76	724.68	3.559	688.49	700.37

Appendix (2-13) Fe and Mn⁺⁺ concentrations as a function of H₂A concentration at lab temperature(20 °C). 10 g sandstone with 0.04 l of H₂A solutions, shaken for 2 hours.

[H ₂ A] ppm	Filtration	Without Filtration	Filtration	Without Filtration
	Mn ⁺⁺ ppm		Fe ppm	
100	1.413	1.441	0.382	0.430
40	1.056	1.052	0.097	0.110
20	0.900	0.883	0.050	0.000
10	0.713	0.708	0.000	0.000

Table (2-14) Amount of iron and Mn⁺⁺ released with and without shaking after 4h reaction between 0.04 l of different [H₂A] with 10 g sandstone.

	Mn ⁺⁺ ppm	Mn ⁺⁺ ppm	Fe ppm	Fe ppm	times Mn(S) >Mn	times Fe(S) >Fe
	Yes	No	yes	No		
Shaking [H ₂ A]						
10	1.007	0.245	0.204	-0.099	4.0	
20	1.115	0.260	0.327	0.050	4.25	6.5
40	1.304	0.433	0.519	0.073	3.0	7.0
100	1.812	0.562	1.098	0.210	4.25	5.25

Fe(S)=concentration of iron after shaking , Fe= concentration of iron without shaking

Appendix (2-15) Amount of Mn⁺⁺ and Fe released from sandstone under two situations. First condition shaking under lab temperature and second condition higher temperature without shaking.

[H ₂ A] ppm	Shaking under 20 °C	Without shaker under 73°C	Shaking under 20 °C	Without shaker under 73°C
	Mn ⁺⁺	Mn ⁺⁺	Fe	Fe
10	0.997	0.556	0.04	b.d.l
20	1.176	0.518	0.117	b.d.l
30	1.345	0.898	0.284	b.d.l
40	1.480	1.243	0.432	0.111
100	2.195	1.822	0.489	0.176

Appendix (2- 16) Amount of Fe and Mn⁺⁺ released from 10 g sandstone using inorganic acid (HCl) and organic acid (ascorbic acid) after 4 h gently shaking.

[H ₂ A] ppm	Fe	Mn	pH after acidification	HCl (M)	Fe	Mn	Initial pH
100	1.036	2.073	2.41	2	15.91	5.072	0.02
75	0.704	1.922	2.38	1	12.1	4.728	0.12
50	0.445	1.566	2.36	0.5	9.016	4.467	0.34
25	0.14	1.188	2.37	0.25	5.137	3.799	0.60
0	0	0.762	2.09	0.1	2.792	1.981	1.02
0	0	0.724	2.06	0.1	2.791	1.968	1.04
				0.05	2.650	1.057	1.37
				0.05	2.657	1.057	1.4
				0.025	2.281	0.368	1.65
				0.025	2.233	0.310	1.68
				0.0125	2.050	0.267	2.03
				0.0125	2.071	0.269	2.05
				0.00625	1.706	0.044	2.43
				0.00625	1.681	0.037	2.44
				0	0.318	0.000	4.92
				0	0.320	0.000	5.03

Appendix (2-17) the release of Fe and Mn⁺⁺ using very dilute HCl. b.d.l. = below detection limit.

[HCl](Mm)	Fe ppm	Mn ⁺⁺ ppm	pH After interaction with sst	Initial pH
0.162	b.d.l	0.929	4.92	3.84
0.162	b.d.l	0.908	4.84	3.84
0.00064	b.d.l	0.860	5.04	4.73
0.00064	b.d.l	0.882	5.08	4.73

Appendix (2-18) Amount of iron and Mn released from 10 g sandstone under unwashed and acid washed (12.5 mM HCl) conditions.

[H ₂ A] ppm	Mn ⁺⁺ ppm		Fe ppm		pH after acidification and separated from sediment	
	washing	unwashed	washing	unwashed	wishing	unwashed
100	1.821	2.903	3.026	0.990	2.12	2.14
75	1.686	2.666	2.356	0.619	2.11	2.15
50	1.445	2.262	1.286	0.422	2.1	2.13
25	1.154	1.846	0.918	0.149	2.13	2.09
15	0.860	1.436	0.191	0	2.1	2.13
0	0.542	0.748	b.d.l	b.d.l	2.14	2.12

Appendix (2-19) amount of iron and Mn^{++} released from 10 g sandstone unwashed and dilute HCl - washed sandstone by ascorbic acid .

[H ₂ A] ppm	Unwashed sandstone			H ₂ A ppm	Washed sandstone by diluted HCl		
	Mn	Fe	pH		Mn	Fe	pH
100	3.159	1.429	4.75	91.25	0.954	1.529	3.88
100	3.262	1.507	4.73	91.25	1.097	1.458	3.76
75	2.541	0.859	4.77	68.43	0.981	1.243	3.75
75	2.842	0.937	4.76	68.43	1.153	1.030	3.89
50	2.398	0.435	4.86	45.62	0.858	0.674	3.81
50	2.663	0.489	4.83	45.62	0.845	0.634	3.82

Appendix (2-20) Concentration of iron and Mn in the washing supernatants for, HCl , and for first and second washing by DIW .

Washing samples	Fe ppm	Mn ⁺⁺ ppm	pH
Diluted HCl(1)	b.d.l	2.902	2.03
Diluted HCl(1)	b.d.l	2.836	2.05
Diluted HCl(1)	b.d.l	2.939	2.04
Diluted HCl(1)	b.d.l	2.780	2.06
First washed 1	b.d.l	0.349	2.76
First washed 2	b.d.l	0.396	2.74
First washed 3	b.d.l	0.364	2.77
Second washed 1	b.d.l	b.d.l	3.43
Second washed 2	b.d.l	b.d.l	3.46
Second washed 3	b.d.l	b.d.l	3.55
Second washed 4	b.d.l	b.d.l	3.51

Appendix (2-21) Amount of iron and Mn released from 10 g sst unwashed and washed sst by calcium chloride

[H ₂ A] ppm	Fe ppm		Mn ⁺⁺ ppm		pH	
	unwashed	washed by CaCl ₂	unwashed	washed by CaCl ₂	Unwashed	Washed
100	1.448	0.128	2.463	0.473	4.82	5.06
100	1.369	0.054	2.612	0.529	4.83	5.11
75	0.882	0.000	2.350	0.300	4.88	5.28
75	0.868	0.000	2.384	0.272	4.89	5.21
50	0.374	0.000	1.991	0.103	5.05	5.32
50	0.352	0.000	2.002	0.193	4.99	5.35

Appendix (2-22) Amount of iron and Mn^{++} released from different washing stages for sandstone samples

Washing samples	Fe ppm	Mn ⁺⁺ ppm	pH
CaCl ₂ (1)	b.d.l	2.325	4.8
CaCl ₂ (2)	b.d.l	2.380	4.82
CaCl ₂ (3)	b.d.l	2.322	4.72
First washing(1)	b.d.l	0.304	5.05
First washing(2)	b.d.l	0.291	5.08
First washing(3)	b.d.l	0.322	5.09
Second washing (1)	b.d.l	b.d.l	5.38
Second washing(2)	b.d.l	b.d.l	5.34

Chapter 3

Appendix (3-1) Phreeqc model for dissolution of KMnO₄ in water at different pHs under equilibrium conditions

pH	Mn(2) Mol/kg H ₂ O	Mn(7) Mol/kg H ₂ O	Cl Mol/kg H ₂ O	Mn total Mol/kg H ₂ O	Mn(7)/Mn	log(Mn(7)/Mn)
3.2	6.86E-04	1.70E-18		6.86E-04	2.48E-15	-14.60587519
4	6.86E-04	4.20E-16		6.86E-04	6.12E-13	-12.21307483
5	6.82E-04	4.20E-13		6.82E-04	6.16E-10	-9.210535085
7	6.86E-04	4.20E-07		6.86E-04	6.12E-04	-3.213340639
8	4.88E-04	1.98E-04		6.86E-04	2.89E-01	-0.539658925
8.5	1.24E-04	5.61E-04		6.85E-04	8.19E-01	-0.08672771
8.6	5.30E-05	6.32E-04	1.56E-04	6.85E-04	9.23E-01	-0.034973493
8.8	not converged					

Appendix (3-2) Absorbance of pure KMnO₂ at different pHs.

Samples of KMno4	ml	0.5 HNO ₃ (μl)	76.25 Mm NaOH (μl)	pH	R ₁	R ₂	R ₃	Average absorbance	% difference *
1	10	0	0	6.68	1.435	1.433	1.43	1.433	0.00
2	10	0	0	6.49	1.44	1.442	1.443	1.442	0.00
3	10	5	0	3.46	1.442	1.44	1.437	1.440	0.14
4	10	10	0	3.12	1.44	1.44	1.439	1.440	0.14
5	10	15	0	2.89	1.435	1.436	1.436	1.436	0.42
6	10	20	0	2.78	1.426	1.421	1.421	1.423	1.32
7	10	0	5	7.08	1.428	1.431	1.427	1.429	0.90
8	10	0	10	8.81	1.431	1.43	1.427	1.429	0.86
9	10	0	15	9.79	1.429	1.427	1.426	1.427	0.99
10	10	0	20	10.06	1.428	1.428	1.426	1.427	0.99

*%difference of absorbance percentage between the absorbance of KMnO₄ without any addition of acid or base and the absorbance of KMnO₄ after adding tiny drops of nitric acid or NaOH. R₁ to R₃ are repeat measurements of absorbance.

Appendix (3-3) The absorbance of different [KMnO₄] ranging from 20 to 200 ppm

[KMnO ₄] ppm	Absorbance at 530nm			
	abs1	abs2	abs3	average
200	2.795	2.795	2.795	2.795
180	2.508	2.508	2.508	2.508
160	2.207	2.207	2.207	2.207
140	1.896	1.896	1.896	1.896
120	1.583	1.583	1.583	1.583
100	1.271	1.271	1.271	1.271
80	1.263	1.263	1.263	1.262
60	0.949	0.949	0.949	0.949
40	0.634	0.634	0.634	0.634
20	0.318	0.318	0.318	0.318

Appendix (3-4) the results of measuring H₂A using 100 ppm KMnO₄ and using 40 ppm KMnO₄

[H ₂ A] ppm	100 KMnO ₄	40 KMnO ₄	Colour of mixture using 40 ppm KMnO ₄	Colour of mixture using 100 ppm KMnO ₄
	Average absorbance			
100	0.193	-0.096	colourless	colourless
80	0.288	-0.080	colourless	Very pale yellow
60	0.395	-0.069	colourless	Pale yellow
40	0.485	0.029	pale yellow	Dark yellow
20	0.568	0.122	pink	Pink
0	0.665	0.214	pink	Pink

Appendix (3-5a) Absorbance of 40 ppm of KMnO₄ containing different levels of ferric iron

Fe(III) ppm	Absorbance at 530nm				average	Different of absorbance from blank
	R ₁	R ₂	R ₃	R ₄		
0*	0.338	0.338	0.339	0.34	0.339	-0.332
0*	0.342	0.342	0.341	0.339	0.341	0.330
20	0.340	0.340	0.339	0.340	0.340	-0.037
10	0.341	0.343	0.339	0.342	0.341	0.403
8	0.343	0.341	0.343	0.342	0.342	0.694
6	0.342	0.342	0.341	0.343	0.342	0.621
4	0.342	0.343	0.343	0.344	0.343	0.911
2	0.342	0.342	0.343	0.341	0.342	0.621

*zero ppm of ferric iron (considered blank or control samples)

Appendix (3-5b) Absorbance of 100 ppm of KMnO_4 containing different levels of ferric iron

Fe ppm	R_1	R_2	R_3	average	% different on compare with zero iron	Just iron solution		After adding KMnO_4	
						ph	Eh	Eh	Eh
10	0.663	0.658	0.66	0.660	0.707	2.57	273.4	2.87	254.7
5	0.659	0.658	0.659	0.659	0.455	2.62	260.3	3.08	241.6
3.5	0.663	0.661	0.661	0.662	0.907	2.83	247.7	3.34	226.2
2.5	0.663	0.662	0.66	0.662	0.907	3.06	242.4	3.43	220.4
1.25	0.66	0.66	0.658	0.659	0.556	3.29	272.2	3.62	206.1
0	0.657	0.657	0.656	0.657	0.152	4.7	132.9	4.69	148.9
0	0.655	0.654	0.655	0.655	-0.153	4.8	134.6	4.89	151.2

Appendix (3-6) The absorbance of different $[\text{H}_2\text{A}]$ in absence and presence of 4 ppm of Fe(III) .

H_2A ppm	Absorbance		% different
	0 ppm Fe^{+++}	4 ppm Fe^{+++}	
90	0.257	0.252	2.09
80	0.302	0.308	-1.75
60	0.414	0.403	2.64
40	0.480		
20	0.570	0.558	2.12
0	0.660	0.660	-0.01

Appendix (3-7) Absorbance of KMnO_4 in presence of different $[\text{FeII}]$

Ferrous iron Fe(II) ppm	Absorbance				% difference, absent and present FeII
	R_1	R_2	R_3	average	
0	0.540	0.540	0.541	0.540	
0	0.540	0.541	0.541	0.541	-0.03
0.321	0.538	0.537	0.537	0.537	0.59
0.625	0.536	0.536	0.536	0.536	0.83
1.25	0.529	0.530	0.530	0.530	2.00
2.5	0.522	0.521	0.522	0.522	3.48
5	0.515	0.510	0.515	0.513	5.03
10	0.452	0.453	0.453	0.453	16.25

Appendix (3-8) Method to prepare different [H₂A] solutions containing 4 and 1 ppm of ferrous iron (Fe)

Fe ⁺⁺ ppm concentration	Fe ⁺⁺ ppm volume ml	H ₂ A ppm concentration	H ₂ A ppm volume ml	desire solution mix	total volume volume ml
40	10	100	90	90 H ₂ A + 4 Fe ppm	100
20	20	100	80	80 H ₂ A + 4 Fe ppm	100
10	40	100	60	60 H ₂ A + 4 Fe ppm	100
5	80	100	20	20 H ₂ A + 4 Fe ppm	100
100	4	0	0	0 H ₂ A +4 Fe ppm	100
10	10	100	90	90 H ₂ A + 1 Fe ppm	100
5	20	100	80	80 H ₂ A + 1 Fe ppm	100
2.5	40	100	60	60 H ₂ A + 1 Fe ppm	100
1.25	80	100	20	20 H ₂ A + 1 Fe ppm	100
100	1	0	0	0 H ₂ A + 1 Fe ppm	100

Appendix (3-9) Absorbance after adding 1 and 4 ppm of Fe⁺⁺ to H₂A

[H ₂ A] ppm	Absorbance 0 ppm Fe	Absorban ce Fe 4 ppm	Absorban ce Fe 1 ppm	% different of absorbance with 4 ppm Fe	% different of absorbance with 1 ppm Fe	apparent H ₂ A 0 ppm Fe ⁺⁺	apparent [H ₂ A](ppm) 4 ppm Fe ⁺⁺	apparent [H ₂ A](ppm) 1 ppm Fe ⁺⁺
90	0.164	0.176	0.162	7.11	-1.22	91.10	88.42	91.56
80	0.217	0.227	0.216	4.60	-0.61	78.83	76.53	79.14
60	0.319	0.314	0.315	-1.46	-1.15	55.53	56.60	56.37
40	0.368	0.377		2.63		44.26	42.03	
20	0.464	0.466	0.467	0.43	0.79	22.18	21.72	21.34
0	0.568	0.553	0.561	-2.70	-1.23	-1.89	1.63	-0.28

Appendix (3-10) pH of various H₂A solutions before and after adding KMnO₄ in the presence and absence of ferrous iron

samples	before add KMnO ₄	After add KMnO ₄
	pH	pH
90 H ₂ A	3.74	4.28
80 H ₂ A	3.72	4.34
60 H ₂ A	3.87	4.49
40 H ₂ A	4.04	4.67
20 H ₂ A	4.4	4.8
0 H ₂ A	5.61	
90 H ₂ A +4Fe	3.74	3.82
80 H ₂ A +4Fe	3.74	3.83
60 H ₂ A +4Fe	3.97	4.16
20 H ₂ A +4Fe	4.21	4.26
0 H ₂ A +4Fe	4.86	4.13
90 H ₂ A +1Fe	3.75	3.94
80 H ₂ A +1Fe	3.81	4.01
60 H ₂ A +1Fe	3.92	4.14
20 H ₂ A +1Fe	4.42	4.55
0 H ₂ A + 1Fe	4.99	4.88

Appendix (3-11) effect of presence of [Mn⁺⁺] on the absorbance of KMnO₄.

[Mn ⁺⁺] ppm	R ₁	R ₂	R ₃	average	% of absorbance increase
10	0.576	0.577	0.576	0.576	22.10
5	0.513	0.513	0.514	0.513	8.76
2.5	0.487	0.485	0.486	0.486	2.97
1.25	0.481	0.48	0.48	0.480	1.77
0.625	0.475	0.474	0.473	0.474	0.42
0	0.471	0.473	0.472	0.472	0.00

Appendix (3-12) Preparation of various solutions containing different concentrations of ascorbic acid and Mn^{++} .

[Mn]ppm	Mn ppm	[H ₂ A] ppm	AA ppm	desire solution	total volume
	volume (ml)		volume (ml)	mix	volume (ml)
40	10	100	90	90 H ₂ A + 4 Mn ppm	100
20	20	100	80	80 H ₂ A + 4 Mn ppm	100
10	40	100	60	60 H ₂ A + 4 Mn ppm	100
5	80	100	20	20 H ₂ A + 4 Mn ppm	100
100	4	0	0	0 H ₂ A + 4 Mn ppm	100
10	10	100	90	90 H ₂ A + 1 Mn ppm	100
5	20	100	80	80 H ₂ A + 1 Mn ppm	100
2.5	40	100	60	60 H ₂ A + 1 Mn ppm	100
1.25	80	100	20	20 H ₂ A + 1 Mn ppm	100
100	1	0	0	0 H ₂ A + 1 Mn ppm	100

Appendix (3-13) Average absorbance of ascorbic acid in absence and presence of 1 and 4 ppm of Mn^{++}

[H ₂ A] ppm	Absorbance		
	0 ppm Mn	4 ppm Mn	1 ppm Mn
90	0.246	0.268	0.252
80	0.273	0.301	0.283
60	0.337	0.357	0.341
40	0.375	0.418	
20	0.412	0.434	0.421
0	0.469	0.510	0.479

Appendix (3-14) pH of various H₂A solutions before and after adding KMnO₄

samples	before add KMnO ₄	after KMnO ₄		Samples	before add KMnO ₄	after KMnO ₄		Samples	before add KMnO ₄	after KMnO ₄
	pH	pH			pH	pH			pH	pH
90 H ₂ A +4 Mn	3.81	3.84		90 H ₂ A +1 Mn	3.82	3.95		90 H ₂ A	3.81	4.0
80 H ₂ A +4 Mn	3.82	3.83		80 H ₂ A +1 Mn	3.81	4.2		80 H ₂ A	3.8	4.07
60 H ₂ A +4 Mn	3.93	3.9		60 H ₂ A +1 Mn	3.94	4.31		60 H ₂ A	3.88	4.2
20 H ₂ A +4 Mn	4.21	3.97		20 H ₂ A +1 Mn	4.14	4.27		20 H ₂ A	4.31	4.39
0 H ₂ A +4 Mn	5.67	4.12		0 H ₂ A +1 Mn	5.66	4.81		0 H ₂ A	5.47	5.34

Table (3-15) Absorbance of H₂A under oxic and anoxic conditions for different times.

	4.5 h	4.5 h	28 h	28 h	52 h	52 h	126 h	126 h
H ₂ A ppm	oxic	anoxic	oxic	anoxic	oxic	anoxic	oxic	anoxic
100	0.3097	0.3133	0.3193	0.3317	0.3196	0.3777	0.3206	0.4610
80	0.4100	0.4163	0.4113	0.4237	0.4083	0.4353	0.4320	0.4580
60	0.5087	0.5137	0.5083	0.5077	0.5133	0.5170	0.5184	0.5240
40	0.5883	0.5917	0.5877	0.5947	0.5967	0.5990	0.6030	0.6197
20	0.6783	0.6763	0.6787	0.6807	0.6890	0.6850	0.6970	0.6950
0	0.7680	0.7763	0.7687	0.7623	0.7597	0.7697	0.7633	0.7653

Chapter 4

Appendix (4-1) Absorbance of standard ascorbic acid solutions for sorption experiment (E1) using 20 g sandstone.

AA ppm	ab1	ab2	ab3	average
40	0.2233	0.2233	0.2266	0.224
30	0.2865	0.2832	0.2935	0.288
20	0.3343	0.3385	0.3385	0.337
10	0.3787	0.3881	0.3801	0.382
5	0.4059	0.4077	0.4077	0.407
2.5	0.4262	0.4262	0.4294	0.427
SLOPE	-191.892			
Intercept	83.988			

ab = absorbance for repeat measurements 1 to 3.

Appendix (4-2) Absorbance of samples (H₂A+SST) using 20 g sandstone , and various [H₂A] (E₁)

samples H ₂ A ppm	ab1	ab2	ab3	average	C ₁ ppm	C ₀ ppm	Mass g	C ₁ after correction* ppm	Sorbed S(mg/g)
30	0.339	0.338	0.342	0.340	18.80	30	20	17.33	0.026
30	0.336	0.336	0.336	0.336	19.47	30	20	17.99	0.025
25	0.359	0.363	0.362	0.361	14.63	25	20	13.16	0.024
25	0.363	0.363	0.365	0.364	14.17	25	20	12.69	0.025
20	0.381	0.378	0.386	0.382	10.75	20	20	9.28	0.022
20	0.384	0.384	0.384	0.384	10.32	20	20	8.85	0.023
15	0.389	0.389	0.394	0.391	8.94	15	20	7.47	0.015
15	0.388	0.398	0.395	0.393	8.49	15	20	7.02	0.016
10	0.408	0.407	0.407	0.407	5.86	10	20	4.39	0.011
10	0.411	0.406	0.408	0.408	5.63	10	20	4.15	0.012
diw	0.430	0.430	0.429	0.430	1.53	0	20	0.06	-0.0001
diw	0.430	0.431	0.430	0.430	1.41	0	20	-0.06	0.0001

* for DIW concentrations

Appendix (4-3) Absorbance of samples (H_2A +sst) using 15 g sandstone, and various $[H_2A]$ (E_2)

samples H_2A ppm	Ab1	Ab2	Ab3	average	C_1	C_0	Mass g	C_1 after correction* ppm	Sorbed S(mg/g)
30	0.2786	0.2753	0.2786	0.2775	19.713	30	15	18.0793	0.031789
30	0.2786	0.2786	0.2786	0.2786	19.494	30	15	17.86036	0.032372
25	0.2819	0.2898	0.2898	0.2871	17.789	25	15	16.15526	0.023586
25	0.2858	0.2931	0.2931	0.2906	17.092	25	15	15.45863	0.025444
20	0.302	0.302	0.3053	0.3031	14.618	20	15	12.98392	0.01871
20	0.3095	0.3095	0.3095	0.3095	13.344	20	15	11.71008	0.022106
15	0.3254	0.3254	0.3212	0.324	10.458	15	15	8.824025	0.016469
15	0.3286	0.3254	0.3286	0.3275	9.754	15	15	8.120757	0.018345
10	0.3506	0.3506	0.3462	0.3491	5.455	10	15	3.821533	0.016476
10	0.3538	0.3494	0.3494	0.3508	5.110	10	15	3.476533	0.017396
diw	0.3707	0.3676	0.3707	0.3696	1.368	0	15	-0.26538	0.000708
diw	0.369	0.368	0.364	0.3670	1.899	0	15	0.265384	-0.00071

* for DIW concentrations

Appendix (4-4) Absorbance of standard ascorbic acid solutions at the beginning and the end of sorption experiment (E_3)

H_2A ppm	In the beginning of experiment			average	In the end of experiment			average	Different % of absorbance
	ab1	ab2	ab3		ab1	ab2	ab3		
20	0.572	0.571	0.573	0.572	0.575	0.578	0.578	0.572	0.87
40	0.489	0.487	0.488	0.488	0.494	0.495	0.494	0.488	1.29
60	0.399	0.397	0.396	0.3973	0.404	0.402	0.4	0.397	1.17
80	0.296	0.291	0.289	0.292	0.302	0.297	0.295	0.292	2.05
100	0.214	0.209	0.207	0.21	0.202	0.202	0.198	0.210	-4.44
120	0.083	0.077	0.067	0.0756	0.082	0.075	0.072	0.076	0.88

% different of absorbance between first and last measurement

Appendix (4-5) Results of sorption experiment (E₃) with different concentrations of H₂A with a fix mass of sandstone (10g).

Samples No.	[H ₂ A] ₀ ppm	average absorbance	[H ₂ A] _t	[H ₂ A] ₀ - [H ₂ A] _t ppm	sorbed mg/g	% difference*
1	120	0.168	106.504	13.496	0.054	11.25
2	120	0.168	106.574	13.426	0.054	11.19
3	100	0.347	68.880	31.120	0.124	31.12
4	100	0.345	69.440	30.560	0.122	30.56
5	80	0.408	56.058	23.942	0.096	29.93
6	80	0.418	54.096	25.904	0.104	32.38
7	60	0.480	40.994	19.006	0.076	31.68
8	60	0.483	40.434	19.566	0.078	32.61
9	40	0.553	25.580	14.420	0.058	36.05
10	40	0.555	25.160	14.840	0.059	37.10
11	20	0.624	10.657	9.343	0.037	46.72
12	20	0.621	11.357	8.643	0.035	43.21

[H₂A]₀ = initial concentration of ascorbic acid

[H₂A]_t = concentration of ascorbic acid after 2 h reaction with sandstone

Difference % = ([H₂A]₀ - [H₂A]_t) / initial [H₂A]₀ / 100

Appendix (4-6 a) Absorbance and drift-corrected absorbance according to the order of samples in the analysis for sorption experiment (E₄)

Standard	First av A	Last av A	delA	1	2	3	4	5	6	7	8	9	10
40	0.079	0.095	-0.016	0.063	0.071	0.074	0.075	0.076	0.076	0.077	0.077	0.077	0.077
30	0.125	0.145	-0.020	0.106	0.115	0.119	0.120	0.121	0.122	0.122	0.123	0.123	0.123
25	0.143	0.166	-0.023	0.121	0.132	0.136	0.137	0.139	0.139	0.140	0.140	0.141	0.141
20	0.172	0.188	-0.016	0.156	0.164	0.166	0.168	0.168	0.169	0.169	0.170	0.170	0.170
15	0.188	0.202	-0.014	0.175	0.181	0.184	0.185	0.185	0.186	0.186	0.186	0.187	0.187
10	0.203	0.221	-0.018	0.185	0.194	0.197	0.199	0.199	0.200	0.200	0.201	0.201	0.201
5	0.223	0.238	-0.015	0.208	0.216	0.218	0.219	0.220	0.221	0.221	0.221	0.221	0.222
3	0.233	0.251	-0.018	0.216	0.224	0.227	0.229	0.230	0.230	0.231	0.231	0.231	0.231
			Slope	-240.905	-243.193	-243.895	-244.235	-244.434	-244.566	-244.659	-244.728	-244.782	-244.825
			Intercept	55.401	57.850	58.665	59.072	59.316	59.479	59.595	59.682	59.750	59.804
			r2	0.99	0.99	0.99	0.99	0.99	0.99	0.99	0.99	0.99	0.99

Appendix (4-6 b) Absorbance and drift-corrected absorbance according to the order of samples in the analysis for sorption experiment (E₄) (continued)

Standard	First av A	Last av A	delA	11	12	13	14	15	16	17	18	19	20
40	0.079	0.095	-0.016	0.078	0.078	0.078	0.078	0.078	0.078	0.078	0.078	0.078	0.078
30	0.125	0.1445	-0.0195	0.123	0.123	0.124	0.124	0.124	0.124	0.124	0.124	0.124	0.124
25	0.143	0.1655	-0.0225	0.141	0.141	0.141	0.141	0.142	0.142	0.142	0.142	0.142	0.142
20	0.1715	0.1875	-0.016	0.170	0.170	0.170	0.170	0.170	0.171	0.171	0.171	0.171	0.171
15	0.188	0.2015	-0.0135	0.187	0.187	0.187	0.187	0.187	0.187	0.187	0.187	0.187	0.187
10	0.203	0.221	-0.018	0.201	0.202	0.202	0.202	0.202	0.202	0.202	0.202	0.202	0.202
5	0.223	0.238	-0.015	0.222	0.222	0.222	0.222	0.222	0.222	0.222	0.222	0.222	0.222
2.5	0.233	0.2505	-0.0175	0.231	0.232	0.232	0.232	0.232	0.232	0.232	0.232	0.232	0.232
			Slope	-244.86	-244.89	-244.91	-244.93	-244.95	-244.97	-244.98	-244.99	-245.01	-245.02
			Intercept	59.848	59.885	59.916	59.943	59.966	59.986	60.004	60.020	60.034	60.047
			r2	0.995	0.995	0.995	0.995	0.995	0.995	0.995	0.995	0.995	0.995

Appendix (4-7) Calculated [H₂A] after correction and sorbed values for experiment (E₅)

No.	Mass in g	C _o	Samples order	Absorbance 1	Absorbance 2	[H ₂ A] ppm	Sorbed mg/g
1	2	25	2g 25 ppm	0.16	0.16	16.857	0.16
2	2	20	2g 20 ppm	0.179	0.178	14.440	0.11
3	2	30	2g 30 ppm	0.141	0.141	24.276	0.11
4	2	10	2g 10 ppm	0.219	0.218	5.707	0.09
5	2	30	2g 30 ppm	0.14	0.139	25.217	0.10
6	2	25	2g 25 ppm	0.157	0.157	21.082	0.08
7	2	10	2g 10 ppm	0.218	0.217	6.381	0.07
8	2	20	2g 20 ppm	0.177	0.176	16.487	0.07
9	5	25	5g 25 ppm	0.169	0.17	18.259	0.05
10	5	10	5g 10 ppm	0.223	0.222	5.330	0.04
11	5	20	5g 20 ppm	0.188	0.188	13.814	0.05
12	5	30	5g 30 ppm	0.151	0.15	23.029	0.06
13	5	15	2g 15 ppm	0.196	0.196	11.913	0.02
14	5	15	5g 15 ppm	0.204	0.204	9.976	0.04
15	5	15	2g 15 ppm	0.196	0.196	11.955	0.02
16	5	30	5g 30 ppm	0.15	0.15	23.241	0.05
17	5	15	5g 15 ppm	0.204	0.204	10.028	0.04
18	5	20	5g 20 ppm	0.187	0.186	14.329	0.05
19	5	25	5g 25 ppm	0.168	0.168	18.874	0.05
20	5	10	5g 10 ppm	0.222	0.222	5.654	0.03

Appendix (4-8) Drift of absorbance of [KMnO₄] (5ml [KMnO₄] +5ml of deionised water) over different times at 530nm.

time min	[KMnO₄] 40 ppm	[KMnO₄] 80 ppm	% absorbance increase for 40 [KMnO₄] ppm	% absorbance increase for 80 [KMnO₄] ppm
0	0.358	0.695		
5	0.359	0.710	0.37	2.16
10	0.370	0.714	3.36	2.66
15	0.378	0.735	5.52	5.50
25	0.394	0.749	9.26	7.30
35	0.404	0.777	11.50	10.65
46	0.419	0.798	14.76	12.99
52	0.432	0.806	17.32	13.81
55	0.431	0.807	17.09	13.92
58	0.431	0.807	16.98	13.92
61	0.435	0.807	17.78	13.92
64	0.434	0.806	17.58	13.81

Appendix (4-9) Absorbance with recording time for sorption experiment E₅.

Recording time	Actual time	Standard [H ₂ A] ppm or samples	Absorbance			
			1	2	3	average
0	05:56	40	0.1858	0.1858	0.1833	0.185
2	05:58	30	0.2449	0.2424	0.2449	0.244
3	05:59	20	0.2939	0.2867	0.2867	0.289
4	06:00	10	0.3386	0.3438	0.3361	0.340
6	06:02	5	0.3681	0.3631	0.3575	0.363
8	06:04	2.5	0.3851	0.3909	0.3826	0.386
10	06:06	10 g sst 30 ppm	0.3207	0.3207	0.3207	0.321
12	06:08	10 g sst 30 ppm	0.313	0.3157	0.3207	0.316
14	06:10	10 g sst 25 ppm	0.3383	0.3411	0.3436	0.341
16	06:12	10 g sst 25 ppm	0.3411	0.3436	0.3359	0.340
18	06:14	15 ppm	0.3281	0.3256	0.3256	0.326
19	06:15	20 ppm	0.3011	0.3011	0.3059	0.303
21	06:17	10 g sst 20 ppm	0.3621	0.3626	0.365	0.363
22	06:18	10 gsst 20 ppm	0.3541	0.3596	0.3621	0.359
24	06:20	10 g sst 15 ppm	0.3762	0.3811	0.3843	0.381
26	06:22	10g sst 15 ppm	0.3762	0.3811	0.3811	0.379
27	06:23	15 ppm	0.3381	0.3357	0.3383	0.337
29	06:25	20 ppm	0.3109	0.3109	0.3132	0.312
31	06:27	10 g sst 10 ppm	0.4008	0.4018	0.4072	0.403
32	06:28	10g sst 10 ppm	0.4017	0.4017	0.4078	0.404
34	06:30	10 g diw	0.4262	0.4201	0.4301	0.425
36	06:32	15 ppm	0.3406	0.3406	0.3481	0.343
37	06:33	20 ppm	0.3182	0.3132	0.3157	0.316
41	06:37	40	0.213	0.2117	0.214	0.2129
42	06:38	30	0.2781	0.2754	0.2614	0.2716
43	06:39	20	0.3254	0.3206	0.3206	0.3222
45	06:41	10	0.3724	0.3748	0.3699	0.3724
46	06:42	5	0.4002	0.3992	0.3998	0.3997
48	06:44	2.5	0.4141	0.4136	0.4189	0.4155

Appendix (4-10) Absorbance values arranged according to time and concentration for sorption experiment E₅.

time (min)	[H ₂ A] ppm						
	2.5	5	10	15	20	30	40
8	0.3862						
48	0.4155						
6		0.3629					
46		0.3997					
4			0.3395				
45			0.3724				
18				0.3264			
27				0.3374			
36				0.3431			
3					0.2891		
19					0.3027		
29					0.3117		
37					0.3157		
43					0.3222		
2						0.2441	
42						0.2716	
0							0.1850
41							0.2129
Intercept	0.3803	0.3574	0.3363	0.3106	0.2870	0.2427	0.1850

Red colour of absorbances represent ascorbic acid alone without sandstone

Appendix (4-11) Absorbance obtained by subtracting the initial absorbance value from the intercept (Appendix 4-10) for each [H₂A] for sorption experiment E₅ .

Time min	2.5	5	10	15	20	30	40
8	0.0059						
48	0.0352						
6		0.0055					
46		0.0424					
4			0.0032				
45			0.0361				
18				0.0158			
27				0.0267			
36				0.0325			
3					0.0021		
19					0.0157		
29					0.0246		
37					0.0287		
43					0.0352		
2						0.0014	
42						0.0289	
0							0.0000
41							0.0279
SLOPE	0.0008						

Appendix (4-12) Absorbance before and after correction, to determine [H₂A] for sorption experiment E₅ .

Samples	Mass of sst (g)	time min	pH	Average absorbance	Correct the absorbance	[H ₂ A] ppm	[H ₂ A] ppm after zero ppm
40	Standard solution	0	4.22	0.1850	0.1850	40.051	
30		2	4.32	0.2441	0.2425	28.769	
20		3	4.41	0.2891	0.2867	20.092	
10		4	4.6	0.3395	0.3363	10.362	
5		6	4.88	0.3629	0.3582	6.082	
2.5		8	4.92	0.3862	0.3799	1.822	
10 g 30	10	10	4.84	0.3207	0.3128	14.977	16.834
10g 30	10	12	4.82	0.3165	0.3070	16.117	17.973
10 g 25	10	14	4.85	0.3410	0.3300	11.615	13.471
10 g 25	10	16	4.88	0.3402	0.3276	12.081	13.938
15	Control samples	18	4.58	0.3264	0.3122	15.090	
20		19	4.49	0.3027	0.2877	19.900	
10 g 20	10	21	4.88	0.3632	0.3467	8.337	10.194
10 g 20	10	22	4.9	0.3586	0.3412	9.401	11.257
10 g 15	10	24	4.87	0.3805	0.3616	5.408	7.265
10g 15	10	26	4.86	0.3795	0.3590	5.927	7.784
15	Control samples	27	4.6	0.3374	0.3161	14.339	
20		29	4.57	0.3117	0.2888	19.688	
10 g 10	10	31	4.87	0.4033	0.3788	2.033	3.889
10 g 10	10	32	4.86	0.4037	0.3785	2.096	3.953
10 g 0	10	34	4.91	0.4255	0.3986	-1.856	0
15	Standard solution	36	4.60	0.3431	0.3147	14.607	
20		37	4.48	0.3157	0.2865	20.135	
40		41	4.22	0.2129	0.1806	40.916	
30		42	4.35	0.2716	0.2385	29.551	
20		43	4.44	0.3222	0.2883	19.789	
10		45	4.61	0.3724	0.3369	10.259	
5		46	4.86	0.3997	0.3634	5.047	
2.5		48	4.92	0.4155	0.3777	2.2577	

Appendix (4-13) Final [H₂A] after correction and calculated sorbed values for sorption experiment (E₅).

Samples	c₀ ppm	c₁ ppm	Mass (g)	sorbed mg/g
1	30	16.8341	10	0.0527
2	30	17.9738	10	0.0481
3	25	13.4716	10	0.0461
4	25	13.9380	10	0.0442
5	20	10.1942	10	0.0392
6	20	11.2576	10	0.0350
7	15	7.2654	10	0.0309
8	15	7.7840	10	0.0289
9	10	3.8898	10	0.0244
10	10	3.9530	10	0.0242

Chapter 5

Appendix (5-1) steps to determine the selectivity coefficient of groups pairs of cations in sandstone .

samples	Mn ++ ppm	Mg ++ ppm	k+ ppm	ca++ ppm	Na+ ppm	Ph	
diw (1)	1.132	3.726	5.936	21.435	9.863	4.98	
diw(2)	1.129	3.63	6.033	21.47	8.794	4.88	
diw(3)	1.186	3.5	6.195	20.8	9.893	4.86	
diw(4)	1.207	4.109	6.345	20.48	8.842	4.83	
0.25M of src12.6H2O (1)	2.855	7.958	9.757	141.5	10.163	4.22	
0.25M of src12.6H2O (2)	2.738	8.223	10.43	147.8	9.049	4.31	
0.25M of src12.6H2O (3)	2.523	8.275	10.35	145.9	9.618	4.35	
0.25M of src12.6H2O (4)	3.041	8.123	9.97	136.3	10.156	4.32	
Average DIW	1.2	3.7	6.1	21.0	9.3	4.9	
	ppm	ppm	ppm	ppm	ppm	mol/L	
SrCl2-avDIW 1	1.7	4.2	3.6	120.5	0.8	0.000047	
SrCl2-avDIW 2	1.6	4.5	4.3	126.8	-0.3	0.000036	
SrCl2-avDIW 3	1.4	4.5	4.2	124.9	0.3	0.000032	
SrCl2-avDIW 4	1.9	4.4	3.8	115.3	0.8	0.000035	
Concs in contact with sst							
mol/L 1	0.00005191	0.00032749	0.00024954	0.00353750	0.00044187	0.00422000	
mol/L 2	0.00004978	0.00033840	0.00026675	0.00369500	0.00039343	0.00431000	
mol/L 3	0.00004587	0.00034053	0.00026471	0.00364750	0.00041817	0.00435000	
mol/L 4	0.00005529	0.00033428	0.00025499	0.00340750	0.00044157	0.00432000	
10	g	0.04	L				
55	24.3	39.1	40	23	1		
2	2	1	2	1	1		cec (meq/100g)
meq/100g 1	0.0246	0.1388	0.0371	2.4091	0.0142	0.0000	2.6
meq/100g 2	0.0229	0.1475	0.0440	2.5351	-0.0052	0.0000	2.7
meq/100g 3	0.0198	0.1493	0.0432	2.4971	0.0047	0.0000	2.7
meq/100g 4	0.0273	0.1443	0.0393	2.3051	0.0141	0.0000	2.5
av cec comp (meq/100g)	0.0236	0.1450	0.0409	2.4366	0.0069	0.0000	2.7
%	0.9	5.5	1.5	91.8	0.3	0.0	100.0
equiv fraction 1	0.0094	0.0529	0.0142	0.9182	0.0054	0.0000	
equiv fraction 2	0.0083	0.0538	0.0160	0.9237	-0.0019	0.0000	
equiv fraction 3	0.0073	0.0550	0.0159	0.9201	0.0017	0.0000	
equiv fraction 4	0.0108	0.0570	0.0155	0.9111	0.0056	0.0000	
a (m)	6.00E-10	8.00E-10	3.00E-10	6.00E-10	4.00E-10	1.00E-10	
gamma 1	5.91E-01	6.13E-01	8.63E-01	5.91E-01	8.68E-01	8.51E-01	
gamma 2	5.86E-01	6.09E-01	8.60E-01	5.86E-01	8.66E-01	8.49E-01	
gamma 3	5.76E-01	5.99E-01	8.55E-01	5.76E-01	8.61E-01	8.43E-01	
gamma 4	5.87E-01	6.10E-01	8.61E-01	5.87E-01	8.66E-01	8.49E-01	
activity 1	3.07E-05	2.01E-04	2.15E-04	2.09E-03	3.83E-04	3.59E-03	
activity 2	2.92E-05	2.06E-04	2.30E-04	2.17E-03	3.41E-04	3.66E-03	
activity 3	2.64E-05	2.04E-04	2.26E-04	2.10E-03	3.60E-04	3.67E-03	
activity 4	3.25E-05	2.04E-04	2.20E-04	2.00E-03	3.82E-04	3.67E-03	
	Kca/mn	Kca/mg	Kca/k	Kca/ca - check	Kca/na	Kca/h	
sample 1	1.44	1.61	0.08	1.00	1.74	8.89E+07	
sample 2	1.49	1.57	0.07	1.00	10.78	1.68E+08	
sample 3	1.59	1.56	0.07	1.00	14.74	2.19E+08	
sample 4	1.37	1.57	0.07	1.00	1.69	1.64E+08	
average	1.47	1.58	0.07		1.71		

Appendix (5-2) effect of add various concentration of Fe on the concentration of rest cations from the sandstone interaction with various concentration of Fe

Samples Add Fe ppm	Ca ⁺⁺	Mg ⁺⁺	Na ⁺	k ⁺	Fe	Mn ⁺⁺
	ppm					
20	23.84	5.04	7.71	6.96	11.55	1.90
20	23.92	4.71	7.69	6.94	11.36	1.66
15	22.20	4.64	6.62	6.86	8.07	1.59
15	23.18	4.84	8.36	6.47	7.31	1.68
10	21.12	4.56	7.33	6.29	4.64	1.59
10	20.58	4.45	6.69	6.46	4.95	1.38
5	19.14	4.15	8.47	6.39	2.01	1.27
5	18.79	4.20	8.17	6.63	2.42	1.28
2.5	17.65	4.06	7.68	5.94	1.26	1.15
2.5	17.82	4.50	7.51	6.13	1.13	1.24
0	16.78	3.91	6.31	6.43	0.00	0.91
0	16.85	4.35	6.49	5.86	0.00	0.94

Appendix (5-3) results of Phreqcee model on the interaction of DIW +sst in present various concentration of FeCl₂ .

sim	state	soln	dist_x	time	step	pH	pe	Ca	Mg	Na	K	Fe	Mn	Cl	ppmFe				
1	i_soln	1	-99	-99	-99	7		12	4.20E-04	1.70E-04	2.78E-04	1.57E-04	7.16E-06	1.67E-05	1.65E-03	0.40113		4.01E-01	
1	i_exch	1	-99	-99	-99	7		12	4.20E-04	1.70E-04	2.78E-04	1.57E-04	7.16E-06	1.67E-05	1.65E-03	0.40113		4.01E-01	
1	react	1	-99	0	1	6.98846	3.96127	4.34E-04	1.76E-04	2.82E-04	1.59E-04	2.87E-05	1.73E-05	1.74E-03	1.60978		1.61E+00		
1	react	1	-99	0	2	6.97759	3.68782	4.47E-04	1.81E-04	2.85E-04	1.62E-04	5.05E-05	1.79E-05	1.83E-03	2.82985		2.83E+00		
1	react	1	-99	0	3	6.95629	3.42946	4.74E-04	1.92E-04	2.91E-04	1.66E-04	9.70E-05	1.89E-05	2.01E-03	5.43105		5.43E+00		
1	react	1	-99	0	4	6.93644	3.29678	4.99E-04	2.02E-04	2.97E-04	1.70E-04	1.45E-04	1.99E-05	2.19E-03	8.12616		8.13E+00		
1	react	1	-99	0	5	6.9177	3.21285	5.23E-04	2.11E-04	3.02E-04	1.73E-04	1.95E-04	2.09E-05	2.37E-03	10.9273		1.09E+01		
Averages																			
								Averages											
Fe o	Ca++ mg	Mg++ mg	Na+ mg/k+	mg/l	Fe++ mg	Mn++ mg	'Cl'	Fe o	Ca++ mg	Mg++ mg	Na+ mg/k+	mg/l	Fe++ mg	Mn++ mg	'Cl'	ppmFe			
0	16.82	4.13	6.40	6.14	0.00	0.92	58.55	0	0.00042	0.00017	0.00028	0.00016	0	1.7E-05	0.00165	0	0	57.8705	0.00163
2.5	17.74	4.28	7.60	6.04	1.19	1.19	64.24	4.5E-05	0.00044	0.00018	0.00033	0.00015	2.1E-05	2.2E-05	0.00181	1.1925	2.5	62.628	0.00177
5	18.97	4.17	8.32	6.51	2.22	1.28	69.06	8.9E-05	0.00047	0.00017	0.00036	0.00017	4E-05	2.3E-05	0.00195	2.215	5	66.7413	0.00188
10	20.85	4.51	7.01	6.37	4.80	1.48	74.78	0.00018	0.00052	0.00019	0.0003	0.00016	8.6E-05	2.7E-05	0.00211	4.795	10	70.6789	0.00199
15	22.69	4.74	7.49	6.66	7.69	1.63	83.61	0.00027	0.00057	0.0002	0.00033	0.00017	0.00014	3E-05	0.00236	7.69	15	77.5705	0.00219
20	23.88	4.87	7.70	6.95	11.46	1.78	91.64	0.00036	0.0006	0.0002	0.00033	0.00018	0.0002	3.2E-05	0.00258	11.455	20	83.1131	0.00234
								56	40.00	24.30	23.00	39.10	56.00	55.00	35.50				
Averages																			
								Averages											
Fe o	Ca++ mg	Mg++ mg	Na+ mg/k+	mg/l	Fe++ mg	Mn++ mg	'Cl'	Fe o	Ca++ mg	Mg++ mg	Na+ mg/k+	mg/l	Fe++ mg	Mn++ mg	'Cl'				
0	16.82	4.13	6.40	6.14	0.00	0.92	58.55	0	0.00042	0.00017	0.00028	0.00016	0	1.7E-05	0.00165				
2.5	17.74	4.28	7.60	6.04	1.19	1.19	64.24	4.5E-05	0.00044	0.00018	0.00033	0.00015	2.1E-05	2.2E-05	0.00174				
5	18.97	4.17	8.32	6.51	2.22	1.28	69.06	8.9E-05	0.00047	0.00017	0.00036	0.00017	4E-05	2.3E-05	0.00183				
10	20.85	4.51	7.01	6.37	4.80	1.48	74.78	0.00018	0.00052	0.00019	0.0003	0.00016	8.6E-05	2.7E-05	0.00201				
15	22.69	4.74	7.49	6.66	7.69	1.63	83.61	0.00027	0.00057	0.0002	0.00033	0.00017	0.00014	3E-05	0.00218				
20	23.88	4.87	7.70	6.95	11.46	1.78	91.64	0.00036	0.0006	0.0002	0.00033	0.00018	0.0002	3.2E-05	0.00236				
								56	40.00	24.30	23.00	39.10	56.00	55.00	35.50				

Appendix (5-4) sorption experiment data for adsorption of Mn^{++} (from Mn standard for FAAS)
on the surface of sandstone by assume $[Mn^{++}]_o$ as explain in below table .

Mn^{++} ppm (C_o)	Mn^{++} ppm (C_i)	Estimated $[Mn]_o$ (ppm)	Corr C_1	S	S [$=(CoC_1+avDIW)V/M$]
20	20.63	1.2	19.43	0.00228	0.00568
20	19.7	0.3	19.4	0.0024	0.0094
15	16.16	1.7	14.46	0.00216	0.00356
15	16.18	1.7	14.48	0.00208	0.00348
10	12.66	3.15	9.51	0.00196	-0.00244
10	12.55	3.05	9.5	0.002	-0.002
5	7.86	3.3	4.56	0.00176	-0.00324
5	7.79	3.2	4.59	0.00164	-0.00296
2.5	3.53	1.25	2.28	0.00088	0.00408
2.5	3.45	1.2	2.25	0.001	0.0044
0	1.87	2	-0.13	0.00052	0.00072
0	1.99	2.1	-0.11	0.00044	0.00024
	0				

Chapter 6

(6-1): Raw and corrected results for final experiment under biotic and abiotic conditions using initial H₂A =100 ppm for different time intervals .

	Raw Fe & Mn Data (ppm)		Corrected Fe & Mn Data (ppm)								Raw H2A Data		Corrected H2A Data		0.264	0.0921
			Corrected for Mn & Fe IE using phreeqc									ppm		-3.96	0.0921	0.0465
for 100 ppm																
[H2A] ppm	time h	Mn bio	Mn abio	Fe bio	Fe Abio	Mn bio	Mn abio	Fe bio	Fe Abio	time h	biotic	abiotic	biotic	abiotic	biotic	abiotic
100	4.5	2.69		1.19		5.06		1.34		4.5	73.71		82.05		82.6	
100	4.5	2.67		1.18		5.06		1.34		4.5	72.16		80.44		81.0	
100	4.5	2.7		1.04		5.19		1.16		4.5	71.5		80.17		80.8	
100	4.5		0.66		0.09		2.2		0.08	4.5		92.25		94.16		94.8
100	4.5		0.54		0.2		1.65		0.22	4.5		92.86		94.16		94.8
100	4.5		0.59		0.21		1.93		0.25	4.5		92.4		93.96		94.6
100	16	3.69		1.43		7.43		1.57		16	47.32		59.15		60.8	1.7
100	16	3.48		1.14		7.03		1.26		16	53.42		64.98		66.6	1.7
100	16	3.52		1.19		7.19		1.29		16	59.94		71.57		73.2	1.7
100	16		0.74		0.36		2.48		0.45	16		72.42		74.32		76.0
100	16		0.72		0.43		2.31		0.56	16		84.02		85.90		87.6
100	16		0.79		0.4		2.6		0.47	16		81.44		83.71		85.4
100	24	3.81		2.17		7.71		2.38		24	37.75		48.62		51.0	2.4
100	24	3.72		2		7.49		2.2		24	40.44		51.28		53.7	2.4
100	24	3.66		1.9		7.39		2.08		24	39.05		49.85		52.2	2.4
100	24		0.82		0.53		2.77		0.65	24		69.5		71.91		74.3
100	24		0.83		0.5		2.77		0.59	24		70.63		73.10		75.5
100	24		0.73		0.44		2.37		0.53	24		69.5		71.65		74.0
100	49	4.4		2.53		8.95		2.74		49	17.66		30.16		34.9	4.7
100	49	4.24		2.46		8.55		2.69		49	16.79		28.80		33.5	4.7
100	49	4.26		2.69		8.55		2.96		49	15.78		27.42		32.1	4.7
100	49		0.63		0.43		2.02		0.53	49		55.62		58.11		62.8
100	49		0.59		0.42		1.85		0.53	49		52.7		55.04		59.7
100	49		0.59		0.38		1.85		0.47	49		52.2		54.54		59.2

(6-2): Raw and corrected results for final experiment under biotic and abiotic conditions using initial H₂A =80 ppm for different time intervals

		Raw Fe & Mn Data (ppm)				Corrected Fe & Mn Data (ppm)						Raw H2A Data	Corrected H2A Data		0.264	0.0921
												ppm		-3.96	0.0921	0.0465
		for 80 ppm				Corrected for Mn & Fe IE using phreeqc						[H2A]	[H2A]	corrected for [Mn]	Corr for Degradation	
[H2A] ppm	time h	Mn bio	Mn abio	Fe bio	Fe Abio	Mn bio	Mn abio	Fe bio	Fe Abio	time h	biotic	abiotic	biotic	abiotic	biotic	abiotic
80	4.5	2.62		0.85		5.05		0.96		4.5	57.14		65.862		66.5	
80	4.5		0.45		0.1		1.44		0.06	4.5		70.68		70.68		70.8
80	16	3.38		0.86		6.83		0.96		16	34.42		46.132		47.8	
80	16		0.62		0.31		2.02		0.35	16		63.56		63.56		63.7
80	24	3.48		1.7		6.99		1.9		24	30.05		40.525		42.9	
80	24		0.63		0.27		2.02		0.35	24		48.32		48.32		48.4
80	49	3.59		1.19		7.29		1.3		49	14.13		26.032		30.7	
80	49		0.49		0.25		1.44		0.29	49		29.08		29.08		29.2

(6-3): Raw and corrected results for final experiment under biotic and abiotic conditions using initial H₂A =40 ppm for different time intervals

													H2A Correction		degrdation	
						Corrected Fe & Mn Data (ppm)							-3.96		0.0921	
	for 40 ppm					Corrected for Mn & Fe IE using phreeqc							corr for [Mn]		bio	abio
[H2A] ppm	time h	Mn bio	Mn abio	Fe bio	Fe Abio	Mn bio	Mn abio	Fe bio	Fe Abio	time h	biotic	abiotic	biotic	abiotic		
40	4.5	1.19		0.42		4.14		0.52		4.5	29.1		33.00		33.59	
40	4.5		0.35		0		1.14		0.01	4.5		35.21		36.60		37.19
40	16	1.25		0.53		4.36		0.66		16	16.9		20.82		22.48	
40	16		0.45		0.21		1.44		0.29	16		27.62		28.99		30.65
40	24	1.48		0.79		5.11		0.97		24	13.28		17.60		20.00	
40	24		0.32		0.23		1.1		0.35	24		18.57		19.39		21.78
40	49	1.76		1.19		5.89		1.36		49	4.59		9.25		13.94	
40	49		0.28		0.14		0.86		0.45	49		13.48		14.32		19.01

(6-4): Raw and corrected results for final experiment under biotic and abiotic conditions using initial H₂A =60 ppm for different time intervals

		Raw Fe & Mn Data (ppm)				Corrected Fe & Mn Data (ppm)					Raw H2A Data		Corrected H2A Data		0.264	0.0921
											ppm		-3.96		0.0921	0.0465
	for 60 ppm					Corrected for Mn & Fe IE using phreeqc					[H2A]	[H2A]	corrected for [Mn]		Corr for Degradation	
[H2A]ppm	time h	Mn bio	Mn abio	Fe bio	Fe Abio	Mn bio	Mn abio	Fe bio	Fe Abio	time h	biotic	abiotic	biotic	abiotic	biotic	abiotic
60	4.5	2.41		0.65		4.47		0.74		4.5	39.03		47.31		47.91	
60	4.5	2.55		0.6		4.85		0.69		4.5	43.59		52.52		53.12	
60	4.5	2.31		0.56		4.26		0.62		4.5	40.87		48.93		49.53	
60	4.5		0.44		0		1.32		0.01	4.5		41.94		43.68		44.28
60	4.5		0.37		0.01		1.1		0.01	4.5		50.47		51.92		52.51
60	4.5		0.46		0		1.38		0.01	4.5		51.60		53.42		54.02
60	16	2.9		0.73		5.74		0.81		16	26.27		36.33		37.99	
60	16	2.88		0.77		5.62		0.85		16	27.93		37.84		39.50	
60	16	2.42		0.64		4.53		0.72		16	24.22		32.56		34.22	
60	16		0.55		0.23		1.71		0.28	16		33.03		34.76		36.42
60	16		0.51		0.25		1.6		0.28	16		39.47		41.00		42.66
60	16		0.6		0.24		1.87		0.28	16		37.50		39.41		41.07
60	24	3.41		1.25		6.81		1.39		24	18.27		29.34		31.74	
60	24	3.27		1.29		6.49		1.45		24	16.03		26.47		28.87	
60	24	3.4		1.29		6.85		1.42		24	15.57		26.53		28.92	
60	24		0.64		0.35		2.15		0.45	24		35.20		37.05		39.45
60	24		0.5		0.24		1.65		0.28	24		32.70		34.21		36.61
60	24		0.42		0.28		1.21		0.35	24		33.91		35.03		37.42
60	49	3.56		1.24		7.27		1.39		49	3.75		15.44		20.13	
60	49	3.4		1.33		6.81		1.45		49	2.23		13.11		17.80	
60	49	3.37		1.31		6.81		1.45		49	2.02		12.82		17.51	
60	49		0.44		0.26		1.21		0.35	49		24.33		25.57		30.26
60	49		0.49		0.25		1.49		0.34	49		23.08		24.53		29.23
60	49		0.4		0.2		1.1		0.28	49		20.66		21.86		26.55

(6-5): Raw and corrected results for final experiment under biotic and abiotic conditions using initial H₂A =20 ppm for different time intervals

																	degredation
						Corrected Fe & Mn Data (ppm)					H2A	H2A	-3.96			0.09	
	for 20 ppm					Corrected for Mn & Fe IE using pl				for 20 ppm			corr for [Mn]	H2A	H2A		
[H2A]	time h	Mn bio	Mn abio	Fe bio	Fe Abio	Mn bio	Mn abio	Fe bio	Fe Abio	time h	biotic	abiotic	biotic	abiotic	Biotic	Abiotic	
20	4.50	1.07		0.35		3.70		0.44		4.5	11.27		14.83		15.43		
20	4.50	1.10		0.38		3.82		0.46		4.5	10.89		14.51		15.11		
20	4.50	1.18		0.29		4.18		0.32		4.5	10.69		14.80		15.40		
20	4.50		0.40		0.00		1.21		0.01	4.5		15.81		17.39		17.99	
20	4.50		0.31		0.00		0.91		0.00	4.5		15.32		16.55		17.15	
20	4.50		0.26		0.00		0.72		0.01	4.5		16.86		17.89		18.49	
20	16.00	1.34		0.45		4.60		0.53		16.0	6.25		10.68		12.34		
20	16.00	1.39		0.40		4.77		0.47		16.0	6.93		11.66		13.31		
20	16.00	1.31		0.49		4.85		0.56		16.0	6.63		10.86		12.52		
20	16.00		0.34		0.19		0.87		0.36	16.0		12.42		13.40		15.05	
20	16.00		0.40		0.18		1.24		0.33	16.0		13.18		14.41		16.07	
20	16.00		0.34		0.17		1.20		0.34	16.0		12.73		13.75		15.40	
20	24.00	1.71		0.66		5.77		0.76		24.0	2.02		7.51		9.90		
20	24.00	1.81		0.60		6.05		0.64		24.0	3.79		9.79		12.19		
20	24.00	1.65		0.46		5.65		0.52		24.0	3.63		9.27		11.66		
20	24.00		0.20		0.23		0.46		0.35	24.0		10.64		10.98		13.38	
20	24.00		0.17		0.20		0.21		0.35	24.0		10.56		10.84		13.24	
20	24.00		0.15		0.22		0.17		0.34	24.0		10.32		10.49		12.88	
20	49.00	1.90		0.85		6.23		0.97		49.0	0.40		6.27		10.97		
20	49.00	1.92		0.73		6.33		0.82		49.0	0.43		6.61		11.31		
20	49.00	1.90		0.66		6.21		0.76		49.0	0.29		6.53		11.23		
20	49.00		0.26		0.13		0.55		0.17	49.0		8.39		9.17		13.86	
20	49.00		0.13		0.14		0.10		0.17	49.0		9.97		10.21		14.91	
20	49.00		0.20		0.13		0.26		0.17	49.0		8.95		9.49		14.19	

(6-6 A) pH and Eh for biotic and abiotic experiments for initial H₂A = 100 ,60 and 20 ppm

100 ppm H ₂ A	biotic	Abiotic	biotic	Abiotic
time h	Ph	Ph	Eh(mv)	Eh(mv)
4.5	4.44		157	
4.5	4.45		160.3	
4.5	4.39		164.1	
4.5		5.15		109
4.5		4.87		130.5
4.5		4.83		132.9
16	4.52		157.5	
16	4.55		153	
16	4.54		152.1	
16		5.01		108
16		4.4		160
16		4.9		127
24	4.56		151.6	
24	4.51		153.5	
24	4.35		152.7	
24		4.92		128.8
24		4.85		132.5
24		4.94		127.5
49	4.71		144.1	
49	4.64		145.5	
49	4.65		146.2	
49		4.95		125.8
49		4.99		122.8
49		5.03		121.2

60 ppm	biotic	Abiotic	biotic	Abiotic
time h	ph	ph	Eh(mv)	Eh(mv)
4.5	4.54		152.1	
4.5	4.54		152	
4.5	4.58		149.2	
4.5		5.22		103.5
4.5		5.16		113
4.5		5.12		114.5
16	4.68		143.8	
16	4.65		145.3	
16	4.71		142.7	
16		5.21		107.5
16		4.9		128.2
16		5.11		114.6
24	4.56		150.4	
24	4.57		149.9	
24	4.61		147.5	
24		4.89		130
24		5		123.5
24		5.1		117
49	4.78		137.5	
49	4.76		137.1	
49	4.75		137	
49		5.02		121.5
49		4.94		126.7
49		5.15		114.7

20 ppm	biotic	A biotic	biotic	A biotic
time h	ph	ph	Eh(mv)	Eh(mv)
4.5	4.73		140.2	
4.5	4.72		141.1	
4.5	4.74		139	
4.5		5.14		111
4.5		5.24		108
4.5		5.45		96
16	4.8		137.1	
16	4.8		136	
16	4.78		136.9	
16		5.43		94.7
16		5.4		99.2
16		5.46		95
24	4.75		141.5	
24	4.79		141	
24	4.79		140.7	
24		5.17		113
24		5.27		107
24		5.23		109.2
49	4.81		134	
49	4.84		133.7	
49	4.78		133.1	
49		5.1		117.5
49		5.46		95.2
49		5.3		105.5

(6-6 B) pH and Eh for biotic and abiotic experiments using initial $H_2A = 80$ and 40 ppm

80 ppm	biotic	abiotic	biotic	abiotic
H ₂ A ppm	ph	ph	Eh(mv)	Eh(mv)
4.5	4.46		157.6	
4.5		4.91		126.5
16	4.6		148.3	
16		4.7		139
24	4.53		153.1	
24		4.92		128.5
49	4.72		141.8	
49		5.29		105

40 ppm	biotic	Abiotic	biotic	Abiotic
time h	ph	ph	Eh(mv)	Eh(mv)
4.5	4.66		144.6	
4.5		5.17		109.5
16	4.74		139.5	
16		5.16		116.8
24	4.62		146.8	
24		5.12		116
49	4.83		133.6	
49		5.2		111.8